DOCTOR OF SCIENCES

Unravelling the effects of proton irradiation on macrophages in cancer

Genard, Géraldine

Award date:
2018

Awarding institution:
University of Namur

University of Namur (UNamur)
Faculté des Sciences – Département de Biologie
Namur Research Institute for Life Sciences (NARILIS)
Unité de Recherche en Biologie Cellulaire (URBC)
Rue de Bruxelles, 61; B-5000 Namur, Belgique

UNRAVELING THE EFFECTS OF PROTON IRRADIATION ON MACROPHAGES IN CANCER

Original dissertation presented
by **Géraldine GENARD**
for the degree of
Doctor of Sciences

Members of the jury:

Prof. Carine MICHIELS (Supervisor)
Unité de Recherche en Biochimie et Biologie Cellulaire (URBC)
NARILIS, UNamur, Namur

Prof. Stéphane LUCAS (co-supervisor)
Laboratoire d'Analyses par Réactions Nucléaires – Physique de la Matière et du Rayonnement (LARN – PMR)
NARILIS, UNamur, Namur

Prof. Yves POUMAY
Laboratoire Cellules et Tissus
Unité de Recherche en Physiologie Moléculaire (URPhyM)
NARILIS, UNamur, Namur

Prof. Olivier FERON
Institut de Recherche Expérimentale et Clinique Pôle de Pharmacologie et de Thérapeutique (IREC - FATH)
UCL, Woluwé-Saint-Lambert

Prof. Peter HUBER
Imaging and Radiooncology
Molecular Radiooncology
Deutsches Krebsforschungszentrum (DKFZ) Heidelberg, Germany

Prof .Anne-Catherine HEUSKIN (Chair woman)
Laboratoire d'Analyses par Réactions Nucléaires – Physique de la Matière et du Rayonnement (LARN – PMR)
NARILIS, UNamur, Namur

May, 30th 2018

Remerciements

En ce jour, c'est une étape qui se clôture. Mais c'est aussi la fin d'une longue histoire. Je ne vous cache pas que c'est avec un petit pincement au cœur que je rédige les dernières lignes de ce manuscrit après les quatre belles années que j'ai vécu en URBC. En débutant cette thèse, je me doutais que l'investissement serait important, que les expériences ne fonctionneraient pas du premier coup (je n'ai pas été déçue !) et que je devrais faire face à ma personnalité plutôt réservée et un manque de confiance en soi pour arriver au bout. Mais j'avais oublié de prendre en compte un élément important. Un élément qui m'aiderait à aller de l'avant et à me surpasser : cet élément c'est une toute une série de personnes qui de près ou de loin m'ont soutenue et aidée durant ces quatre années. Par ces quelques lignes, j'aimerais vous montrer à quel point vous avez été précieux pour moi.

I would like to thank all the members of my thesis jury: Prof. Peter Huber, Prof. Olivier Feron, Prof. Yves Poumay, Prof. Stéphane Lucas and Prof. Carine Michiels. I also specially thank Prof. Anne-Catherine Heuskin, the chairwoman of my thesis jury. Thank for the time you spent on my thesis and the constructive remarks and discussion that emerged during and following the private defense.

La première personne à qui je dois énormément, c'est ma promotrice Carine Michiels. Sans ses encouragements, son soutien et sa « positive attitude », je n'y serais jamais arrivée. Grâce à vous, j'ai concrétisé l'envie de faire une thèse. Certes, je n'ai pas eu le parcours de thèse le plus facile. Et pourtant, peu importe la situation, vous avez toujours été là, vous m'avez aiguillée et redirigée quand je m'éloignais un peu trop de mes objectifs, et ce, même quand vos fonctions vous ont éloignées du laboratoire. Ces quatre années ont été formatrices pour moi, autant sur le plan professionnel que personnel et vous y avez grandement contribué.

Je tiens également à remercier mon co-promoteur, Stéphane Lucas, qui m'a accueillie au sein de son laboratoire de physique, le LARN, et qui m'a emmené dans l'univers de la radiobiologie. Grâce à votre accueil, j'ai également découvert que la conception selon laquelle un physicien ressemblait à un geek de « Big Bang Theory » était erronée.

Si j'ai eu l'occasion de réaliser cette thèse, c'est aussi en grande partie grâce aux soutiens financiers du Télévie (FNRS), de l'Université de Namur et de l'institut Narilis. Le Télévie m'a permis de « travailler » durant ces quatre années. Je dis bien « travailler » car comme l'a dit un célèbre auteur, « en choisissant un travail que l'on aime, on n'aura pas à travailler un seul jour de sa vie ». Cette formidable organisation m'a également permis de rencontrer tout une série de personnes, d'enfants et de malades, durant les activités qu'elle organise. Des personnes qui nous rappellent ce pourquoi on s'est lancé dans l'aventure qu'est la thèse, et avec qui j'ai pu partager ma passion à de nombreuses reprises. J'aimerais aussi remercier Nathalie Caron pour m'avoir permis de terminer cette thèse, tout en revoyant mon cours de physiologie générale et en développant mes capacités didactiques. Enfin, sans l'institut Narilis, et la contribution de Virginie, je n'aurais pu assister à de belles conférences et profiter de ces occasions pour visiter des villes qui m'étaient alors inconnues.

Un grand merci aux « séniors » de l'URBC, à savoir les professeurs Thierry Arnould, Martine Raes, Patsy Renard et Florence Chainiaux. J'en profite pour remercier Thierry de s'être attelé à la tâche difficile qu'est la gestion du laboratoire. Certes la tâche n'est pas aisée mais c'est avec beaucoup de succès que vous l'avez menée à bien et j'en souhaite autant à Patsy qui reprendra le flambeau en septembre prochain.

J'ai beaucoup parlé de mes quatre années en URBC, mais il est certain que j'ai passé beaucoup de journées (et parfois des nuits !) auprès de l'accélérateur. Un grand merci aux physiciens qui m'ont accueillie parmi eux et qui, assez rapidement, m'ont donné le surnom de « Gégé », un surnom que je n'avais pourtant jamais supporté jusqu'alors. Aujourd'hui, je ne voudrais pour rien au monde qu'on me surnomme autrement. Merci pour les pauses cafés, les repas et surtout les tartes anniversaires ou « rentrée d'air » que l'on a partagés. Merci à Anne-Catherine Heuskin d'avoir pris le temps de m'expliquer l'ensemble des protocoles pour le montage des chambres, l'ensemencement des cellules, etc. alors qu'elle n'était pas loin d'accoucher. Je remercie également Tijani pour toute l'aide qu'il a pu m'apporter durant les journées d'irradiation. Merci à Greg, Ben, Romain, Sha et Polo pour les beaux moments que j'ai partagé en votre compagnie. Je n'oublie pas non plus Adri, Félicien, Julien, Pablo, Christophe, Rémy, Cécile, Stella, Pavel, Ornella et tous les autres qui ont su égayer mes journées au LARN. Yvon et Louis Lambotte, je vous remercie également de m'avoir aidée à développer les grandes chambres d'irradiation. Et bien sûr, Seb, merci d'avoir partagé ce beau séjour à Budapest avec moi. Merci aussi pour toutes nos discussions scientifiques et moins scientifiques.

J'en viens maintenant à remercier l'équipe HIF/TumHyp pour tous leurs bons conseils, les discussions et surtout les gâteaux que nous avons partagés pendant nos réunions. Un grand merci à Benjamin pour toutes les discussions scientifiques mais aussi pour ses nombreux encouragements qui m'ont souvent réconciliés avec moi-même et m'ont poussé à donner le meilleur de moi-même. Tu as énormément apporté à notre équipe. Il y a une personne sans qui cette fin de thèse n'aurait pas été possible. La Little Miss Sunshine du labo, Ank, je ne saurais comment te remercier pour tout l'aide que tu m'as apportée, tes conseils et tes explications précieuses. Seb M. et Thomas, vous nous avez prouvé que la chimie était nécessaire à la compréhension de certains mécanismes biologiques. Merci également de m'avoir émerveillé avec l'arc-en-ciel de jus de chou rouge pendant les activités Télévie. Merci Pastelle de m'avoir laisser t'initier à la recherche et je suis très heureuse de mon côté d'avoir eu à encadrer une étudiante qui en voulait autant. Je remercie aussi mes compagnons de macrophages, François et Victor (et anciennement Marie G. et Céline T). On n'aura jamais vu autant de troc en matière de flasque de THP-1. Notre médecin attitré, Eléonore, est un comble à elle toute seule, puisque c'est elle qu'il a fallu secourir d'un malaise pendant une présentation (je te charrie !). Merci d'avoir partagé quelques cours de Zumba avec moi et d'avoir égayer mes journées de manipes par tes petites conneries et ton humour. Camille, je te passe la « patate chaude » ! Blague à part, c'est un honneur de savoir que « son bébé » va grandir entre de bonnes mains. Je te souhaite le meilleur pour la suite et je sais que tu as déjà pu faire face aux joies de travailler avec les chambres d'irradiation, mais ne te décourage jamais, ces désagréments font aussi partie de notre apprentissage et tu en seras d'autant plus satisfaite à la ligne d'arrivée. Enfin, Kathleen et Sophie, deux personnes qui me sont chères au sein de cette équipe. Vous avez toujours su trouver les mots pour m'encourager en cas de stress, panique total et crise de nerf, alors un grand merci!

Leen, Julie, Marino et plus récemment, Damien, Alexis et Camille, merci d'avoir apporté un peu de jeunesse dans notre équipe URBC. Je vous souhaite beaucoup de succès pour la suite.

Ensuite, il y a des personnes sans qui le laboratoire ne pourrait pas tourner. Antoine, je te remercie infiniment pour les innombrables RT-qPCR et MNAse assay que tu as pris en charge. Ton aide m'a été précieuse et, en passant, tes citations du jour vont beaucoup me manquer ! Guy, le bisouteur du labo mais aussi un pilier du labo. Ta bonne humeur et tes tournées bisous vont beaucoup me manquer aussi. Maude, tu es passée de collègue à colloc' et enfin au statut d'amie. Merci pour l'année durant laquelle tu as supporté mes manies, mon désordre et le reste. Tu es l'une des rares personnes qui a eu l'occasion de voir à quel point j'étais difficile à vivre^^. Un grand merci à la team « confocale », Noëlle et Catherine, sans qui nos journées seraient bien plus remplies. Merci Martine pour tes encouragements, et tes précieux conseils sur les THP-1. Marc, le seul qui se prend pour le Dieu du labo et un homme parfait ! Ton humour et tes petits pics ont toujours détendu l'atmosphère. Le problème c'est que quand on s'attaque à quelqu'un, il faut toujours attendre le retour de bâton^^. Viviane, en plus d'être une super secrétaire, tu es devenue une amie qui m'est très chère. Je te remercie aussi car tu as toujours trouvé les mots pour m'aider à aller de l'avant. Enfin, Patricia, je tenais également à te remercier pour tes belles paroles qui chaque matin me mettait de bonne humeur.

Durant ma thèse, ce sont également de belles amitiés qui se sont développées, au sein de l'URBC mais également en dehors. Je remercie tout d'abord l'équipe « Paillette » de m'avoir fait découvrir un monde nouveau et de m'avoir montré combien il était plaisant de se sentir unique et différente. Un merci tout particulier à mes trois voisines de bureau : Marie T., Elise et Aude. Votre soutien et vos conseils m'ont aidé à traverser les moments difficiles de la thèse. Vos voyages et vos discussions m'ont permis de sortir la tête hors des manipes et des analyses. Enfin, je vous remercie pour toutes vos attentions qui m'ont énormément touchées. Mélanie et Marie, merci de m'avoir tenu compagnie dans la rédaction de thèse ! We did it ! Ton autodérision et ton humour m'auront été d'une grande aide durant cette fin de thèse, Mélanie. Bush, I wish you all the best for your futur plans. I will always be your URBC's sister. Emilie, derrière ton attitude un peu rude se cache une personne sensible et adorable. Courage, tu es presqu'au bout ! Ma petite Val, tu fais également partie de mes belles rencontres. Je retiens surtout de toi nos échanges de recettes « healthy », nos conversations à n'en plus finir ainsi que tes bourdes mémorables. Hélène, merci de m'avoir fait partager ton mariage et tes 30 ans. Elo et Jeff, je vous félicite encore pour la petite merveille que vous avez conçue et pour les futures à venir. J'espère que vous avez changé de GPS et n'emprunterez plus jamais les chemins de boues. Je crois que Geoffrey s'en souviendra longtemps (et votre voiture est marquée à vie). Céline et Victor, deux collègues qui sont également devenus des amis. Merci Victor pour les séances running. Céline, tu m'as toujours épaté par ta force de caractère alors ne laisse pas tomber ! Dans le même univers, je remercie Romain d'avoir partagé de nombreuses séances détentes le long du halage. Mais pas que, merci aussi pour tout le reste ! Une autre belle rencontre que je me dois de mentionner est celle de Sahar, Adel et Maryam. Ton attitude positive face à toute épreuve et ta gentillesse m'ont toujours impressionnées Sahar. Vous formez une belle famille tous les trois. Je remercie également Pierre, Romain, Conrard, Marie-Paule, Arvind, Ali, Maxime, Claire, Ophélie, Nassim, Fabrice et Flo pour leur présence, les soirées, les Mojitos, les soirées « Cap 30 » ou Renois et les retrouvailles pour certains. Je ne pourrais clôturer ce paragraphe sans citer mon coach sportif. Tu m'as tout appris de la course à pied et maintenant on ne peut plus m'arrêter. C'est toujours

un plaisir de venir le samedi aux courses du Challenge du BW, pour courir mais aussi pour retrouver l'ambiance qui s'est créée grâce à toute votre équipe.

Kathleen, Morgane et Sophie (la team « Melman ») vous êtes sans aucun doute les trois personnes qui me sont devenues les plus chères durant cette thèse. C'est une belle amitié qui nous réunit en tant que quatuor. Nos délires, nos coups de gueule, nos soirées cookies, nos pauses thé/café vont énormément me manquer. Kathleen, tu as toujours été là pour moi, m'a fait revivre mon enfance en m'emmenant à Disneyland Paris et m'a aidé à relativiser sur beaucoup de choses. Aujourd'hui, nous attendons bébé Melman avec impatience ! Morgane, tu es un peu ma semblable, ma compagne de « cerveau torture », ce qui fait qu'on a très facile à se comprendre. Avec le recul, on ne peut faire que rire de nos conneries ! Sophie, je crois que sans ton soutien, la fin de ma thèse aurait été impossible. Tu n'entendras bientôt plus mes « j'ai faim », « c'est quand qu'on mange » et puis « j'ai trop mangé, je dois vomir ». Mais je suis certaine qu'ils ne te manqueront pas ! On est un peu devenu les inséparables du labo alors que beaucoup de choses nous opposaient au départ. Je pense que tout a commencé autour d'un Mojito, notre passion commune^^. Je ne me fais pas de soucis au sujet de notre amitié car je sais qu'elle perdurera encore longtemps ! N'hésites pas à m'appeler à la rescousse en fin thèse, je te rendrai la pareille avec plaisir ! Je remercie également ta maman, Petchaye, de m'avoir accueilli à bras ouverts lors de mes quelques city-trips à Paris et de m'avoir aidé à confectionner jupe et robe.

Enfin, je remercie les personnes qui me sont le plus chers : mes parents et ma sœur. Je les remercie d'avoir supporté mes absences, mes caprices, mes conneries, mes histoires de macrophages et protonthérapie, et d'avoir été aux petits soins pour moi. J'ai des parents et une sœur formidables et je pense qu'on n'a jamais été aussi soudé qu'aujourd'hui. Merci pour tout, je vous dois énormément.

En plus d'être le principal constituant du microenvironnement tumoral, les macrophages associés aux tumeurs (TAMs) jouent un rôle essentiel dans la progression tumorale. En effet, ils interviennent dans les processus d'angiogenèse, de répression immunitaire, d'invasion et de métastases. Depuis longtemps, les TAMs se voient identifiés aux macrophages de type M2. Ce phénotype est caractérisé par des propriétés anti-inflammatoires et des fonctions pro-tumorales. On distingue à l'opposé de cet état d'activation alternatif des macrophages, un état d'activation classique, aussi appelé phénotype M1. Les macrophages de phénotype M1 sont, quant à eux, associés à des propriétés pro-inflammatoires, un potentiel de phagocytose et ont un rôle antitumoral. De façon intéressante, des changements du microenvironnement tumoral peuvent facilement modifier la polarisation des macrophages d'un phénotype M2 vers M1, ou inversement. Par conséquent, la reprogrammation des TAMs grâce aux thérapies représente un outil thérapeutique prometteur afin d'induire une régression tumorale. Divers types de chimiothérapie et d'immunothérapie ont déjà réussi à induire une reprogrammation des TAMs, associée à une régression tumorale. Toutefois, n'étant pas localisé, ce type de thérapie peut induire une réaction inflammatoire systémique. Pour éviter ces effets, la radiothérapie locale représente une stratégie séduisante. Jusqu'à maintenant, les rayons X et rayons γ n'ont pas pu induire une reprogrammation des TAMs. Néanmoins, comme la radiothérapie est un domaine en constante évolution, de nouvelles avancées en matière de radiothérapie ont vu le jour, c'est le cas de la protonthérapie. En comparaison à la radiothérapie conventionnelle, la protonthérapie offre divers avantages physiques et représente donc un outil thérapeutique puissant pour éliminer les tumeurs de façon très précise. La protonthérapie est d'autant plus intéressante qu'elle a démontré des effets radiobiologiques différents de la radiothérapie conventionnelle. C'est pourquoi, étudier les effets de l'irradiation par protons sur les macrophages, et plus précisément sur leur reprogrammation, permettrait de réévaluer considérablement la fréquence d'utilisation de la protonthérapie comme traitement contre le cancer.

Dans ce travail, les effets de l'irradiation par protons ont été évalués sur des cultures de macrophages M0 (non polarisés), M1 et M2 et des co-cultures de macrophages M2 et cellules cancéreuses. Nous avons démontré que les macrophages M1 étaient plus radioresistants que les autres phénotypes à des doses moyennes d'irradiation par protons. Cette radiorésistance est probablement due à une cinétique différente des systèmes de détection et de réparation des dommages à l'ADN. Elle ne peut néanmoins pas être expliquée par une différence de la compaction de la chromatine dans les macrophages M1 avant l'irradiation. Par contre, les macrophages M1 sont capables de mieux gérer une exposition aux espèces réactives de l'oxygène (ROS), comparés aux macrophages M0 et aux macrophages M2. Une gestion des ROS plus efficace pourrait grandement contribuer à la radiorésistance des macrophages M1 à l'irradiation par protons. De plus, cette étude a également permis de décrypter, tout du moins en partie, comment l'utilisation de doses modérées (5 et 10 Gy) d'irradiation par protons, mais pas les rayons X, reprogramme des macrophages M0 et M2. En effet, en activant l'hétérodimère NFκB p50 – p65, l'irradiation par protons permet aux macrophages M0 d'acquérir un phénotype M1, et pousse les macrophages M2 à adopter un phénotype que l'on pourrait situer à l'intermédiaire des phénotypes M1 et M2. Ces résultats ont été confirmés par la combinaison d'un inhibiteur de la kinase IKK (Bay-117082) à l'irradiation par protons. En effet, lorsque la

translocation nucléaire de NFκB est entravée, l'irradiation par protons ne peut plus promouvoir la reprogrammation des macrophages. Étant donné que les dommages à l'ADN et le stress oxydatif sont intimement liés à l'activation de NFκB, une activation plus importante de NFκB pourrait expliquer que l'irradiation par protons soit plus efficace que les rayons X pour induire une reprogrammation des macrophages. Enfin, nous avons également développé et validé un système de co-culture pour les macrophages M2 et la lignée de cellules cancéreuses A549. Les premiers résultats ont montré que la repolarisation des macrophages M2, induite par l'irradiation par protons, n'est pas influencée par la présence de cellules cancéreuses. Par ailleurs, en exposant les macrophages M2 à une dose de 10 Gy (protons), nous avons également relevé qu'une voie sensible à la présence d'ADN cytoplasmique (cGAS/STING) était activée dans les macrophages co-cultivés avec les cellules cancéreuses. Il s'agit d'une voie de signalisation essentielle pour générer une réponse immunitaire anti-tumorale, initiée par les TAMs.

Pour conclure, les résultats obtenus au cours de ce travail ont permis d'étudier les effets de l'irradiation par protons sur les macrophages. Nous avons mis en évidence l'efficacité de la protonthérapie pour reprogrammer les macrophages M2 en un phénotype proche de celui des macrophages M1. Par ailleurs, nous avons montré, dans des co-cultures, que les cellules cancéreuses ne semblent pas influencer cette reprogrammation dans les conditions expérimentales utilisées. Dès lors, une meilleure compréhension de l'ensemble des mécanismes moléculaires par lesquels l'irradiation par protons permet la reprogrammation des macrophages ainsi que la validation de ces résultats par des études *in vivo*, permettraient de mettre en lumière le potentiel de la protonthérapie pour reprogrammer les macrophages au sein des tumeurs.

In addition to be the most abundant constituents of the tumor microenvironment, tumor-associated macrophages (TAMs) influence key processes in tumor progression, including angiogenesis, immunosuppression, invasion and metastasis. For a long time, TAMs have been associated to a M2-like phenotype, characterized by anti-inflammatory properties and pro-tumoral functions. This alternative activation state of macrophages contrasts with the classical activation state, also referred to as the M1 phenotype. M1-like macrophages are associated to pro-inflammatory, phagocytic and anti-tumoral roles. Interestingly, microenvironmental changes in tumor may easily switch the phenotype from M2 to M1, or inversely. Therefore, re-educating TAMs with treatment modalities represents a promising therapeutic strategy to elicit tumor regression. Several chemotherapies and immunotherapies have successfully triggered a reprogramming of TAMs and a concomitant tumor regression. However, these therapies are not localized and could thus trigger a systemic inflammatory response. For this reason, local radiotherapy represents an attractive alternative. Until now, X-rays and γ-rays have not succeeded to reprogram TAMs. As radiotherapy is a continuously evolving field, new types of advanced radiotherapy have emerged, such as protontherapy. By presenting several physical advantages over conventional radiotherapy, protontherapy is a powerful therapeutic tool used to precisely target the tumor. Interestingly, proton beam therapy has demonstrated different radiobiological effects on tumors. Therefore, understanding the effect of proton irradiation on macrophages, and more specifically on their reprogramming, could allow to re-evaluate the use rate of protontherapy for cancer treatment.

In this work, the effects of proton irradiation were investigated on M0 (unpolarized), M1 and M2 macrophages, as well as on co-cultures of M2 macrophages and cancer cells. We demonstrated that M1 macrophages are the most radioresistant phenotype to moderate doses of proton irradiation. This radioresistance is probably due to a different kinetic of DNA damage detection and repair. Interestingly, the evaluation of heterochromatin level before irradiation cannot explain the radioresistance of M1 macrophages. However, this phenotype better faces reactive oxygen species (ROS) exposure compared to M0 and M2 macrophages. A better ROS management could thereby contribute to the radioresistance of M1 macrophages. The present study also determined, at least in part, how moderate doses (5 and 10 Gy) of proton irradiation, but not X-ray radiation, triggered macrophage reprogramming in M0 and M2-like macrophages. By targeting NFκB p65, proton irradiation educated M0 macrophages to adopt a M1-like phenotype and reprogrammed M2 macrophages to acquire a mixed M1/M2 phenotype. These results were confirmed by the use of an IKK inhibitor (Bay-117082) in combination with proton irradiation. When nuclear translocation of NFκB was prevented, proton irradiation failed to induce macrophage reprogramming. As DNA damage and oxidative stress are intimately correlated to NFκB p50 – p65 activation, we suggested that proton irradiation induces a stronger NFκB activation compared to X-rays, thereby explaining the effective macrophage reprogramming. Finally, we set-up experiments for co-culture between M2 macrophages and A549 cancer cells. Our preliminary results revealed that proton-induced macrophage reprogramming is not influenced by the presence of cancer cells. Exposure to 10 Gy of protons also triggered cytosolic DNA-sensing pathway (cGAS/STING) in M2 macrophages co-cultured

with cancer cells. In other reports, this signaling pathway was shown to be essential for triggering immune antitumor responses, initiated by TAMs.

In conclusion, the results obtained during this work allowed to study the effects of proton irradiation on macrophages. We evidenced the efficacy of proton irradiation to reprogram M2 macrophages into a phenotype close to the M1 one. In addition, we demonstrated, in co-cultures, that cancer cells do not seem to influence this reprogramming in our experimental settings. For the future, the identification of the molecular mechanisms by which proton irradiation induces macrophage reprogramming as well as the validation of our results by *in vivo* experiments, should underpin the huge potential of protontherapy for targeting TAMs in tumors.

Abbreviation List

ABCA1: ATP-binding cassette transporter 1
ALTAIS: accélérateur linéaire tandétron pour l'analyse et l'implantation des Solides
AMPK: AMP-activated protein kinase
ANG-2: angiopoietin-2
ANK: ankirin repeat domain
AP-1: activator protein 1
APC: antigen-presenting cell
Arg1: arginase 1
ATM: ataxia telangiectasia mutated
ATP: adenosine triphosphate
ATR: ataxia telangiectasia and Rad3 related
B-TIL: B tumor-infiltration lymphocytes
BAFF-R: B cell activation factor receptor
BAK: Bcl-2 homologous antagonist killer
BAX: Bcl-2-associated X protein
Bcl-2: B-cell lymphoma protein 2
Bmpr2: bone morphogenetic protein receptor 2
BPM: beam profile monitor
BRCA2: breast cancer 2
Breg: B regulatory cell
BTK: Burton tyrosine kinase
c/EBPβ: CCAAT/enhancer-binding protein β
CAFs: cancer-associated fibroblasts
CAM: cell adhesion molecules
CC: coiled coil domain
CCL: chemokine (C-C motif) ligand
CCR: chemokine (C-C motif) receptor
CD: cluster of differentiation
CDD: charge-coupled device
CDNs: cyclic dinucleotides
cGAMP: cyclic GMP-AMP
cGAS: cyclic GMP-AMP synthase
Chk1/2: checkpoint kinase 1 or 2
CL: clodrolip
COX2: cyclooxygenase 2
CpG-ODN: unmethylated cytosine-guanine (CpG) oligodeoxynucleotides
CSF-1: colony-stimulating factor 1
CSF-1R: colony-stimulating factor 1 receptor
CTL: cytotoxic lymphocyte
CTLA4: cytotoxic T lymphocyte protein 4
CXCL: chemokine (C-X-C motif) ligand
CXCR: chemokine (C-X-C motif) receptor
DAG: diacylglycerol
DAMPs: damage-associated molecular patterns
DCs: dendritic cells
DDR: DNA damage response
DMXXA: 5,6 dimethylxanthenone-4 acetic acid
DNA: deoxyribonucleic acid
DNA-PKcs: DNA-dependent protein kinase, catalytic subunit
DNAM-1: DNAX accessory molecule 1
DSB: double-strand break
EBAO: ethidium bromide – acridine orange
ECM: extracellular matrix
EGF: epidermal growth factor
EMT: epithelial mesenchymal transition
EndMT: endothelial mesenchymal transition
ER: endoplasmic reticulum
ERK: extracellular signal-regulated kinase
FAS: fatty acid synthesis
FAO: fatty acid oxidation
FcRγ: Fc receptor γ
FDA: food and drug administration
FGF: fibroblast growth factor
FIH1: factor inhibiting HIF1
FITC: fluoresceine isothiocyanate
FRβ: folate receptor β
Fra1: fos-related antigen 1
FSP-1: fibroblast secreted protein-1
GATA3: GATA-binding protein 3

GM-CSF: granulocyte-macrophage colony-stimulating factor
HDAC11: histone deacetylase 11
HDI: high doses of irradiation
HIF: hypoxia-inducible factor
HLA: human leukocyte antigen
HLA-DR: human leukocyte antigen-cell surface receptor
HLH: helix-loop-helix domain
HMGB1: alarmin high motility group box 1
HO-1: heme oxygenase 1
hPBMC: human peripheral blood monocyte-derived cells
HR: homologous recombination
HRE: hypoxia response element
HRG: histidine-rich glycoprotein
hSSB1: human single-strand DNA binding protein 1
IAP: inhibitor of apoptosis
ICD: immunogenic cell death
IDO: indoleamine-2,3-dioxygenase
IFI16: interferon gamma inducible factor 16
IFN: interferon
IFNAR: type I interferon receptor
IFP: intratumoral fluid pressure
Ig: immunoglobulin
IGF: insulin-like growth factor
IκB: inhibitory kinase of NFκB
IKKs: IκB kinases
IL: interleukin
IL-1R: interleukin 1 receptor
IMRT: intensity-modulated radiation therapy
iNOS: inducible nitric oxide synthase
IR: ionizing radiation
IRAK: interleukin-1 receptor-associated kinase
IRF: interferon regulatory factor
JAK1: janus kinase 1
JNK: c-Jun N-terminal kinase
KLF: Kruppel-like factor
LDI: low doses of irradiation
LEC: lymphatic endothelial cells
LET: linear energy transfer
LLC: Lewis lung carcinoma
LncRNA: long non-coding RNA
LPS: lipopolysaccharide
LTβR: lymphotoxin β-receptor
LZ: leucin zipper-like motif
M-CSF: monocyte colony-stimulating factor
mAb: monoclonal antibody
Mal: MyD88-adaptor-like
MAMs: metastasis-associated macrophages
MAPK: mitogen-activated protein kinase
MARCO: pattern recognition scavenger receptor
MCL-1: induced myeloid leukemia cell differentiation protein
MCP-1: monocyte chemoattractant protein 1
MDI: moderate doses of irradiation
MDSCs: myeloid-derived suppressor cells
MHC: major histocompatibility complex
miRNA: micro RNA
MMP: metalloproteinase
MnSOD: manganese superoxide dismutase
MPK1: mitogen-activated protein kinase 1
MRC1: mannose receptor-C1
MRN: Mre11 – Rad50 – Nbs1
mTORC: mechanistic target of rapamycin complex
MyD88: myeloid differentiation primary response 88
NAC: N-acetyl cysteine
NADPH: nicotinamide adenine dinucleotide
NBD: NEMO-binding domain
NEMO: NFκB essential modulator (IKKγ)
NFκB: nuclear factor kappa B
NHEJ: non-homologous end joining
NIK: NFκB-inducing kinase
NK: natural killer
NKG2: NK cell receptor G2

NKT: natural killer lymphocytes
NLRs: NOD-like receptors
NO: nitric oxide
NOD: nucleotide binding and oligomerization domain
NOX: NADPH oxidase
NRE: NFκB response elements
Nrf2: nuclear erythroid derived 2-related factor
NSCLC: non-small cell lung cancer
OAR: organ at risk
OER: oxygen enhancement ratio
OXPHOS: oxidative phosphorylation
PAK1: p21 protein-activated kinase 1
PAMPs: pathogen-associated molecular patterns
PARP: poly(ADP - ribose) polymerase
PBMC: peripheral blood mononuclear cell
PD-1: programmed cell death 1
PD-L1: programmed cell death ligand 1
PDA: pancreatic ductal adenocarcinoma
PDCD4: programmed cell death protein 4
PEC: peritoneal exudate cells
PET: positron emission tomography
PGE_2: prostaglandin E_2
PHD: prolyl hydroxylase
PI3Kγ: phosphoinositide kinase 3 γ
PIASy: SUMO E3 ligase protein inhibitor of activated STATy
PIDD: p53-induced protein with a death domain
PIGF: placental growth factor
PIPS: Passivated Implanted Planar Silicon
PKC: protein kinase C
PKNOX1: PBX/knotted 1 homeobox
PMA: phorbol-12-myristate-13-acetate
PMN : polymorphonuclear cell
PPARγ: peroxisome proliferator-activated receptor γ
PPP: pentose phosphate pathway
PPRs: pattern recognition receptors
PTEN: phosphatidylinositol-3,4,5-triphosphate 3-phosphatase
RANK: receptor activator for nuclear kappa B
RANTES: regulated on activation, T cell expressed and secreted
RBBP8: retinoblastoma binding protein 8
RBE: radiobiological effectiveness
REDD1: regulated in development and DNA damage response 1
RELMα: resistin-like molecule α
RIP1: receptor interacting protein 1
rhIFNγ: recombinant human IFNγ
RNA: ribonucleic acid
RNS: reactive nitrogen species
RNI: reactive nitrogen intermediate
Rock2: Rho-associated protein kinase 2
ROS: reactive oxygen species
RR-CDG: cyclic diguanine
RT: radiotherapy
RT-qPCR: reverse transcription quantitative polymerase chain reaction
SCLC: small-cell lung cancer
SDF-1: stromal cell-derived factor 1
SHIP1: SH-2 containing inositol 5' polyphosphatase 1
STAT: signal transducer and activator of transcription
STING: stimulator of interferon gene
SOBP: spread-out Bragg peak
SOCS: suppressor of cytokine protein
SSB: single-strand break
SUMO: small ubiquitin-like modifier
TA: transactivation domain
TAMs: tumor-associated macrophages
TBK1: TANK-binding kinase 1
TCA: tricarboxylic cycle
TCR: T cell receptor
TGFβ: transforming growth factor
$T_H1/2$: T helper 1 or 2

Tie2: angiopoietin receptor 2
TILs: tumor-infiltrating lymphocytes
TIRAP: TIR domain-containing adaptor
TLRs: Toll-like receptors
TLS: tertiary lymphoid structure
TME: tumor microenvironment
TMEM: tumor microenvironment of metastasis
TNFα: tumor necrosis factor α
TNFR: tumor necrosis factor receptor
TP: thymidine phosphorylate
TRAF6: TNFR-associated factor 6
TRAIL-R2: TNFα-related apoptosis-inducing ligand receptor
Treg: T regulatory lymphocyte
TREX1: three prime repair exonuclease 1
TRIF: TIR domain-containing adaptor inducing IFNβ
VCAN: versican, extracellular matrix proteoglycan
VEGF: vascular endothelial growth factor
VEGFR: vascular endothelial growth factor receptor
VMAT: volumetric modulated arc therapy
WBI: whole body irradiation
WT: wild-type
XRCC4: X-ray repair cross-complementing protein 4
ZA: zoledronic acid
ZF: zing-finger domain

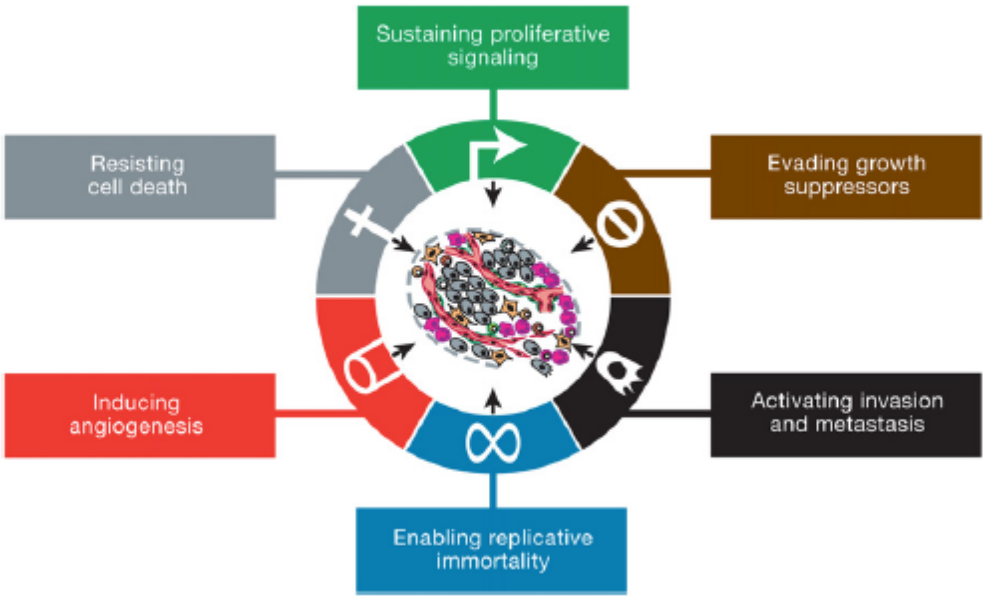

Figure I.1 - Hallmarks of cancer
Hanahan and Weinberg suggested in 2000 that the tumor growth is based on six acquired capabilities: self-sufficiency in growth signals, insensitivity to anti-growth signals, tissue invasion and metastasis, limitless replicative potential, sustained angiogenesis and evading apoptosis *(Hanahan and Weinberg 2000).*

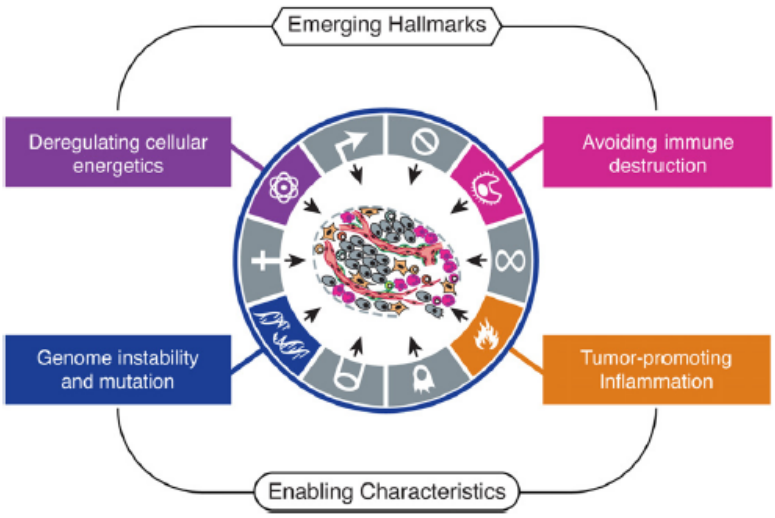

Figure I.2 – Enabling characteristics and emerging hallmarks
In 2011, Hanahan and Weinberg described two enabling characteristics (genome instability and mutation, and tumor-promoting inflammation) that influence tumor development. They also proposed emerging hallmarks (deregulating cellular energetics and avoiding immune destruction) that explained extrinsic influence on cancer cells and on tumor fate *(Hanahan and Weinberg 2011).*

Cancer is an insidious disease that was already noticed in 1600 BC in an Egyptian papyrus. Nowadays, cancer remains one of the two leading worldwide causes of death despite the better understanding of its mechanism and the improvement of diagnosis and treatments.

The development of a tumor occurs through genetic alterations that transform one normal cell into a cancer cell. These mutations conferred advantages to neoplastic cells within a given environment *(Junttila and de Sauvage, 2013; McGranahan and Swanton, 2017a)*. Based on the intrinsic changes observed in neoplastic cells, Hanahan and Weinberg described six hallmarks of tumors: a self-sufficiency in growth signals, insensitivity to anti-growth signals, tissue invasion and metastasis, limitless replicative potential, sustained angiogenesis and evading apoptosis (***Figure I.1***) *(Hanahan and Weinberg, 2000, 2011)*. Tumors had long been described as a multistep process where only genetic alterations drove the progressive transformation of normal cells into highly malignant cells *(Foulds, 1954; Nowell, 1976)*. However, these cell masses were depicted more recently as complex heterogenic tissues *(Hanahan and Weinberg, 2000)*. Indeed, transformed cells recruit numerous host cells at the tumor site to educate and take advantage of them. Tumors are thus populated by multiple normal resident and recruited accessory cells, which create an extracellular matrix and a microenvironment that support tumor growth. In addition to stromal and vascular cells, immune cells significantly influence the fate of tumors. Therefore, Hanahan and Weinberg proposed two additional emerging hallmarks that depend on extrinsic factors: the deregulation of cellular energy and the evasion to the immune destruction *(Hanahan and Weinberg, 2011)* (***Figure I.2***).

Immuno-oncology is a quite recent area of research and medicine that focuses both on the understanding of the immune system responsibilities in tumorigenesis, and on therapies that improve the intrinsic potential of cancer patients in developing an immune response against cancer. The immune surveillance represents a significant barrier to tumor formation and progression. However, cancer cells are able to educate the immune system by modifying the microenvironment and then evade from the immune surveillance *(Hanahan and Weinberg, 2011)*. The collaboration of the immune system with malignant cells then allows the creation of an immunosuppressive microenvironment that significantly contributes to tumor growth *(Kim et al., 2007; Teng et al., 2008).* By maintaining bidirectional relationships with cancer cells and other recruited cells, tumor-associated macrophages (TAMs) actively participate to the immunosuppressive microenvironment. However, changes in the tumor microenvironment (e.g. immunostimulatory microenvironment, acute inflammation) or other stimulations (e.g. therapies, bacteria, pro-inflammatory cytokines) may affect the activation state of TAMs, or in other words their polarization and drive the acquisition of an antitumor phenotype. TAMs were therefore the subject of numerous studies aiming at targeting these cells in order to reverse the fate of tumors. A lot of successful therapies targeting TAMs have thus been developed and include chemotherapies, immunotherapies and radiotherapy *(See Chapter 3).*

Conventional radiotherapy (X-rays, γ-rays), as one of the most often used treatment for cancer, has been demonstrated to exert conflicted effects on the immune system. On one side, radiotherapy is able to induce the activation of the immune system in tumors and on the other

side, it may consolidate the immunosuppressive microenvironment. Although presenting the advantage to be a local treatment, RT is associated with numerous adverse effects (e.g. fibrosis, nausea, vascular damage) due to the irradiation of healthy tissue surrounding the tumor. In order to improve radiotherapeutic treatments, the delivered dose must be maximized at the tumor site, while being minor at the surrounding healthy tissues. Thanks to physical properties, charged particle therapy has the advantage to better spare healthy tissues while exhibiting a greater efficacy on cancer cells. Charged particle therapy mainly uses beams of protons, carbon ions or helium nuclei (alpha particles). Nowadays, protontherapy remains the most used charged particle therapy and is already frequently exploited for the treatment of cancers near organ at risk (e.g. brain, spinal cord and optic nerve) and for pediatric cancers *(Joiner and Kogel, 2009)*. However, the biological effects of protontherapy on the immune system are poorly characterized.

In this context, the present work aims to unravel the effect of proton irradiation on macrophages, and more precisely on their reprogramming towards a pro-inflammatory phenotype, associated with antitumor functions. As TAMs are at the heart of this thesis, their roles in tumors will be addressed in the first part of the introduction. The understanding of signaling pathways involved in macrophage polarization will be the subject of the second chapter. A third chapter will report the effects of therapies, and more specifically of radiotherapy, on macrophage polarization. Finally, a brief comparison of conventional radiotherapy and charged particle therapy will be performed in the fourth chapter.

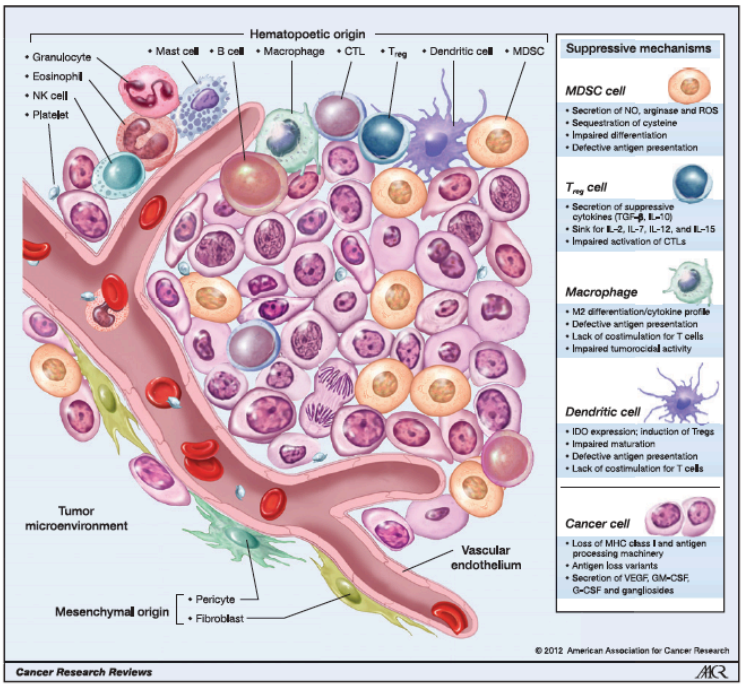

Figure I.3 - Tumor microenvironment
A tumor is composed of malignant cells and a multitude of host infiltrating and recruited cells. These cells include *stromal cells* (cancer-associated fibroblasts (CAFs), endothelial cells and pericytes), *innate immune cells* (tumor-associated macrophages (TAMs), dendritic cells (DCs), natural killer cells (NK cells), myeloid-derived suppressor cells (MDSCs), granulocytes) and *adaptive immune cells* (B and T lymphocytes, and NK T cells) *(Kerkar and Restifo 2012).*

BOX 1: Innate and adaptive immune system

The **innate immunity** (also called natural or native immunity) provides the early line of defense against microbes or injured cells. This mechanism rapidly reacts after infections or trauma. The innate immunity comprises chemical and physical barriers (e.g. epithelium, antimicrobial products), phagocytic cells (neutrophils and macrophages), dendritic cells, natural killers and blood proteins (e.g. complement system). Macrophages and dendritic cells are both antigen-presenting cells (APCs) that can trigger the activation of T lymphocytes. A key characteristic of the innate immune system is the lack of specificity.
The **adaptive immunity** (also called specific or acquired immunity) distinguishes different microbial and nonmicrobial substances and may adapt the response for each case. This response appears later than the innate defense, but is more specific. Adaptive immunity also responds more vigorously to repeated exposure to the same substance, known as memory. The adaptive immune system comprises B lymphocytes and T lymphocytes *(Abbas 2015).*

Chapter 1: Crosstalk between tumor-associated macrophages (TAMs) and the tumor microenvironment

1.1. Immunity in cancer: a double-edged sword

More than 30 years ago, tumors have been defined as "wounds that do not heal" in reference to the close resemblance between these lesions and the granulation tissue of healing skin wound. Indeed, tumors are lesions with chronic unresolved inflammation where cell proliferation, survival and migration are managed by multiple factors and cell types *(Arwert et al., 2012; Dvorak, 1986)*. In addition to malignant cells, all solid tumors contain different lineage subsets, including stromal cells (cancer-associated fibroblasts (CAFs), endothelial cells and pericytes), myeloid-lineage cells (TAMs, dendritic cells (DCs), natural killer (NK) cells, myeloid-derived suppressor cells (MDSCs) and granulocytes) and lymphoid-lineage cells (B and T lymphocytes, and NKT cells) (***Figure I.3***) *(Hanahan and Weinberg, 2011; Tlsty and Coussens, 2006)*. The immune system (BOX 1), comprising the two last lineage cells, plays conflicting roles in tumorigenesis. On the one hand, the immune system contributes to cell transformation through chronic inflammation and promotes tumor growth by releasing pro-tumoral mediators (e.g. IL-10, TGFβ) or by shaping the immunogenicity of cancer cells. In other words, the immune system applies a high selective pressure on cancer cells that have the ability to initiate an immune response (so-called the immunogenicity) and only poor immunogenic malignant cells survive. On the other side, the immune system also prevents tumor growth by immune surveillance by recognizing cancer cells and eliminating them. This recognition is mainly performed by the crosstalk between antigen-presenting cells (APCs) and T lymphocytes. Moreover, the innate immune cells, such as macrophages, can also recognize cancer cells and kill them *(Noy and Pollard, 2014; Schreiber et al., 2011).*

In the following sections, the dual function of the immune system in cancer progression will be detailed mainly by describing the role of chronic inflammation in cancer initiation and the immunoediting concept. The emphasis will also be put on the TAMs and their opposite roles in controlling the tumor fate: regression or promotion.

1.1.1. Cancer-related inflammation

Rudolf Virchow was the first to propose a connection between inflammation and tumorigenesis in 1863. He noticed that tumors often develop at sites of chronic inflammation and that these tumors contain a high proportion of inflammatory cells *(Balkwill and Mantovani, 2001)*. Over the past decades, a lot of efforts were made to understand the link between inflammation and cancer *(Mantovani et al., 2008a)* and it appears that two pathways co-exist to make this connection. The *intrinsic pathway* relies on the induction of neoplasia by genetic events and thereby on the generation of an inflammatory microenvironment. In the *extrinsic pathway*,

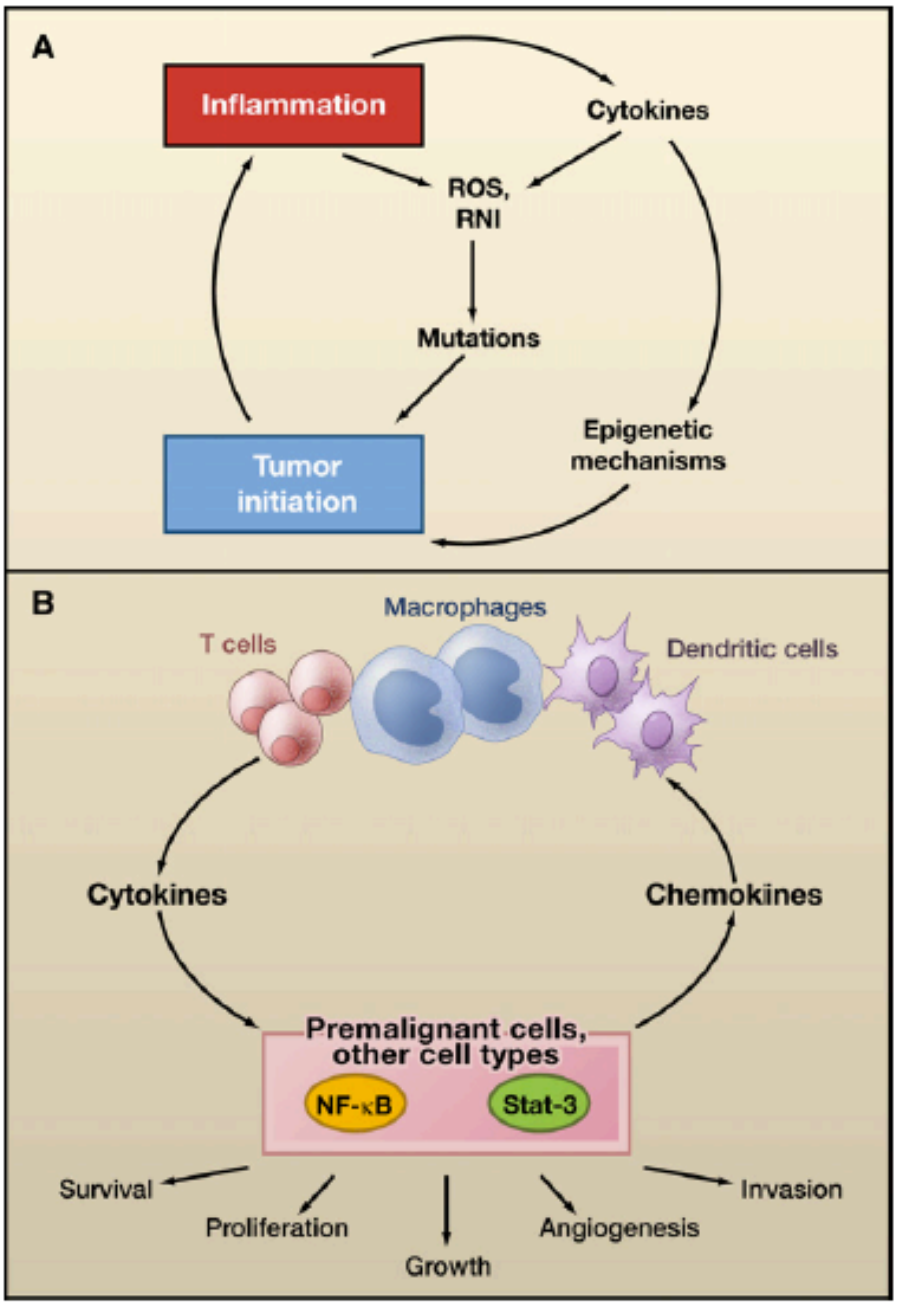

Figure I.4 - Chronic inflammation and tumor initiation and promotion

(**A**) *Chronic inflammation induces tumor initiation*. Inflammatory cells promote malignant transformation of normal cells through the production of reactive compounds such as reactive oxygen species (ROS) and reactive nitrogen intermediates (RNI). Mutations and epigenetic changes are the results of cytokines released by the inflammatory cells. Once initiated, the tumor contributes to the inflammatory environment.

(**B**) *Chronic inflammation promotes tumor growth*. Malignant cells release chemokines that recruit inflammatory cells (including mainly TAMs and T cells) into the tumor. Inflammatory cells produce cytokines that activate key transcription factors, such as STAT3 and NFκB in malignant cells. These transcription factors control protumoral properties in cancer cells, including survival, proliferation, growth, angiogenesis and invasion *(Grivennikov, Greten et al. 2010).*

inflammation makes susceptible to cancer initiation. These two pathways converge and result in the activation of transcription factors in malignant cells that consolidate the inflammatory environment, promoting tumor growth *(Mantovani et al., 2008a).*

Intrinsic pathway - The cancer initiation may be induced by several factors, such as carcinogens, radiation, inherited genetic mutations or viral infections *(Schreiber et al., 2011)*. During malignant transformation, the activation of some oncogenes in cancer cells initiates the establishment of an inflammatory microenvironment. Indeed, the release of chemokines favors the recruitment of several inflammatory effectors, mainly including TAMs and T cells. In order to re-establish the homeostasis, recruited inflammatory cells secrete cytokines and prostaglandins that activate transcription factors (such as nuclear factor kappa B (NFκB), hypoxia-inducible factor 1 (HIF1), activator protein 1 (AP-1) and signal transducers and activation of transcription 3 (STAT3)) in cancer cells. These mediators and then the activation of transcription factors often promote tumor growth. Therefore, the cytokine and chemokine expression patterns control the immune and inflammatory milieu as well as the tumor growth *(Grivennikov et al., 2010; Mantovani et al., 2008a).*

Extrinsic pathway – It is now well demonstrated that chronic inflammation also augments the risk of developing cancer. For example, chronic infections (e.g. *Helicobacter pylori,* hepatitis C virus or schistosomes), autoimmune diseases (inflammatory bowel disease), tobacco smoking, obesity or idiopathic inflammation all predispose to malignant transformation whereas, the use of anti-inflammatory agents prevents tumorigenesis in many cases. It is important to note that while low-grade chronic inflammation may induce carcinogenesis, acute inflammation has been mostly associated to tumor regression. This difference probably relies on different effectors involved in acute and chronic inflammation. How inflammatory cells contribute to tumorigenesis (***Figure I.4 A***)? Recruited inflammatory cells (mainly TAMs and neutrophils) release mutagenic mediators such as reactive oxygen species (ROS) and other mediators like cytokines (e.g. tumor-necrosis factor α (TNFα), interleukin 6 (IL-6) and IL-1β), metalloproteinases (MMPs) and prostaglandin E_2 (PGE_2) (***Figure I.4 B***). This inflammatory microenvironment directly leads to DNA damage or affect DNA repair system and cell cycle checkpoints. In more details, reactive compounds, including ROS and reactive nitrogen species (RNS) induce DNA damage and genomic instability, thus accelerating the malignant transformation of normal cells. In the same line, it was also shown that the release of TNFα by inflammatory cells promotes ROS accumulation in malignant cells. The connection between inflammation and cancer initiation is also reflected by the induction of cancer-related epigenetic modifications, such as DNA methylation or silencing of genes by non-coding RNA sequences, mostly elicited by inflammatory mediators (such as IL-1β) secreted by TAMs. Finally, an inflammatory environment supports the malignant transformation by impeding the DNA repair machinery (e.g. mismatch repair system, base insertions or deletions) or by activating survival and proliferation pathways in cancer cells. For instance, inflammatory cells produce cytokines and growth factors that confer stem cell-like properties to malignant cells through the activation of STAT3, as well as promote survival in malignant cells through the activation of NFκB. Altogether, these elements indicate that chronic inflammation plays a major role in cancer initiation by increasing the mutation rate in normal cells *(Colotta et al., 2009; Grivennikov et al., 2010; Qian and Pollard, 2010).*

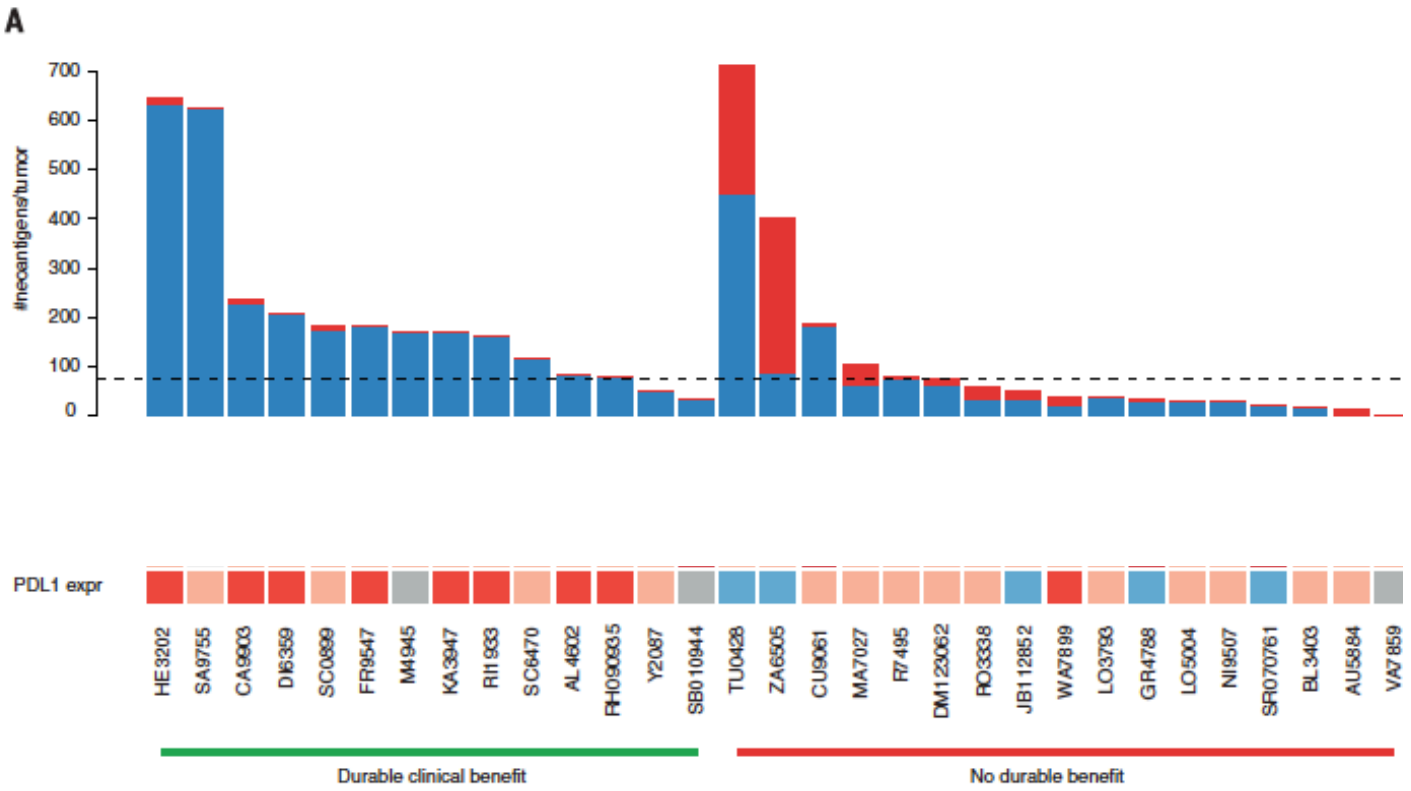

Figure I.5 – Neoantigen burden and clinical benefit of immunotherapy (immune checkpoint blockade)
Proportion of clonal (blue) and subclonal (red) neoantigens per tumor and associated expression of immune checkpoint (PD – L1 ; programmed cell death ligand 1). A high proportion of clonal neoantigens correlates to a high homogeneity upon neoantigen landscape. A homogeneous antigen landscape is associated with a durable clinical benefit for immunotherapy (immune checkpoint blockade) due to a high PD-L1 (immune checkpoint) expression. On the contrary, a high proportion of subclonal neoanigens is associated to a high heterogeneity upon the neoantigen landscape. A heterogeneous antigen landscape is linked to poor durable benefit of immunotherapy *(McGranahan et al., 2016).*

In this inflammatory context, TAMs, as the most representative inflammatory cells in tumors, play a central role in tumor initiation and tumor promotion *(Grivennikov et al., 2010; Mantovani and Sica, 2010)*.

1.2. The role of the immunity in cancer promotion: the cancer immunoediting concept

The tumor fate depends on the immunogenicity of the tumor, or in other words, on the ability of malignant cells to stealth from the activation of the immune system *(Dunn et al., 2004)*. Therefore, more a tumor is immunogenic, more this tumor is susceptible to be eliminated by the immune system. Indeed, cancer cells expose on their surfaces, different molecules (so-called neoantigens) that can be recognized by the immune system. In this context, both innate and adaptive immune systems have been shown to significantly contribute to the tumor eradication. However, while the immune system represents a significant barrier to the tumor formation and progression, cancer cells are able to evade from the immune surveillance and to educate the immune system by modifying the tumor microenvironment *(Hanahan and Weinberg, 2011; Kim et al., 2007; Teng et al., 2008).* A tumor is thus considered as edited when there is an immunoselection of malignant cell clones that display a reduced immunogenicity. These events are the bases of the cancer immunoediting concept. This concept is divided in three phases: elimination, equilibrium and evasion *(Noy and Pollard, 2014; Schreiber et al., 2011)* that will be described here under.

1.2.1. Cancer cell recognition: the neoantigen landscape

There is compelling evidence that cancer cells are recognized by the immune system. Mutations or transcriptional aberrations lead to the formation of new epitopes, so-called neoantigens. These neoanigens are formed by silent or non-silent mutations in diverse proteins or may also be generated by overexpressed normal proteins, subjected to immune system recognition *(McGranahan and Swanton, 2017b; Schreiber et al., 2011)*. However, as the tumor grows, there is a selection of cancer cell clones that lack immunodominant rejection antigens *(Mittal et al., 2014).* This immunoselection, induced by the pressure from the intact immune system, allows poor immunogenic cancer cells to survive in an immunocompetent host *(Shankaran et al., 2001)*. It explains why the transfer of poor immunogenic cancer cells from an immunocompetent host to an immunocompetent or immunodeficient recipient mouse always generated a new tumor, while the injection of high immunogenic cancer cells from an immunodeficient host to an immunocompetent mice induced tumor rejection in half of the cases *(Schreiber et al., 2011).* As a whole, the immune system plays opposite roles: it allows cancer cell recognition for tumor elimination while it applies a selective pressure on cancer cells that drives immunoselection.

In addition, while the immune system drives the immunoselection of cancer cell clones, the neoantigen landscape of tumor is also able to shape the antitumor immunity. The neoantigen landscape or burden is the number of mutational loads per tumor. This comprises clonal and subclonal neoantigens. Clonal mutations are identified in all malignant cells while subclonal mutations are present in only a subset of cancer cells. Indeed, clonal and subclonal neoantigens are distinct mutational processes that operate at different times along the tumor evolution *(McGranahan and Swanton, 2017b).* Therefore, once the tumor is established, the neoantigen

BOX 2: Lymphocytes

Two lymphocyte populations can be distinguished in the adaptive immunity: B lymphocytes and T lymphocytes.

B lymphocytes produce antibodies that recognize antigens for the elimination of extracellular pathogen (or transformed cells).

After their activation by antigen-presenting cells, mature **T lymphocytes** directly interact with infected cells (or transformed cells) to eliminate intracellular pathogens (or cancer cells). T cells can be classified in two major groups, based on their T cell receptors (TCRs): γδ and αβ. αβ T cells are further classified according to their effector functions: helper or cytotoxic. **T helper** (T_H) lymphocytes ($CD4^+$) activate phagocytes, such as macrophages, to kill phagocytized pathogens (or phagocytized transformed cells), or activate B lymphocytes for antibody response. **Cytotoxic T** lymphocytes ($CD8^+$, CTLs) directly destroy infected cells (or cancer cells). **NKT cells**, another αβ T cell subset, express characteristic of both NK and T cells. NKT cells, as well as **γδ T cells,** are rare populations that recognize non-protein antigens, such as lipids, phosphorylated molecules or alkyl amines *(Grivennikov, Greten et al. 2010, Abbas 2015).*

landscape may be homogeneous or heterogeneous through the genomic diversity of subclonal neoantigen populations. These neoantigens activate the immune system. Especially, the presentation of neoantigens to naive T cells allows the activation of these cells and then the tumor infiltration by effector T cells that eliminate malignant cells *(McGranahan et al., 2016).* In a recent study, it has been demonstrated that the infiltration of the tumor microenvironment by effector T cells is higher in patients with a homogeneous neoantigen landscape. Thus, a high number of clonal neoantigens is associated with a longer overall survival of patients. Indeed, patients with low intratumor heterogeneity upon the neoantigen landscape have longer survival than patients carrying high intratumor heterogeneity (***Figure I.5***), and these patients are better responders to immunotherapy, such as immune checkpoint inhibitors *(McGranahan et al., 2016; McGranahan and Swanton, 2017b).* In addition, the neoantigen landscape in different metastases from the same patient may be also completely different. Recently, a case study reported evidences of high neoantigen heterogeneity between metastases in a single patient, leading to divergent immune activation, different tumor microenvironment and diverse tumor genetics within tumors. This means that treatment may differently affect the metastases in one patient by differently interacting with the diverse tumor microenvironment and immune effectors of each metastasis *(Jimenez-Sanchez et al., 2017)*.

1.2.2. Elimination phase

The cancer immunosurveillance process is a well known concept developed long time ago *(Burnet, 1970; Thomas, 1959)***.** The immune system is efficiently able to protect host against the development of primary tumors by eliminating newly transformed cells *(Stutman, 1970).* It was well demonstrated by the higher recurrence of carcinogen-induced and spontaneous cancers in mice lacking adaptive immune system (immunodeficient mice) compared to mice carrying an intact immune system (immunocompetent mice). These experiments revealed the crucial role of the adaptive immune system, and more specifically of T lymphocytes, in tumor suppression. The killing of cancer cells occurs mostly through the secretion of interferon γ (IFNγ) and perforin *(Shankaran et al., 2001)*. In reality, more than being restricted to the adaptive immunity, the detection and the elimination of cancer cells occur through the interplay of the innate and adaptive immune systems (***Figure I.6***). Different kinds of neoantigens may be detected by the innate immune system. For example, dying cancer cells release nucleic acids and damage-associated molecular pattern (DAMPs), sensed by antigen presenting cells (APCs), such as dendritic cells (DCs) and M1-like tumor-associated macrophages (M1-TAMs) *(Woo et al., 2015)*. Activated APCs are then able to prime the activation of naive T cells (BOX 2) in lymph nodes by presenting the antigens. In this context, type I interferon (IFN I, e.g. IFNα or IFNβ) plays a key role in the activation of T cells against tumor-associated antigens. Once activated by APCs, cytotoxic lymphocytes (CTLs or $CD8^+$ T cells) and natural killer cells are both susceptible to recognize neoantigens exposed by cancer cells and thereby to recruit all members of the innate and adaptive immune systems to eliminate malignant cells. Another body of evidence has pointed the role of macrophages in the elimination of cancer cells, notably through phagocytosis *(Mittal et al., 2014; Woo et al., 2015)*. Altogether, it suggests a key role of the innate immune system in the detection of cancer cells and the priming of T cells to elicit their antitumor functions *(Mittal et al., 2014).*

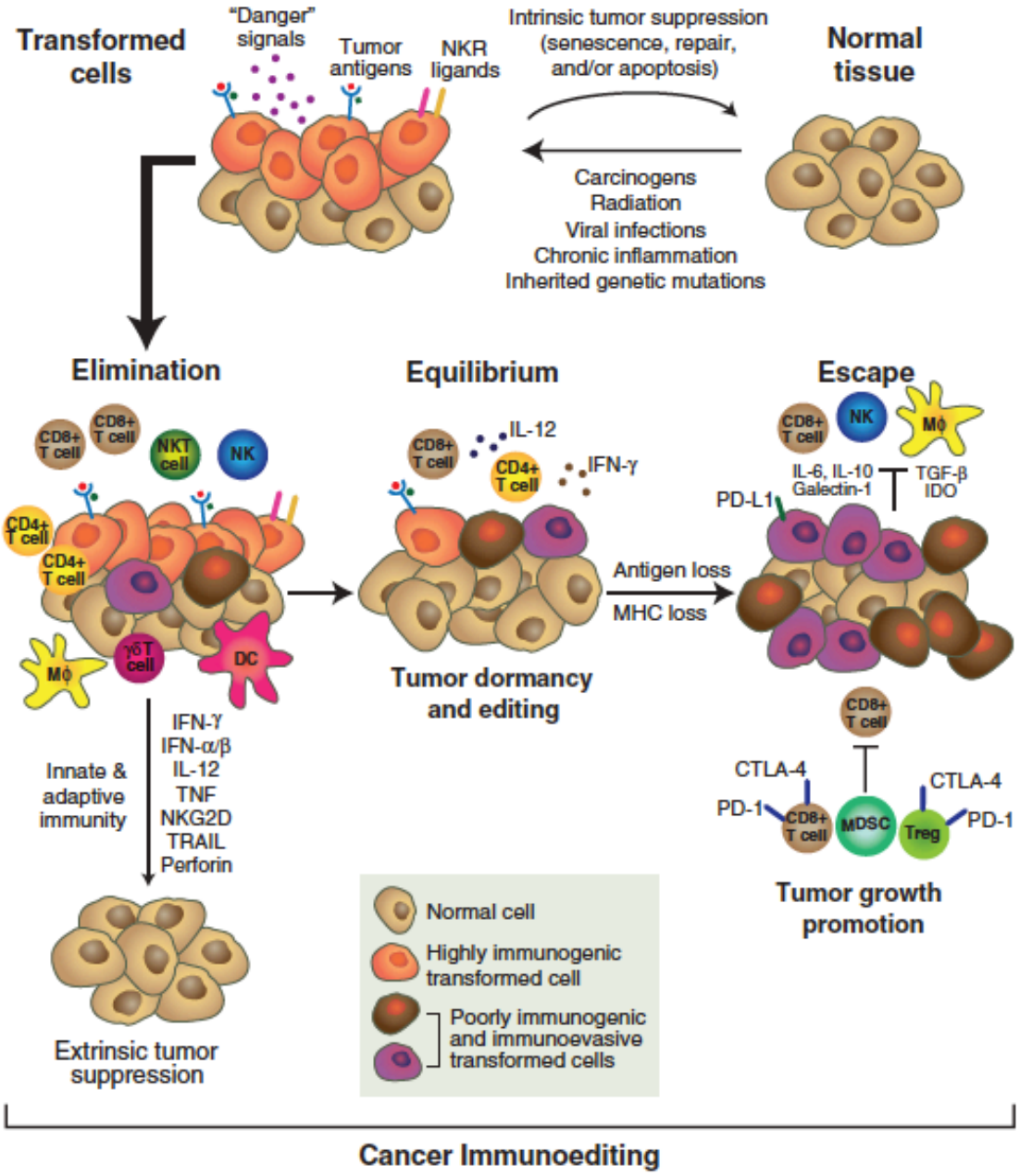

Figure I.6 – Cancer immunoediting

The cancer immunoediting process relies on three phases: elimination, equilibrium and escape. The transformation of normal cells into malignant cells may be caused by several extrinsic (carcinogens, radiation, viral infections, chronic inflammation) and intrinsic (genetic mutations) factors that contribute to tumor development. Transformed cells expose on their surface several antigens that can be recognized by the immune system. During the first phase, innate (NK cells, macrophages, DCs) and adaptive ($CD4^+$ lymphocytes, $CD8^+$ lymphocytes and NKT cells) immune cells eliminate cancer cells (***elimination phase***). In the second phase, a balance between the tumor suppression applied by the adaptive immune system ($CD4^+$ lymphocytes, $CD8^+$ lymphocytes) and the tumor growth keeps the tumor in dormancy (**equilibrium *phase***). Due to a selective pressure from the immune system, only cancer cell clones with reduced immunogenicity survive. In the third phase, the edited clones start to proliferate and educate the immune system to sustain tumor growth. Tumor growth is also promoted by some cells from the innate (macrophages, MDSCs) and adaptive (Treg) immune system while other effector cells (NK cells, CD8+ CTL) are excluded from the tumor (***escape phase***) *(Schreiber, Old et al. 2011).*

1.2.3. Equilibrium phase

If some cancer cells survive to the elimination phase, the immune system, and mostly the adaptive immune system, keeps residual cancer cells in a dormancy state (***Figure I.6***). The tumor dormancy is maintained by an immune-mediated balance: the presence of CTLs, NK cells and γδ T cells (BOX 2) favors tumor elimination while the NKT cells, T regulatory lymphocytes (Treg) and myeloid-derived suppressor cells (MDSCs) promote tumor growth. The evolution of a dormancy state towards the evasion state is driven by a progressive lack of tumor specific antigens and a decreased cross-presentation of tumor antigens. In addition, although in the elimination phase, an immunostimulative microenvironment (e.g. IFNγ, TNFα, IL-12) recruits the immune effectors, in the equilibrium phase, a balance between an immunostimulative (IL-12 and IFNγ) and an immunosuppressive microenvironment (IL-10 and transforming growth factor β (TGFβ)) maintains tumors in dormancy. This phase may be the longest one since cancer cells may reside in patients for decades before eventually generating primary tumors or distant metastases *(Mittal et al., 2014; Schreiber et al., 2011)*.

1.2.4. Evasion phase

In the evasion phase, an immunosuppressive microenvironment predominates and a new interplay between the innate and the adaptive immune system leads to the immunoselection of poorly immunogenic cancer cells, promoting tumor outgrowth (***Figure I.6***). This is made feasible by a reduced immune recognition of tumor-specific antigens, a decreased cross-presentation of tumor antigens, an increased resistance of cancer cells to the immune system and a supporting immune system *(Mittal et al., 2014)*. The reduced immune recognition of neoantigens is linked to the selection of cancer cell clones with low immunogenicity or to changes in the neoantigen landscape. For example, some cancer cells can evade macrophage phagocytosis by expressing high levels of « don't eat me signals » such as cluster of differentiation 47 (CD47), and/or low levels of « eat me signals » such as calreticulin *(O'Sullivan et al., 2012).* Also, an immunosuppressive microenvironment predominates and fuels tumor growth. This immunosuppressive microenvironment comprises mediators like vascular endothelial growth factor (VEGF), TGFβ, IL-10, IL-23. All these mediators are released by different contributors that mainly gather Treg, MDSCs, DCs and M2-like TAMs. In addition, these factors play key role in the immunosuppression and more specifically in T cell anergy. T cell anergy may also be induced by the binding of negative co-stimulatory molecules (e.g. programmed cell death ligand 1 (PD-L1)). Emphazing the role of M2-like macrophages in this process, the secretion of several macrophage-derived factors including polyamines, monocyte colony-stimulating factor (M-CSF), VEGF, IL-10 and TGFβ highly benefits to tumor growth, angiogenesis and metastasis *(Mantovani et al., 2008b; Mittal et al., 2014).*

1.3. Tumor-associated macrophages: friends or foes?

Macrophages are phagocytic cells, playing key roles in the innate immunity *(Gosselin et al., 2014)*. Their monocytic precursors are efficiently recruited into the tumor site by VEGF, colony-stimulating factor 1 (CSF1), chemokine (C-C motif) ligand 2 (CCL2) and chemokine (C – X – C

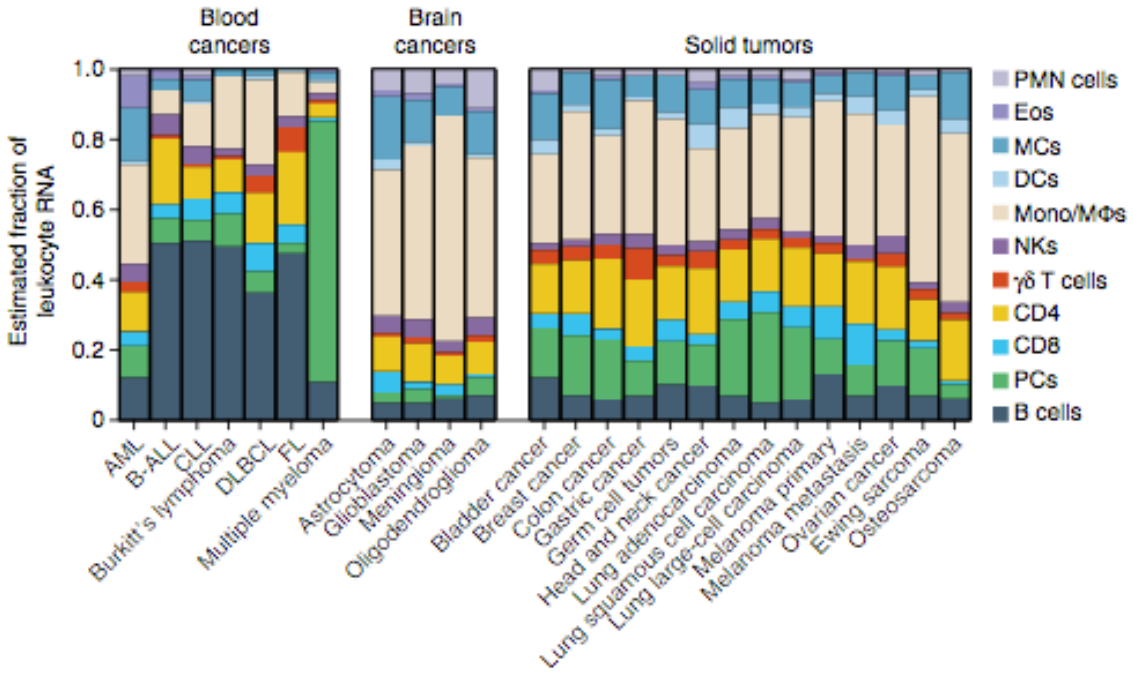

Figure I.7 – Leukocyte proportion in 25 human cancers
Estimated mRNA fraction of different leukocyte subsets in 25 human cancers. PMN, polymorphonuclear cells; Eos, eosinophils; MCs, myeloid –derived suppressor cells; DCs, dendritic cells; Mono/MΦs, monocytes/macrophages; NKs, natural killers; γδ T cells; CD4, $CD4^+$ T lymphocytes; CD8, $CD8^+$ T lymphocytes; PCs, plasmocytes; B cells, B lymphocytes. Estimated macrophage fraction represents up to 50% of the leukocyte population in brain and solid tumors *(Gentles, Newman et al. 2015).*

Figure I.8 – Linear scale of macrophage classification
The classification of tumor-associated macrophages (TAMs) relies on a dual phenotype designation, also observed in steady state: M1 macrophages (or so-called classically activated macrophages) or M2 macrophages (referred to as alternatively activated macrophages). These two phenotypes can be featured as a linear scale where M1 and M2 phenotypes represent the two extremes and between which exists a multitude of intermediate phenotypes *(Mosser and Edwards 2008).*

motif) ligand 12 (CXCL12). Once recruited into the tumors, monocytes differentiate into tumor-associated macrophages (TAMs) *(Lin et al., 2001; Yuan et al., 2016)*. The pro-tumoral functions of TAMs have been highlighted by numerous studies. For example, depletion of macrophages by chlodronate liposome or anti-CSF1 therapy reduces tumor progression *(Klug et al., 2013; Komohara et al., 2014; Zeisberger et al., 2006)*. However, the anti-tumoral functions of TAMs have also been demonstrated at early stages of tumorigenesis *(Mittal et al., 2014)* and by the action of diverse treatments that reprogram TAMs to elicit their anti-tumoral functions (See Chapter 3). As TAM population represents up to 50 % of host infiltrating cells (***Figure I.7***) within the tumor *(Gentles et al., 2015; van Ravenswaay Claasen et al., 1992)*, the fate of the tumor may widely be influenced by their activation state.

Macrophages exhibit a high plasticity leading to their classification in two distinct phenotypes with opposite functions in tumors. The M1 phenotype, also called classical activation state, plays key roles in tumor eradication by displaying pro-inflammatory, phagocytic and anti-tumoral activities, while the M2 phenotype, referred to as an alternative activation state, is involved in tumor growth by holding anti-inflammatory and pro-tumoral functions (***Figure I.8***). This classification follows the one found in cancer-free organisms, as M1 macrophages exhibit pathogen phagocytic abilities while M2 macrophages are requested for infection-free healing circumstances *(Biswas and Mantovani, 2010)*. In most cancer, M1-like TAMs are found in tumor at early stages of the disease (*elimination phase*) whereas M2-like TAMs gradually replenish the macrophage pool as the tumor grows (*evasion phase*). Actually, the transition from a M1 to a M2 phenotype occurs through the switch from an immunostimulative to an immunosuppressive microenvironment *(Mittal et al., 2014; Movahedi et al., 2010)*. The tumor infiltration by TAMs with a M1 phenotype is linked to a positive prognosis for patients while the presence of M2-like macrophages is strongly associated to a worse prognosis in most of cancer types. It has to be noted that the total tumor-infiltrating macrophages (CD68+) are correlated with a good outcome for colorectal or prostate cancer patients while it is mostly associated to a poor prognosis in other cancer types (***Figure I.9***) *(Fridman et al., 2017).*

Macrophages interact with the adaptive immune system: M1 macrophages facilitate the activation of T helper 1 (T_H1) lymphocytes (cfr BOX 2), while M2 macrophages promote T_H2 cell development *(Biswas and Mantovani, 2010)*. M1 macrophages also have the ability to present antigen, prime T cell activation and facilitate the development and the activation of NK cells *(Ansell and Vonderheide, 2013).* These abilities, as well as their cytotoxic functions mediated by ROS, MMPs and TNFα productions, are completely aborted under anti-inflammatory conditions *(Guiducci et al., 2005; Kerkar and Restifo, 2012)*. M2-like TAMs produce low levels of pro-inflammatory cytokines (e.g. IL-1β, TNF-α, IL-12, IL-6) and high levels of anti-inflammatory cytokines (e.g. IL-10) and immunosuppressive factors (e.g. TGFβ, VEGF) *(Sica and Mantovani, 2012)*. However, the classification of TAMs along the binary M1/M2 phenotypes is an oversimplification of the reality, as a multitude of macrophage subsets are usually noticed in tumors. Indeed, TAMs express different pattern of gene expression in function of their localization (e.g. close to blood vessels), the local microenvironment (e.g. hypoxia) and their origins (tissue resident macrophages or blood monocytes), reflecting the high plasticity and the heterogeneity of these myeloid cells. Based on their functions, at least six different subpopulations of TAMs co-exist in tumors. These different macrophage subsets share features of both M1 and M2 populations, which attest of the complexity of macrophage classification

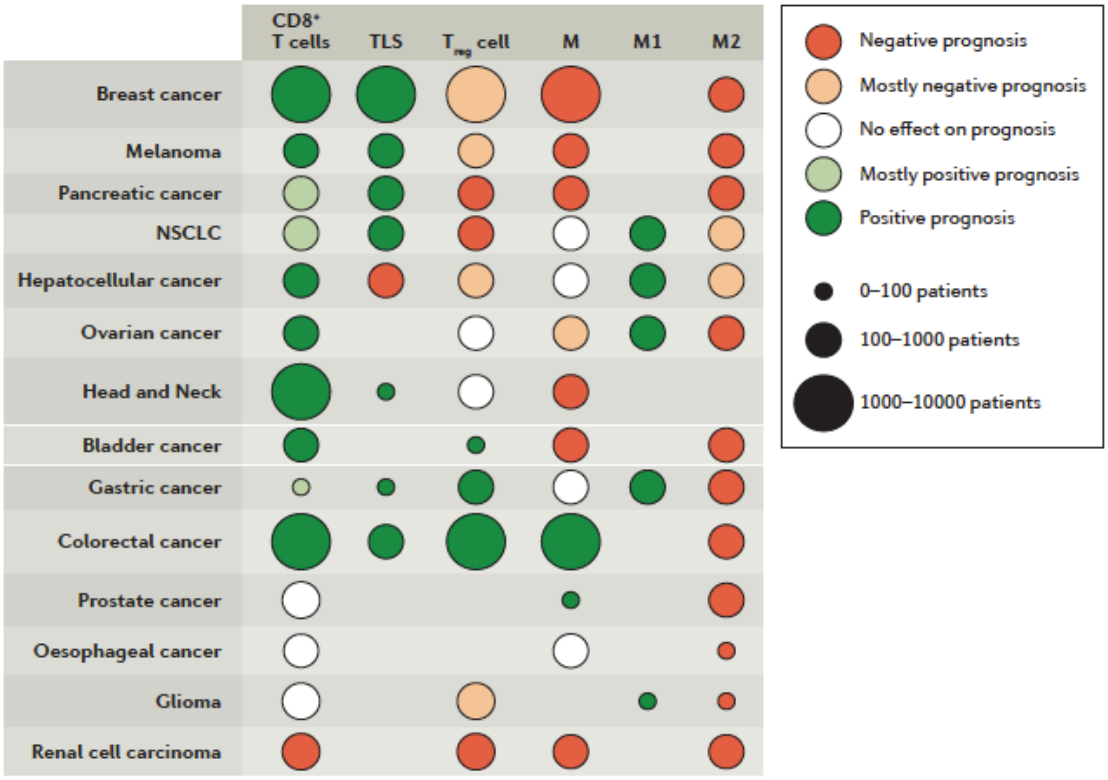

Figure I.9 – Prognosis of patients with cancers based on the immune infiltrate
The presence of $CD8^+$ T lymphocytes, tertiary lymphoid structure (TLS), T regulatory cells, $CD68^+$ macrophages, M1-like macrophages and M2-like macrophages was analyzed in patients with cancers. Data from more than 200 studies were included in this analysis. The size of the circle indicates the number of patients enrolled in the studies. The color indicates the prognosis of patients: red for « negative prognosis », orange for « mostly negative prognosis », white for « no statistically significant correlations », light green for « mostly positive prognosis » and green for « positive prognosis » *(Fridman, Zitvogel et al. 2017).*

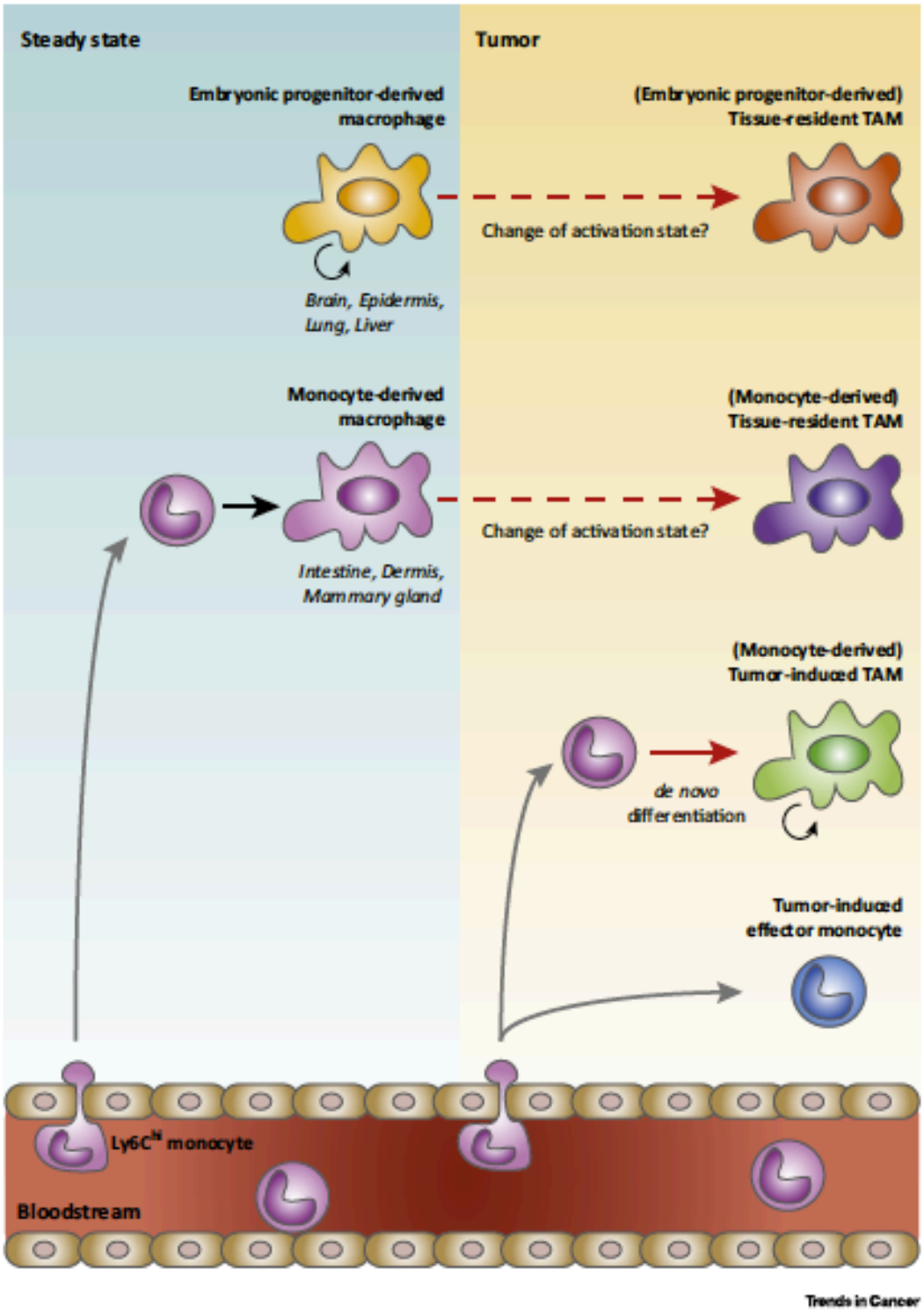

Figure I.10 – Origin of tumor-associated macrophages (TAMs)
During steady state (left panel), tissue-resident macrophages are derived from self-maintaining of embryonic progenitors or from the migration (grey arrow) of circulating blood monocytes into tissues. In tumors (right panel), TAMs derived from the activation (red dashed arrows) of tissue-resident macrophages or from migration (grey arrows) of circulating blood monocytes. These last ones can directly differentiate (red arrow) into TAMs when entered into the tumor *(Franklin and Li 2014).*

(Mittal et al., 2014; Qian and Pollard, 2010). The diverse macrophages subpopulations will be described in the following sections, by covering their origins and their different functions.

2. Ontogeny of tumor-associated macrophages

2.1. Macrophage origin

During embryogenesis, yolk sac erythro-myeloid progenitors invade healthy tissues and give rise to tissue-resident macrophages, whereas in adulthood, tissue-resident macrophages are self-maintained locally or are replaced by circulating monocyte-derived macrophages from hematopoietic origin *(Gomez Perdiguero et al., 2015)*. Therefore, two classes of macrophages co-exist in tissues: resident and infiltrating macrophages. Two exceptions are however noticed: microglia is only generated from the self-maintaining of yolk-sac progenitors *(De Palma, 2016; Hoeffel and Ginhoux, 2015; Zhu et al., 2017)* while intestinal macrophage pool is continuously replenished by adult blood monocytes (***Figure I.10 – left panel***) *(Zhu et al., 2017)*. In addition, recent studies have reported differences between tissue-resident macrophages. The analysis of chromatin landscape in tissue-resident macrophages from different tissues revealed distinct populations. Moreover, as macrophages derive from different origins and are maintained upon distinct local microenvironments in tissues, these cells present diverse functions and co-exist within the same tissue *(Lavin et al., 2014; Zhu et al., 2017).* The different chromatin landscapes between distinct macrophage subsets drive distinct expression patterns *(Gosselin et al., 2014; Lavin et al., 2014)*. Interestingly, fully differentiated macrophages acquire a new chromatin landscape when transferred in a new host tissue, meaning that tissue-resident macrophages may be completely reprogrammed *(Lavin et al., 2014)*. All these features reflect the high plasticity of macrophages in their functions and identities.

2.2. TAM ontogeny

The attraction of TAMs into tumors is carried out by several factors including chemokines (CCL2, CCL5, CCL7, CXCL3 and CXCL12) and chemoattractants (CSF1, VEGFA) *(Biswas and Lewis, 2010; Komohara et al., 2014)*. These factors bind to chemokine (C – C motif) receptors (CCR) or to CSF-1 and VEGF receptor (CSF1R; VEGFR).
It was thought for a long time that in pathological settings such as cancer, the major source of macrophages comes from circulating classical monocytes (or inflammatory monocytes), even in brain tumors *(De Palma, 2016; Hashimoto et al., 2013)*. Accordingly, the study of TAM origin in a mouse mammary tumor model revealed that $CCR2^{+}$ inflammatory monocytes are actively recruited into the tumor by CCL2. Indeed, the tracking of transferred $CCR2^{+}$ monocytes from $CCR2^{GFP}$ reporter mice into congenically $CCR2^{DTR}$ PyMT mice, lacking $CCR2^{+}$ monocytes, showed an infiltration and a differentiation of these monocytes into TAMs in tumors. These observations were confirmed by a distinguishable phenotype of TAMs from their neighbored mammary tissue-resident macrophages *(Franklin et al., 2014)* (***Figure I.10 – right panel***). Similar experiments in mammary tumors and breast metastasis *(Movahedi et al., 2010; Qian et al., 2011)* and other experiments in colorectal cancer (MC38 tumor-bearing mice) also showed that TAMs were bone-marrow-derived *(Gordon et al., 2017).* In addition to circulating blood monocytes, monocytes from the spleen also contribute to a lesser extent to the monocyte-derived TAM

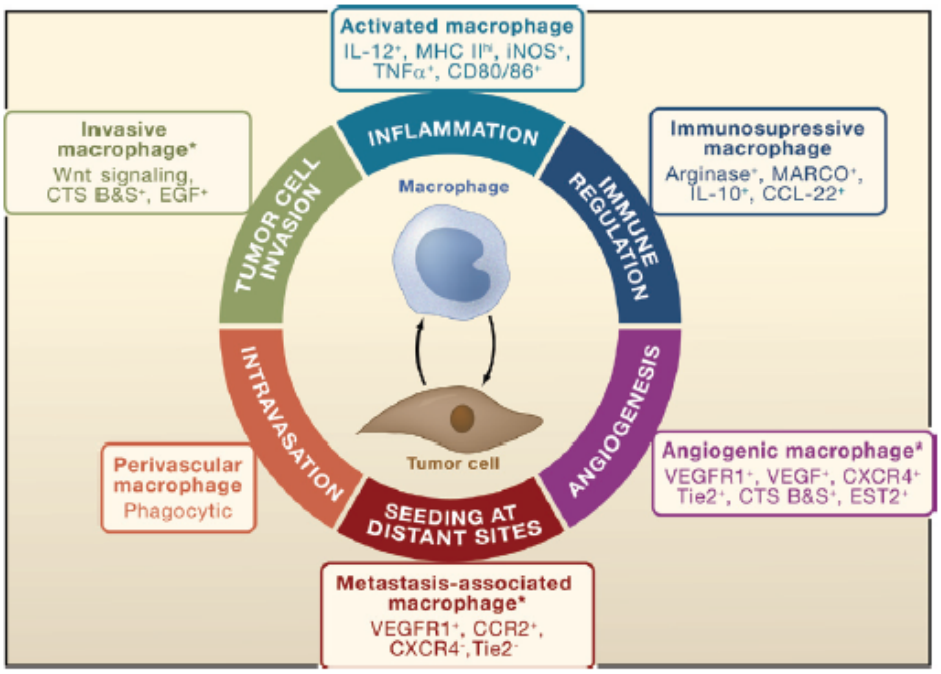

Figure I.11 – Key tumorigenic features associated to macrophages
The diagram represents six macrophage phenotypes present in tumors, related to six distinct functions in tumorigenesis. These subpopulations are all defined by the expression of specific macrophage markers (CD11b, F4/80 and CSF-1R) but are associated to a specific pattern of gene expression induced by different environmental cues *(Qian and Pollard 2010).*

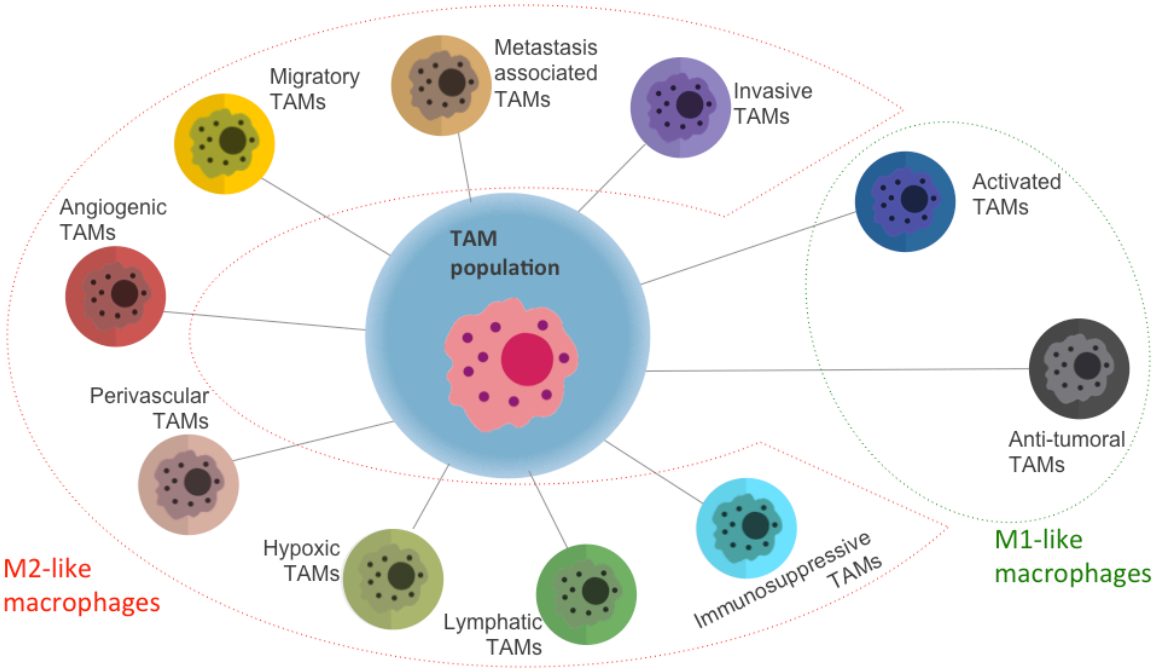

Figure I.12 – TAM subpopulations
Diagram of TAM populations with a M1-like (activated TAMs and anti-tumoral TAMs) or M2-like phenotype (invasive TAMs, metastasis-associated TAMs, migratory TAMs, angiogenic TAMs, perivascular TAMs, hypoxic TAMs, lymphatic TAMs and immunosuppressive TAMs) *(Genard Géraldine).*

population *(Shand et al., 2014).* Differently, DeNardo and his colleagues observed that TAMs derived from circulating monocytes as well as from the expansion of tissue-resident macrophages in a pancreatic tumor model. While monocyte-derived TAMs shape the immune responses by sampling tumor antigens, tissue-resident-derived TAMs have pro-fibrotic activities that fuel tumor growth. It suggests that macrophages from different origins respond to inflammatory cues with distinct activities *(Zhu et al., 2017)*. However, in an orthotopic colorectal cancer model, the remodeling of the extracellular matrix (ECM), as a part of the fibrotic activities of TAMs, was executed only by monocyte-derived TAMs *(Afik et al., 2016).* In line with the observations reported by DeNardo and his colleagues, the study of macrophage ontogeny in glioma and brain metastases also revealed that both bone-marrow-derived macrophages and tissue-resident microglia infiltrated the tumors. These two subsets of TAMs presented distinct education patterns, related to different transcription factor networks and chromatin landscapes. In addition, while microglial TAMs were enriched for expression of chemokines associated to a pro-inflammatory response, bone-marrow-derived macrophages presented a wound healing response *(Bowman et al., 2016).* Based on multiple studies, it was proposed that TAMs derive from surrounding tissues as the tumor size is small, while monocytes replenish TAM burden as the tumor grows and the intratumor vasculature is built *(Komohara et al., 2014)*.
In addition, some defined TAM populations have also been associated to specific origin and localization. For example, perivascular TAMs are mostly derived from circulating monocytes expressing the angiopoietin receptor Tie2 *(Lewis et al., 2016).* Besides circulating monocytes and tissue-resident macrophages, the monocytic myeloid-derived suppressor cells (M-MDSCs) also appear as a potential source for the TAM reservoir, as these cells are strongly recruited to the tumor site and rapidly differentiate into TAMs *(Kumar et al., 2016).*

All these studies suggest that the origin of TAMs may differ from a cancer site to another, and that heterogeneous TAM populations co-exist in tumor. These different macrophage subpopulations come from distinct origins and fulfill distinct functions, promoting or not tumor growth.

3. Role of TAMs and their interactions with cells from the tumor microenvironment

Qian and Pollard described six different types of TAMs, mostly related to a M2-like phenotype. These six types of macrophages are associated to specific patterns of gene expression and distinct roles in tumors. They include activated macrophages, invasive macrophages, metastasis-associated macrophages, perivascular macrophages, angiogenic macrophages and immunosuppressive macrophages *(Qian and Pollard, 2010)* (***Figure I.11***). Other macrophage types including migratory macrophages, hypoxic macrophages, lymphatic macrophages and anti-tumoral macrophages are also described in the literature (***Figure I.12***). The roles fulfilled by all these macrophage subtypes mainly include tumor initiation, tumor promotion, tumor metastasis and angiogenesis. In addition, macrophages hold a particular interaction with other immune cells, favoring immunosuppression.

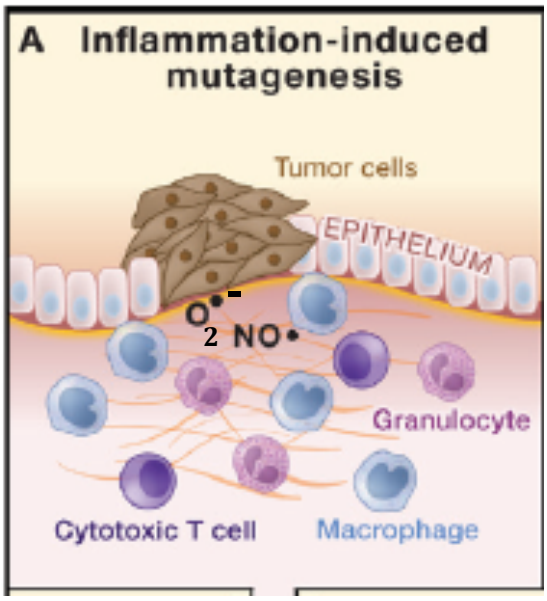

Figure I.13 – Activated macrophages
Chronic inflammation, induced by diverse components (e.g. pathogens), promotes the transformation of normal epithelial cells into malignant cells. This transformation is potentiated by reactive nitric and oxygen species released mainly by macrophages into the tumor microenvironment *(Qian and Pollard 2010).*

3.1. Tumor initiation: contribution of *activated macrophages*

As described earlier, chronic smoldering inflammation is well known to create an enabling environment for cancer initiation and promotion. Inflammatory cells, and mostly TAMs, may initiate malignant transformation of normal cells notably through the release of reactive compounds (ROS, RNI) (***Figure I.13***). In addition, chronic inflammation promotes tumor growth by enhancing the release of growth factors by inflammatory cells. It was effectively demonstrated that an inflammatory microenvironment contributes to the genetic instability in the neoplastic cells while an anti-inflammatory microenvironment prevents tumor initiation. As a vicious circle, the mutagenesis in cancer cells induces the recruitment of inflammatory cells at the tumor site. The recruited activated macrophage subset is a pro-inflammatory macrophage population that creates a microenvironment suitable for malignant cell population. This population shares a common M1-like phenotype by expressing IL-12, the major histocompatibility complex II (MHC II), the inducible nitric oxide synthase (iNOS), TNFα, CD80 and CD86 *(Grivennikov et al., 2010; Noy and Pollard, 2014; Qian and Pollard, 2010).* In this inflammatory context, NFκB and STAT3 regulate the expression of several important genes in TAMs. For example, the activation of the heterodimer p50 – p65 (NFκB) in macrophages mediates the production of IL-6, IFNγ and TNFα that contribute to tumorigenesis, once enough mutations had driven malignant transformation in epithelial cells *(Noy and Pollard, 2014)*. As STAT3 controls the production of anti-inflammatory cytokines such as IL-10, the ablation of STAT3 hampers the anti-inflammatory response and promotes tumor initiation. In line with these observations, the suppression of IL-10 also enhanced carcinogen-induced tumorigenesis *(Qian and Pollard, 2010)*. Once the tumor has emerged, activated macrophages are rapidly replaced by pro-tumoral M2-like TAMs. These changes are occurring during the transition from benign to invasive cancer and are associated to a switch from a T_H1-like (e.g. TNFα, IL-6, IFNγ, IL-12) towards a T_H2-like (e.g. IL-4, TGFβ, IL-10, CSF-1) microenvironment *(Mittal et al., 2014).*

3.2. Tumor promotion and metastasis: interplay between TAMs, malignant cells and cancer-associated fibroblasts (CAFs)

The epithelial – mesenchymal transition (EMT) is a key mechanism through which transformed epithelial cells acquire abilities to invade and disseminate. This transition is associated to morphological changes, increased motility, matrix-degrading enzyme expression and increased resistance to apoptosis. The microenvironment plays a key role in this process. More specifically, macrophages maintain a tight interaction with cancer cells by supporting their intravasation in blood vessels, their migration and dissemination in secondary sites and by preparing and supporting their evolution in a new microenvironment *(Hanahan and Weinberg, 2011)*.

3.2.1. Invasive macrophages

Invasive macrophage population is a subset of macrophages that promotes intravasation of cancer cells and that initiates the EMT. Cancer cells release CSF1 that recruits macrophages into the tumor. Once recruited, macrophages secrete endothelial growth factor (EGF), activating the migratory capability of cancer cells. The involvement of the CSF1 – EGF axis in tumor metastasis

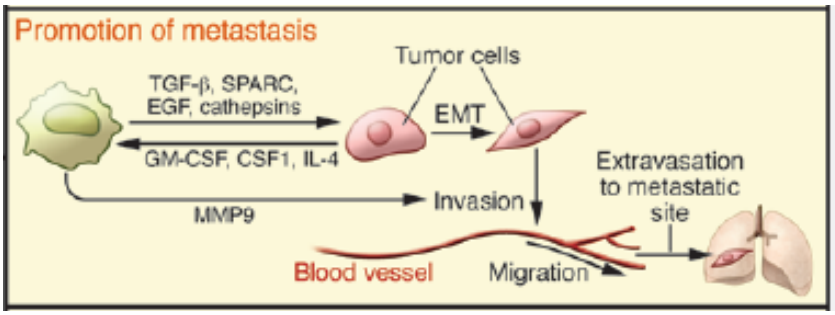

Figure I.14 – Promotion of invasiveness by TAMs

Cancer cells attract TAMs into the tumor site by secreting factors such as CSF1 and contribute to the immunosuppressive phenotype of macrophages by releasing IL-4. In return, invasive TAMs release several factors, including TGFβ and EGF, that contribute to the epithelial mesenchymal transition (EMT) of malignant cells, to their migratory profile and then to their extravasation in blood circulation *(Ugel, De Sanctis et al. 2015).*

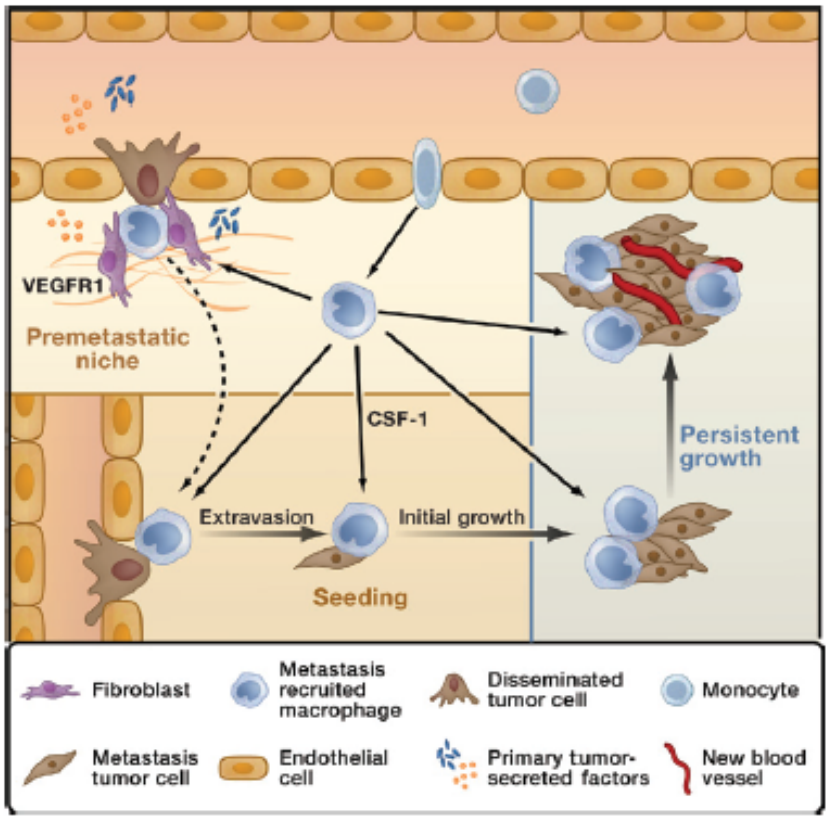

Figure I.15 – TAMs promote invasion and metastasis of malignant cells

TAMs are recruited to the premetastatic niches by several factors including CSF-1, CCL2 and other factors. Once recruited, macrophages show tight interactions with fibroblasts to prepare the extracellular matrix. These niches enhance and attract invasive cancer cells to form a new mass. Once recruited, cancer cells accumulate in the metastatic lesion and interact with fibroblast and macrophages, mostly through CSF-1 and VEGFR *(Qian and Pollard 2010).*

is further confirmed by the fact that the inhibition of CSF1 – EGF signaling pathway aborts migration and chemotaxis of both cells *(Wyckoff et al., 2004; Wyckoff et al., 2007) (**Figure I.14**)*. While CSF1 – EGF axis plays a major role in cell invasion, it is not exclusive, since other factors such as chemokines and cytokines may also influence cancer cell migration. For instance, the release of the chemokine CCL18 by macrophages promotes the invasiveness of cancer cells by enhancing the EMT in breast cancer models and patients *(Su et al., 2014)*. Also, the co-migration of macrophages and cancer cells is initiated by another chemokine, CXCL12, released by malignant cells, fibroblasts or pericytes *(Qian and Pollard, 2010)*. Moreover, TAMs promote a stem cell-like phenotype in cancer cells through the secretion of cytokines like TGFβ in a hepatocellular carcinoma mouse model. Indeed, TGFβ induced cancer stem cells to undergo EMT *(Fan et al., 2014)*. Finally, matrix remodeling by proteolytic destruction also enhances the escape of cancer cells. For example, TAMs release matrix metalloproteinases (MMPs), including MMP2 and MMP9, which favor malignant cell invasion *(Kitamura et al., 2007)*.

Besides a tight synergy between cancer cells and TAMs in tumor invasion, cancer-associated fibroblasts (CAFs) also influence the migratory profile of cancer cells by themselves or in concert with TAMs (***Figure I.15***). CAFs play key roles in the recruitment of macrophages, neutrophils and lymphocytes to the tumor site by secreting a variety of chemokines and pro-inflammatory cytokines, including IL-6, IL-8, and TNFα *(Xing et al., 2010).* The cooperation between malignant cells and CAFs allowed macrophage recruitment during prostate carcinoma progression. Indeed, co-culture experiments revealed that the recruitment and the differentiation of monocytes were synergized by CXCL12 (or stromal-derived growth factor-1 (SDF-1)) and by CCL2 (or monocyte chemotactic protein-1 (MCP-1)), released by CAFs and malignant cells respectively. Once differentiated, M2-like TAMs contribute to the invasiveness of malignant cells and to angiogenesis *(Comito et al., 2014)*. In hypoxic conditions, CXCL1 and IL-6 were shown to be important chemoattractants for TAMs and CAFs in bladder cancer. In return, recruited TAMs and CAFs both supplied CXCL1 and other growth factors that promote tumor invasion *(Miyake et al., 2016).*

3.2.2. Metastasis-associated macrophages

While the here above experiments highlighted the influence of macrophages on the migratory profile of cancer cells, they also modified the metastatic site (***Figure I.15***). Even before malignant cells invade a metastatic site, the formation of pre-metastatic niches, populated by $CD11b^+$ $VEGFR1^+$ myeloid cells, influence the homing of circulating cancer cells *(Noy and Pollard, 2014).* In line with these observations, TAM depletion in a CCR2- colorectal cancer model induced changes in ECM composition, as the protein expression of different types of collagen, glycoproteins, proteoglycans and ECM-modulators was modified. The results evidenced the contribution of TAMs to the production and the organization of collagenous matrix through their interactions with CAFs. Indeed, the interplay between CAFs and TAMs allows the formation of ECM niches suitable for metastasis, notably by enhancing collagen (I and XIV) expression in CAFs *(Afik et al., 2016).* Metastasis-associated macrophages (MAMs) are $CCR2^+$, $VEGFR1^+$, $Ly6C^-$, $F4/80^+$ *(Noy and Pollard, 2014).*

BOX 3: Parabiosis

Parabiosis relies on the surgical union of two animals connected through the elbow and knee joints and by attachment of the skin. This surgical process allows the formation of a microvasculature by natural wound-healing processes (inflammation) and thus permits the sharing of immune cells. As partners share circulating factors, such as circulating antigens, cross immune reactions are prevented. The initial experiment was performed by Paul Bert in 1864 and slightly evolved by the input of Bunster and Meyer in 1933. Parabiosis enables to examine the contribution of the circulating cells like monocytes, from one animal in the other. For example, by using an ubiquitous GFP expressing mouse and a wild-type mouse, it is possible to follow GFP positive cells *(Kamran, Sereti et al. 2013, Scudellari 2015).*

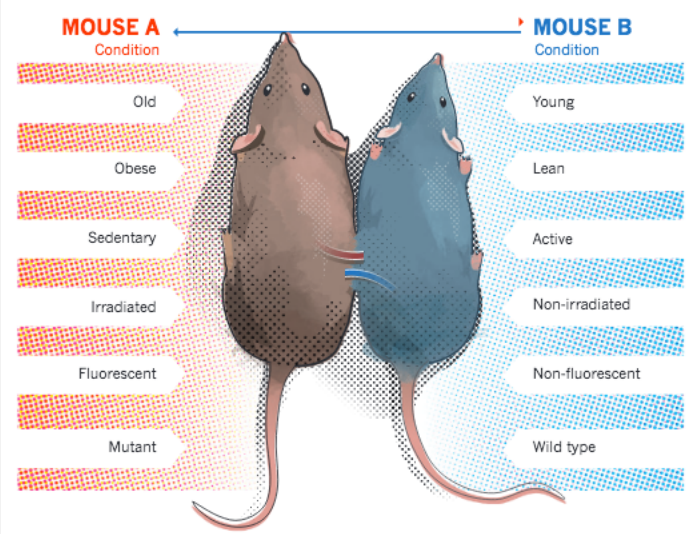

3.2.3. Migratory macrophages

Although macrophages may induce invasiveness and metastasis of cancer cells through paracrine secretions, macrophages may also fuse with cancer cells and acquire migratory activities. The metastatic properties linked to the fusion between cancer cells and host cells was reported a long time ago *(Kerbel et al., 1983)*. Indeed, the surgical union of two organisms sharing the blood circulation, or so-called parabiosis (BOX 3), revealed the fusion between fluorescent-labeled TAMs and cancer cells in intestinal tumors. These hybrids exhibited a transcriptomic identity shared by both parental cells and acquired a migratory behavior. Therefore, while masquerading as host immune cells and then avoiding immunosurveillance, these hybrids navigated the circulatory system and promoted metastasis *(Powell et al., 2011).* While the occurrence of this macrophage – cancer cell fusion was shown to be very low (0.1% to 7.6%) in a spontaneous breast cancer model *(Lizier et al., 2016)*, this phenomenon was also detected in peripheral blood from melanoma patients *(Clawson et al., 2015)*. The migratory conversion of TAMs was also noticed in breast, ovarian and colorectal cancers after the phagocytosis of cancer cell apoptotic bodies. Indeed, foreign DNA elements, from apoptotic bodies containing cancer genes, were incorporated into open chromatin regions or transactivated some silenced genes in phagocytic TAMs. This genetic transfer generated a unique macrophage subpopulation, harboring stem-cell markers, escaping from immunosurveillance and promoting metastasis *(Zhang et al., 2017)*. These experiments, among others, have highlighted another type of macrophages with metastatic functions: the migratory macrophages. The identification of these macrophages relies on the presence of malignant cell DNA fragments.

3.3. Angiogenesis, intravasation and extravasation: crosstalk between TAMs and the circulatory system

The framework of new vessels involves endothelial cells and pericytes. The tumor endothelial cells differ from the normal endothelial cells by several markers, including specific growth factor receptors and integrins *(Ruoslahti, 2002)*. The pericytes are mesenchymal cells that support the quiescent endothelium, mainly by secreting angiopoietin. These cells also participate to the vascular basement for newly formed vessels *(Hanahan and Weinberg, 2011)*. A key feature of the tumor vasculature is its abnormal structure, generally leading to hypoxic and acidotic regions in tumor.

As the tumor is growing, its metabolic and nutritional needs are increasing. The formation of a vascular network allows the tumor to meet these needs. Angiogenesis is the formation of new blood (angiogenesis) and lymphatic (lymphangiogenesis) vessels in order to supply the tumor in nutrients, oxygen and immune cells, and also to remove waste products. This process is influenced by the release of pro-angiogenic factors in the microenvironment *(Nishida et al., 2006)*. During angiogenesis, a crucial role is attributed to immune inflammatory cells, mostly including TAMs but also Tie2-expressing monocytes, MDSCs, DCs, mast cells and neutrophils. Altogether, these cells secrete factors such as cytokines (e.g. VEGF, TGFβ, fibroblast growth factor (FGF), TNFα), chemokines (e.g. CXCL8/IL-8), matrix metalloproteinases (e.g. MMP-9),

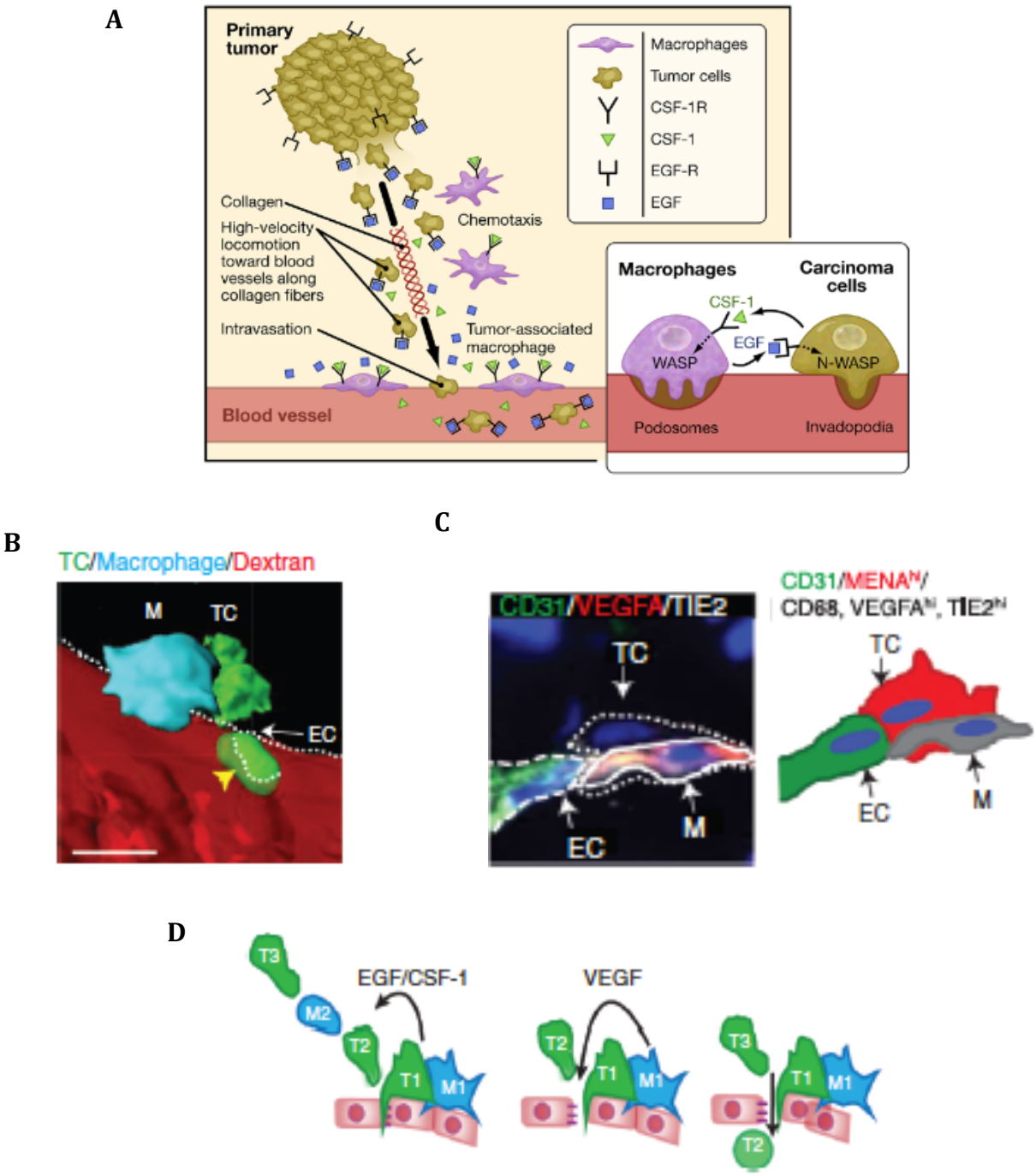

Figure I.16 – The role of perivascular TAMs in intravasation and metastasis
A tight interaction between macrophages and cancer cells drive the extravasation of cancer cells. (**A**) A paracrine loop (CSF-1 – EGF) between cancer cells and macrophages allows the co-migration of both cells to blood vessels and then the extravasation and dissemination of cancer cells. (**B**) Real-Time imaging allowed the 3D reconstruction of cancer cell intravasation (yellow arrow) at the luminal surface of endothelium (EC, red). The intravasation of cancer cells (TC, green) is made possible by their interaction with perivascular macrophages (M, cyan). (**C**) Perivascular macrophages are a distinct subset which is characterized by high levels of VEGF-A and a high expression of the Tie2 receptor. (**D**) The EGF – CSF1 axis promotes the co-migration of cancer cells and TAMs to the tumor vasculature. Then, the release of VEGF-A by $Tie2^{+}$ TAMs induces a local and transient vascular permeability, allowing the intravasation of cancer cells and their subsequent migration *(Harney, Arwert et al. 2015)*.

ROS, nitric oxide (NO) and a multitude of other mediators that regulate angiogenesis *(Hanahan and Coussens, 2012).*

3.3.1. Angiogenic macrophages

During early tumorigenesis, an angiogenic switch allows the activation of quiescent endothelial cells to form new vessels. This activation is elicited by the presence of diverse signals mostly represented by VEGF, CSF1 and FGF *(Hanahan and Weinberg, 2011)*. Pollard and his colleagues showed that TAMs play a crucial role in this angiogenic switch, as the inhibition of macrophage recruitment by anti-CSF1 monoclonal antibody suppressed vasculogenesis and tumor growth *(Riabov et al., 2014)*. Indeed, angiogenic macrophages are recruited mainly by CSF1 and CXCL12, a ligand for chemokine (C – X – C) motif receptor 4 (CXCR4) *(Qian and Pollard, 2010)*. It was also observed that the angiogenic switch in a mammary cancer model was mediated through the release of the WNT family ligand (WNT7B), by macrophages, then inducing the production of VEGF-A by vascular endothelial cells *(Yeo et al., 2014)*. Moreover, macrophages release VEGF to promote neoangiogenesis, and this is well demonstrated by the abortion of the angiogenic switch when the expression of VEGFA is abrogated in myeloid cells. Finally, by degrading the extracellular matrix through the release of MMP9, macrophages also make extracellular storage of VEGF available for endothelial cell activation. Overall, angiogenic macrophages are $VEGFR1^+$, $VEGF^+$ and $CXCR4^+$ *(Qian and Pollard, 2010).*

3.3.2. Perivascular macrophages and monocytes

Perivascular TAMs integrate a distinct subset of macrophages, localized close to blood vessels and known for enhancing the intravasation of cancer cells. Recruited notably by CXCL12, this macrophage subtype expresses high levels of the angiopoietin receptor (Tie2), metalloproteinases (such as MMP9), VEGF-A and PDGFβ *(Lewis et al., 2016)*.
The angiopoietin 2 (ANG2) is a proangiogenic cytokine, released by activated endothelial cells, that recruits perivascular $Tie2^+$ TAMs in the vicinity of the tumor vasculature. Once recruited, this macrophage subset contributes to the intravasation of cancer cells, and thereby to metastasis. Indeed, perivascular macrophages act by clustering nearby the vasculature, as it was demonstrated in xenograft mammary tumor-bearing mice. This process involves the EGF – CSF1 axis which promotes the co-migration of cancer cells and TAMs to blood vessels. In more details, a paracrine loop is established between cancer cells and macrophages in the initial stages of metastasis. The chemotaxis of carcinoma cells to blood vessels occurs in response to EGF, secreted by perivascular TAMs. In turn, CSF1, released by malignant cells, attracts stromal TAMs to co-migrate with cancer cells. CSF1 also induces the secretion of EGF by TAMs, then promoting the paracrine loop between cancer cells and TAMs. In this process, collagen fibers direct TAMs and cancer cells towards the blood vessels and more specifically to a specific space, named the tumor microenvironment of metastasis (TMEM). Once in the proximity of blood vessels, actin regulators modify the cytoskeleton of cells and allow them to execute intravasation *(Condeelis and Pollard, 2006)*. More recently, it was shown that the release of VEGF-A by $Tie2^+$ TAMs induced a local and transient vascular permeability, allowing the intravasation of cancer cells and their following migration (***Figure I.16***) *(Harney et al., 2015).* Perivascular TAMs are

identifiable by their high expression of Tie2, VEGF-A, MMP9, cyclooxygenase 2 (COX2) and CXCR4 (Riabov et al., 2014) and are probably the same as invasive macrophages.

A large panel of studies also revealed a specific population of monocytes, the Tie2-expressing monocytes. This monocytic lineage is characterized by the expression of Tie-2 and displays key roles in angiogenesis, tumor growth and metastasis in several cancer models *(Turrini et al., 2017; Venneri et al., 2007)*. Indeed, this monocytic subtype can be distinguished from Tie2+ macrophages by their cell surface markers: $Tie2^+$ monocytes are $CD11b^+$, $F4/80^+$,$MRC1^{high}$, $CD11c^-$ while $Tie2^+$ macrophages are $CD11b^+$, $F4/80^+$, $MRC1^{low}$, $CD11c^+$. Also, these monocytes highly express blood remodeling genes, insulin-like growth factor 1 (IGF1) and genes involved in the regulation of epithelial cell proliferation *(Wang et al., 2016a)*. The recruitment of this monocyte subpopulation is performed by CSF1. This factor upregulated the expression of Tie2 in monocytes in a mouse model of breast cancer *(Forget et al., 2014).* The angiopoietin, by its binding to the Tie2 receptor, leads to an elevated expression of IL-10 in $Tie2^+$ monocytes, suppressing T cell proliferation and promoting T regulatory (Treg) lymphocytes *(Coffelt et al., 2011).* As Tie2+ monocytes play key roles in angiogenesis, the targeting of ANG2 or Tie2 in pancreatic and breast cancer models suppressed angiogenesis and hampered the association of $Tie2^+$ monocytes with blood vessels *(Mazzieri et al., 2011)*.
This monocyte subset is rare in the blood of healthy humans but it is found at high levels in peripheral blood and intriguingly within tumor in cancer patients. These Tie2+ monocytes represent the main monocytic population in tumors *(Venneri et al., 2007)* and are usually related to a negative prognosis for most cancer types *(Turrini et al., 2017).*

3.3.3. Hypoxic macrophages

Hypoxic areas are zones placed at distance from the nearest capillary or close to abnormal structure of the vasculature, resulting in transient blood flow *(Michiels et al., 2016)*. The lack of oxygen and nutrients creates a specific microenvironment that stimulates the formation of a new network of vessels with chaotic branching structures *(Carmeliet and Jain, 2011)* and that recruits different types of host cells, including TAMs. The recruitment of macrophages to hypoxic regions is elicited by the secretion of chemoattractants, mainly including VEGF and endothelin *(Murdoch and Lewis, 2005).* Once recruited in hypoxic zones, macrophages express low levels of CCR2, impeding their chemotaxis to other tumor areas that would be mediated by CCL2 *(Sica et al., 2000a)*. This macrophage subset is also influenced by phenotypic changes due to the activation of hypoxia-inducible factor 1 (HIF1). Indeed, hypoxia enhances the stability of HIF1α and HIF2α in TAMs and this stabilization is regulated by the PTEN/Pi3Kγ/AKT pathway *(Joshi et al., 2014)*. Finally, all these biological activations trigger the expression of pro-angiogenic genes, such as *Vegf*, and of other genes (e.g. arginase 1 (*Arg1)*) *(Colegio et al., 2014; Qian and Pollard, 2010)*. Interestingly, more than influencing macrophage phenotype, hypoxia fine-tunes the phenotype of M2-like MHC-II^{low} TAMs in Lewis lung carcinoma (LLC) bearing mice. This is made by upregulating the expression of specific genes, such as *Hif1α, Vegf-a, Ang2, Igf1, Egf and Nos2 (iNOS)* that are not highly expressed in these macrophages in normoxic areas, and by promoting the angiogenic activities of this macrophage subtype *(Laoui et al., 2014)*. Therefore, hypoxic TAMs are characterized by a higher expression of HIF1α, HIF2α and VEGF compared to the normoxic macrophage population.

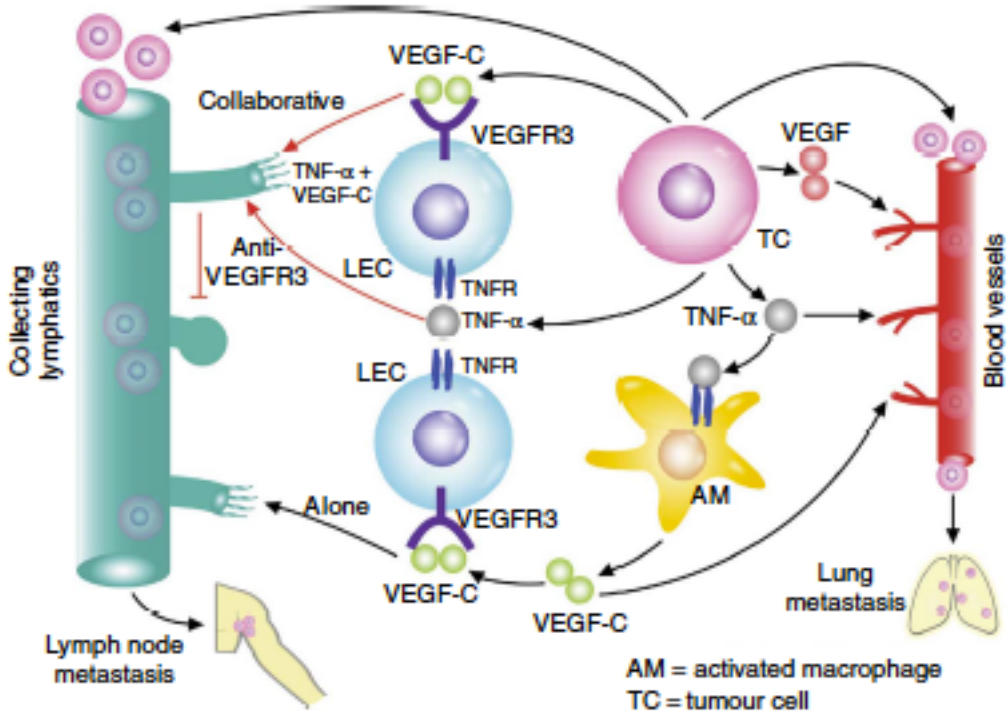

Figure I.17 – Lymphatic macrophages
TNFα, released by malignant cells (tumor cell, TC), stimulates the production of VEGF-C through the activation of TNF1R in TAMs (activated macrophages, AC). In return, VEGF-C stimulates the VEGF receptor 3 (VEGFR3) expressed by lymphatic endothelial cells (LEC) and promotes, in concert with TNFα, lymphangiogenesis and then lymph node metastasis *(Ji, Cao et al. 2014)*.

3.3.4. Lymphatic macrophages

Cells forming lymphatic vessels are closely related to the endothelial cells from blood vessels. In tumors, the lymphatic vessels are invaded by cancer cells, promoting the seeding of metastasis at secondary sites *(Hanahan and Weinberg, 2011)*. Only few studies have analyzed the interactions between lymphatic endothelial cells and TAMs. However, these interactions have been observed in several cancers, including gastric, breast and cervical cancers *(Ding et al., 2014; Ding et al., 2012; Go et al., 2016)*. Further studies are needed to evaluate the mechanisms involved in the macrophage-mediated lymphangiogenesis but it has already been observed that TAMs induce lymphangiogenesis through VEGF-C release *(Ding et al., 2012)*. Indeed, TNFα, released by malignant cells, stimulates the production of VEGF-C through the activation of TNF1R in TAMs. Once released, VEGF-C activates VEGFR3 on lymphatic endothelial cells and promotes, in concert with TNFα, lymphangiogenesis that facilitates metastasis dissemination *(Ji et al., 2014)* (***Figure I.17***). In addition to promote new blood vessel development, the WNT family, a major actor in tumor development, is also involved in lymphangiogenesis. While WNT7B stimulates the production of VEGF-A by angiogenic macrophages, WNT5A promotes the production of VEGF-C by lymphatic macrophages *(Shao et al., 2016; Yeo et al., 2014)*. This macrophage subtype expresses high levels of VEGF-C and WNT5A, and is also $TNFR1^+$.

3.4. Immunosuppressive TAMs: interactions with the immune system

3.4.1. TAM interplay with the innate immune system

The innate immune system and more specifically, the myeloid lineage, comprises dendritic cells, tumor-associated macrophages, monocytes, myeloid-derived suppressor cells, mast cells and granulocytes. The main functions of these cells are the antigen capture for degradation (macrophages) or presentation (dendritic cells), tissue repair and effector functions (mast cells, monocytes and granulocytes). One of the most important features of myeloid-lineage cells is their high plasticity driven by the environmental cues *(Palucka and Coussens, 2016)*. Tumor-infiltrating inflammatory cells have been reported to participate to the tumor growth and to the angiogenesis in addition to support migration and invasion of cancer cells *(Mantovani, 2010)*.

3.4.1.1. Myeloid-derived suppressor cells (MDSCs)

Myeloid-derived suppressor cells (MDSCs) are immunosuppressive precursors of dendritic cells, macrophages and granulocytes *(Ansell and Vonderheide, 2013)*. In cancer-free organism, the non-suppressor myeloid cells participate to the homeostasis of normal tissues when the organism has to face infection or injury. In tumor, MDSCs are induced into a suppressive state and show an immature phenotype *(Kerkar and Restifo, 2012)*. In fact, in peripheral lymphoid organs, the prominent MDSC population accounts for polymorphonuclear MDSC (neutrophils), while in tumor, MDSCs are widely represented by monocytes. The recruitment of these cells into tumors is mainly driven by CCL2 and CCL5 factors *(Kumar et al., 2016).* Once recruited, these cells favor neoangiogenesis and metastasis. MDSCs also prevent the immunosurveillance by impeding

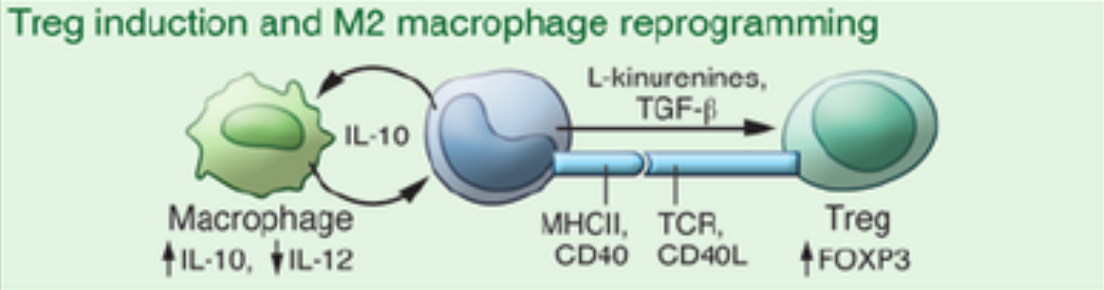

Figure I.18 – Crosstalk between TAMs and MDSCs
A paracrine loop operates between MDSCs and TAMs, which favors immunosuppressive characteristic of TAMs and MDSCs. MDSCs release IL-10 that decreases IL-12 production in TAMs and promotes IL-10 secretion. In turn, the decreased IL-12 production by TAMs stimulates MDSCs to further release IL-10. MDSCs are then able to activate Tregs and thus favor immunosuppression *(Ugel, De Sanctis et al. 2015).*

antigen presentation performed by dendritic cells and by inhibiting T cell activation and NK cell cytotoxicity *(Hui and Chen, 2015)*. In addition, they favor an immunosuppressive microenvironment thereby regulating Treg cell expansion and activation *(Ansell and Vonderheide, 2013)*. In order to perform all these functions, MDSCs act through the production of high amounts of NO, ROS and immunosuppressive cytokines such as IL-10 and TGFβ, and/or deprive T cell from key nutrition factors including L-arginine *(Kerkar and Restifo, 2012; Kumar et al., 2016).* Regarding all these functions, MDSCs directly correlate with a poor prognosis when their densities are high in the tumor microenvironment *(Fridman et al., 2017)*.

A tight interaction occurs between MDSCs and TAMs, favoring the immunosuppressive functions of TAMs, thus promoting tumor growth. MDSCs skew macrophages into a M2-like phenotype through the release of IL-10, thus decreasing IL-12 production in TAMs in a breast cancer model. This crosstalk is exacerbated by TAMs themselves. Indeed, the decrease in IL-12 production by macrophages stimulates MDSCs to further release IL-10. As IL-12 is critical for T cell priming while IL-10 promotes T cell anergy, this TAM – MDSC crosstalk participates to the immunosuppressive microenvironment (***Figure I.18***) *(Sinha et al., 2007).* Another study in mammary and colon cancer models confirmed these results. IL-10, produced by MDSCs, reduced the production of IL-6, IL-12 and TNFα in TAMs while it increased NO release *(Beury et al., 2014)*. It was also demonstrated that the activation of the high motility group box 1 (HMGB1) played a pivotal role in the immunosuppressive TAM – MDSCS crosstalk by facilitating the differentiation and the suppressive activity of MDSCs. Interestingly, HMGB1 enhanced the IL-10 production in MDSCs *(Parker et al., 2014)*.

3.4.1.2. Dendritic cells (DCs)

DCs are antigen-presenting cells playing key roles for bridging innate and adaptive immunity. These cells exert an antigen-presenting function by presenting the antigen to T cells through the classical MHC class I or II molecules or through the non-classical cluster of differentiation 1 (CD1), and thus have the ability to induce antigen-specific T-cell response *(Palucka and Coussens, 2016).* However, in tumors, these professional APCs fail to prime T cells due to microenvironmental factors, such as VEGF, CSF-1, IL-6 and IL-10 *(Kerkar and Restifo, 2012)*. Indeed, in the presence of immunosuppressive cytokines, such as IL-10, DCs remain in an immature stage and lead to T-cell suppression *(Ruffell et al., 2014)*.
Therefore, the immature DCs express low levels of co-stimulatory and MHC class I and II molecules and fail to present antigen to lymphocytes, thus disrupting T cell activation. These immature DCs also express high levels of indoleamine 2,3-dioxygenase (IDO) which degrades acid tryptophan, an amino acid essential for T cell activation *(Kerkar and Restifo, 2012).* The prognosis linked to DC infiltration depends on the maturity of these cells in tumors *(Chang et al., 2014).*

Interactions between DCs and T lymphocytes through receptors and co-stimulators (e.g. B7 – CD28), or cytokines (e.g. IL-12, IFN, IL-15) are needed for the differentiation of naive $CD8^+$ T cells into cytotoxic T lymphocytes (CTL) *(Palucka and Coussens, 2016)*. However, in tumors, TAMs are widely recognized as driving immune suppression. Furthermore, they play key roles in trapping DCs in an immature stage, impeding T cell activation. More precisely, the release of IL-10 by M2-like TAMs inhibits DC functions and IL-12 production by these APCs *(Ruffell et al.,*

2014). Other studies also showed that $Tie2^+$ monocytes also inhibit DC functions by decreasing the human leukocyte antigen-cell surface receptor (HLA-DR) expression in DCs *(Ibberson et al., 2013).*

3.4.1.3. Natural killer (NK) cells

NK cells are members of the innate lymphoid cell family. This cell subset recognizes malignant cells notably through the expression of HLA-DR class I *(Wang et al., 2017a)* and are highly involved in the resistance to tumor engraftment *(Hui and Chen, 2015).* The recognition of abnormal cells, due to their loss of MHC class I or by ligands activating NK cells, triggers cytotoxic functions, cytokine production and proliferation in NK cells. Activated NK cells release proteins by degranulation such as perforin and granzymes that mediate cell killing *(Morvan and Lanier, 2016)*. NK cells also secrete abundant amounts of TNFα and IFNγ, through which they induce cancer cell apoptosis *(Ansell and Vonderheide, 2013),* and release other cytokines and chemokines that participate to the recruitment of myeloid cells and T cells *(Morvan and Lanier, 2016).* However, cancer cells develop many strategies to escape detection and elimination by NK cells. Also, immunosuppressive soluble factors, such as PGE_2 and TGFβ promote tumor progression by depleting NK cells in tumors and by blocking their maturation process *(Morvan and Lanier, 2016)*. All these features explain the correlation between a high number of effective NK cells and a good prognosis in cancer patients *(Pasero et al., 2015; Xu et al., 2016)*.

Depending on their phenotype, TAMs may activate or repress NK cells. Interestingly, *in vitro* experiments revealed the reciprocal activation of NK cells and M1-like macrophages. In more details, LPS-activated macrophages (M1-like macrophages) secrete IL-12 and IL-18 that trigger the activation of NK cells and their cytotoxic functions. In return, activated NK cells release T_H1-type cytokines, such as IL-12, TNFα and IFNγ that triggers M1-like polarization in macrophages. In contrast, IL-4 polarized macrophages (M2-like macrophages) fail to activate NK cells. *(Bellora et al., 2014; Bellora et al., 2010)*. In tumors, patrolling monocytes, stimulated by cancer exosomes, prevent lung metastasis formation through the release of IL-15, an activator of NK cells *(Kubo et al., 2017; Plebanek et al., 2017)*. Otherwise, macrophages also activate NK cells through trans-presentation of IL-15 by their IL-15Ra *(Chenoweth et al., 2012)*. As M2-like macrophages and TAMs express low amounts of « protective » HLA class I molecules, NK cells are able to kill them. However, TGFβ secreted in the tumor microenvironment, mostly by TAMs, inhibits the cytotoxic functions of NK cells *(Morvan and Lanier, 2016)*. Indeed, TGFβ downregulates the expression of NKp30 and NKG2D, both NK receptors allowing the recognition and the killing of malignant cells *(Castriconi et al., 2003)*. As a whole, NK cells and TAMs mutually influence each other by the release of diverse soluble factors.
The mutual influence between NK cells and TAMs might also be induced by cell-to-cell contact through the direct interaction between receptors and co-stimulators. For instance, TAMs reduce NK-cell degranulation and IFNγ production, possibly through the reduction of the expression of NKp46 (NK cell receptor p46) and DNAM-1 (DNAX accessory molecule 1), two NK cell receptors that play major roles in macrophage killing and cytotoxicity respectively *(Bellora et al., 2010)*. Other examples are the stimulation of NKG2A-Qa1 (NK cell receptor G2A, cluster Qa1) that allows macrophages to avoid lysis by NK cells *(Bodduluru et al., 2015)* or the binding of HLA-G

BOX 4: T lymphocyte subpopulations in cancer

CD4+ T helper and T regulatory lymphocytes

Like macrophages, naive CD4+ T helper (T_H) lymphocytes can be polarized in three distinct phenotypes: T_H1, T_H2 or T_H17. T_H1-polarized CD4+ T cells in conjunction with cytotoxic CD8+ T cells promote macrophage cytotoxic activity through the secretion of IL-2, TNFα and IFNγ *(Stout and Bottomly 1989)* and upregulate antigen processing and MHC molecule expression in APCs *(DeNardo, Barreto et al. 2009).* Conversely, T_H2-polarized CD4+ T cells secrete diverse cytokines (such as IL-4, IL-10 and IL-13) driving T-cell anergy and loss of T-cell mediated cytotoxicity T_H2 cytokines also enhance immunosuppressive T regulatory cells (Tregs) and promote a M2-like phenotype in TAMs *(Palucka and Coussens 2016)*. Naive CD4+ T lymphocytes may also be polarized towards T_H17 lymphocytes. T_H17 lymphocytes are T helper cell lineage producing IL-17 and are characterized by ambivalent functions: tumor regression through antitumor functions or tumor progression through induction of angiogenesis. Besides, T regulatory cells (Tregs) have the ability to inhibit APCs and effector T cells, as well as, to release immunosuppressive cytokines (e.g. IL-10 and TGFβ). The release of TGFβ by Tregs notably interferes with cytotoxic functions of CTLs. Therefore, these cells mediate immune suppression and lead to immune evasion by the tumor *(Qi, Huang et al. 2013)*.

CD8+ T cells (Cytotoxic T cells or CTLs)

CD8+ cytotoxic T cells (CTLs) represent the major neoplastic cell killer through their cytotoxic functions. Their differentiation from naive CD8+ T cells to CTLs is encountered by APCs in lymphoid organs. CTLs perform their cytotoxic function through different mediators including granzyme A or B and perforin. This cell type can specifically recognized cancer cells via receptors that have a high affinity for antigens *(Palucka and Coussens 2016)*. Inside the tumor, CD8+ T cells have to face the immunosuppressive microenvironment and regulatory cells as Tregs and myeloid cells. Cancer cells are able to escape from the immune system notably through the activation of negative regulatory pathways, also called checkpoint regulators, such as programmed cell death ligand 1 or 2 (PD-L1 and PD-L2) or cytotoxic T-lymphocyte protein 4 (CTLA4). These ligands are able to inhibit the activity of T cells *(Chen, Zhang et al. 2017)*.

(macrophages) to NKG2D (NK cells) that subsequently represses the cytotoxic activity of NK cells *(Noy and Pollard, 2014)*.

3.4.2. TAM interactions with the adaptive immune cells

As described above, the immune system plays a dual role in tumor. The elimination of malignant cells is driven by APCs, mainly dendritic cells and macrophages, through the activation of CTLs in tumor-draining lymph nodes. After T-cell priming, CTLs migrate into the tumor to specifically eliminate malignant cells through degranulation or through ligand/receptor pathway *(van der Woude et al., 2017)*. However, this process is mainly inhibited by an immunosuppressive microenvironment and several cell-cell interactions that induce T-cell anergy. Furthermore, B cells also play key role in the induction of an immunosuppressive microenvironment.

3.4.2.1. B cells

As B cells represent a heterogeneous population, opposite immune responses are attributed to distinct B cell subpopulations in tumors. On one side, tumor-infiltrating B lymphocytes (B-TIL) secrete immunoglobulins (Ig) as well as angiogenic and anti-inflammatory mediators (such as VEGF or IL-10), which contribute to T-cell depletion and to the recruitment of MDSCs. B cells also promote tumor growth through the secretion of TGFβ, ECM degradation and the recruitment of TAMs at the tumor site. On the other side, B-TIL are also able to enhance T-cell activity ($CD4^+$ and $CD8^+$ T cells) and to elicit tumoricidal effects by secreting granzyme B or antibodies. For example, $CD20^+$ B cells acts as APCs and contribute to the survival and the proliferation of tumor-infiltrating T cells (TILs) *(Tsou et al., 2016)*.
In addition, B regulatory cells (Breg) are a separate subset, considered as IL10-producing B cells *(He et al., 2014).* This subset activates plasma B cells by secreting IgM and promotes metastasis by converting $CD4^+$ T cells into immunosuppressive T regulatory cells.
The infiltration of B cells in tumor is associated with good prognosis in some tumors, including breast and lung cancers while mature plasma cells are linked to a unfavorable clinical outcome in lung carcinomas *(Tsou et al., 2016).*

The phenotype of TAMs is widely influenced by the presence of B cells into the tumor microenvironment. Co-culture system of B cells, macrophages and B16 melanoma cells revealed that B cells drive the polarization of macrophages into a M2-like phenotype through the release of IL-10 *(Wong et al., 2010).* Another study revealed the role of IgG to induce pro-tumoral functions (angiogenesis, tissue remodeling and tumor growth) in macrophages through the activation of Fc receptor γ (FcRγ) *(Andreu et al., 2010)*. Indeed, in a pancreatic cancer model, the stimulation of FcRγ by B cells activated the Burton tyrosine kinase (BTK) and programmed macrophages towards a M2-like phenotype in a phosphoinositide kinase 3 γ (PI3Kγ)-dependent mechanism *(Gunderson et al., 2016).*

3.4.2.2. T cells

Another lymphoid compartment of the tumor microenvironment is the T cell lineage. This population comprises γδT cells, $CD4^+$ T cells, $CD8^+$ T cells and NKT cells (BOX 4).

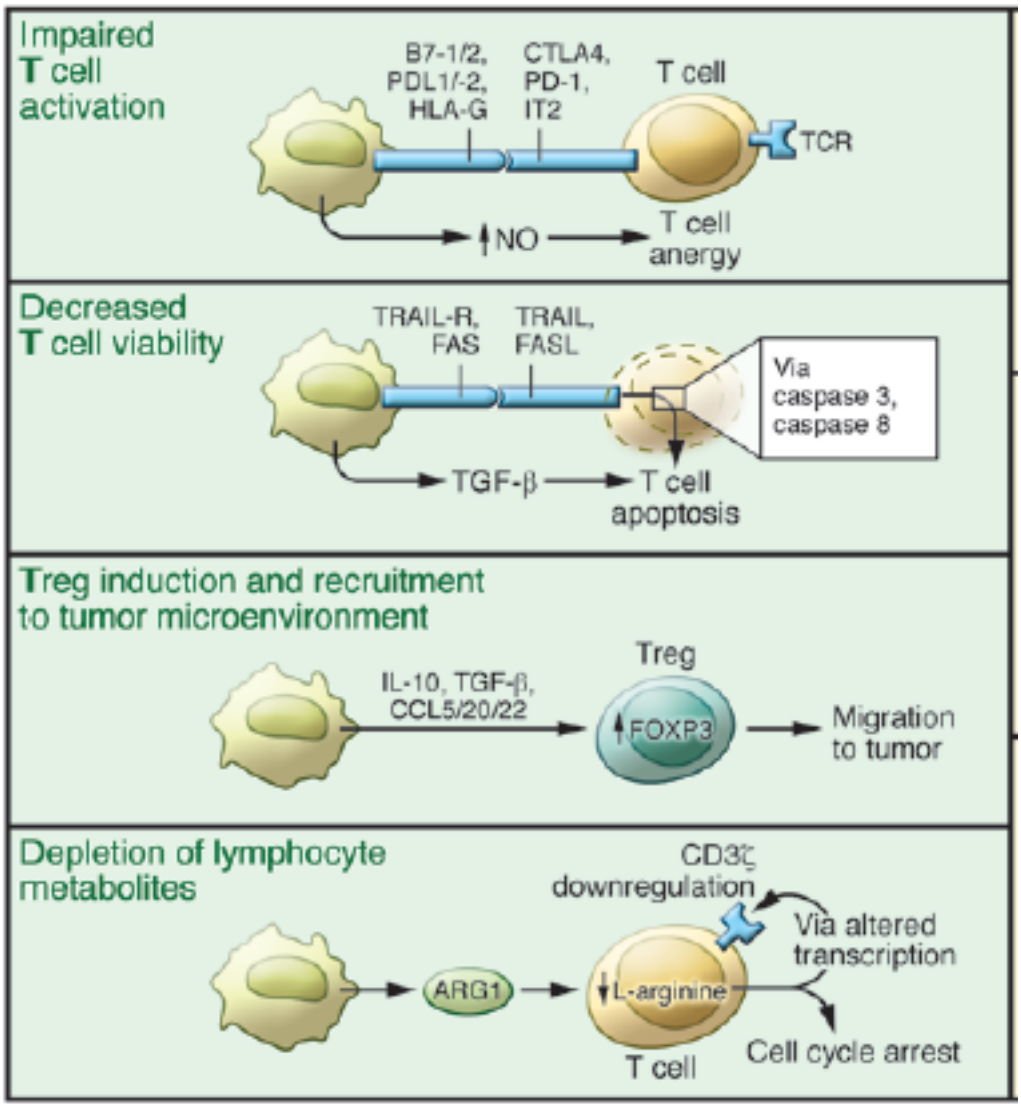

Figure I.19 - Interplay between TAMs and T lymphocytes

TAMs influence T cells in several ways: (**A**) macrophages impair T cell activation through the binding of inhibitory ligands (B7-1, B7-2, PD-L1, PD-L2, HLA-G) to checkpoint receptors (CTLA4, PD-1 and IT2). (**B**) TAMs induce T cell apoptosis through the activation of FAS ligand and TRAIL in T cells. (**C**) Macrophages also activate and recruit regulatory T cells to the tumor microenvironment by releasing diverse cytokines (IL-10 and TGFβ) and chemokines (CCL5, CCL20 and CCL22). (**D**) Finally, TAMs deplete T cell by producing arginase 1 (Arg1) that catalyzes the transformation of arginine, an essential metabolite for T cells, into NO *(Ugel, De Sanctis et al. 2015)*

The presence of lymph nodes in periphery of tumors allows the antigen presentation by APCs to T cells and the priming of cancer-specific T cells. Primed T cells then travel via the circulatory system to the tumor *(Joyce and Fearon, 2015).* The recognition of the neoantigens expressed on malignant cell membranes is mediated by both $CD4^+$ and $CD8^+$ T cells *(Gajewski et al., 2013)*. However, the number of effector T cells into the tumor is largely reduced and an exclusion phenomenon is observed. The reasons for this exclusion are the preferential recruitment of immune cells over others *(Quail and Joyce, 2013)*, the trapping of T cells in the stroma surrounding the tumor and the inhibition of the T cell extravasation from the vascular system to the tumor *(Joyce and Fearon, 2015)*. In addition, even when T cells overcome this exclusion barrier and reach the intratumoral areas, an immunosuppressive microenvironment leads to T cell anergy. This immunosuppressive microenvironment includes immunosuppressive cytokines (IL-10 and TGFβ), chemokines, PD-1/PD-L1 axis, IDO, ROS and hypoxia *(Gajewski et al., 2013).* Therefore, tumor immune cell infiltrates present a high heterogeneity between patients. Indeed, a tumor is so-called « hot » when infiltrated by a large number of suppressive T-cell (T-cell inflamed), or is conversely pretended as « cold » if tumor-infiltrating lymphocytes (TILs) are absent or trapped in the tumor margin (T-cell non-inflamed) *(van der Woude et al., 2017)*.
Mostly, the TIL population have been reported to correlate with a positive outcome in cancer patients *(Slaney et al., 2014)*. CTL subset play key roles in tumor regression and their presence is then associated to a good outcome for cancer patients *(Fridman et al., 2017)*. Although in physiological condition, Tregs play major functions by maintaining immunological self-tolerance, in cancer, these cells highly infiltrate the tumor and are associated with a poor outcome for patients *(von Boehmer and Daniel, 2013)*.

TAMs and T cells communicate and interact one with each other through the stimulation of receptors in direct contact as well as by the release of a multitude of cytokines, chemokines and enzymes (***Figure I.19***). Firstly, TAMs interfere with T cells by impairing their activation (***Figure I.19a***). In more details, macrophages expose several ligands to checkpoint receptors, such as PD-L1 and ligand of CTLA-4. These inhibitory ligands control the intensity of the immune response. The binding of PD-L1 or PD-L2 on macrophages to the receptor PD-1 on T cells interferes with T cell cytotoxic functions, regulates cell cycle and inhibits their activation *(Noy and Pollard, 2014).* These inhibitory ligands are not exclusively expressed by TAMs as they are also found on cancer cells. A recent publication also revealed the expression of PD-1 on TAMs, a subpopulation associated to low phagocytosis and immunosuppression in colon carcinoma-bearing mice and in patients with colorectal cancers *(Gordon et al., 2017).* The expression of B7-1, B7-2 and probably B7-H3 and B7-H4 ligands by macrophages inhibits T cell activation by their binding to CTLA-4 on T cells *(Komohara et al., 2016; Noy and Pollard, 2014)*. Besides, macrophages also express HLA-G that contributes to T cell inhibition *(Ugel et al., 2015).*
Secondly, TAMs induce T cell apoptosis through the binding of TRAIL-R or FAS-R to their corresponding ligands on T cells (***Figure I.19b***).
In addition, the release of chemokines, such as CCL17, CCL22 also contributes to promote tumor growth by stimulating the infiltration of natural Tregs into the tumor (***Figure I.19c***). This infiltration is attributed to the stimulation of the receptor CCR4 on Tregs by CCL17 and CCL22. Other chemokines, including CCL3, CCL4, CCL5, CCL18 and CCL20, all secreted by TAMs, also intervene in Treg recruitment *(Komohara et al., 2016; Noy and Pollard, 2014; Zheng et al., 2017).* Also, cytokines like TGFβ and IL-10 contribute to the inhibition of T cell proliferation and

activation while promoting survival of Tregs. Indeed, TGFβ inhibits CTLs, T_H1 and T_H2 $CD4^+$ T cells, while IL-10 represses only T_H1 and T_H2 $CD4^+$ helper T cells. High TGFβ expression also promotes macrophage infiltration into the tumor microenvironment and upregulates the transcription factor Foxp3 in $CD4^+$ T cells, inducing regulatory function of T cells (Tregs) *(Noy and Pollard, 2014)*.
Finally, in concert with MDSCs, TAMs produce arginase 1 and iNOS, thus depleting L-arginine in the tumor microenvironment. L-arginine is necessary for T cell functions (***Figure I.19d***). The conversion of L-arginine by arginase 1 also induces the production of ROS that impede T cell proliferation and functions *(van der Woude et al., 2017).*

3.5. Tumor regression: *anti-tumoral macrophages*

Through their anti-tumoral functions, M1-like macrophages are associated to a good prognostic in cancer *(Fridman et al., 2017)*. The roles of anti-tumoral TAMs in tumor suppression are mostly linked to their phagocytic functions and their antigen-presenting properties. In addition, M1-like macrophages produce high levels of reactive compounds (such as ROS and NO) and TNFα, which trigger apoptosis in cancer cells. However, this phenotype is usually absent or limited in tumors due to the immunosuppressive tumor microenvironment. It is why the anti-tumoral functions of TAMs were mainly revealed through the reprogramming of TAMs by anticancer therapies. Especially, the re-education of M2-like TAMs into anti-tumoral M1-like macrophages by chemotherapy, immunotherapy or radiotherapy, may be sufficient to induce tumor regression *(See Chapter 3)*.

4. Future directions

A lot of effort is made to further characterize macrophage functions in tumors. Recently, a mass cytometry study revealed 17 major TAM phenotypes in patients with clear cell renal cell carcinoma. Each macrophage subset would be involved in different functions into tumors and the presence of a phenotype over another would be associated with a worse or a better outcome *(Chevrier et al., 2017)*. Further investigations are needed to associate each macrophage subpopulation with a specific function and other mass cytometry analyses in different cancer types are required to transpose these results for all types of cancer. Nevertheless, the dissection of macrophages phenotypes and their associated functions should allow rethinking the binary M1/M2 classification. Moreover, a better knowledge of macrophage phenotype would allow to specifically target given subsets in order to drive tumor regression.

Chapter 2: Macrophage polarization, distinct signaling pathways

In order to detail the signaling pathways involved in anti- and pro-tumoral functions of macrophages, we will follow the usual macrophage classification, where M1 and M2 macrophages represent two extremes of a linear scale. In a cancer-free context, several conditions such as infections or tissue damage, determine the activation state of macrophages. In tumors, the denomination in M1 – like or M2 – like macrophages is more complex for several reasons. First, the activation state of macrophages is influenced by diverse macrophage origins and by multiple local microenvironments. Second, the tumor microenvironment is perpetually changing over the time and may continuously influence the phenotype of TAMs. Third, the specific function of « kill » or « repair », associated to M1 or M2 macrophages respectively is largely controversial in tumors since a lot of new functions are attributed to tumor-associated macrophages. To deal with such a complexity, it is not surprising that an oversimplification of this heterogenic scheme is necessary to connect phenotype (M1 versus M2) to functions (anti-tumoral versus pro-tumoral) and understand the tumor complexity *(Murray, 2017)*. In this chapter, we will browse the polarization signaling pathways of TAMs by reviewing the effects of different mediators such as cytokines, growth factors, nucleic acids and DAMPs (damage-associated molecular pattern), released in the tumor microenvironment and by analyzing the different signaling pathways involved in macrophage polarization. We will also summarize the effects of non-coding RNAs, hypoxia or some metabolites that also modulate the polarization of macrophages *(Escribese et al., 2012; Van den Bossche et al., 2017).*

1. Influence of the tumor microenvironment on macrophage polarization

1.1. Cytokines and other mediators

Once recruited into the tumor site, mostly by CCL2 and CSF-1 (or M-CSF), monocytes and tissue-resident macrophages are polarized by multiple factors *(Murray, 2017; Wang et al., 2014)*. Cancer-related inflammation is characterized by the presence of diverse cytokines like INFγ and TNFα or by the presence of other mediators such as GM-CSF (or CSF-2) or Toll-like receptor (TLR) ligands. These TLR ligands include microbial products (e.g. lipopolysaccharides; LPS) or cancer cell-derived products. All these factors are able to polarize macrophages towards a pro-inflammatory phenotype, referred to as the classically activated state or M1 macrophages. As the tumor grows, the pro-inflammatory microenvironment is switched to an immunosuppressive microenvironment. It is well accepted that the presence of IL-4, IL-10, IL-13, TFG-β and CSF-1 (M-CSF) within the tumor microenvironment allows the polarization of macrophages towards an anti-inflammatory phenotype, so-called the alternative activation state or M2 macrophages. This is induced by the binding of these factors to specific receptors, including IL-4Rα, IL-10R, TGFβR and CSF-1R. The binding of IL-34 on CSF-1R (or CD115) also induces M2-like polarization. In addition to cytokines, growth factors, such as EGF, lipids or PGE_2 also favor a M2-like phenotype, associated with pro-tumoral functions. *In vitro* models mainly use INFγ and LPS or GM-CSF to polarize macrophages into M1 phenotype, while IL-4 and IL-13 or M-CSF are

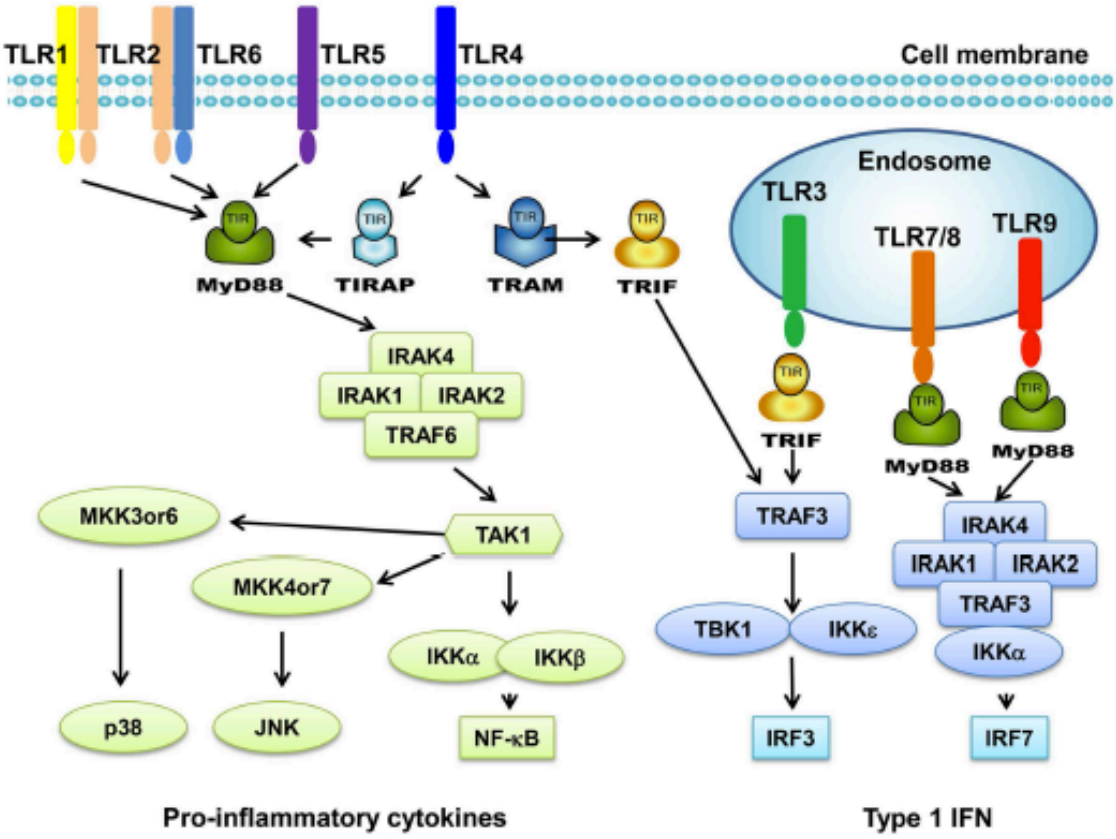

Figure I.20 – Toll-like receptors (TLRs) and related- signaling pathways

TLR family is composed of 10 members that are localized on cell membrane for TLR1, TLR2, TLR4, TLR5 and TLR6 while TLR3, TLR7, TLR8 and TLR9 are intracellular TLRs and required for nucleic acid recognition. Furthermore, TLR1 and TLR6 are stimulated only when they are heterodimerized with TLR2. Two different signaling pathways are triggered after TLR activation: the MyD88-dependent and MyD88-independent pathways. Upon stimulation, the cytoplasmic portion of TLR3, TLR4, TLR5, TLR7, TLR9 interacts with MyD88 and induces its activation. MyD88 then recruits different actors that trigger the activation of the NFκB axis and the c-Jun N-terminal kinase (JNK), thereby promoting the transcription of several pro-inflammatory cytokines. TLR3 and TLR4 also activate the MyD88 independent pathway that triggers IRF3 and NFκB and induces the production of IFNβ *(Zhao, Zhang et al. 2014)*.

applied to obtain M2 macrophages. This approach closely reproduces the interaction between $CD4^+$ T cells and macrophages, since T_H1 (e.g. IFNγ) or T_H2 (IL-4, Il-10 and IL-13) cytokines, released by T helper lymphocytes influence macrophage polarization. It was also shown that eosinophils and neutrophils produce IL-4 and IL-13 that induce M2-like polarization *(Jeannin et al., 2017; Mantovani et al., 2013; Murray, 2017; Wang et al., 2014; Zheng et al., 2017).*

1.2. Cancer cell –derived molecules and pattern recognition receptors (PRRs)

The activation of pattern recognition receptors (PRRs) is triggered by pathogen-associated molecular patterns (PAMPs) upon infection or by damage-associated molecular patterns (DAMPs), released from tissue destruction or by apoptotic or necrotic cells. These danger signals include alarmins (such as HMGB1), ATP and other mediators, as well as nucleic acids from dying cells *(Patidar et al., 2017).* In tumors, PRR activation regulates proliferation of malignant cells, cell survival and death, ROS production, angiogenesis and tissue remodeling and repair. Among PRRs, toll-like receptors (TLRs) and nucleotide binding and oligomerization domain (NOD)-like receptors (NLRs) are both receptors that, once activated, regulate NFκB and MAPK signaling pathways in macrophages *(Wang et al., 2014).*

The TLR family consists of 10 members and each member recognizes a specific component of pathogens (such as LPS) or element from host or cancer cells *(Takeda and Akira, 2004)*. Some examples are described here under. Self-DNA released from dying cancer cells activates TLR4. miRNAs in circulating cancer cell-derived exosomes triggers the activation of TLR7/8. Tumor-derived dsRNA or siRNA are recognized by TLR3 while tumor mitochondrial DNA activates TLR9 *(Patidar et al., 2017)*. TLR1, TLR2, TLR4, TLR5 and TLR6 are localized on cell membrane while TLR3, TLR7, TLR8 and TLR9 are intracellular TLRs and are required for nucleic acid recognition *(Zhao et al., 2014)*. The TLR signaling pathway shares a lot of similarities with the IL-1R signaling axis *(Takeda and Akira, 2004)*. Briefly, two different signaling pathways are triggered after TLR activation: the MyD88-dependent and MyD88-independent pathway (***Figure I.20***). Upon stimulation, the cytoplasmic portion of TLR3, TLR4, TLR5, TLR7, TLR9 interacts with MyD88 and induces its activation. MyD88 then recruits TIR domain-containing adaptor (TIRAP) and MyD88-adaptor-like (Mal) for their activation. Once stimulated, these adaptors performed the activation of the interleukin-1 receptor-associated kinase 4 (IRAK-4), which is followed by the phosphorylation of IRAK-1. Phosphorylated IRAK-1, together with the TNFR-associated factor 6 (TRAF6), dissociates from the receptor to recruit other complexes that drive the activation of the NFκB axis and the c-Jun N-terminal kinase (JNK), thereby promoting the transcription of several pro-inflammatory cytokines. Another member of IRAK family, IRAK-M, negatively regulates this pathway by inhibiting the association of MyD88 to the TLR cytoplasmic portion *(Takeda and Akira, 2004)*.
In addition, TLR3 and TLR4 also mediate the MyD88-independent pathway, which leads to the activation of the interferon regulatory factor 3 (IRF3) and NFκB, through the activation of IκB kinases ε (IKKε) and IKKι by the TIR domain-containing adaptor inducing IFNβ (TRIF). The activation of MyD88-independent pathway induces the production of IFNβ *(Takeda and Akira, 2004).*

In murine models of melanoma, the expression of IRAK-1 and TRAF6 is reduced in TAMs when compared to peritoneal macrophages, impeding the M1-like polarization of macrophages. In addition, the high expression of IRAK-M in TAMs, but not in peritoneal macrophages, abrogates MyD88 and TLR4 or TLR9 association *(Banerjee et al., 2011)*. Even upon LPS stimulation, normally triggering the activation of TLR4, IRAK-M promotes MyD88 degradation *(Standiford et al., 2011)*. However, MyD88-independent pathway is partially functional in TAMs and is responsible for the production of IL-10. Indeed, TLR3 stimulation in TAMs from melanoma bearing mice promoted the release of IL-10 and TGFβ while decreasing the expression of IL-12 through the decrease in histone phosphorylation at promoter region. These modifications are generated by the activation of extracellular signal-regulated kinase (ERK) *(Banerjee et al., 2011)*. Until now, the association between TLR members and macrophage phenotype is poorly characterized. However, it seems that TLR1, TLR2, TLR3 TLR8 stimulation would induce a M2 phenotype while the activation of TLR3, TLR4, TLR7 and TLR9 would promote the classical activation (M1) in macrophages *(Banerjee et al., 2011; Patidar et al., 2017; Peng et al., 2013; Wang et al., 2014).*

The activation of NLRs in TAMs has been less much studied than was TLR stimulation. The activation of these intracellular receptors positively or negatively regulates NFκB. Indeed, the activation of most NLRs contributes to inflammation in tumorigenesis by triggering the inflammasome. In contrast, NLRC3 and NLRP12, both inhibit the canonical NFκB signaling pathway by targeting TRAF6 or IRAK1 respectively *(Allen, 2014)*.

1.3. Angiopoietin 2

The angiopoietin 2 (Ang2) polarizes macrophages towards a M2-like phenotype by its binding to the Tie2 receptor, thereby inducing the inhibition of NFκB and HIF1α in tumor *(Tyagi et al., 2009)*. This M2-like polarization is translated into a high expression of M2 markers (CD206 and IL-10) and angiogenic markers (MMP2, VEGF, COX2, cathepsin B and thymidine phosphorylate (TP)), while there is a low level of M1 markers such as IL-6, IL-12 and TNFα *(Coffelt et al., 2011; De Palma and Naldini, 2011; Forget et al., 2014; Lewis et al., 2007)*. This is added to the fact that IL-10 and CSF-1 are also able to upregulate the expression of Tie2 in human peripheral blood mononuclear cells (PBMC) *(Forget et al., 2014; Garcia et al., 2014)*. Ang2 is mainly released by endothelial cells and cancer cells. However, the mechanism through which Ang2 impedes the pro-inflammatory phenotype in macrophages is poorly understood and needs further investigations.

2. Signaling pathways

Different signaling pathways are triggered after the stimulation of receptors. The signaling pathways are usually complementary and overlap to induce a specific phenotype. Depending on mediators released in the tumor microenvironment, activated signaling pathways modulate macrophage polarization towards M1-like, M2-like or mixed M1/M2 phenotype, with more or less robustness. NFκB is a central signaling axis of macrophage polarization, as well as the IRF/STAT pathway. However, other signaling pathways may also modulate the activation state of macrophages.

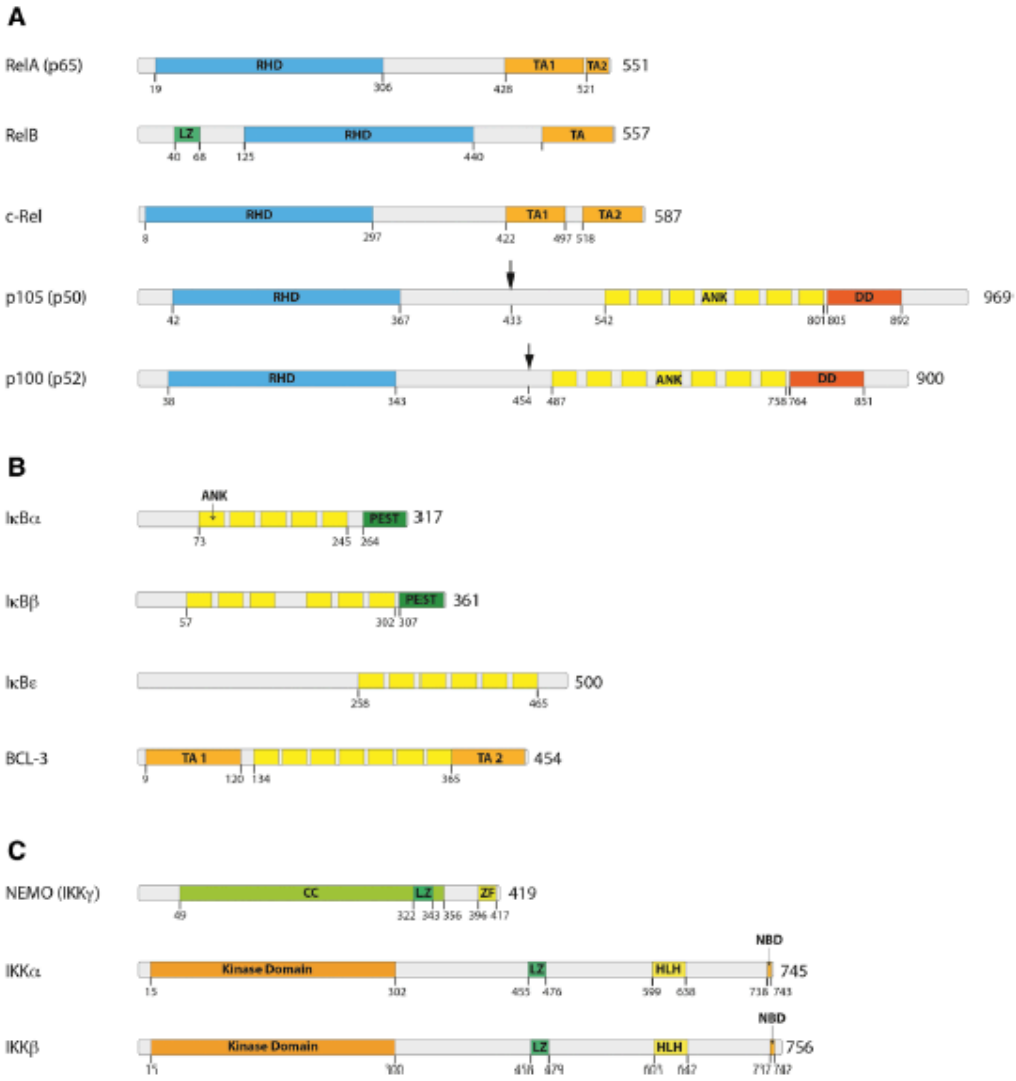

Figure I.21 – NFκB family members, inhibitory kinases of NFκB (IκB) and IκB kinases

(A) The NFκB family consists of 5 members: RelA (p65), RelB, c-REL, NFκB1 (p105) and NFκB2 (p100). A Rel homology domain (RHD), allowing DNA binding, as well as homo- and heterodimerization, composes each member of the NFκB family. RelA, RelB and c-Rel are characterized by transactivation domains (TAs) that are essential for transcriptional activity. p105 and p100 are processed in p50 and p52 by the cleavage of the inhibitory ankirin repeat domain (ANK). Indeed, in the pro-forms (p105 and p100), the ankirin repeat domains are linked to the RDH domain and prevent DNA binding.

(B) The IκB family is composed by 4 members: IκBα, IκBβ, IκBε and BCL-3. These members consist of ankirin repeat domains (ANK) that mediate the inhibition of NFκB. PEST domains contain proline, glutamate, serine and threonine. BCL-3 differs from the other members by containing TA domains that are necessary for transcriptional activity when this member is associated to NFκB dimers for DNA binding.

(C) There are three IKK proteins that form a complex: IKKγ (NEMO), IKKα and IKKβ. NEMO differs from the two others IKK members by its CC (coiled-coil domain) and ZF (zing-finger domain) domains. The three members possess a LZ domain (leucin zipper-like motif) while only IKKα and IKKβ have HLH (helix-loop-helix domain), NBD (NEMO-binding domain) domains and a kinase catalytic domain *(Hoesel and Schmid 2013)*.

2.1. NFκB

2.1.1. NFκB signaling pathway

NFκB was first discovered in B cells as a nuclear factor binding to the enhancer element of the immunoglobulin kappa light-chain. In reality, NFκB is expressed in nearly all cell types. NFκB consists of homodimers or heterodimers of the Rel family members comprising RelA (or p65), RelB, c-Rel, NFκB1 and NFκB2 (***Figure I.21. A***). These two last members are pro-forms that are processed to p50 and p52 respectively. Indeed, p50 and p52 are formed by the cleavage of the inhibitory ankyrin repeat domains of their respective pro-forms *(Hoesel and Schmid, 2013)*. All members are characterized by a Rel homology domain that mediates their DNA binding and dimerization. RelA, RelB and c-Rel contain transactivation domains (TAs) which are essential for transcription activity, while dimers of p50 and p52 lack this transactivation domain and act as transcriptional repressors *(Biswas and Lewis, 2010; Hagemann et al., 2009)*. NFκB targets different genes and is thus connected to diverse functions. Indeed, the expression of target genes is differently regulated by the different NFκB dimers, in function of their differential preferences for variations of the DNA-binding sequence (***Figure I.21. B***). In resting cells, inhibitor of NFκB (IκB) proteins (IκBα, IκBβ and IκBε) sequester NFκB dimers in the cytoplasm by binding their DNA-binding domain, thereby making them transcriptionally inactive *(Hoesel and Schmid, 2013).*

Three different NFκB pathways exist: the canonical or classical NFκB pathway involving p50 and p65 subunits, the non-canonical or non-classical NFκB pathway requiring p52 and RelB and the atypical NFκB pathway (***Figure I.22***) *(Biswas and Lewis, 2010; Hoesel and Schmid, 2013)*. In the canonical pathway, the stimulation of TLRs, IL-1R or TNFR allows the activation of IKK complex composed by IKKα, IKKβ and IKKγ (also called NEMO for NFκB essential modulator) (***Figure I.21. C***). Once IKKβ is phosphorylated, IKK complex triggers the phosphorylation, the ubiquitination and the degradation of IκB, releasing NFκB dimer. Freed NFκB dimer translocates into the nucleus to activate the transcription of pro-inflammatory target genes (TNFα, IL-1β, IL-6, IL-12, CCLs, CXCLs and SOCS3) or pro-survival genes (B-cell lymphoma protein 2 (Bcl-2), Fas receptor, Fas ligand, A20) *(Biswas and Lewis, 2010; Karin and Ben-Neriah, 2000; Sica and Mantovani, 2012; Wang et al., 2014).* In the non-canonical pathway, the stimulation of CD40, the receptor activator for nuclear kappa B (RANK), the B-cell activation factor (BAFF-R) or the lymphotoxin β-receptor (LTβR) activates IKKα through the NFκB-inducing kinase (NIK). The activation of IKKα induces the proteosomal processing of p100 into p52, releasing the heterodimer p52 – RelB that activates the transcription of target genes. In the atypical pathway, genotoxic stress activates the ataxia telangiectasia mutated (ATM) checkpoint kinase that subsequently recruits NEMO into the nucleus. The sumoylation, followed by the ubiquitination of NEMO, allows the complex NEMO/ATM to return into the cytosol to phosphorylate IKKβ and then to trigger the activation of the canonical NFκB pathway.

These three different pathways are activated by the stimulation of receptors (e.g. TLRs, TNFR or CD40) or through intracellular modulators (e.g. ROS, DNA damage or MAPK). For example, NFκB closely interacts with MAPK, including JNK and p38. While p38 acts as a cofactor in NFκB activation, JNK usually inhibits NFκB pathway. Other kinases have also been reported to modulate NFκB pathways, such as PKC or PI3K-Akt. Finally, mRNAs encoding different NFκB

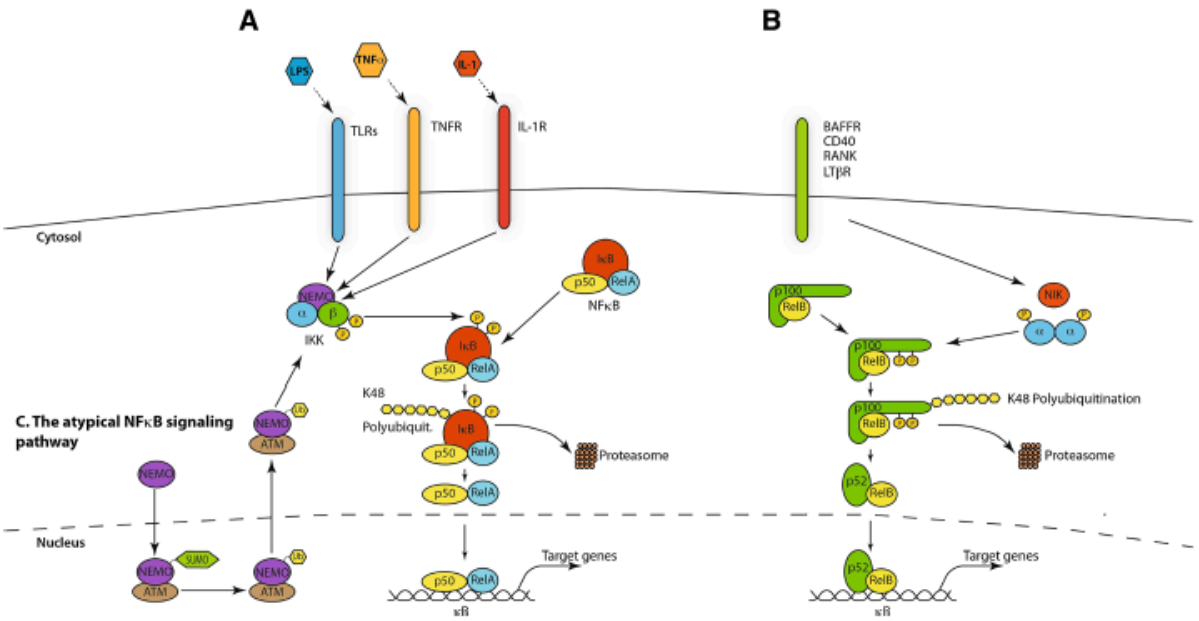

Figure I.22 – NFκB signaling pathways

There are three different NFκB pathways: the canonical or classical NFκB pathway, the non-canonical or non-classical NFκB pathway and the atypical NFκB pathway.

In the *canonical pathway*, the stimulation of TLRs, IL-1R or TNFR allows the activation of IKK complex triggering the phosphorylation, the ubiquitination and thereby the degradation of IκB. Freed NFκB dimer translocates into the nucleus to activate the transcription of pro-inflammatory target genes.

In the *non-canonical pathway*, the stimulation of CD40, the receptor activator for nuclear kappa B (RANK), the B-cell activation factor (BAFF-R) or the lymphotoxin β-receptor (LTβR) activates IKKα through the NFκB-inducing kinase (NIK). The activation of IKKα induces the proteosomal processing of p100 into p52, releasing the heterodimer p52 – RelB that activates the transcription of target genes.

In the *atypical pathway*, genotoxic stress activates the ataxia telangiectasia mutated (ATM) checkpoint kinase that subsequently recruits NEMO into the nucleus. The sumoylation, followed by the ubiquitination of NEMO, allows the complex NEMO/ATM to return to the cytosol to phosphorylate IKKβ and then to trigger the activation of the canonical NFκB pathway *(Hoesel and Schmid 2013)*.

subunits are targeted by diverse miRNAs that fine-tune their expression, hence the activity of NFκB. In return, NFκB also regulates miRNA transcription, such as the processing and the maturation of Let-7 miRNA family *(Hoesel and Schmid, 2013)*.

2.1.2. Role of NFκB in TAMs

In macrophages, the active heterodimer p50 – p65 allows the transcription of pro-inflammatory genes (e.g. IL-6, IL-8, IL-12, TNFα), promoting the M1 phenotype, while the inhibitory homodimer NFκB p50 – p50 impedes the activation of pro-inflammatory genes by competing with the binding of the heterodimer p50 – p65 at the promoter region of these genes. In addition, the repressive homodimer p50 – p50 is necessary for the transcription of COX2, IL-10 and TGFβ *(Biswas and Lewis, 2010)*.
In TAMs, the p65 subunit is involved in inflammation–mediated tumor initiation through the transcription of IL-6, TNFα and IL-1β. However, as the tumor grows, a switch in NFκB dimers, from p50 – p65 towards p-50 – p50, allows TAMs to be re-educated towards an anti-inflammatory and immunosuppressive phenotype *(Biswas and Lewis, 2010; Hagemann et al., 2009).*

2.1.3. Localization of NFκB in TAMs

The localization of NFκB p50 and p65 subunits may reveal a lot on their activity. Interestingly, TAMs from mice and human ovarian cancers showed nuclear localization for NFκB p50, while NFκB p65 was sequestered in the cytoplasm, even upon LPS-mediated TLR stimulation. The defective activation of p65 NFκB correlated with a reduced pro-inflammatory cytokines in TAMs *(Saccani et al., 2006)*. In line with these observations, the cytoplasmic localization of NFκB p65 was also observed in microglia and TAMs derived from glioblastoma *(Mieczkowski et al., 2015)*. Besides the defective nuclear translocation of NFκB p65, this subunit is also subjected to proteosomal degradation in cytoplasm or nucleus *(Karin and Ben-Neriah, 2000; Tanaka et al., 2007)* or may also be eliminated by TLR2-dependent selective autophagy in hepatoma-educated macrophages. In the last case, NFκB p65 was ubiquitinated and directed in aggresome-like structures, recognized by autophagosomes and then degraded by fusion with lysosomes. This mechanism was shown to be dependent on TLR2 stimulation, as NFκB p65 activation was restored in hepatoma-educated TLR2 $^{-/-}$ macrophages. Furthermore, this mechanism relied on the activation of ERK1/2 *(Chang et al., 2013)*. Another receptor involved in p65 subunit degradation is IL-10R and its blockade re-established NFκB p65 – p50 in macrophages *(Sica et al., 2000b)*.

2.1.4. Inactivation of NFκB in TAMs

In order to understand the influence of NFκB signaling in myeloid cells on tumor growth, several groups used the targeting of IKKβ in myeloid cell lineage. These experiments generated conflicting results. On one side, several studies revealed the beneficial effect of NFκB inactivation on tumor growth. For example, deletion of IKKβ in myeloid cells reversed tumor progression in colon and hepatic cancer mice models *(Greten et al., 2004; Maeda et al., 2005)*. In

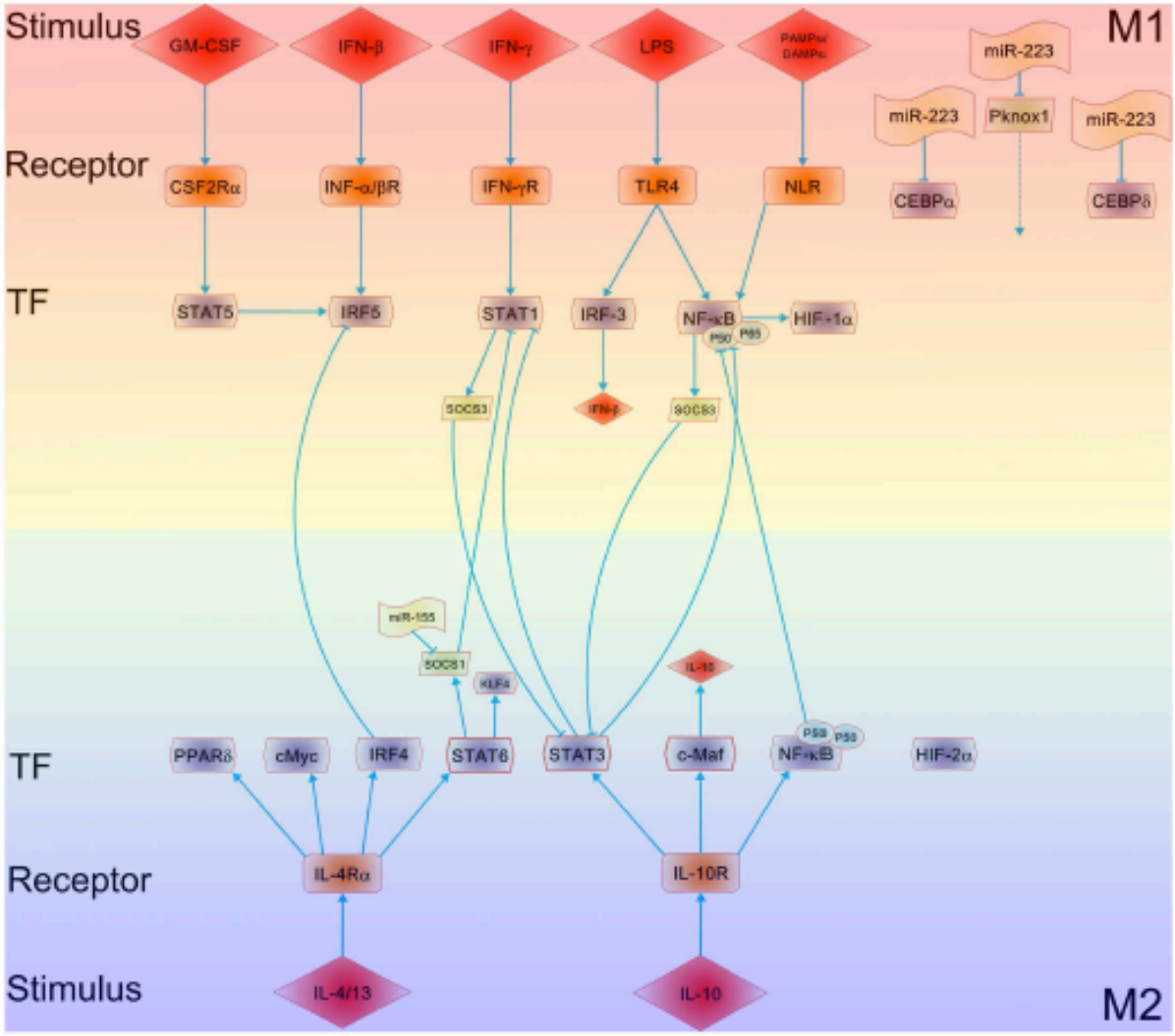

Figure I.23 – Overview of signaling pathways involved in macrophage polarization
IRF/STAT pathway is a major axis in macrophages polarization as the balance between activated STAT1 and STAT3/STAT6 finely tunes macrophage phenotype. STAT1, IRF3/5 and NFκB p65 – p50 predominate in M1 macrophage polarization and are associated with pro-inflammatory and cytotoxic functions, while STAT3/STAT6, IRF4 and NFκB p50 – p50 trigger M2 phenotype and control anti-inflammatory and immunosuppressive functions. In this signaling network, SOCS1 and SOCS3 are both inhibitors of STAT1 and STAT3 respectively, that reinforce one or the other activated IRF/STAT pathway. Other mediators, such as PPARδ, cMyc, c-Maf, also contribute to M2 polarization. Finally, hypoxia is also involved in the activation status of macrophages: HIF1α is associated to M1 phenotype while HIF2α promotes M2 polarization *(Wang, Liang et al. 2014)*.

addition, the adoptive transfer of IKKβ-inhibited BMDMs or TAMs reduced tumor growth in an ovarian cancer model *(Hagemann et al., 2008)*. On the other side, other studies evidenced that myeloid deletion of IKKβ in other cancer models, such as angiosarcoma or melanoma, was associated with tumor growth *(Yang et al., 2014a; Yang et al., 2012)*. Furthermore, the inducible expression of IKK, and then the activation of NFκB in macrophages aborted lung metastasis emergence and was associated with a pro-inflammatory phenotype in lung macrophages. However, these effects were observed only when the inducible activation was performed before tumorigenesis *(Connelly et al., 2011)*. The divergence of the results regarding IKKβ targeting may be due to the use of different cancer models. In addition, the targeting of IKKβ generated myeloid cell lineage with inactivation for several NFκB members, impeding to define the precise role of each subunit.

Other groups have investigated the specific targeting of p50 or p65 subunit. For instance, fibrosarcoma and melanoma tumor growth was slowed in NFκB p50-deficient mice and in $p50^{-/-}$ bone marrow chimera, due to tumor infiltration by M1-like TAMs *(Saccani et al., 2006)*. In addition, peritoneal macrophages, that were tumor-educated with condition medium from colon cancer cell line (colon-26), were repolarized from M2 to M1-like macrophages upon p50 siRNA-mediated silencing *(Kono et al., 2014)*. In this way, it could be speculated that, in the absence of the repressive homodimer NFκB p50 – p50, TAMs would be easily reprogrammed towards the M1 phenotype through the activation of complementary pathways. The specific targeting of p65 in myeloid cells revealed antitumor properties in a glioblastoma model. Indeed, the suppression of the p65 subunit in myeloid cells allowed the polarization of the microenvironment in an immunocompetent one, reducing the presence of $CD206^{+}$ macrophages (M2) and MDSCs while increasing the number of $CD86^{+}$ dendritic cells, $CD86^{+}$ M1 macrophages and T cells *(Achyut et al., 2017)*. A lot of different myeloid cells contribute to the fate of tumor: macrophages (TAMs), monocytes MDSCs, neutrophils, eosinophils, basophils and microglia in the case of brain tumor. Therefore, by targeting p65 in myeloid cells, several cell types may be differently influenced and thus favor or repress tumor growth. It is why, in order to precisely study the involvement of the heterodimer p50 - p65 in TAM phenotype and its influence on tumor growth, NFκB p65 should be specifically targeted in TAMs.

2.2. IRF/STAT

The interferon regulatory factors (IRF) and the signal transducers and activators of transcription (STAT) signaling pathway is one of the most important axis regulating macrophage polarization (***Figure I.23***). This signaling pathway comprises diverse members (STAT 1 – 6 and IRF 1 – 9) that differently modulate macrophage polarization: STAT1, STAT5, IRF1, IRF3 and IRF5 are known to induce M1 polarization while STAT3, STAT6 and IRF4 are involved in M2 polarization.

2.2.1. M1 activation

Numerous studies have revealed the activation of STAT1 and STAT5 in M1 macrophages upon the binding of IFNγ to IFNγR or CSF2 (or GM-CSF) to CSF2Rα. In the same line, type I IFNs, such as IFNα and IFNβ, also activate the transcription factor STAT1 upon their binding to the type I

interferon receptor (IFNAR) *(Wang et al., 2014)*. The regulation of STAT1 is performed through the inhibition of this transcription factor by the suppressor of cytokine protein 1 (SOCS1), itself regulated by STAT6 (M2-like transcription factor) *(Zhou et al., 2014)*. Besides, GM-CSF promotes the phosphorylation of STAT5 that subsequently activates IRF5 *(Wang et al., 2014)*. IRF5 is also activated by IRF1 through IFNβ stimulation that leads macrophages to adopt a M1-like phenotype *(Xie et al., 2016)*. Indeed, IRF5 subsequently interacts with NFκB p65 to enhance the expression of IL-12 and IL-23 *(Amici et al., 2017)*. Regarding other IRF members, the stimulation of IFNγR and TLRs triggers the activation of IRF3. IRF8 also contributes to the M1 macrophage polarization by its binding to TRAF6 thus inducing TNFα, IL-1β and IL-12 secretion *(Amici et al., 2017; Zhao et al., 2006)*. Actually, a lot of pro-inflammatory cytokines and PAMPs may trigger the activation of IRF/STAT pathway and lead to M1 polarization *(Amici et al., 2017)*. The activation of these transcription factors drives the expression of different pro-inflammatory mediators such as TNFα, IL-1β, IL6, IL-12, IL-23, ROS and iNOS in macrophages *(Amici et al., 2017; Zheng et al., 2017).*

2.2.2. M2 activation

The activation of IRF/STAT signaling is also triggered in M2-like macrophages by stimuli such as IL-4, IL-10 or IL-13. Indeed, IL-4 or IL-13 activates STAT6 through the stimulation of IL4Rα whereas IL-10 binds to IL-10R and stimulates STAT3 *(Wang et al., 2014)*. The polarization of macrophages towards the M2 phenotype also includes the activation of IRF4 via the binding of IL-4/IL-13 to IL-4Rα. The activation of these transcription factors allows the transcription of genes like IL-10 and TGFβ, associated to the M2 polarization of macrophages *(Mantovani and Locati, 2013)*. As in M1 macrophages, this axis is regulated by inhibitory proteins. Specifically, SOCS3, activated by STAT1 and NFκB p50 – p65, mediates the regulation of STAT3 by inhibiting this transcription factor (Wang et al., 2014).

2.2.3. IRF/STAT in TAMs

In most tumors, TAMs present a reduced level of M1-like IRF/STAT transcription factors (STAT1, IRF1, IRF7 and IRF8) and an increased activation of M2-associated IRF/STAT transcription factors (STAT3, STAT6 and IRF4). Indeed, compared to macrophages that are not educated by cancer cells such as peritoneal macrophages, TAMs present a higher phosphorylated STAT3 in mice bearing mammary tumors (D1-DMBA-3). This activation status in TAMs is correlated to a M2-like phenotype and to promotion of tumor growth *(Rodriguez et al., 2013)*. It explains why STAT3 silencing in TAMs reduced the tumor growth in hepatocellular carcinoma cancer model *(Wan et al., 2014)*. In the same line, the expression of STAT6 was upregulated in M2-like tumor-educated macrophages co-cultured with colorectal cancer cells (CT26) *(Chen et al., 2016b)*. STAT6 was also activated in TAMs from breast cancer patients and the inhibition of this transcription factor in mouse bearing breast carcinoma (4T1) induced a decreased in M2 markers and was associated with tumor regression *(Binnemars-Postma et al., 2018).* In patients with clear cell renal cell carcinoma, IRF4 was upregulated in TAMs and correlated with a poor prognosis *(Dannenmann et al., 2013)*. Indeed, the activation of IRF4 was shown to be dependent on the mechanistic target of rapamycin complex 2 (mTORC2) activation in M2-like TAMs through an increased glucose metabolism. It is why the loss of mTORC2 activity

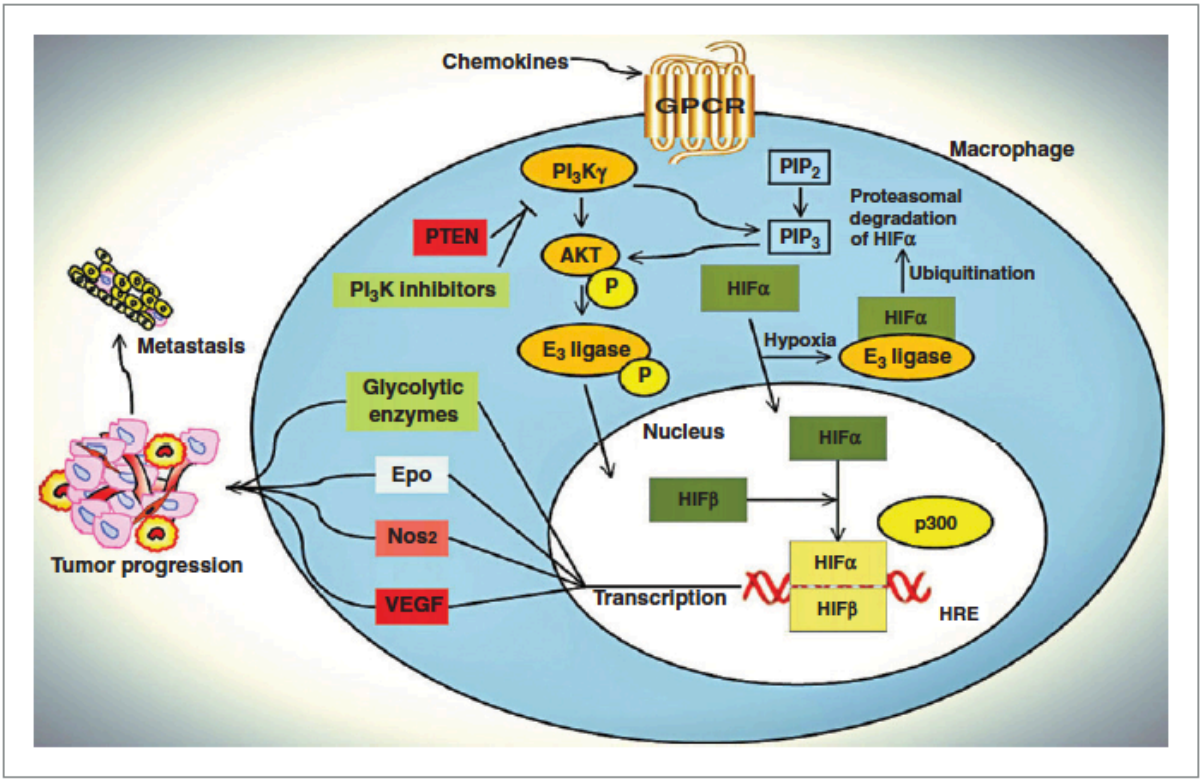

Figure I.24 – PTEN/PI3Kγ/Akt signaling pathway

Activated PI3Kγ recruits Akt and the mechanistic target of rapamycin complex 2 (mTORC 2), which allows the activation of Akt. The Akt-mediated phosphorylation, and then the degradation of an E3 ligase allow HIFα to translocate into the nucleus. Consequently, the association between HIFα and HIFβ induces the transcription of genes that promote tumor growth and metastasis. In this axis, the phosphatase and TENsin homolog (PTEN) is a negative regulator of the PI3Kγ/Akt *(Joshi, Singh et al. 2014)*.

in melanoma B16-bearing mice repressed tumor growth by decreasing IRF4 in TAMs *(Huang et al., 2016b)*.
In contrast, TAMs present a lower phosphorylated STAT1 level in mice bearing mammary tumors (DA-DMBA-3) *(Rodriguez et al., 2013)*. The activation of STAT1 was only observed in premalignant lesions and was associated to M1-like macrophages and cancer-related inflammation *(Mori et al., 2015)*. As some miRNAs may prevent the activation of STAT1, the suppression of miRNA-processing enzyme DICER induced an increased expression of STAT1 and a reprogramming of TAMs towards a M1-like antitumor phenotype *(Baer et al., 2016)*. IRF3 was also shown to be absent in TAMs from fibrosarcoma-bearing mice while it was translocated into nucleus after LPS treatment, a TLR ligand known to induce M1-like phenotype *(Biswas et al., 2006)*. The activation of IRF8 is more controversial. A study revealed the involvement of IRF8 in TAMs, stimulated by CXCL16, in suppressing liver metastasis in colorectal cancer *(Kee et al., 2014)*. However, in glioblastoma, a high level of IRF8 in hypoxic TAMs drove the release of CCL4, promoting cancer cell invasion *(Wang et al., 2016b)*. Another study also suggested that the inhibition of IRF8 in TAMs was beneficial for tumor regression in a fibrosarcoma model *(Strauss et al., 2015)*. Other studies revealed that the activation of IRF1 and IRF7 in TAMs triggered their anti-tumor properties. For example, the transduction of primary macrophages with adenoviral vectors of constitutively active forms of IRF7 induced IFN release that triggers anti-tumor properties of TAMs *(Goubau et al., 2009; Romieu-Mourez et al., 2006)*. Also, mitochondrial fission, driven by a mitochondrial outer membrane protein after TLR4 stimulation, promoted IRF1 activation in TAMs and was associated with IL-12a production and anti-tumor immune response *(Gao et al., 2017)*.
Therefore, the IRF/STAT pathway linked to M1 polarization is aborted in TAMs, while the IRF/STAT transcription factors associated to the M2 phenotype are upregulated. Furthermore, this pathway is closely interconnected to NFκB and these pathways may act together to finely tune the polarization of TAMs *(Wang et al., 2014)*.

2.3. PI3Kγ/Akt pathway

The phosphoinositide 3 kinase p110γ (PI3Kγ) and serine-threonine protein kinase Akt pathway (***Figure I.24***) is activated by the stimulation of TLR or other receptors (e.g. IL1-0R). Indeed, several factors such as TGFβ and IL-10, promote M2-like polarization through the activation of PI3Kγ/Akt pathway *(Antoniv and Ivashkiv, 2011; Zhang et al., 2016)*. Activated PI3Kγ recruits Akt, also known as protein kinase B, and mTORC 2, which allows the activation of Akt *(Vergadi et al., 2017)*. Phosphorylated Akt then activates mTORC1, which also acts as a negative regulator of Akt. It was shown that mTORC1 contributes to the M1-like phenotype while mTORC2 promotes the M2-like phenotype *(Mazzone et al., 2017)*.
In TAMs, as in M2-like macrophages, PI3Kγ is necessary for the activation of Akt, mTOR and the CCAAT/enhancer-binding protein β (c/EBPβ). These factors trigger the expression of anti-inflammatory and immunosuppressive factors such as Arg1, TGFβ and IL-10 *(Wenes et al., 2016)*. It is why the inhibition or the deletion of PI3Kγ led to the expression of pro-inflammatory cytokines like IL-12, IFNγ and NOS2 (iNOS), by promoting NFκB activation *(Kaneda et al., 2016)*. PI3Kγ was also involved in HIFα stabilization in TAMs from a Lewis lung cancer mouse model. Briefly, p110γ (PI3Kγ) controlled the stabilization of HIF1α and HIF2α, allowing the transcription of target genes (e.g. VEGF). The transcription of these genes thereby favored to

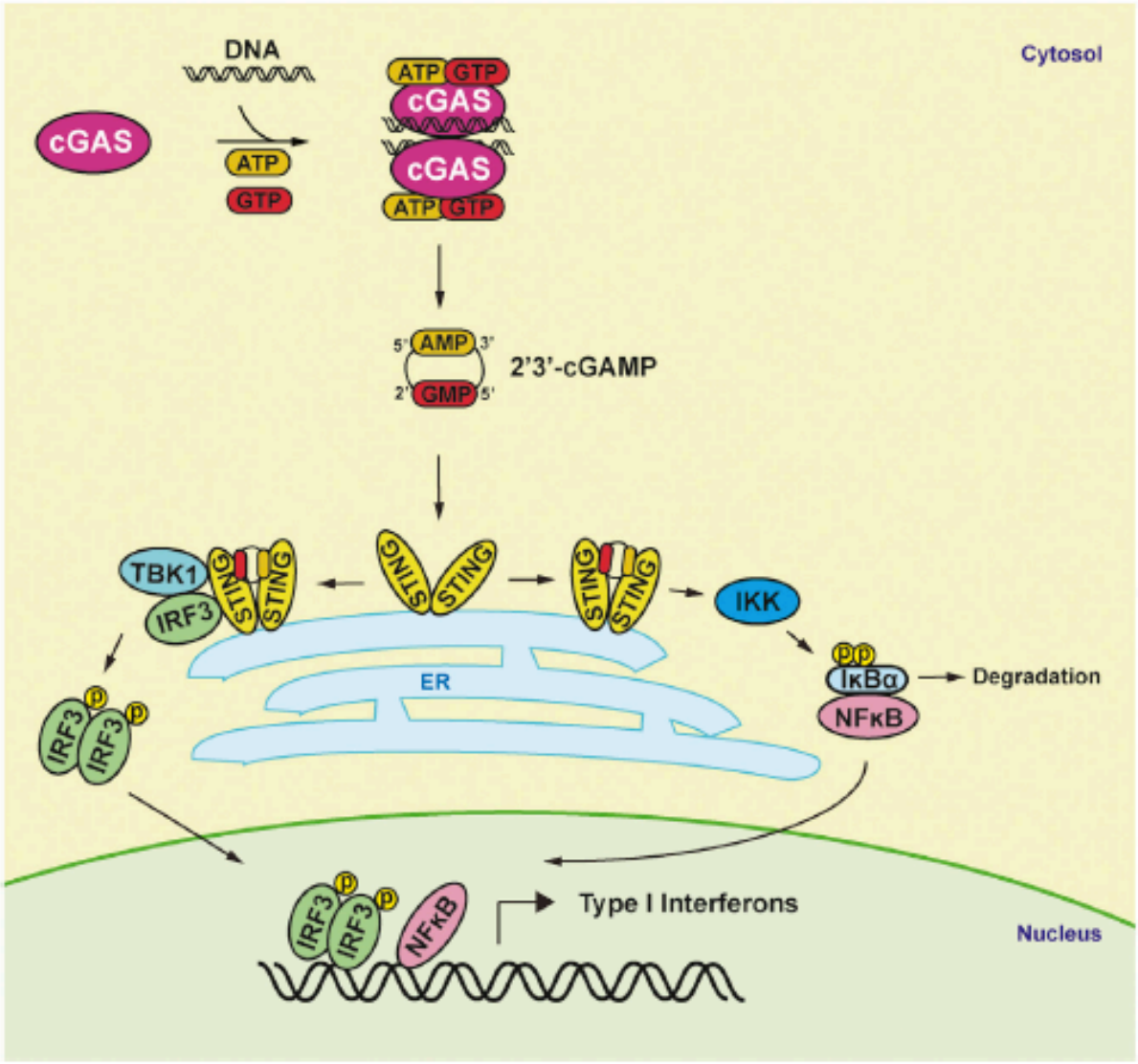

Figure I.25 – cGAS/STING pathway

Cytosolic DNA triggers the activation of cGAS, allowing the synthesis of 2'3'cGAMP from ATP and GTP. This ligand binds STING dimers that recruit TBK1 for the activation of IRF3. STING may also activate IKK, releasing NFκB from IκBα sequestration. IRF3 dimers and NFκB work together to finally induce IFN I gene transcription *(Cai, Chiu et al. 2014)*.

angiogenesis, metastasis and tumor growth *(Joshi et al., 2014)*. In addition, the inhibition of c/EBPβ by miR-155 skewed macrophages in a M1-like phenotype and prevented the expression of Arg1 *(Wu et al., 2016)*. In contrast, the activation of mTORC1 was also responsible for a metabolic switch in macrophages that inhibited angiogenesis and prevented metastasis *(Wenes et al., 2016)*

The phosphatase and TENsin homolog (PTEN) is a negative regulator of the PI3Kγ/Akt as the loss of PTEN increased Akt activity and impeded the M1 phenotype induced by LPS *(Sahin et al., 2014)*. In a tumor context, PTEN $^{+/-}$ prostate cancer bearing mice exhibited a higher TAM infiltration that was related to bigger tumor size *(Fang et al., 2013)*. These results were confirmed by a decreased expression of TNFα in prostate cancer patients with a low PTEN mRNA levels *(Armstrong et al., 2016)*. In contrast, the overexpression of PTEN in Raw264.7 macrophages co-cultured with breast carcinoma cells (4T1) led to an increased protein expression of iNOS and a decrease in Arg1 protein levels *(Li et al., 2015a).*

2.4. cGAS/STING

Double and single stranded DNA or RNA from bacteria or extracellular pathogens, as well as DNA from dying cancer cells or damaged cells may polarize macrophages. TLR3 and TLR7 are both pattern-recognition receptors that detect double and single stranded DNA in macrophages *(Akira, 2006; Beutler et al., 2006)*. The activation of TLRs by tumor-derived DNA contributes to the polarization of TAMs towards a M1 phenotype. Cyclic GMP-AMP synthase (cGAS) is an intracellular sensor for all forms of structured DNA (or double strand DNA) that activates innate immune responses *(Chen et al., 2016a)*. In more details, the binding of cytosolic DNA to cGAS induces a conformation change in the active site of cGAS, generating cyclic GMP-AMP (cGAMP) from ATP and GTP. cGAMP acts as a second messenger and binds to the endoplasmic-reticulum (ER)-membrane stimulator of interferon gene (STING). This binding promotes a conformational change and then the activation of STING, leading to its trafficking from the ER to the Golgi apparatus. During this process, STING recruits and activates the TANK-binding kinase 1 (TBK1) which in turn phosphorylates the transcription factor IRF3. The phosphorylation of IRF3 allows the dimerization of IRF3 and then the nuclear translocation of this transcription factor. STING also activates the kinase IKK, leading to the subsequent nuclear translocation of NFκB. IRF3 and NFκB work concomitantly to increase the expression of pro-inflammatory genes, such as TNFα, IL-1β and IL-6. This process can be inhibited by TREX1 (three-prime repair exonuclease 1), a cytoplasmic exonuclease, which degrades cytoplasmic DNA (***Figure I.25***) *(Cai et al., 2014; Chen et al., 2016a)*.
Other DNA sensors were also discovered, including DAI, DDX41, DNA-PK and IFI16 *(Chen et al., 2016a)*. Interferon gamma inducible factor 16 (IFI16) binds to single and double-stranded DNA and is required for cGAS/STING pathway signaling in macrophages. IFI16 also participates to the recruitment and the activation of TBK1 in STING complex. It has to be noted that IFI16 does not have any analog in mice *(Jonsson et al., 2017)*.

In tumor, the activation of cGAS by cancer cell-derived DNA is usually found in phagocytes and triggers an anti-tumor immunity. The activation of cGAS by self cytosolic DNA also triggers cGAS/STING pathway and leads to IFN signaling *(Chen et al., 2016a)*. Interestingly, it was shown

that the activation of STING by its agonist 5,6, dimethylxanthenone-4 acetic acid (DMXXA) reprogramed M2-like macrophages towards a M1 phenotype in a non-small cell lung carcinoma bearing mice *(Corrales et al., 2016)*. Bacterial cyclic dinucleotides (CDNs) such as cyclic di-guanine (RR-CDG) may also bind to STING. The combination of RR-CDG to radiotherapy blocked the M2 polarization of bone marrow-derived macrophages by decreasing IL-10 secretion. This treatment also increased the secretion of TNFα in TAMs from a Panc02 mouse model *(Baird et al., 2016)*. Furthermore, macrophage depletion using clodronate liposome abrogated the antitumor effects associated to STING activation by intratumoral administration of cGAMP *(Ohkuri et al., 2017)*. Therefore, it seems that the cGAS/STING pathway is an essential activator of the M1 phenotype in tumor. Surprisingly, STING also phosphorylates STAT6, associated to the polarization of macrophages towards a M2 phenotype. However, until now, this part of the cGAS/STING pathway has been poorly studied *(Ohkuri et al., 2018)*.

3. Non coding RNA (microRNA and long non-coding RNA)

M1						
miRNA	**Inhibited target genes**	**Model**	**M1**	**M2**	**TAM**	**Ref**
miR-155	SOCS1, SHIP1, Bcl-6 (⊣ *NFκB*), C/EBPβ (→*Arg1*), IL-13Rα1 (→*Stat6*)	IFNβ, TNFα, IL-1, MG-CSF, and TLRs	→	⊣		*(Wu et al., 2016)*
miR-125a-5p	A20 (⊣NFκB) VEGFR1	LPS (THP-1) LPS + IFNγ (BMDMs)	→	⊣		*(Wu et al., 2016)* (Melton et al., 2016)
miR-125b-5p	IRF4, A20	IFNγ	→			*(Wu, Dai et al. 2016)*
miR-21 (inhibited by PGE_2)	Stat3, SOCS1		→			*(Wu, Dai et al. 2016)*
miR-342-5p	Bmpr2, Akt1 → miR-155	LPS/IFNγ	→			*(Wu, Dai et al. 2016)*
miR-33	AMPK (↘ FAO, ↗ glycolysis)	LPS/IFNγ	→	⊣		*(Wu, Dai et al. 2016)*
miR-101	ABCA1, MKP1 (⊣MAPK)	LPS	→			*(Wu, Dai et al. 2016)*
Let-7e	TLR4	LPS	→			*(Wu, Dai et al. 2016)*
miR-98	TLR4 (→ IL-10)	LPS	→			*(Wu, Dai et al. 2016)*
miR-148a-3p (activated by Notch)	PTEN (⊣AKT→*NFκB, ROS*)	GM-CSF + LPS/INFγ or IL-4	→	⊣		(Huang et al., 2017)
miR-130a	PPARγ	M-CSF or IFNγ NSCLC patients	→	⊣	⊣	*(Lin et al., 2015)*
miR-16	PD-L1 (⊣ T cell activation)	Peritoneal macrophages + INFγ or IL-4	→			*(Jia et al., 2016)*

M2						
miRNA	**Inhibited target genes**	**Model**	**M1**	**M2**	**TAM**	**Ref**
miR-125a-5p	KLF13 (T cell activation)	GM-CSF vs M-CSF (BMDMs)	⊣	→		*(Banerjee et al., 2013)*
miR-124	C/EBPα	IL-4, IL-13		→		*(Wu, Dai et al. 2016)*
miR-378-3p	IL-4Rα, PI3K, AKT	IL-4		→		*(Wu, Dai et al. 2016)*
miR-223	Pknox1	IL-4		→		*(Wu, Dai et al. 2016)*
miR-187	TNFα, IκBζ (→IL-12p40, IL-6)	IL-10		→		*(Wu, Dai et al. 2016)*
miR-146a (activated by PPARγ)	IRAK1/2, TRAF6, IRF5 Notch1	 LPS/IFNγ	⊣	→		*(Huang et al., 2016a)* *(Wu, Dai et al. 2016)*
miR-146b	TLR4, MyD88, IRAK1, TRAF6	LPS	⊣			*(Wu, Dai et al. 2016)*
miR-21 (activated by CSF1 → PI3K)	PDCD4 (→*NFκB,* ⊣ *IL-10)*, IL-12p35, PTEN ERK1/2, NFκB p65	LPS CSF-1	⊣	 →		*(Wu, Dai et al. 2016)* (Caescu et al., 2015)
miR-125b-5p	TNFα	LPS	⊣			*(Wu, Dai et al. 2016)*
Let-7c	C/EBPδ, PAK1 (→*NFκB*)	M-CSF	⊣	→		*(Wu, Dai et al. 2016)*
Let-7f	A20	LPS	⊣			*(Wu, Dai et al. 2016)*

TAMs						
miRNA	**Inhibited target genes**	**Model**	**M1**	**M2**	**TAM**	**Ref**
miR-940 (activated by hypoxia)	unknown (miRNA delivered by cancer cell-secreted exosomes)	Co-culture U937 with SKOV3 cells (ovarian cancer) + patients		→	→	*(Chen et al., 2017)*

miR-146a (inhibited by NFκB p50)	*Cfr M2 miRNAs*	TAMs		→	→	*(Li et al., 2015b)*
miR-145	HDAC11 (⇥*IL-10, VEGF*) TLR4 (→*IL-12p40, TNF*)	THP-1, NOMO-1 DLD-1 xenograft mice (colorectal cancer)		→	→	*(Shinohara et al., 2017)*
miR-21a	TLR8 (human) TLR7 (murine) ligand (miRNA delivered by cancer cell-secreted exosomes) (→*NFκB* →*TNFα, IL-6*)	Lung cancer model	→		→	*(Fabbri et al., 2012)*
miR29a	TLR8 ligand (miRNA delivered by cancer cell-secreted exosomes) (→*NFκB* →*TNFα, IL-6*)	Lung cancer model	→		→	*(Fabbri et al., 2012)*
miR-155 (activated by STAT1 and inhibited by Tim-3)	C/EBPβ, SOCS1 (⇥ JAK1/STAT1)	Co-cultured IL-4 polarized BMDMs+ LLC cells	→	⇥	⇥	*(Cai et al., 2012; Jiang et al., 2016; Yu et al., 2013)*
Let-7b	STAT3/AKT	LPS/IFNγ or IL-4 or co-cultured PBMCs with PC3 (prostate carcinoma)	→	⇥	⇥	*(Wang et al., 2016c)* *(Huang et al., 2016c)*
miR-125a (activated by Notch)	FIH1, IRF4	Isolated TAMs IL-4 or LPS/IFNγ polarized BMDMs	→	⇥	⇥	(Zhao et al., 2016)
miR-125b	*Cfr M1 miRNAs*	SK-LU1 (lung cancer) exosome on J774.A1		⇥	⇥	(Trivedi et al., 2016)
miR-511-3p	Rock2 (→ *IRF4*)	IL-4, IL-13		⇥	⇥	*(Wu, Dai et al. 2016)*
miR-720	GATA3	IL-4/IL-13 (THP-1) + breast cancer patients	→	⇥	⇥	*(Zhong and Yi, 2016)*
miR-222 (inhibited by NFκB p50)	CXCR4, CXCL12	Isolated TAMs		⇥	⇥	(Li et al., 2015b)
miR-23a	A20 (⇥NFκB) JAK1/STAT6	Isolated TAMs	→	⇥	⇥	*(Ma et al., 2016)*

miR-27a	IRF4/PPARγ	Isolated TAMs	⟶	⊣	⊣	*(Ma et al., 2016)*
miR-19a-3p	Fra1 (⊣VEGF, STAT3)	4T1 breast cancer model Polarized RAW264.7	⟶	⊣	⊣	*(Yang et al., 2014b)*

Legend: ⊣ for « inhibit »; ⟶ for « activate »

BOX 5: Non-coding RNAs

microRNAs (miRNAs): miRNAs are small non-coding RNA of approximately 22 nucleotides that mediate gene silencing by controlling the translation of mRNA into proteins. While some miRNAs regulate the expression of specific target genes, others are master regulators of hundreds of genes simultaneously. This regulation is achieved by mRNA degradation or by the inhibition of the translation initiation *(Esteller 2011).*

Long non-coding RNA (lncRNAs): lncRNAs are a heterogeneous group of non-coding transcripts longer than 200 nucleotides that mediate epigenetic modifications of DNA by recruitment of chromatin remodeling complexes. In this way, LncRNAs regulate the expression of neighboring genes and distant genomic sequences *(Esteller 2011).* In addition, LncRNAs can mimic and compete with nuclear receptors or transcription factors for consensus DNA binding. These sequences also control the functions of regulatory miRNAs and form complex with regulatory proteins. Finally, lncRNAs may directly interact with functional domains of proteins and regulate signal transduction *(Liu, Sun et al. 2015).*

A multitude of non-coding RNAs (BOX 5) was shown to interfere with macrophage polarization. These last years, a lot of studies revealed the contribution of miRNAs to macrophage polarization through the specific targeting of polarization-regulating mRNAs. Some of these miRNAs promote the M2-like phenotype while others trigger the M1-like phenotype (***Table 1 – M1/M2***). Recent studies have also focused on the effects of miRNAs required for the M2-like polarization of TAMs (***Table 1 - TAMs***). A large panel of miRNAs contributes to TAM polarization. For this reason, the suppression of miRNA activity, induced by the inactivation of the miRNA-processing enzyme DICER, promoted the M1-like TAM reprogramming. A specific miRNA family, Let-miRNAs, also takes part to macrophage polarization. Therefore, the rescue of Let-7a, Let-7d-5p or Let-7e (Let-7 miRNA family) in DICER deficient TAMs restored the M2-like phenotype *(Baer et al., 2016).*

Besides miRNAs, the function of LncRNAs in macrophage polarization is also an emerging research area. A recent study pointed the different profile of lncRNA expression in unpolarized, M1 and M2 macrophages *(Huang et al., 2016d).* For example, LncRNA cox-2 inhibits M2-like macrophage polarization while promoting the anti-tumoral functions of M1-like macrophages. Indeed, LncRNA cox-2 prevented immune evasion, angiogenesis, tumor growth and metastasis in a hepatocellular carcinoma model *(Ye et al., 2018).* The expression of some of these lncRNAs is regulated by NFκB, STAT6 and TNFα signaling pathways in cancer *(Liu et al., 2015).*

4. Hypoxia – induced polarization

It is well known that hypoxia triggers a M2-like phenotype in M1 macrophages and reinforces the M2 phenotype in M2 macrophages *(Leblond et al., 2016; Raggi et al., 2017)*. As described in chapter 1 (section 3.2.3. hypoxic macrophages), hypoxia also influences and fine-tunes the pro-tumoral phenotype of TAMs. For example, PMA-differentiated THP-1 macrophages and human peripheral blood mononuclear cells (h-PBMCs) were polarized towards an M2 phenotype ($CD163^+$, $CD206^+$) when co-cultured with hypoxia-primed breast cancer cells *(Tripathi et al., 2014).* These results were confirmed in a glioblastoma model where TAMs were recruited in hypoxic areas and adopted a M2-like phenotype *(Leblond et al., 2016)*. However, Laoui and his colleagues showed that hypoxia rather influences M2-like TAMs functions than promoting their M2 phenotype. Indeed, well-oxygenated tumors presented similar abundance of TAMs subsets, namely MHC-II^{high} (M1) macrophages and MHC-II^{low} (M2) macrophages, while in hypoxic tumor areas more MHC-II^{low} macrophages were recruited. Furthermore, MHC-II^{low} macrophages in well-oxygenated and hypoxic areas differed by their hypoxia-sensitive gene expression and angiogenic activity but hypoxia did not alter their M2 marker expression *(Laoui et al., 2014)*. Besides chronic hypoxia, intermittent or cycling hypoxia may also exist in tumors. Indeed, anarchical structure of tumor blood vessels creates fluctuation in the tumor blood perfusion and is characterized by periods of reoxygenation that occur in a cyclic way *(Brown, 1979)*. Intermittent hypoxia can be mimicked by the exposition of mice to alternative cycles of hypoxia (e.g. 8% oxygen), followed by reoxygenation (21% oxygen). Intermittent hypoxia, established as 8% oxygen for 4h per day, in a Lewis lung carcinoma (LLC) spontaneous metastasis model promoted non-small cell lung cancer metastasis by enhancing M2 macrophage polarization. The M2 polarization in lung metastasis was driven by an activation of ERK 1/2 *(Zhang et al., 2014)*. In another study, 20 cycles/hour of 90 seconds to 6% oxygen followed by reoxygenation (21% oxygen) 12 hours a day, also showed a shift of M1 phenotype towards M2 polarization *(Almendros et al., 2014).*

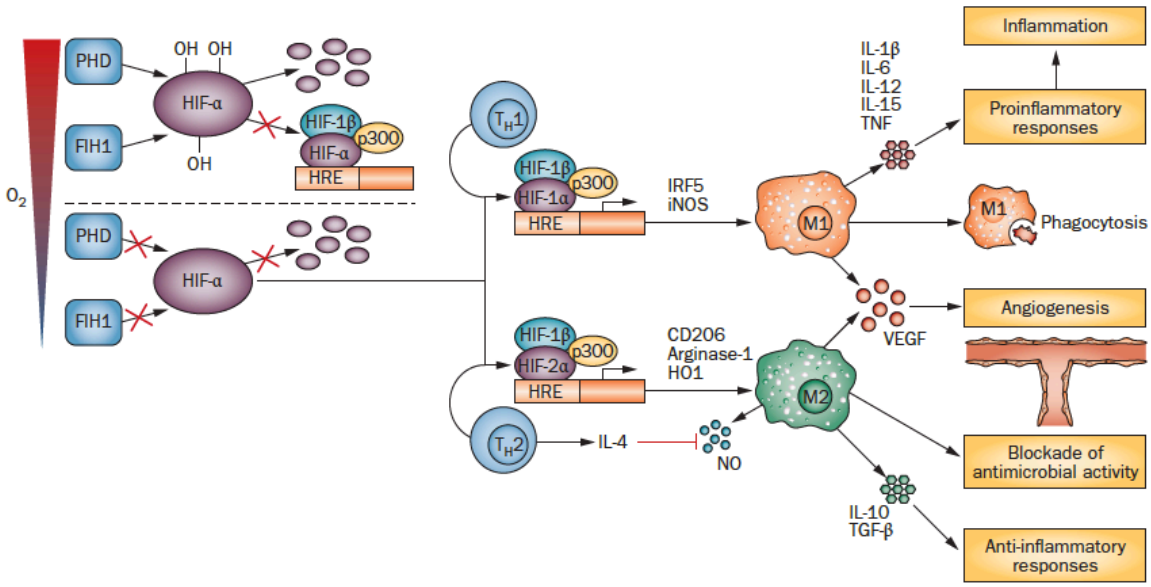

Figure I.26 – Hypoxia-regulated macrophage polarization

The hydroxylation of HIFα by prolyl hydroxylase (PHD) and factor inhibiting HIF-1 (FIH1) leads to the degradation and transcriptional inactivation of HIF1α and HIF2α. PHD and FIH1 need oxygen to be functional and are then inactive under hypoxia. Therefore, low levels of oxygen allow HIFα to translocate into the nucleus and to promote the transcription of target genes by its dimerization with HIF1β and its association to hypoxia response element (HRE). T_H1 cytokines activate HIF1α, increasing iNOS levels, NO synthesis and inducing a M1 activation state (IRF5 activation), while T_H2 cytokines activate HIF2α, thus suppressing NO synthesis and promoting arginase 1 (Arg1) expression, associated to a M2 phenotype *(Konisti, Kiriakidis et al. 2012)*.

Regarding the molecular pathways intervening in hypoxia-induced TAM phenotype, there are two isoforms of HIF, referred to as HIF1α and HIF2α, that are respectively associated with M1 and M2 phenotype (***Figure I.26***). Indeed, the activation of PI3Kγ in hypoxic BMDMs phosphorylates Akt, that itself activates an E3 ligase by phosphorylation. As non-activated E3 ligase sequesters HIFα, its activation allows HIFα to translocate into the nucleus. The association between HIFα and HIFβ induces the transcription of genes that promote tumor growth and metastasis *(Joshi et al., 2014)*. The knockout of HIF-1α skewed macrophages in a M2 phenotype in a spheroid tumor model, as it was evidenced by a decreased expression of TNFα, IL-6 and iNOS. In the same study, the absence of HIF1α also promoted the pro-angiogenic functions of macrophages *(Werno et al., 2010)*. Moreover, pro-inflammatory cytokines stimulate HIF1α. Once activated, HIF1α increases iNOS levels and NO synthesis, and induces a M1 activation state. In contrast, T_H2 cytokines stimulate HIF2α, then suppressing NO synthesis and promoting arginase 1 (Arg1) expression, associated to a M2 phenotype *(Escribese et al., 2012)*. However, the dichotomic association between HIFα isoforms and macrophage phenotype is not fully understood and remains conflicting as HIF1α was also shown as a M2 activator. Indeed, HIF1α drove an M2-like TAM polarization in lung and melanoma cancer models. The activation of HIF1α in TAMs triggered the expression of VEGF and Arg1, responsible for angiogenesis and tumor growth respectively *(Colegio et al., 2014)*. In addition another study showed that HIF1α was similarly expressed in MHC-II^{high} (M1) and MHC-II^{low} (M2) macrophages while the expression of HIF2α was higher in MHC-II^{low} macrophages *(Laoui et al., 2014)*. Further investigations are thus needed to fully establish the link between HIFα subunit and macrophage phenotype.

5. Metabolic reprogramming

The metabolism of TAMs is similar to the metabolism of IFNγ and LPS polarized macrophages (M1). Indeed, pro-inflammatory macrophages (M1) exhibit an aerobic glycolysis and an enhanced pentose phosphate pathway (PPP) whereas their oxidative phosphorylation (OXPHOS) is impaired and they present a disrupted tricarboxylic cycle (TCA, Krebs cycle) in favor to the fatty acid synthesis (FAS). In contrast, anti-inflammatory macrophages (M2) show glycolytic metabolism with an intact TCA coupled to high OXPHOS but a reduced PPP and a FAS that fuels the fatty acid oxidation (FAO) (***Figure I.27***) *(Van den Bossche et al., 2017).*

Indeed, a lot of studies revealed the metabolic reprogramming of TAMs by the tumor microenvironment *(Liu et al., 2017).* In homeostatic conditions and under stress, ATP is essential for cellular functions. The energy pool is provided by the transformation of uptaken glucose in ATP by glycolysis and tricarboxylic cycle. The intervention of oxygen is fundamental for ATP production. Oxygen serves as an electron acceptor in the electron transport chain during the mitochondrial OXPHOS. When oxygen is limited, cells reprogram their metabolism to produce ATP through glycolysis, which is then associated with lactate production. However, despite the presence of oxygen in tumors, TAMs increase glycolysis (2 ATP/ glucose) and lactate production while reducing mitochondrial respiration (OXPHOS: 34 ATP/glucose). This phenomenon was described as the *Warburg effect* or the aerobic glycolysis *(El Kasmi and Stenmark, 2015; Liu et al., 2017)*. These metabolic changes promote metastasis in human pancreatic ductal carcinoma by enhancing angiogenesis, extravasation and EMT *(Penny et al., 2016).*

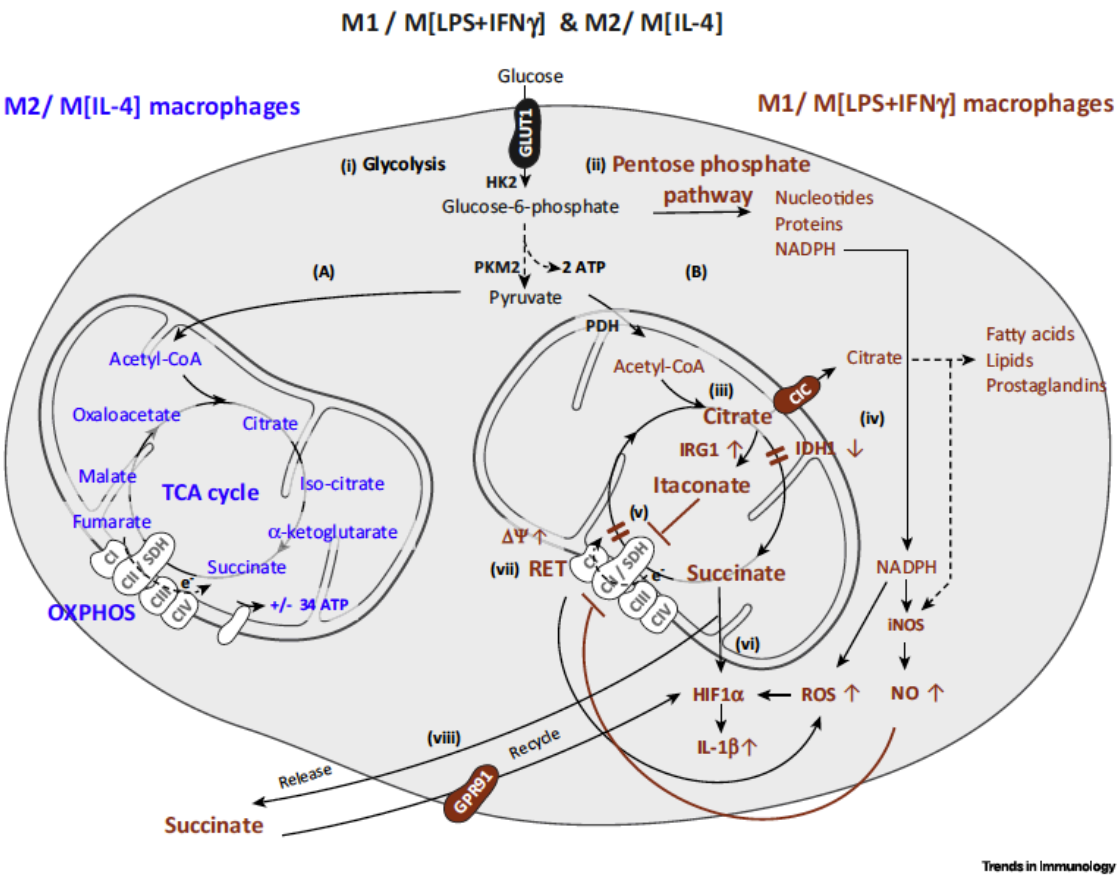

Figure I.27 – Metabolism-regulated macrophage polarization

(A) Anti-inflammatory macrophages (M2) show glycolytic metabolism (*i*) with an intact tricarboxylic cycle (TCA, Krebs cycle) coupled to a high oxidative phosphorylation (OXPHOS). However, this phenotype also presents a reduced pentose phosphate pathway (PPP) and a fatty acid synthesis (FAS) that fuels the fatty acid oxidation (FAO). **(B)** In contrast, pro-inflammatory macrophages (M1) exhibit an aerobic glycolysis (*i*) and an enhanced PPP (*ii*) while their OXPHOS is impaired and they present a disrupted TCA (*iii*) in favor to the FAS. The disruption of TCA is marked by an accumulation of citrate (*v*) and succinate (*vi*) that stabilize HIF1α. Consequently, the succinate released by macrophage generates a positive feedback loop, reinforcing the M1 phenotype (*viii*). In addition, the mitochondrial hyperpolarization (*vii*) drives mitochondrial ROS and IL-1β production *(Van den Bossche, O'Neill et al. 2017)*.

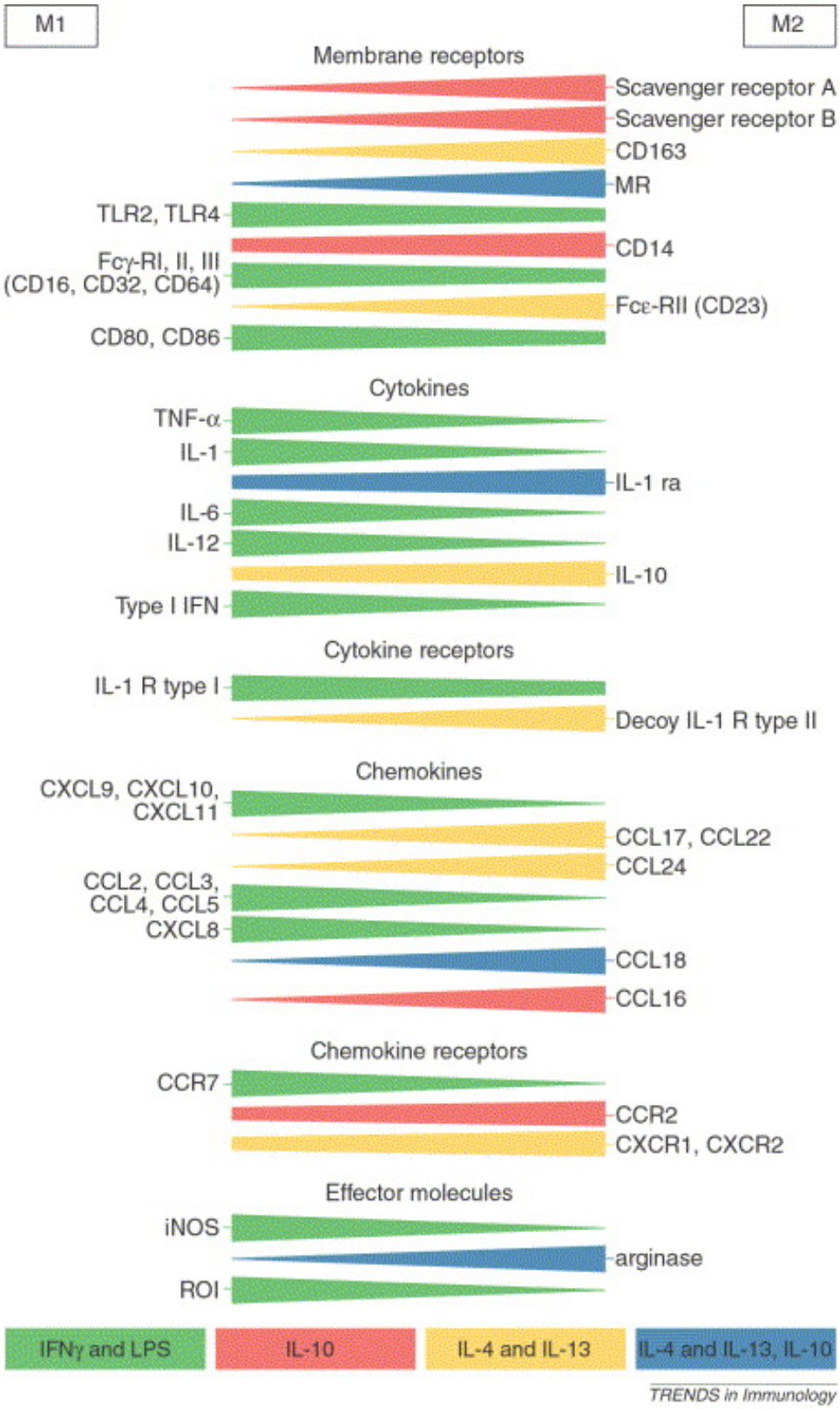

Figure I.28 – List of M1 and M2 markers *(Mantovani, Sozzani et al. 2002)*

In hypoxic areas or stressed conditions, the glycolytic metabolism is reduced in TAMs. In these conditions, the inhibitor regulated in development and DNA damage response 1 (REDD1) negatively regulates mTORC1 in macrophages, thus reducing glucose uptake and favoring glucose availability for endothelial cells. It hence leads, in concert with pro-angiogenic factors, to disorganized tumor vasculature and metastasis *(Wenes et al., 2016)*.

6. M1 and M2 classification

The classification of TAMs according to their M1 or M2 phenotype is based on several markers (**Figure I.28**). Unless a lot of effort is made to find new M1 or M2 markers that could clearly discriminate these two macrophage subsets, this classification is not well defined. Indeed, a lot of M1 markers are also expressed in M2-like macrophages and inversely. For example, Arg-1 is a M2 marker, while it is also highly induced in M1-like mycobacteria-infected macrophages *(Murray et al., 2014).* Another example is IL-10 that is expressed in M1 macrophages but much more in M2 macrophages *(Murray, 2017)*. Moreover, as multiple TAM phenotype exist in tumors, this classification becomes obsolete. It is thus difficult to link a phenotype to a specific function. In addition, it should be noted that differences exist between mouse and human regarding markers associated to macrophage polarization.

7. Conclusions and future directions

Macrophages in tumors gather multiple subtypes and it is difficult to classify these subtypes as M1 or M2 macrophages. Depending on their location into the tumor, and thereby according to the mediators available in the tumor microenvironment, TAMs exhibit a phenotype close to M2 macrophages or a mixed M1/M2 phenotype. Downstream the binding of mediators to their respective receptors, multiple signaling pathways drive macrophage polarization. These signaling axes are interconnected and in most cases overlap each other to finely tune the polarization of macrophages. The signaling pathways described in this chapter are not exclusive, as other signaling axes have also been reported to influence macrophage polarization. Furthermore, with the advent of sequencing and new technologies, the mapping of TAM polarization pathways is more and more complete and reveals the contribution of new signal transduction pathways.
In addition to cytokines, the oxygen level, metabolic products or cells from the microenvironment also regulate the activation status of macrophages as well as their metabolic pathways. Indeed, TAMs adapt to the tumor microenvironment and adopt a metabolism close to the one of M1 macrophages, while their activated signaling pathways resemble more to the one of M2 macrophages. Therefore, a lot of studies try now to connect metabolism to signaling axes in order to further characterize TAMs.

As TAMs are the most abundant infiltrating cells in tumors and as they hold a pro-tumoral phenotype close to M2 macrophages, an increasing interest has emerged for the reprogramming of TAMs towards a M1-like phenotype, associated to antitumor functions. The targeting of one or the other signaling pathway involved in macrophage polarization is sufficient to modify the phenotype of TAMs and generate tumor regression. In the next chapter, the influence of

chemotherapies, immunotherapies and radiotherapy on macrophage polarization will be detailed. This review has been published in *Frontiers in Immunology* on July 2017.

Chapter 3: Reprogramming of tumor-associated macrophages with anticancer therapies: radiotherapy versus chemo- and immunotherapies

Erratum:

- p.7: High Doses of Irradiation (HDI): *3 x 20 Gy* (5th line)
- p. 7: High Doses of Irradiation (HDI): 3 x 6 Gy (31st line)

frontiers in Immunology

REVIEW
published: 14 July 2017
doi: 10.3389/fimmu.2017.00828

Reprogramming of Tumor-Associated Macrophages with Anticancer Therapies: Radiotherapy versus Chemo- and Immunotherapies

*Géraldine Genard[1,2], Stéphane Lucas[2] and Carine Michiels[1]**

[1] URBC – NARILIS, University of Namur, Namur, Belgium, [2] Laboratory of Analysis by Nuclear Reaction (LARN/PMR) – NARILIS, University of Namur, Namur, Belgium

Tumor-associated macrophages (TAMs) play a central role in tumor progression, metastasis, and recurrence after treatment. Macrophage plasticity and diversity allow their classification along a M1–M2 polarization axis. Tumor-associated macrophages usually display a M2-like phenotype, associated with pro-tumoral features whereas M1 macrophages exert antitumor functions. Targeting the reprogramming of TAMs toward M1-like macrophages would thus be an efficient way to promote tumor regression. This can be achieved through therapies including chemotherapy, immunotherapy, and radiotherapy (RT). In this review, we first describe how chemo- and immunotherapies can target TAMs and, second, we detail how RT modifies macrophage phenotype and present the molecular pathways that may be involved. The identification of irradiation dose inducing macrophage reprogramming and of the underlying mechanisms could lead to the design of novel therapeutic strategies and improve synergy in combined treatments.

Keywords: tumor-associated macrophages, reprogramming, polarization immunotherapy, chemotherapy, radiotherapy, nuclear factor kappa B, reactive oxygen species

OPEN ACCESS

Edited by:
Anahid Jewett, University of California, Los Angeles, United States

Reviewed by:
Nejat K. Egilmez, University of Louisville, United States
Benjamin Bonavida, University of California, Los Angeles, United States

****Correspondence:***
Carine Michiels
carine.michiels@unamur.be

Specialty section:
This article was submitted to Cancer Immunity and Immunotherapy, a section of the journal Frontiers in Immunology

Received: *25 April 2017*
Accepted: *30 June 2017*
Published: *14 July 2017*

Citation:
Genard G, Lucas S and Michiels C (2017) Reprogramming of Tumor-Associated Macrophages with Anticancer Therapies: Radiotherapy versus Chemo- and Immunotherapies. Front. Immunol. 8:828. doi: 10.3389/fimmu.2017.00828

Abbreviations: AMPK, AMP-activated protein kinase; AP-1, activator protein 1; Arg 1, arginase 1; ATM, ataxia telangiectasia mutated; C/EBPβ, CCAAT-enhancer-binding proteins; CCL, chemokine ligand; CCR2, C–C chemokine receptor type 2; CD206, cluster of differentiation 206 or mannose receptor; CL, clodrolip; COX, cyclooxygenase; CpG-ODN, unmethylated cytosine-guanine (CpG) oligodeoxynucleotides; CSF-1, colony-stimulating factor 1; CSF-1R, colony-stimulating factor 1 receptor; CTLA4, cytotoxic T lymphocyte-associated protein 4; CXCL12, C–X–C motif chemokine 12; ECM, extracellular matrix; ERK, extracellular signal-regulated kinase, FDA, food and drug administration; FRβ, folate receptor β; HDI, high doses of irradiation; HIF, hypoxia-inducible factor; HLA-DR, human leukocyte antigen-cell surface receptor; HO1, heme oxygenase 1; HRG, histidine-rich glycoprotein; IFNγ, interferon γ; IL, interleukin; iNOS, inducible nitric oxide synthase; IR, ionizing radiation; IRF, interferon-regulatory factor; JNK, c-Jun N-terminal kinase; KLF4, Kruppel-like factor 4; LDI, low doses of irradiation; LET, linear energy transfer; LLC, Lewis lung cancer; LPS, lipopolysaccharide; mAb, monoclonal antibody; MAPK, mitogen-activated protein kinase; MARCO, pattern recognition scavenger receptor; MCP-1, monocyte chemoattractant protein 1; M-CSF, macrophage colony-stimulating factor; MDI, moderate doses of irradiation; MHC, major histocompatibility complex; MMP, matrix metalloproteinase; MnSOD, manganese superoxide dismutase; MPK1, MAPK phosphatase 1; MRC1, mannose receptor-C 1; NAC, *N*-acetyl cysteine; NADPH, nicotinamide adenine dinucleotide; NEMO, NFκB essential modulator; NFκB, nuclear factor kappa B; NK, natural killer; NO, nitric oxide; NOX, NADPH oxidase; Nrf2, nuclear erythroid derived 2-related factor; p38, MAPK; PAMPs, pathogen-associated molecular patterns; PD-1, programmed cell death 1; PD-L1, programmed death ligand 1; PDA, pancreatic ductal adenocarcinoma; PEC, peritoneal exudate cells; PI3Kγ, phosphoinositide 3-kinase gamma; PlGF, placental growth factor; PPARγ, peroxisome proliferator-activated receptor gamma; RANTES, regulated on activation, T cell expressed and secreted; RELMα, resistin-like molecule alpha; RNS, reactive nitrogen species; ROS, reactive oxygen species; RT, radiotherapy; STAT, signal transducer and activator of transcription; SUMO, small ubiquitin-like modifier; TAMs, tumor-associated macrophages; TGFβ, transforming growth factor β; TLR, toll-like receptor; TNFα, tumor necrosis factor α; TRAIL-R2, TNFα-related apoptosis-inducing ligand receptor; VCAN, versican, extracellular matrix proteoglycan; VEGF, vascular endothelial growth factor; ZA, zoledronic acid.

INTRODUCTION

In 1863, Rudolf Virchow was the first to highlight the infiltration of leukocytes in tumor, thereby proposing a link between inflammation and tumorigenesis. Two centuries later, an inflammatory microenvironment within the tumor is part of the hallmarks of cancer (1). In fact, in emerging cancer disease, inflammation is a two-edge sword. On the one hand, the immune system can recognize tumor cells and kill them. On the other hand, chronic inflammation promotes cancer invasion, angiogenesis, and immunosuppression (2, 3). In this context, the immune system was assigned tumor immunoediting functions. The emergence of neoplastic cells induces an inflammatory environment, contributing to the rejection of the tumor (the *elimination phase*). However, the immune system establishes a selective pressure on cancer cells hence selecting resistant cells (the *equilibrium phase*). Finally, tumor evades from the immune system and moves into the *escape phase* (4). This last phase can occur through different mechanisms: reduced immune recognition, increased cancer cell resistance or survival, and immunosuppressive tumor microenvironment (5). In this process, macrophages act as an orchestrator of inflammation and are the main players of immunosurveillance. In the elimination phase, transformed cells are recognized and their antigens are presented to the effectors of the immune system by macrophages, promoting antitumor immunity (6). However, in the escape phase, macrophages play an important role in tumor progression by stimulating angiogenesis, metastasis, tumor growth, and immunosuppression notably through the secretion of polyamines, M-CSF, vascular endothelial growth factor (VEGF), IL-10, and transforming growth factor β (TGFβ) (5).

COMPLICITY OF TUMOR-ASSOCIATED MACROPHAGES (TAMs) IN TUMOR PROGRESSION

More than 50% of tumor-infiltrating cells are macrophages, named TAMs (7, 8). The recruitment and accumulation of TAMs into tumors are initiated by macrophage chemoattractants [e.g., CCL2/monocyte chemoattractant protein 1 (MCP-1), colony-stimulating factor 1 (CSF-1)] and it is well established that TAMs drive tumor progression (9, 10). In fact, cancer prognosis is closely linked to the number of TAMs with an inverse correlation: increased number of TAMs is associated with a reduced cancer patient survival (11). In healthy tissues, macrophages offer a remarkable plasticity to efficiently respond to environmental cues (12). In tumors, an identical plasticity is described: TAMs are educated by the tumor microenvironment, providing multiple phenotypes with a range of functions (13). TAM phenotypes can be featured as a linear scale where M1 and M2 phenotypes represent the two extremes, similarly to the T_H1–T_H2 classification (**Figure 1**). M1 macrophages are recognized as classically activated macrophages and show enhanced ability to phagocyte pathogens. More importantly, these cells have antitumoral properties. Macrophages can also be polarized into the M2 phenotype, the alternative activated state of macrophages. M2 macrophages are requested in infection-free healing circumstances and have pro-tumoral functions. The polarization of macrophages can be driven by different microenvironmental molecules and leads to the production by the macrophages of different cytokines and chemokines. M1 macrophages are activated during acute inflammation by toll-like receptor (TLR) ligands [lipopolysaccharide (LPS)] or T_H1 cytokines [interferon γ (IFNγ)–tumor necrosis factor α (TNFα)]. M1 macrophages display an enhanced production of pro-inflammatory cytokines (TNFα and interleukins: IL-1β, IL-2, IL-6, IL-12, IL-23), reactive oxygen species (ROS), nitric oxide (NO) and present antigens *via* major histocompatibility complex class II molecules (14). Stimulation of macrophages with IL-4/IL-13, IL-10, TGFβ, or glucocorticoids leads to the M2 phenotype and the subsequent production of anti-inflammatory cytokines (IL-10, TGFβ) that have an inhibitory effect on cytotoxic $CD8^+$ T cells. Macrophages with M2 phenotype also express cell surface scavenger receptor (CD206), hemoglobin receptor (CD163) and produce extracellular matrix (ECM) components (14–16). M2 macrophages facilitate the resolution of inflammation and promote tissue repair by T_H2 response, tissue remodeling, and immune tolerance. They also favor tumor growth (17, 18). This phenotype can be subclassified into M2a, M2b, or M2c according to the roles these macrophages exert (19). In cancer disease, TAMs usually exhibit a M2 phenotype and participate to tumor angiogenesis, tumor invasion and metastasis, immunosuppression and cell activation. All these features led Qian and Pollard to classify TAMs in six functional subtypes: angiogenic, immunosuppressive, invasive, metastasis associated, perivascular, and activated macrophages (20).

MOLECULAR PATHWAYS FOR M1–M2 POLARIZATION

The polarization of macrophages is influenced by several mechanisms driven by transcription factors and miRNAs (**Figure 1**). The activation of macrophages into M1 or M2 phenotype is mainly induced by interferon-regulatory factor/signal transducer and activator of transcription (IRF/STAT) signaling pathways. IRF3, IRF5, STAT1, and STAT5 are responsible for driving M1 polarization while IRF4, STAT3, and STAT6 provide M2 activation signals (14, 21). Besides IRF/STAT transcription factors, hypoxia also influences macrophage polarization. The lack of oxygen can activate hypoxia-inducible factors (HIF) differently in M1 versus M2 macrophages. Indeed, T_H1 cytokines are able to induce HIF1α stabilization, triggering M1 response whereas HIF2α is activated by T_H2 cytokines in M2 macrophages. These differences rely on the ability of HIF1 and HIF2 to, respectively, activate or suppress NO synthesis (22). Furthermore, nuclear factor kappa B (NFκB) fulfills a central role in the pro-inflammatory macrophages (M1). Indeed, the active heterodimer NFκB (p50–p65) promotes the transcription of inflammatory genes while the inhibitory heterodimer NFκB (p50–p50) prevents the transcription of these genes in anti-inflammatory macrophages (M2). Other transcription factors including AP-1, Kruppel-like factor 4 and PPARγ can modulate the activated state of macrophages. Finally, miRNA also interfere with the polarization of macrophages. Among miRNAs of interest, miR127, miR155, and miR223 are key regulators of M1 polarization (23, 24). In contrast, miR146-a promotes M2 polarization while decreasing the expression of M1 markers (25).

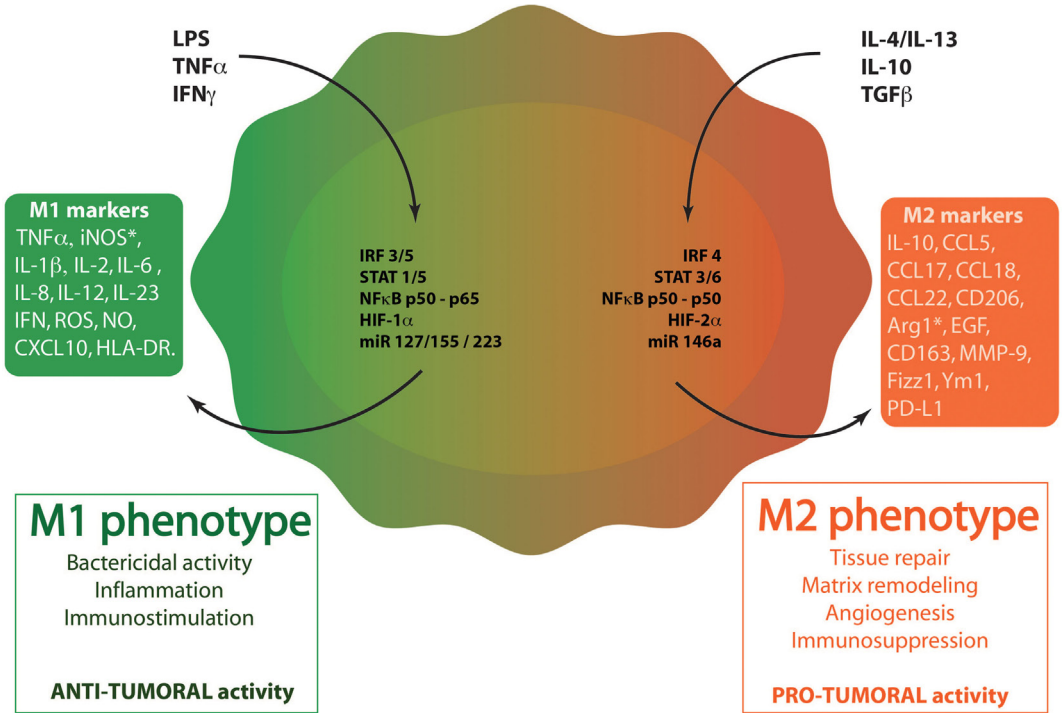

FIGURE 1 | Macrophage polarization. Through the binding to their respective receptors, M1 stimuli [lipopolysaccharide (LPS), tumor necrosis factor α (TNFα), and interferon γ (IFNγ)] trigger the activation of several transcription factors. These factors include interferon-regulatory factor/signal transducer and activator of transcription (IRF/STAT) family members (IRF3, IRF5, STAT1, and STAT5), the active nuclear factor kappa B (NFκB) heterodimer (p50–p65) and HIF1. miR127, miR 155, and miR223 also regulates M1 polarization. When polarized in M1-like phenotype, macrophages produce specific cytokines (TNFα, IL-1β, IL-2, IL-6, IL-12, IL-23, IFNγ), chemokines (CXCL10) and other molecules [reactive oxygen species (ROS), nitric oxide (NO), inducible nitric oxide synthase (iNOS), human leukocyte antigen-cell surface receptor (HLA-DR)]. M1 phenotype plays key roles in inflammation, immunostimulation and an antibacterial and antitumoral responses. M2 stimuli [IL-4, IL-13, IL-10, and transforming growth factor β (TGFβ)] bind to ILR4α, ILR10, or TGFβR to induce M2-like phenotype in macrophages. These stimuli activate several transcription factors: IRF/STAT family members (IRF4, STAT 3, and STAT6), the inhibitory NFκB homodimer (p50–p50) and HIF2. miR14a also influences M2 polarization. When polarized in M2-like phenotype, macrophages produce specific cytokines (IL-10), chemokines (CCL5, CCL17, CCL18, CCL22), and other proteins (CD163, CD206, Arg1, MMP-9, Fizz-1, Ym-1, and PD-L1). M2 macrophages exert diverse functions, such as tissue repair, matrix remodeling, angiogenesis, immunosuppression, and favor tumor growth.

TARGETING TAMs WITH CHEMOTHERAPY OR IMMUNOTHERAPY

In response to microbial signals, tissue damage, cytokines and metabolic products, monocytes, and macrophages from healthy tissues are able to undergo reprogramming (12, 21, 26, 27). The pro-tumoral functions of TAMs and their ability to be reprogrammed, from M2-like macrophages toward M1 phenotype, make them an attractive target for anticancer therapies. Currently, different approaches have been proposed to modulate TAMs: (1) depletion of TAMs; (2) inhibition of circulating monocyte recruitment into the tumor; (3) blockade of M2 phenotype; and (4) enhanced activation of M1 macrophages or reprogramming of TAMs toward M1-like macrophages (27, 28). Each of these approaches will be detailed here under (**Figure 2**).

Depletion of TAMs

Three alternatives are available to destroy TAMs in tumor (**Figure 2A**). The first way is the use of chemical compounds, especially bisphosphonates, such as clodronate encapsulated in liposomes [clodrolip (CL)]. These liposomes containing clodronate are phagocyted by macrophages and are disrupted by lysosomal processes, leading to the release of clodronate in the cells. Clodronate is metabolized to an analog of ATP, cytotoxic for macrophages (29). CL is currently used in immune research and clinical trials to eliminate macrophages and phagocytes in multiple malignancies. For example, TAM depletion with CL impaired tumor engraftment, reduced tumor growth, and favored mouse survival in a chronic lymphocytic leukemia model (30). However, despite its effective tumor regression effects, it also induced severe side effects such as sensitivity toward infections and weight loss in mice and patients (31–34). A similar approach was developed using zoledronic acid (ZA), which inhibited tumor progression, angiogenesis, and metastasis in association with sorafenib in two human hepatocellular carcinoma mouse models (34). ZA depleted matrix metalloproteinase 9 (MMP-9) expressing TAMs (M2-like macrophages) but also impaired the differentiation of myeloid cells into TAMs (35). However, ZA, as ibandronate (another bisphosphonate), has generated conflicting results.

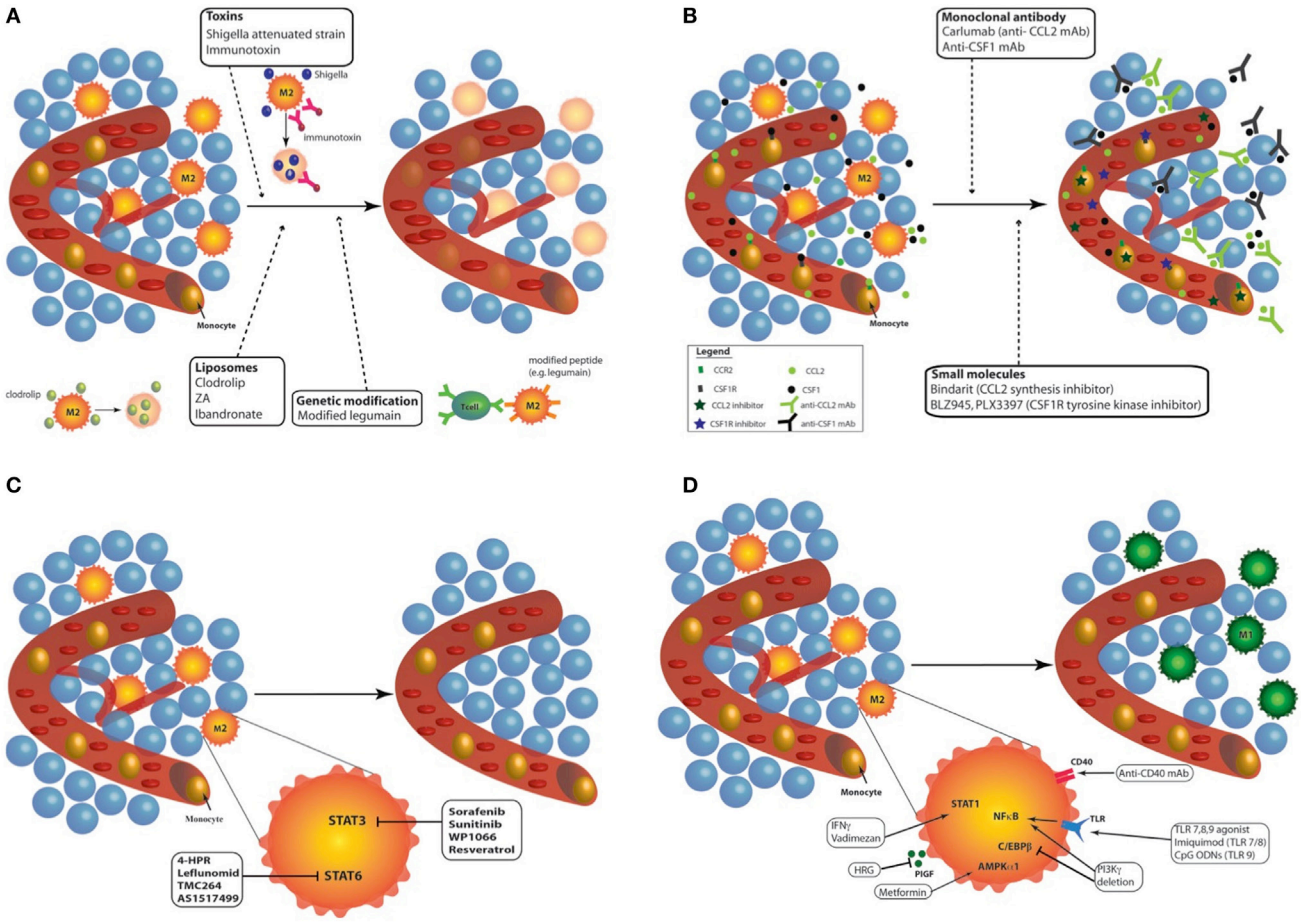

FIGURE 2 | Targeting tumor-associated macrophages (TAMs) with chemo- and immunotherapies. Different approaches have been proposed to modulate TAMs: **(A)** *Depletion of TAMs*: different kinds of treatments are available to destroy TAMs in tumor: toxins (*Shigella flexneri* attenuated strain or immunotoxin), liposome containing bisphosphonates [clodrolip, zoledronic acid (ZA) or ibandronate], and peptide modification to induce cytotoxic lymphocyte activation (e.g., legumain). Depletion of macrophages in tumor induced effective tumor regression in mouse and patients. **(B)** *Inhibition of circulating monocyte recruitment into the tumor*: two main recruitment effectors can be targeted to inhibit the recruitment of monocyte to the tumor site: CCL2/C–C chemokine receptor type 2 (CCR2) and colony-stimulating factor 1 (CSF-1)/CSF1-R. The use of monoclonal antibody against CCL2 (e.g., Carlumab) or CSF-1 inhibits tumor growth in mouse models and humans. Another way to prevent monocyte recruitment to the tumor site is the use of molecule targeting CCL2/CCR2 (e.g., bindarit) or CSF1/CSF1-R (e.g., BLZ945, PLX3397) pathways. **(C)** *Blockade of M2 phenotype*: the blockade of M2 phenotype can be achieved by targeting two main transcription factors: STAT3 (sorafenib, sunitinib, WP1066, and resveratrol) and STAT6 (4-HPR, leflunomid, TMX264, and AS1217499). All these inhibitors provide tumor regression and inhibited angiogenesis. **(D)** *Enhanced activation of M1 macrophages or reprogramming of TAMs toward M1-like macrophages*: TAM reprogramming into M1 macrophages can be achieved through the stimulation of STAT1 (IFNγ, vadimezan), AMPKα1 (metformin), or nuclear factor kappa B [toll-like receptor agonists such as imiquimod or CpG-ODNs; phosphoinositide 3-kinase (PI3Kγ) deletion]. The inhibition of placental growth factor (PlGF) (HRG) and C/EBPβ (PI3Kγ deletion) also leads to effective reprogramming of TAMs toward M1-like macrophages. Finally, by stimulating CD40, monoclonal antibodies (mAbs) against CD40 similarly reprogram TAMs from M2 phenotype to M1 macrophages.

The targeting of MMP-9 positive macrophages was also obtained with dasatinib, a tyrosine kinase inhibitor well tolerated by patients and approved by food and drug administration (FDA) for chronic myeloid leukemia (36). However, dasatinib has been reported to inhibit other immune cells as natural killer (NK) cells and T cells, then aborting tumor immune response. Finally, trabectedin (ET-743), another drug approved by FDA, exhibited a cytotoxic effect against TAMs and showed antitumor activity. This drug was shown to not damage lymphocyte subgroups. This is due to the differential expression of TNFα-related apoptosis-inducing ligand receptor (TRAIL) (TNFα-related apoptosis-inducing ligand) receptor by the different types of leukocytes: trabectedin targets TAMs while human NK cells and $CD8^+$ lymphocytes were resistant to TRAIL-mediated toxicity. In fact, blood monocytes and TAMs expressed higher level of TRAIL-R2 compared to NK cells and $CD8^+$ lymphocytes (37, 38).

A second alternative is the use of toxin-conjugated monoclonal antibodies (mAbs) or attenuated bacteria that kill macrophages. An anti-scavenger receptor A (CD204) antibody conjugated to the saporin toxin reduced the number of vascular leukocytes and inhibited tumor progression in a murine ovarian cancer model (39). An immunotoxin composed of portions of anti-folate receptor beta antibody conjugated

to *Pseudomonas* exotoxin A was also used to deplete TAMs: reduced tumor growth was observed in nude mice bearing C6 glioma xenografts (40). In the same line, *Shigella flexneri* is a bacterial pathogen inducing the apoptosis of macrophages. Galmbacher and his colleagues developed an attenuated strain of *S. flexneri* to infect breast cancer-bearing mice. The treatment led to TAM depletion and to a complete tumor regression in tumor-bearing mice (41).

The last alternative is the activation of cytotoxic T lymphocytes against macrophages. Legumain is an asparaginyl endopeptidase that contributes to the degradation of the ECM and to angiogenesis. TAMs have been found to express abundant amounts of legumain (42). This discovery led Smahel and his team to modify the gene sequence of legumain to enhance the efficacy of immunization against legumain. These modifications induced reduced legumain maturation and impaired cellular localization, and resulted in T helper ($CD4^+$) and cytotoxic ($CD8^+$) lymphocyte-dependent elimination of TAMs (43).

Depletion of macrophages has thus met successful results in the tumor regression in mouse models and patients. However, a systemic depletion of macrophages obviously renders the organism more sensitive to infections and other aggressions. Therefore, these types of treatments need to be localized to the tumor site.

Inhibition of Circulating Monocyte Recruitment into Tumor

The inhibition of CCL2/C–C chemokine receptor type 2 or CSF1/CSF1-R pathways by several methods was shown to efficiently induce tumor regression (**Figure 2B**). CCL2 is a chemokine produced by cancer cells that is responsible for the recruitment of monocytes at the tumor site. CCL2 overexpression in tumor is correlated with macrophage infiltration and poor prognosis in human cancers (44–46). Furthermore, CCL2 is a key actor of metastasis since it enhances the retention of metastasis-associated macrophages in breast cancer metastasis. CCL2 blockade was reported to block the mobilization of monocytes from the bone marrow to the blood in a murine breast cancer model (47). The inhibition of CCL2 by an anti-CCL2 monoclonal antibody (e.g., carlumab) or through the inhibition of its synthesis (e.g., bindarit, trabectedin) prevented the recruitment of macrophages into the tumor site. Most of these treatments are now tested in clinical trials. Carlumab, a human monoclonal antibody against CCL2, was safely used in metastatic castration-resistant prostate cancer (48) and in a phase Ib study in association with other chemotherapy agents (docetaxel, gemcitabine, paclitaxel or carboplatin and pegylated liposomal doxorubicin) (49). This monoclonal antibody led to an efficient depletion of macrophages into the tumor and can significantly delay tumor regrowth following chemotherapy (49). Besides mAb targeting CCL2, other compounds (e.g., bindarit, trabectedin) were found to inhibit the synthesis of CCL2/MCP-1. Bindarit reduced TAM and myeloid-derived suppressor cell infiltration in a breast cancer model and resulted in impaired metastatic disease in a prostate cancer model (50). This treatment also targeted angiogenesis and tumor growth in human melanoma xenografts (51). In addition to deplete TAMs, trabectedin is used to inhibit monocyte recruitment. This drug targets CCL2 synthesis by interacting with the transcription machinery (52) but also modulates the DNA repair machinery (53). In clinic, it is used to treat ovarian and breast cancer as well as soft tissue sarcomas (53, 54).

Colony-stimulating factor 1/CSF1-R signaling drives the recruitment and the differentiation of TAMs toward a M2 phenotype in tumor. CSF1-deficient mice showed a 50% decrease in macrophage infiltration while neutrophil infiltration was increased during tumor progression in a mouse model of pancreatic islet cancer (55). mAbs and small molecules targeting CSF1 (mAb anti-CSF1) or CSF1-R (BLZ945, emactuzumab, PLX3397) were subjected to numerous studies and were shown to deplete macrophages in a tissue-specific manner (56, 57). Overall, CSF1-R inhibitors deplete TAMs and abolish tumor growth, angiogenesis, and metastasis. BLZ945, a highly selective small molecule inhibitor of CSF1-R tyrosine kinase, attenuated the turnover rate of TAMs while increasing the number of $CD8^+$ T cells in murine cervical and breast carcinoma models (56). In addition, blockade of CSF-1/CSF1-R by mAb anti-CSF1 or with PLX2297 (a small molecule targeting the tyrosine kinase domain of CSF1-R) was reported to reprogram remaining TAMs at the tumor site to support antitumor immunity in pancreatic cancer mouse models (58). PLX3397 also delayed the recurrence of glioblastoma after radiation by modifying the recruitment and polarization of myeloid cells in an intracranial xenograft model (59). However, orally administered PLX3397 showed no efficacy for human glioblastoma in a phase II study (60). Other chemoattractants for macrophages such as VEGF, C–X–C motif chemokine 12, CCL4 are also under investigation and may be considered as potential targets to inhibit macrophage recruitment and hence tumor progression.

Blockade of M2 Phenotype

Two main transcription factors have been largely reported to block M2 polarization: STAT 3 and STAT6 (**Figure 2C**). Tyrosine kinase inhibitors (sunitinib and sorafenib) inhibit STAT3 in macrophages. Sorafenib was shown to restore the secretion of IL-12 while suppressing IL-10 expression in prostaglandin E2-conditioned macrophages, indicating a reverse effect on the immunosuppressive cytokine profile in TAMs (61). Inhibition of STAT3 with WP1066 reversed immune tolerance in patients with glioblastoma multiforme. This treatment stimulated the secretion of pro-inflammatory cytokines and activated T cells (62). In the same line, resveratrol has also been used to suppress M2-like polarization of TAMs with parallel inhibition of tumor growth in a mouse lung cancer xenograft model. The blockade of M2-like polarization of TAMs by resveratrol was linked to the decreased activity of STAT3 (63).

Similarly, fenretinide (4-HPR) inhibited the phosphorylation of STAT6 and skew M2 polarization. In a colorectal mouse model, the effects were accompanied by a reduction in the number of M2-like macrophages in tumor and by an inhibition of angiogenesis (64). Other inhibitors of STAT6 activation (TMC264, AS1517499) were developed but no one underwent clinical studies (65–67).

Enhanced Activation of M1 Phenotype or Reprogramming of TAMs toward M1-Like Macrophages

Several options are currently used to select M1 phenotype from TAMs or to reprogram TAMs from M2 to M1 phenotype: TLR agonists, mAb targeting inhibitory proteins of M1 phenotype as well as other compounds (**Figure 2D**). TLR agonists represent a promising antitumor therapy. However, different agonists have been shown to promote different immune responses. Imiquimod is a ligand of TLR7 and acts mainly by increasing the number of infiltrating $CD43^+$ lymphocytes. This TLR agonist was found to induce the nuclear translocation of NFκB in J774A macrophages, leading to the production of pro-inflammatory proteins, such as TNFα, IL-6, IL-12, and CCL2 (68). The combination of topical imiquimod with low doses of cyclophosphamid and radiotherapy (RT) revealed a synergic antitumor effect and an increased survival response. This allowed the prevention of recurrence, with tumor rejection over 2 months after the end of treatment in a cutaneous breast cancer model (69). Multiple phase I and phase II clinical trials for imiquimod resulted in the use of topical application of imiquimod in clinic for skin metastasis and carcinomas. Synthetic unmethylated cytosine-guanine (CpG) oligodeoxinucleotides (CpG-ODNs) also offered high immunostimulatory activity. These molecules act by enhancing the production of pro-inflammatory cytokines, such as TNFα, IL-6 and IL-12, in macrophages and by upregulating NFκB activity in these cells. Indeed, these nucleotides are frequently found in viral and bacterial genomes and are recognized as pathogen-associated molecular patterns by TLR9 (70–72). Multiple studies aimed to improve the delivery of these CpG-ODNs by coupling them to gold nanoparticles for example (73). Combination of CpG-ODNs with other therapies, such as anti-CD40 exhibited promising results associated with the repolarization of TAMs (74, 75), even in poorly immunogenic cancer models such as a preclinical glioma model (76).

Another alternative to favor cytotoxic functions of TAMs is the stimulation of CD40 with mAbs. CD40 mAbs have demonstrated antitumor T-cell responses in mouse models of cancer and in clinical trials (77). Macrophages also express CD40 in their plasma membrane. Anti-CD40 mAbs were shown to promote macrophage tumoricidal activity, especially through enhanced secretion of NO and TNFα. Hence, it could induce $CD8^+$ T cell-dependent inhibition of tumor growth and metastasis (78–80). Clinical studies revealed objective tumor response in solid tumors (81). Since anti-CD40 mAbs can induce programmed death ligand 1 (PD-L1) upregulation in TAM and tumor-infiltrating monocyte plasma membrane, the blockade of PD-L1 axis combined with anti-CD40 and anti-CTLA-4 (anti-cytotoxic T-Lymphocyte-associated protein 4) mAbs showed extensive survival in colon and breast cancer models (77). Finally, MARCO is a pattern recognition scavenger receptor and is expressed by immunosuppressive TAMs. The targeting of this receptor is a new promising way to treat mammary carcinoma, colon carcinoma, and melanoma through the reprogramming of immunosuppressive TAMs toward a pro-inflammatory phenotype and by increasing tumor immune response (82).

A third alternative to reprogram TAMs is the use of different chemical compounds. The most famous one is IFNγ (83), approved by the FDA. In the same line, a small flavonoid-like compound, vadimezan (DMXAA), was found to repolarize macrophages in M1 phenotype. Reprogrammed macrophages then released cytokines and chemokines, including high local levels of TNFα, to induce a subsequent $CD8^+$ T cell activation (84). Vadimezan has been the subject of numerous preclinical studies and clinical trials. Alternatively, macrophage phosphoinositide 3-kinase γ (PI3Kγ) was shown to control a critical switch between immune suppression and activation. Selective deletion of PI3Kγ simultaneously activates NFκB and inhibits C/EBPβ in macrophages. In combination with anti-PD-L1, PI3Kγ depletion promoted tumor regression and prolonged survival in head and neck, lung, and breast cancer murine models (85). The plasma protein histidine-rich glycoprotein (HRG) is also able to block TAMs into a M1 phenotype through the downregulation of the expression of the placental growth factor (PlGF), a member of the VEGF family. In mice, HRG promoted antitumor immune responses and normalization of the vessel network (86). Finally, metformin was shown to skew TAMs polarization into a pro-inflammatory phenotype, partially through AMPKα1 activation. This effect was concomitant with a decrease in the number of metastases in Lewis lung cancer intravenous model (87).

While depletion of macrophages induced toxicities in mouse models and humans, the inhibition of macrophage/monocyte recruitment is one of the most used therapies in clinical studies. This type of therapy is usually combined to chemotherapy or RT and generated encouraging results in patients. On the other hand, the reprogramming of TAMs by chemotherapies or immunotherapies seems another very attractive way to target macrophages in tumors. However, there is a huge need for clinical studies to confirm these preclinical data in humans. Furthermore, it has to be noted that these treatments need to be localized to avoid an activation of M1 macrophages outside of the tumor and a systemic inflammatory response.

TARGETING TAMs WITH RT

In addition to target TAMs using chemo- and immunotherapies, it is also possible to influence the macrophage polarization with RT. Herein, we explore how low linear energy transfer (LET) radiotherapies (X-rays and γ-rays) can repolarize TAMs *in vitro* and *in vivo*. In a first part, the doses which have to be applied to the tumor in order to induce TAM reprogramming will be described and in a second part, the mechanisms involved in RT-induced reprogramming will be detailed.

Macrophage Radioresistance and Recruitment after RT

Macrophages are one of the most radioresistant cells in humans (7). This radioresistance is brought by a huge production of anti-oxidative molecules, such as manganese superoxide dismutase (MnSOD), a scavenger of superoxide (O_2^-) ions. The high expression of MnSOD confers cellular resistance against damaging effects. These damaging effects are mainly produced

by radiation-induced radicals, such as ROS or reactive nitrogen species (RNS). Indeed, the expression of MnSOD was increased after irradiation in THP-1, HL60, and KG-1 myelocytic cell lines. The mechanism of radioresistance conferred to macrophages was shown to be dependent on TNFα signaling. Indeed, endogenous production of TNFα is required for MnSOD expression following ionizing radiation (IR) (88–90). This TNFα-induced MnSOD expression is mediated by PKC-dependent activation of cAMP-responsive element-binding protein-1/ATF-1-like factors and would be dependent on NFκB activation (90–92). Currently, the radioresistance provided by endogenous MnSOD to macrophages is mimicked in healthy cells using MnSOD plasmid/liposome gene therapy to confer radioresistance to healthy cells (93–95).

Radiotherapy is used for more than 50% of cancer patients and showed tumor regression in most of the cases (33, 96). However, in addition to the intrinsic radioresistance of macrophages, IR also elicits a high recruitment of myeloid cells at the tumor site, possibly leading to tumor recurrence and tumor regrowth (59). Depletion of macrophages by liposomal clodronate before IR promoted the antitumor effects of RT and highlighted the role of recruited TAMs in tumor regrowth (90). Macrophage recruitment after IR is mediated by CCL2 and CSF1. Indeed, RT stimulated CSF1 production in prostate cancer and was shown to be responsible for TAM accumulation (97). Similarly, the inhibition of CSF1 receptor with PLX3397 prevented the myeloid cells recruitment after IR, increased survival and postponed the recurrence of glioblastoma in intracranial xenograft models (59). RT also promotes macrophage infiltration, from the peritumoral environment to the tumor site, in a CCL2 dependent way (98, 99). However, to the best of our knowledge, there is no study combining RT to CCL2 inhibition described yet.

Dose-Dependent Effects of Irradiation on Macrophage Reprogramming

Although IR slightly affects the viability of macrophages, radiotherapy modifies the macrophage phenotype. To analyze the effects of radiotherapy on macrophage reprogramming, we classified these effects according to the dose. According to the UNSCEAR (United Nations Scientific Committee on the Effects of Atomic Radiation), low dose of X-ray radiation are doses under 0.1 Gy, but clinically applied low doses are doses under 1 Gy (100). In this review, the irradiation doses were classified as followed: low doses as doses lower than 1 Gy, moderate doses (MDI) as doses ranging from 1 to 10 Gy, and high doses as doses higher than 10 Gy.

High Doses of Irradiation (HDI)

In vitro, M1 Raw264.7 macrophages were reprogrammed toward M2-like macrophages after HDI (20 Gy). Sustained M2 phenotype after irradiation resulted from NFκB p50 activation, leading to high IL-10 production and reduced TNFα secretion. These results were confirmed *in vivo* since HDI (3 Gy × 20 Gy over 3 days) promoted M2-like macrophages at the tumor site, in mice with Panc02 cell xenografts (101). In another study, high doses of X-rays (25 Gy in one shot or 60 Gy fractioned over 3 weeks) increased the number of M2-like TAMs in a murine model of prostate cancer (TRAMP-C1 cell line). This was evidenced by a low inducible nitric oxide synthase (iNOS) level in macrophages and by an increase in Arg1 and COX-2 mRNA expression. Such high doses induced angiogenesis and tumor growth in this cancer model (7). An increased number of M2-like macrophages after high doses of radiation (12 Gy) was also observed in an oral cancer model. The recolonization of tumor by M2-like macrophages elicited the secretion of pro-angiogenic factors that contribute to neoangiogenesis, favoring tumor growth (102). In addition, Seifert et al. similarly described accelerated tumor growth after irradiation (12 Gy) of murine pancreatic tumor models. This was driven by an early infiltration of M2-polarized TAMs into the tumor after radiotherapy and resulted in a subsequent T-cell suppressive response. This T cell response was linked to the upregulation of PD-L1 expression in tumor. The authors showed that RT accelerated the progression of pancreatic dysplasia to invasive carcinoma but also promoted tumor growth in invasive pancreatic ductal adenocarcinoma (PDA). Indeed, a decrease in iNOS, IRF5 and H2eb1 mRNA expression and a higher expression of Arg1, CD206, and PD-L1 were observed in TAMs from pancreatic dysplasia and PDA irradiated with hypofractionated (12 Gy) or fractionated (3 Gy × 6 Gy) doses (103). When TAMs were collected from tumor-bearing mice after RT and transferred to other tumor-bearing mice, tumor growth was accelerated to a higher extent than with unirradiated-macrophage transfer (7). Altogether, these results showed that HDI skew TAMs in a M2-like phenotype (**Table 1**). This is why the blockade of M-CSF, in order to prevent macrophage recruitment, in combination with HDI is attractive. Indeed, it revealed interesting results: M-CSF inhibition combined to RT promotes tumor regression. This reinforces the idea that HDI-irradiated TAMs take part to the tumor growth and tumor radioresistance. Furthermore, high levels of TAM-derived IL-10 elicited T cell anergy in irradiated tumor (103). This is why an adoptive $CD4^+$ T cell transfer has not met any success, except with the use of anti-M-CSF therapy combined to RT. This observation highlights the necessity to reprogram macrophages toward a M1-like phenotype to overcome the immunosuppression and the tumor regrowth after RT.

Moderate Doses of Irradiation (MDI)

In vitro, human unpolarized monocyte-derived macrophages shifted toward M1-like macrophages after MDI (2 Gy × 5). This is highlighted by the upregulation of pro-inflammatory markers (M1 phenotype) such as human leukocyte antigen-cell surface receptor (HLA-DR) and CD86, but also by the downregulation of anti-inflammatory markers (M2 phenotype) such as decreased mRNA expression of CD163, MRC1 (C-type mannose receptor 1, CD206) and versican (ECM proteoglycan) and reduced secretion of IL-10. In these macrophages, phagocytosis, associated with the M1-like phenotype, was increased after MDI while irradiation did not influence the ability of cocultured macrophages to promote the invasion of cancer cells and angiogenesis, features of M2-like macrophages (104). In the same line, unpolarized Raw 264.7 macrophages exhibited a higher expression of M1 markers (iNOS, TNFα, IL-12p70, IFNγ RANTES, and MCP-1) and a higher abundance of the phosphorylated p65 subunit from NFκB after γ-irradiation (2 Gy) (105). The γ-irradiation (2 Gy) of a human

TABLE 1 | Macrophage reprogramming after HDI, MDI, and LDI.

	Reference	Dose	Radiation type	Effect on polarization	Model
HDI	(7)	4 Gy × 5 × 3 week = 60 Gy	X-ray	M2 polarization	Mouse TRAMP-C1 (prostate)
	(101)	20 Gy × 3/day	X-ray	M2 polarization	Mouse Panc02 (pancreas)
	(102)	12 Gy	X-ray	M2 polarization	Human oral cancer (OSC-19 cells)—xenograft
	(103)	12 Gy or 3 × 6 Gy	X-ray	M2 polarization	Orthotopic pancreatic ductal adenocarcinoma model pancreas
MDI	(108)	2 Gy × 5 (10 Gy)	X-ray	Mixed M1/M2 phenotype	Human monocyte-derived macrophages (hMDM) with RKO or SW1463 cells
	(105)	5–10 Gy	X-ray	Increased inducible nitric oxide synthase (iNOS)/nitric oxide (NO) production	Raw 264.7 stimulated with lipopolysaccharide (LPS)/interferon γ (IFNγ)
	(104)	2 Gy × 5	X-ray	Reduced M2 markers	hMDMs
	(107)	2–4 Gy	γ-ray	M1 polarization	Raw 264.7, THP-1, hMDM
	(33)	2 Gy	γ-ray	M1 polarization	Raw 264.7 and peritoneal macrophages from RT5 mice
	(96)	2 Gy	γ-ray	M1 polarization	Tumor-associated macrophages from RT5 mice + CD8 T cell transfer (pancreas)
	(118)	1–2 Gy	X-ray	M2 polarization	Peritoneal macrophages from BALB/c mice + LPS/Raw 264.7
LDI	(105)	0.3–0.6–1.25 Gy	X-ray	Decreased iNOS/NO production	Raw 264.7 stimulated with LPS/IFNγ
	(109)	0.5–1 Gy	X-ray	M2 polarization	Raw 264.7
	(110)	0.5–0.7 Gy	X-ray	M2 polarization	THP-1 monocytes + LPS and monosodium urate crystals
	(111)	0.5–0.7 Gy	X-ray	Reduced M1 markers	THP-1 monocytes + LPS and monosodium urate crystals
	(112)	0.01–0.7 Gy	X-ray	M2 polarization	Peritoneal macrophages/Raw 264.7

Red shading/font means M2 polarization, green shading/font means M1 polarization.
HDI, high doses of irradiation; MDI, moderate doses of irradiation; LDI, low doses of irradiation.

macrophage cell line (U937) also provoked a higher expression of TNFα and IFNγ compared to unirradiated macrophages (106). In another study, $CD11b^+$/Gr-1 peritoneal macrophages from RT5 mice were γ-irradiated (2 Gy) *ex vivo* and showed an increased iNOS expression, related to M1 phenotype (33). Finally, PMA-differentiated macrophages (THP-1), murine macrophages (Raw 264.7) and human monocyte-derived macrophages (hMDM) revealed a pro-inflammatory profile after moderate doses of γ-rays (2 and 4 Gy). This was evidenced by increased mRNA levels for TNFα, IFNγ, IL-6, and IL-23 and higher protein levels for IL-1β and IL-8. While most of the previous studies showed the activation of NFκB p65 for macrophage reprogramming, this last study revealed that IR-induced M1-like phenotype was promoted by the transcriptional expression of IRF5 and was ataxia telangiectasia mutated (ATM)-dependent (107). Altogether, the results from *in vitro* experiment showed that unpolarized macrophages tend to acquire a M1 phenotype after MDI.

In addition to program unpolarized macrophages to M1 phenotype, MDI also potentiated the already acquired M1 phenotype. Indeed, MDI (2 Gy × 5) promoted a pro-inflammatory profile in M1 macrophages stimulated with LPS/IFNγ, as indicated by an increased expression of HLA-DR (104). Another *in vitro* experiment revealed that doses under 1 Gy prevented the polarization of macrophages toward M1 phenotype whereas doses of 5 and 10 Gy promoted the M1 phenotype in murine Raw 264.7 macrophages when stimulated with LPS/IFNγ. This is emphasized by an increased expression of iNOS and a higher NO production in irradiated macrophages (105). In contrast, in hMDMs stimulated with M-CSF and IL-10 (M2 macrophages), MDI did not influence the expression of pro- and anti-inflammatory markers (104). In other words, the effect of MDI on polarized macrophages showed an enhanced M1 phenotype in M1 macrophages but no change in M2 macrophages, meaning that MDI could not reprogram TAMs *in vitro*.

Cocultured experiments were performed between radiosensitive (RKO cells) or radioresistant (SW1463 cells) colorectal cancer cell lines and human unpolarized monocyte-derived macrophages. After irradiation, the mRNA expression of some pro-inflammatory (CCR7, IL1β, CXCL8) markers was decreased whereas the mRNA expression of anti-inflammatory markers was unchanged when macrophages were cocultured with RKO cells. MDI also promoted cancer cell invasion and migration of cocultured RKO cells. However, when macrophages were cocultured with SW1463 cells, there was an upregulation of the expression of pro-inflammatory (CCR7, CD80) and anti-inflammatory markers (IL-10 and CCL18) but no change of cancer cell migration and invasion. It means that following MDI, unpolarized macrophages adopt a different phenotype according to the type of cancer cells with which they interact (108).

Interestingly, *in vivo* experiments revealed promising results. A group of researchers suggested that moderated single dose (2 Gy) of γ-ray was able to completely reprogram TAMs in tumor. Klug and Prakash analyzed M1 (iNOS protein level, NO production) and M2 (Ym-1, Fizz-1 and Arg 1 protein level) markers in $CD11b^+$ peritoneal macrophages from RT5 mice after whole-body irradiation (WBI). While untreated mice exhibited elevated expression of M2 markers in peritoneal macrophages, whole-body irradiated mice revealed increased M1 marker expression and decreased M2 marker expression. However, local irradiation was not able to modify the expression of M1 and M2 markers when measured in tumor tissue lysate. As local MDI (1, 2, and 6 Gy) induced a decline of T cell infiltration, the authors used $CD8^+$ T cell transfer in addition to local irradiation (2 Gy) to induce a shift in the polarization of TAMs toward a M1 phenotype

and to promote T cell infiltration in tumor. Local irradiation in combination with $CD8^+$ T cell transfer induced an enhanced expression of IL-12p40 and IFNγ (M1 markers) and a reduced expression of IL-10 (M2 marker) in tumor tissue lysate. Indeed, the infiltration of tumor by T cells was exclusively dependent on the reprogrammed TAMs. When TAMs was depleted with CL treatment before local irradiation and $CD8^+$ T cell transfer, there was an inhibition of T cell recruitment into irradiated tumors. The infiltration of $CD8^+$ T cell into tumor is made feasible with the normalization of the vasculature. Indeed, pro-inflammatory macrophages elicited the normalization of the vasculature and allowed an efficient T cell transfer, leading to the eradication of the tumor and an increased survival in irradiated RT5 mice. However, it remains elusive how $CD8^+$ T cell transfer impacts TAM reprogramming. Interestingly, local irradiation alone is not able to reprogram TAMs toward a M1-like phenotype. Then, it seems clear that $CD8^+$ T cell transfer plays a role in macrophage reprogramming. The underlying mechanism needs to be further investigated (96) **Table 1** summarized the effects of MDI on macrophage polarization described here above.

Low Doses of Irradiation (LDI)

Low doses of irradiation represents a good alternative in order to bypass the toxicities observed during intensive radiotherapy (HDI) (**Table 1**). However, LDI rather favor the M2 phenotype of TAMs. Indeed, LDI decreased the iNOS level and the NO production in Raw 264.7 macrophages polarized in M1 phenotype, resulting in repolarization of M1 macrophages toward M2 phenotype (105). Other results in favor of a M2-like phenotype were described after low doses of γ-radiation in murine macrophages. Indeed, irradiation of murine macrophages (RAW 264.7) with a dose of 0.5 Gy inhibited MPK1 [mitogen-activated protein kinase (MAPK) phosphatase]. MPK1 dephosphorylates the MAPKs p38, c-Jun and ERK1/2 and the dephosphorylation of p38 was associated with a decrease in TNFα and IL1β levels. Irradiation (0.5 Gy) of RAW264.7 macrophages stimulated with LPS also led to a decrease in p38 phosphorylation and TNFα production (109). In addition, Frey and Lodermann showed that low doses of X-rays (0.5–0.7 Gy) induced an anti-inflammatory phenotype in LPS-activated human THP-1 cells as evidenced by reduced amounts of secreted IL-1β in the medium. This was linked to a lower p65 NFκB nuclear translocation and a weak p38 phosphorylation (110, 111). Closely related to these results, it was also demonstrated that doses under 2 Gy favored the repolarization of M1 macrophages into M2-like macrophages, as evidenced by an increased level of TGFβ in the culture medium. This was associated to a reduced nuclear translocation of p65 NFκB (112).

In conclusion, HDI and LDI show no effect on M2 to M1 macrophage polarization while MDI clearly evoke TAM reprogramming. However, most of studies performed in this field are *in vitro* experiments, i.e., macrophages alone with no contact with cancer cells. Further *in vivo* experiments should reinforce the results obtained by Klug et al. with MDI. Furthermore, to our knowledge, no clinical study has been designed to analyze the effect of MDI on TAM reprogramming. It is thus difficult to transpose these data to the human tumors.

Whole-Body Irradiation

In vivo studies showed that exposure to low doses of WBI in healthy mice activated the innate immune cells including macrophages (113–115) (**Table 2**). In healthy mice, a single dose of WBI resulted in a T_H1 cytokine expression profile whereas fractionated dose irradiation drove a T_H2 shift in spleen and blood of mice (116). In the same line, single low doses (0.075 and 2 Gy) of total body radiation in healthy mice polarized peritoneal macrophages toward M1 phenotype as indicated by increased IL-12 and IL-18 secretion. This polarization is strongly linked to the activation of p65 NFκB and MyD88 a few hours after WBI (117). Only a few studies were published on WBI of tumor-bearing mice, as this treatment is irrelevant for human. However, as WBI would reprogram TAMs, studying the underlying mechanisms could be very helpful. A first study indicated that low doses (0.01–0.1 Gy) of WBI induced opposite effects on macrophages and NK cells in BALB/c radiosensitive mice and C57BL/6 radioresistant mice. Peritoneal macrophages exhibited a M1 phenotype in BALB/c mice, evidenced by an increased production of IL1β, IL-12 and TNFα. However, M2 macrophages were observed in tumor from C57BL/6 mice after WBI, partly elucidating the radioresistance of this mouse strain (118). Klug et al. also showed that peritoneal macrophages from RT5 mice, irradiated with a systemic dose of 2 Gy, revealed a higher iNOS level and NO production whereas the expression of M2 markers was decreased in these macrophages, indicating macrophage reprogramming. Furthermore, macrophages from total body irradiated mice, when transferred to tumor-bearing mice in parallel with $CD8^+$ T cell adoptive transfer, induced tumor regression, similar to local irradiation in combination with $CD8^+$ T cell adoptive transfer (96). In parallel, Prakash et al. described a switch of TAM polarization toward

TABLE 2 | Macrophage reprogramming after WBI.

Reference	Dose	Radiation type	Effect	Model
(113)	0.2 and 2 Gy	γ-ray	M1 polarization	WBI (without tumor)
(117)	0.075 and 2 Gy	X-ray	M1 polarization	WBI (without tumor)
(114)	0.5–6 Gy	X-ray	M1 polarization	WBI (without tumor)
(118)	0.01–0.02–0.1 Gy × 10/day × 2 weeks (LDI)	X-ray	Increased cytotoxic activity and nitric oxide	Macrophages from BALB (L1)/c and C57BL/6 (Lewis lung cancer) mice (WBI)
(96)	0.5–2 Gy × 1 (MDI)	X-ray	M1 polarization	Mouse RT5 insulinoma/Human MeWo melanoma xenograft/Human pancreas
(33)	2 Gy × 2 (MDI)	γ-ray	M1 polarization	Rip1 Tag5 tumor-bearing mouse (WBI)

Green shading means M1 polarization.
WBI, whole-body irradiation.

M1 phenotype when RT5 insulinoma bearing mice were treated by systemic irradiation (2 Gy/week on 2 weeks). Indeed, tumor lysates presented a higher expression of M1 markers [iNOS, pSTAT3, TNFα, IL-12 (p70)] and a lower expression of M2 markers (CD206, Fizz-1, Ym-1 and Arg1). Peritumoral macrophages showed an elevated iNOS expression and NO production after WBI, modifying the tumor microenvironment with the normalization of the tumor vasculature.

To explain the discordance between local irradiation and WBI on the reprogramming of TAMs, the authors suggested that WBI allowed the mobilization of fresh reprogrammed macrophages from various lymphoid organs to infiltrate the tumor site and the surrounding microenvironment. Infiltration of tumor by reprogrammed macrophages can result in the activation of antitumor T-cell responses and can thereby act as an "endogenous vaccine" (33) On the other hand, local irradiation is not able to invite macrophages from lymphoid organs to the tumor site. It could be hypothesized that the transfer of $CD8^+$ T cells would induce macrophage reprogramming in lymphoid organs. The combination of T cell transfer to irradiation would promote the normalization of the tumor vasculature, allowing tumor perfusion by $CD8^+$ T cells and reprogrammed macrophages.

Molecular Pathways Responsible for the Repolarization of TAMs after RT

There are several mechanisms proposed to explain the influence of the irradiation dose on the polarization of TAMs. These mechanisms are partly different from those involved in the reprogramming mediated by chemotherapy and immunotherapy, and they include ROS, DNA damage, p50–p65 NFκB activation, and MAPK phosphorylation. The differences between the different doses could be due to the activation of different pathways according to the dose, i.e., a switch in the NFκB subunit balance for moderate doses while high doses would induce apoptosis.

NFκB Balance

Nuclear factor kappa B plays an important role in the polarization of macrophages. It was shown that M2 macrophages acquired their phenotype under the effect of p50–p50 NFκB homodimer while M1 macrophages are answerable to p50–p65 NFκB heterodimer (24). Once p65–p50 NFκB is translocated into the nucleus, it allows the expression of pro-inflammatory mediators [TNFα, IL-1β, IL-6, IL-12(p40), IFNγ, CXCL10 and NOS2 (14)] whereas p50–p50 NFκB inhibits the expression of these genes. Indeed, several experiments revealed the need for p65 translocation to activate M1 polarization (24, 119). Crittenden and his colleagues evidenced that HDI (60 Gy) produced M2 phenotype through p50–p50 dimer activation, leading to a subsequent IL-10 production (101). In the same line, low X-ray radiation dose (<1 Gy) reduced the translocation of p50–p65 NFκB in M1 activated macrophages (112). LDI on human macrophages and LPS-activated THP-1 macrophages reduced the nuclear amount of p65 NFκB, a phenomenon also correlated to a decreased secretion of IL-1β (M1 cytokine) (110). Interestingly, Teresa Pinto et al. revealed an enhanced phosphorylation of RelA (p65) in macrophages following MDI (2, 6, and 10 Gy), correlated to M1 repolarization (104). Hildebrandt et al. also evidenced the role of NFκB in TAM reprogramming in Raw264.7 macrophages after 2 Gy irradiation (105). In an *in vivo* study, whole-body γ-irradiation (2 Gy)-induced the phosphorylation of NFκB p65 in tumor lysate. The activation of NFκB p65 is closely related to a reprogramming of TAMs toward M1-like macrophages (33) (**Figure 3**).

In sepsis, a sustained activation of macrophages by LPS leads to a tolerance and a reprogramming of macrophages toward M2 phenotype. This reprogramming is driven by p21, involved in the shifting of the balance between p65–p50 and p50–p50 NFκB dimers. Indeed, p21 deficiency is linked to a reduced DNA-binding affinity of the p50–p50 homodimer and a prevalence for the p65–p50 heterodimer in macrophages stimulated with LPS (120, 121). In some cases, ubiquitination is controlled by the phosphorylation of a protein substrate (122). Indeed, some effectors of the DNA repair machinery are described to be involved in the ubiquitin proteasome pathway and regulate p21 protein level in ML-1 cells (myelocytic leukemia cell line) (123). Therefore, a high ubiquitination of p21 would lead to a lower level of p21 protein. This could be correlated with an increased p65–p50 DNA-binding affinity and could potentially favor a M1 phenotype after IR. Further investigations are, however, required to understand the possible role of p21 in regulating the NFκB balance after IR.

ATM Kinase

Radiotherapy induces major effects on cells by creating DNA damage. DNA damage and ROS produced by γ-radiation (2–20 Gy) induced the phosphorylation of ATM in U937 human macrophage cell line (106). When DNA damage appeared, ATM plays a central role in the detection and the activation of the DNA repair machinery [for review see Ref. (124)]. The activation of ATM notably leads to the ubiquitination of NEMO (NFκB Essential Modulator), a subunit of the IKK complex, a few hours

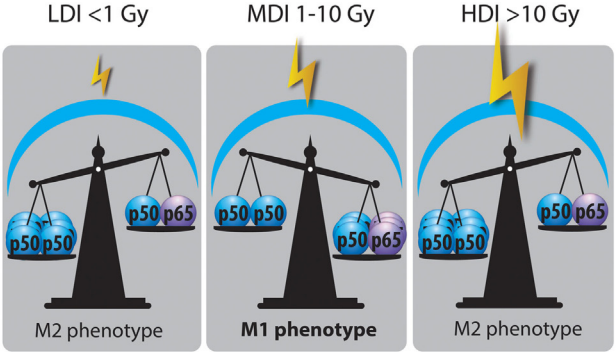

FIGURE 3 | Nuclear factor kappa B (NFκB) balance state after LDI, MDI, and HDI. Irradiation dose showed opposite effects on NFκB balance in macrophages: LDI or doses lower than 1 Gy did not modify the abundance of p50–p50 NFκB in macrophage nucleus after radiation. MDI or doses from 1 to 10 Gy induced a switch of NFκB balance from the inactive homodimer (p50–p50) to the active heterodimer (p50–p65), correlated with a reprogramming of tumor-associated macrophages (TAMs). HDI or doses higher than 10 Gy were not able to change the NFκB balance, skewing TAMs in a M2 phenotype (HDI, high doses of irradiation; MDI, moderated doses of irradiation; LDI, low doses of irradiation).

after macrophage irradiation. The ubiquitination of NEMO is ATM-dependent as indicated by the reduced ubiquitination of NEMO when an ATM inhibitor (Ku5593) was used in combination with γ-rays (125). Ubiquitinylated NEMO then drives the activation of IKK complex in the cytoplasm. This activation goes through ubiquitination of IKβ and the subsequent degradation of this inhibitor by the proteasome. p65–p50 NFκB is, therefore, released in the cytoplasm and free to move into the nucleus where the heterodimer acts as a transcriptional factor [for review see Ref. (126)].

After γ-radiation (2 Gy), the phosphorylation of NEMO was followed by the activation of NFκB (p65). A subsequent upregulation of M1 markers (CD86, CD40, HLA-DR, TNFα, IFNγ) and a reduced secretion of IL-4 (M2 marker) followed the activation of NFκB. These changes are partially generated by elevated ROS content in cells, as indicated by the increase or decrease in the phosphorylation of NEMO when U937 monocytic cells were irradiated and treated with L-buthionine sulphoximine or *N*-acetyl cysteine (NAC), respectively. Indeed, L-buthionine sulphoximine irreversibly inhibits γ-glutamylcysteine synthase, hence depleting GSH level and increasing ROS content. NAC is a potent antioxidant, known to decrease ROS level by increasing GSH levels (106). However, another team showed that γ-rays (0, 3, 6, and 10 Gy) induced NFκB activation in Raw 264.7 macrophages, as highlighted by the degradation of the IKβ protein. The activation of NFκB was related to a higher NO production in macrophages. This phenomenon is dependent on DNA damage more than ROS level, since NAC did not affect NO production and IKβ degradation in irradiated cells (127).

Moreover, modulators of DNA repair, such as Olaparib (PARP inhibitor), increased ATM activation and upregulated IRF5 transcription, resulting in macrophage activation toward a pro-inflammatory phenotype (107). In conclusion, IR is able to induce DNA damage by direct or ROS-dependent interactions with DNA. DNA damage leads to the recruitment of the ATM kinase and DNA repair machinery. Consequently, ATM contributes to the reprogramming of macrophages after irradiation.

Reactive Oxygen Species

Radiation therapy promotes the formation of radicals, such as ROS or RNS in cells. ROS quantities depend on the dose applied to the cells. In macrophages, different ROS concentrations can differently influence the cellular responses and the polarization of macrophages. Indeed, the role of ROS in the polarization of macrophages is not so clear but the most accepted idea is that ROS play key roles in M1 responses (e.g., defense against invading microbes) (128) and regulates M2 polarization (129, 130).

M1 Polarization

The polarization of macrophages toward M1 or M2 phenotype goes through several pathways, including NFκB. There is a balance between the inhibitory heterodimer NFκB (p50–p50) and the active heterodimer NFκB (p50–p65) (24). When this balance leans on one side or the other, macrophages undergo M2 or M1 polarization, respectively. It is also well known that ROS generation mediated the production of pro-inflammatory cytokines (131). Indeed, this ROS production activates MAPK and NFκB pathways (132). It was shown that H_2O_2 enhanced p65 NFκB DNA-binding and promoted p65 NFκB phosphorylation. This NFκB activation is followed by its translocation into the nucleus in macrophage and monocytic cell lines, and then induces M1 polarization (133). In parallel, it was shown that H_2O_2 altered protein–protein interaction of p50–p50 NFκB, therefore reducing p50–p50 NFκB activation, supporting M1 activation (134). As previously said, ROS production is observed after irradiation. This is due to the direct ionization of molecules by incident photons. Another way for γ-irradiation to induce ROS generation is the activation of NADPH oxidase (NOX). The NADPH oxidase (NOX 1 and NOX 2) catalyzes the oxidation of nicotinamide adenine dinucleotide in the $NADP^+ + H^+$ while reducing O_2 in O_2^-, leading to the formation of H_2O_2. γ-irradiation (2 Gy) promoted ROS production in Raw264.7. This ROS production was partly inhibited by the use of NAC and by diphenylene iodonium, a NOX inhibitor. In parallel, the protein expression of NOX2 was increased after γ-irradiation in PMA-differentiated THP-1 cell and in Raw264.7 macrophages. Altogether, these results indicated that moderate doses of γ-irradiation generated NOX2-dependent ROS production. Elevated ROS content yielded ATM activation, as suggested by the absence of ATM phosphorylation in presence of NAC or siNOX2 when Raw264.7 macrophages were irradiated. This NOX2-dependent ATM activation controlled the polarization of Raw 264.7, THP-1 and hMDM in M1-like macrophages, through the regulation of IRF5 transcription. Moreover, in patients, the perturbation of ATM-dependent NOX2 signaling pathway was associated with a decreased iNOS macrophage number and poor tumor responses to radiotherapy (107).

M2 Polarization

Not only, NAPDH oxidase activity drives M1 polarization, but its inhibition conversely triggers M2 polarization. A previous study showed that the inhibition of NOX promoted anti-inflammatory microglial activation (M2 phenotype) during neuroinflammation (135). Furthermore, another group revealed that the deletion of NOX1/2 reduced ROS production during macrophage differentiation. This double knockout is not critical for M1-like polarization of mouse bone marrow-derived macrophages, but prevented M2 polarization, as evidenced by the reduced expression of mCCL17, mCCL24 and RELMα. Indeed, NOX1/2 is crucial for the activation of c-Jun N-terminal kinase (JNK) and extracellular signal-regulated kinase (ERK) MAPKs during monocyte to macrophage differentiation and then affects M2 polarization (136). High concentrations of ROS play a decisive role in the differentiation and the polarization of macrophages into M2 phenotype and antioxidants treatment affected M2 but not M1 macrophage polarization. The use of butylated hydroanysole and other ROS scavengers repressed tumorigenesis by blocking the occurrence of TAMs (129). H_2O_2 stimulates the production of TNFα and activates the transcription factor STAT6, responsible for the expression of M2 markers such as Fizz-1 in macrophages (137, 138).

All these data showed that high concentrations of ROS trigger M2 polarization while smaller concentrations are responsible for M1 polarization. On the one hand, the production of ROS driven by HDI prevents the reprogramming of TAMs toward M1-like

macrophages. On the other hand, LDI induce small ROS production, probably not enough to reach the range of concentrations able to reprogram macrophages. However, MDI allows to reach the right range of ROS concentrations in macrophages to activate p65 NFκB, IRF5, and MAPK notably through ATM activation, hence favoring M1 phenotype.

Further investigations are needed to better understand the effect of IR on the ROS generation in TAMs and the molecular pathways involved in the polarization of macrophages *via* ROS production.

IRF5

Interferon-regulatory factor/signal transducer and activator of transcription (IRF/STAT) signaling is a central pathway in macrophage polarization. IRF can interact with two adaptors, MyD88 and TRIF, downstream of cytokine receptors or TLR. IRF5 and IRF4 are in competition to the binding of MyD88 and the subsequent activation of pro-inflammatory transcription factors, including NFκB. The activation of IRF5 through MyD88 then promotes M1 phenotype in macrophages. As a competitor for MyD88, IRF4 acts as an antagonist and can suppress M1 macrophage polarization. The balance between IFR4 and IRF5 in cells is critical for M2 and M1 polarization, respectively (24, 139).

Only one *in vitro* study established the role of IRF5 in macrophage reprogramming after irradiation. In this study, the authors showed that macrophages acquired a M1-like phenotype after exposition to γ-irradiation (2 Gy). This polarization is made feasible by the activation of NOX2 and ATM, hence driving the transcription of IRF5 (107). While these results are very interesting, the contribution of IRF/STAT pathway to macrophage polarization mediated by irradiation needs to be further investigated *in vivo* and in patients. Furthermore, IRF5 modulation is also known to drive M1 polarization through the activation of NFκB. The link between IRF and NFκB in macrophage reprogramming after radiotherapy should also be considered.

iNOS Level and NO Production

Nitric oxide mediator is a double-edge sword key regulator in tumor progression. On the one hand, NO has antitumoral effects as it promotes DNA damage, elicits cell death, and enhances anticancer therapeutic efficacy. Indeed, patients with lower iNOS expression levels, hence low NO production, showed recurrence of tumors and metastasis after RT. On the other hand, NO mediator is also known for its pro-tumoral effects since it induces antiapoptotic effects and promotes cell cycle, cancer progression, metastasis, angiogenesis, and chemoprotection. High level of iNOS is associated with poor prognosis and tumor-promoting effects (140). It thus seems that critical NO concentrations and iNOS levels finely modulate the fate of the tumor.

High doses of irradiation induced NO production and high iNOS expression level in macrophages. For instance, high doses of γ-irradiation (20 Gy) led to iNOS activation and NO production, favoring tumor growth and recurrence after RT (141). Another *in vivo* study using high doses (25 Gy or 3 Gy × 20 Gy) also generated high level of iNOS in murine macrophages after IR, contributing to the tumor growth (7). NO production contributes to DNA repair by inducing p53, poly(ADP ribose) polymerase and DNA-dependent protein kinase activation, leading to tissue regeneration and tumor regrowth. In addition, NO mediator is related to tumor angiogenesis and promotes reoxygenation. Therefore, targeting iNOS in murine macrophages enhanced postradiotherapeutic efficacy after HDI (141).

On the other hand, WBI (2 Gy × 2 Gy) on RT5 mice induced an increased NO production and iNOS level, enough to induce tumor regression. In addition, *ex vivo* radiation with similar doses on peritoneal macrophages from RT5 mice also stimulated an increased in iNOS level and NO production (33). Indeed, NO can be considered as a free radical and as a source of reactive oxygen and nitrogen species, inducing DNA damage (142). Another team hypothesized that iNOS and NO production induced by MDI (2 Gy) remodeled vasculature allowing cytotoxic lymphocyte recruitment, and subsequent tumor eradication (15). NO leads to higher tumor oxygenation by promoting vasodilatation and hence radiosensitization (142). It can diffuse toward bystander cancer cells leading to their radiosensitization (143).

High doses of irradiation would induce high level of NO in macrophages, leading to cancer progression. Contrarily, MDI drive a slight increase in NO production in macrophages, enough to participate to the reprogramming of TAMs and favoring tumor regression.

MAPK (p38–ERK–JNK)

Mitogen-activated protein kinases are serine threonine kinases activated by diverse stimuli including cytokines and ROS. MAPKs regulate diverse pathways such as cell proliferation, apoptosis, and differentiation. MAPKs include extracellular signal-regulated kinase 1 and 2 (ERK 1/2), JNK and p38. They mediate immune cell functional responses to diverse signals and play a role in macrophage polarization. MAPK kinases (MAPKKs) activate MAPKs through dual phosphorylation on tyrosine and threonine residues (Thr–X–Tyr motif) located in the activation loop of the kinase domain (144). The phosphorylation of MAPK activates pro-inflammatory gene transcription and is correlated with M1-like macrophages. At the opposite, MAPKs are inactivated through dephosphorylation of threonine and/or tyrosine residues within the activation loop by MAPK phosphatase (MKP-1) (145). MKP-1-deficient macrophages exhibit skewed activation profiles: macrophages showed an enhanced pro-inflammatory phenotype in response to IFNγ and TNFα while this deficiency severely suppressed "M2-like" phenotype after IL-4 stimulation (146). Compared to wild-type mice, MKP-1-deficient mice produced greater amounts of TNFα, IL-1β, CCL2, granulocyte/macrophage colony-stimulating factor (GM-CSF), IL-6, IL-10, and IL-12p70 (147, 148).

Mitogen-activated protein kinases are also regulated by ROS and DNA damage (132). Within a few minutes, low doses (0.5 and 1 Gy) of γ-radiation induced a dephosphorylation of both ERK 1/2 and p38 MAPKs. This dephosphorylation depended on MKP-1 and induced the suppression of TNFα production in Raw 264.7 cells. These results correlated with the inability of LDI to reprogram M2 macrophages (109). Another study showed enhanced phosphorylation of ERK 1/2 and p38 following moderated doses (2 Gy) of γ-radiation in resident peritoneal exudate cells. This activation was related to a decreased

dephosphorylation exerted by MKP-1 and was correlated with TNFα production. The explanation relies on the oxidation of the catalytic cysteine of MKP that inactivates the phosphatase, then triggering the activation of MAPK cascade including JNK and p38. These results correlated with the reprogramming of macrophages induced by MDI (149). Conflicting results revealed the inhibition of p38 phosphorylation in macrophages after WBI of tumor-bearing mice. The inhibition of p38 phosphorylation in macrophages allowed the reprogramming of TAMs toward M1 phenotype in tumor. This inhibition could be linked to the upregulation of MKP-1 (33).

Nuclear Erythroid Derived 2-Related Factor (Nrf2)

The Nrf2 is involved in the management of intracellular oxidative stress. It is also known to repress inflammation by inhibiting pro-inflammatory cytokine expression. Indeed Nrf2 is able to bind the close proximity of IL-6, IL-1β, and IL-1α genes in LPS-stimulated macrophages. This binding hence inhibits the recruitment of RNA polymerase II to the transcription start site without affecting the p65 NFκB recruitment. The Nrf2 binding to these genes is independent on ROS level since the use of antioxidant (NAC) did not affect the inhibition of pro-inflammatory gene transcription mediated by Nrf2 (150). The transcription factor Nrf2 was translocated into the nucleus even after 0.1 Gy γ-radiation, leading to the upregulation of antioxidant proteins such as heme oxygenase-1 in Raw 264.7. Nrf2 translocation increased with the dose (0.1–2.5 Gy). The regulation of Nrf2 is mediated by ERK 1/2 pathway after the irradiation of macrophages (121). It is also known that in oxidative stress conditions, p21 interacts with Nrh2 domain of Nrf2, upregulating Nrf2-mediated antioxidant response (151). This could link the Nrf2 pathway to NFκB in the reprogramming of TAMs after IR: the absence of p21 prevents the anti-inflammatory response mediated by Nrf2 and favors the p50–p65 NFκB DNA-binding. The fate of irradiated macrophages would then depend on the connection between ROS level/DNA damage and the downstream-activated pathways.

Overall View Regarding TAM Reprogramming upon Radiotherapy

Local radiotherapy can finely tune the balance between immunosuppression and immune antitumor properties. The shift toward

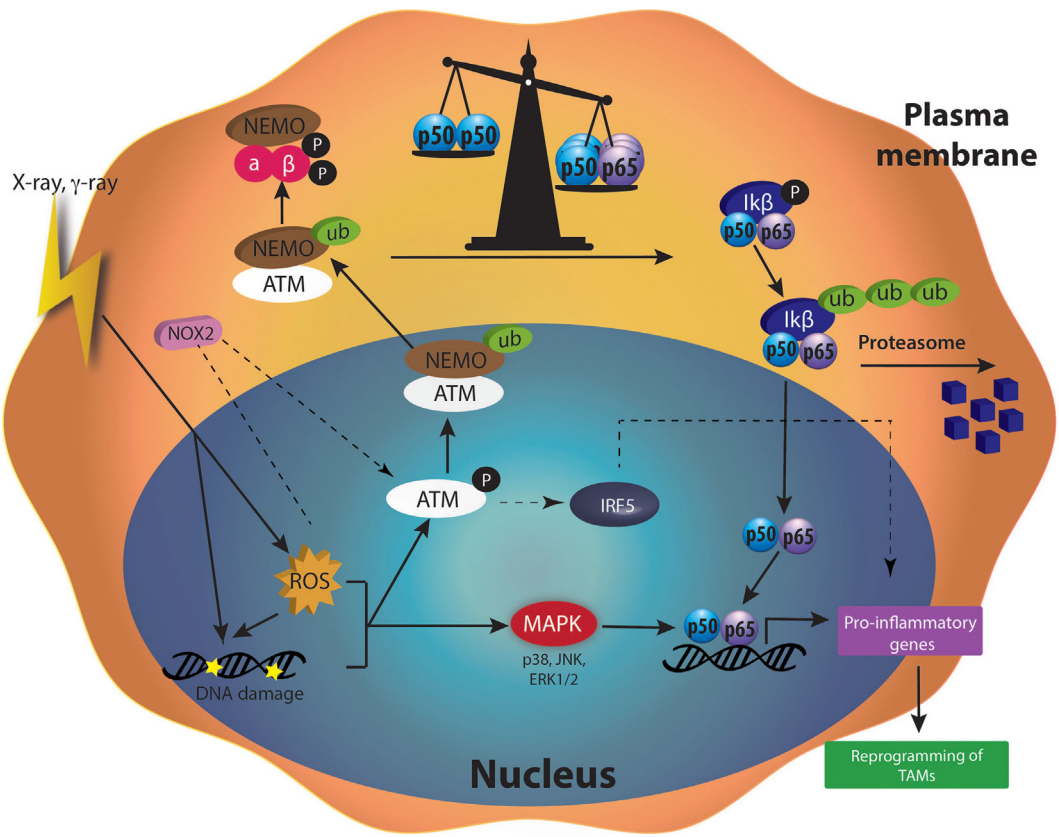

FIGURE 4 | Molecular mechanisms activated after moderated doses of irradiation in tumor-associated macrophages (TAMs). Ionizing radiation (X-rays or γ-rays) induces DNA damage and elevated reactive oxygen species (ROS) content in cells. DNA repair machinery [such as ataxia telangiectasia mutated (ATM)] is activated by DNA damage and initiates the ubiquitination of NFκB essential modulator (NEMO), a subunit of the IKK complex. Therefore, ubiquinated NEMO can drive the activation of IKK complex in the cytoplasm. The degradation of IκB protein by the proteasome allows the release of p50–p65 nuclear factor kappa B (NFκB) in the cytoplasm. p50–p65 NFκB is then translocated into the nucleus and induces the transcription of pro-inflammatory genes, leading to the reprogramming of TAMs. ROS are also able to stimulate mitogen-activated protein kinase (MAPKs). Once phosphorylated, MAPKs also participate to the activation of NFκB and hence, to the transcription of pro-inflammatory genes.

one or the other immune state depends on the dose per fraction, the total dose and the cancer type. Whereas local IR finds difficulties to completely reprogram TAMs, WBI can be helpful in the understanding of TAMs reprogramming since it activates the immune system outside the tumor site, leading to the complete eradication of the tumor. It, thus, seems that local IR needs something more than its sole effects on macrophages to induce a total reprogramming of TAMs and to restore a full immune antitumor response.

The mechanisms underlying macrophage reprogramming after radiation therapy are summarized in **Figure 4**. This figure emphasizes the central role of NFκB in macrophage reprogramming after MDI. Although most of these studies described in this review are promising, there is still a huge need for further investigations and *in vivo* confirmations. Indeed, cancer cell irradiation generates damage-associated molecule patterns (DAMPs), such as high mobility group box 1 (HMGB1). DAMPs bind on their corresponding pattern-recognition receptor, such as TLR4 for HMGB1 in macrophages, triggering a pro-inflammatory phenotype (152). The irradiation then promotes antitumoral responses. However, it is possible that the contact between macrophages and cancer cells could offer the response of macrophages to radiotherapy. Indeed, cancer cells secrete different cytokines and chemokines that could influence the faith of macrophage polarization. More precisely, the type of cancer cells in the tumor can modulate macrophage reprogramming after irradiation, as evidenced by the opposite results acquired with different cancer cell lines in cocultured with macrophages (108).

In parallel, IR can also alter other types of cells in tumor, such as lymphocytes and dendritic cells, as well as the tumor vascularization (152). For example, ablative radiation therapy promotes $CD8^+$ T cell accumulation into the tumor (153, 154). Indeed, single moderate doses (10 Gy) of irradiation mobilized $CD8^+$ T cell through dendritic cells activation hence reducing or eradicating tumor. Therefore, MDI fulfills mobilization of effectors from the immune system and is able to reprogram TAMs in an antitumor phenotype. However, the issue about the fractionation should also be addressed, as in patients the treatments are usually given in several doses. It was shown that hyperfractionation (5 Gy × 4 Gy) could completely abrogate the effect on $CD8^+$ T cell mobilization observed with single high dose (20 Gy) (154). The effects of fractionation on macrophage reprogramming remain elusive and need to be further investigated.

CONCLUSION AND FUTURE DIRECTIONS

Chemo- and immunotherapies, as well as moderate dose of irradiation are able to reprogram TAMs into M1-like macrophages. TAM reprogramming is induced through various mechanisms. These pathways mainly include NFκB, NO production, and STAT1 that can act together. MDI-induced reprogramming is made possible through DNA damage-dependent ATM activation, the production of a specific range of ROS and NO amounts, a shift of the NFκB balance to the active p50–p65 heterodimer, the transcription of IRF5 and the activation of the MAPK pathway. Amongst them, NFκB pathway seems to be a central target for macrophage reprogramming.

Local IR is able to kill cancer cells and to activate the immune system by the release of cancer cell antigens and of immune-associated factors by stromal cells and vascular endothelial cells, but it also depletes T cells and antigen-presenting cells (155). Combined radiotherapy and immunotherapy have shown promising results in reprogramming macrophages and may thus be useful for tumor elimination. However, the choice of T cell adoptive transfer can determine the fate of the tumor and macrophage reprogramming, as $CD8^+$ T cell adoptive transfer is more effective than $CD4^+$ T cell adoptive transfer (96, 103). Indeed, the use of a anti $CD4^+$ T cell therapy combined to γ-irradiation (5 Gy) in a mammary mouse model improved the efficacy of radiotherapy (156). The use of MDI combined to adoptive $CD8^+$ T cell transfer or stimulating $CD8^+$ T cell therapy (such as anti PD-L1/programmed cell death 1) may give promising results as effective anticancer therapies. The transfer of irradiated macrophages was also the subject of numerous studies in murine models. However, human clinical studies using transferred macrophages have also been performed but showed no or few improvements regarding cancer regression (157).

Another avenue to explore would be the effect of high LET particles, for example protons, since protontherapy is more and more developed in clinic. As the mechanism of action is different from that of conventional radiotherapy (X-rays), the effects on macrophage reprogramming could be potentiated. Indeed, charged particles can drive huge NFκB activation compared to X-rays or γ-rays, as shown in HEK/293 cells (158).

Targeting the immune system in cancer diseases demonstrated successful improvement on cancer elimination and has become a highly promising therapy. Therefore, MDI combined to chemo- or immunotherapies targeting macrophage reprogramming could also synergize their effects on tumor regression.

AUTHOR CONTRIBUTIONS

GG wrote the review and designed the figures and the tables. SL and CM supervised the whole work, contributed to writing, and critically revised the paper.

FUNDING

GG is recipient of a Télévie grant (FNRS, Belgium).

REFERENCES

1. Mantovani A. Cancer: inflaming metastasis. *Nature* (2009) 457(7225):36–7. doi:10.1038/457036b
2. Quail DF, Joyce JA. Microenvironmental regulation of tumor progression and metastasis. *Nat Med* (2013) 19(11):1423–37. doi:10.1038/nm.3394
3. Hanahan D, Weinberg RA. Hallmarks of cancer: the next generation. *Cell* (2011) 144(5):646–74. doi:10.1016/j.cell.2011.02.013
4. Schreiber RD, Old LJ, Smyth MJ. Cancer immunoediting: integrating immunity's roles in cancer suppression and promotion. *Science* (2011) 331(6024):1565–70. doi:10.1126/science.1203486
5. Mittal D, Gubin MM, Schreiber RD, Smyth MJ. New insights into cancer immunoediting and its three component phases – elimination,

equilibrium and escape. *Curr Opin Immunol* (2014) 27:16–25. doi:10.1016/j.coi.2014.01.004
6. Gordon S, Martinez FO. Alternative activation of macrophages: mechanism and functions. *Immunity* (2010) 32(5):593–604. doi:10.1016/j.immuni.2010.05.007
7. Tsai CS, Chen FH, Wang CC, Huang HL, Jung SM, Wu CJ, et al. Macrophages from irradiated tumors express higher levels of iNOS, arginase-I and COX-2, and promote tumor growth. *Int J Radiat Oncol Biol Phys* (2007) 68(2):499–507. doi:10.1016/j.ijrobp.2007.01.041
8. van Ravenswaay Claasen HH, Kluin PM, Fleuren GJ. Tumor infiltrating cells in human cancer. On the possible role of CD16+ macrophages in antitumor cytotoxicity. *Lab Invest* (1992) 67(2):166–74.
9. Allavena P, Sica A, Garlanda C, Mantovani A. The Yin-Yang of tumor-associated macrophages in neoplastic progression and immune surveillance. *Immunol Rev* (2008) 222:155–61. doi:10.1111/j.1600-065X.2008.00607.x
10. Noy R, Pollard JW. Tumor-associated macrophages: from mechanisms to therapy. *Immunity* (2014) 41(1):49–61. doi:10.1016/j.immuni.2014.06.010
11. Lewis CE, Pollard JW. Distinct role of macrophages in different tumor microenvironments. *Cancer Res* (2006) 66(2):605–12. doi:10.1158/0008-5472.CAN-05-4005
12. Mosser DM, Edwards JP. Exploring the full spectrum of macrophage activation. *Nat Rev Immunol* (2008) 8(12):958–69. doi:10.1038/nri2448
13. Pollard JW. Tumour-educated macrophages promote tumour progression and metastasis. *Nat Rev Cancer* (2004) 4(1):71–8. doi:10.1038/nrc1256
14. Biswas SK, Mantovani A. Macrophage plasticity and interaction with lymphocyte subsets: cancer as a paradigm. *Nat Immunol* (2010) 11(10):889–96. doi:10.1038/ni.1937
15. De Palma M, Coukos G, Hanahan D. A new twist on radiation oncology: low-dose irradiation elicits immunostimulatory macrophages that unlock barriers to tumor immunotherapy. *Cancer Cell* (2013) 24(5):559–61. doi:10.1016/j.ccr.2013.10.019
16. Qian BZ, Pollard JW. Macrophage diversity enhances tumor progression and metastasis. *Cell* (2010) 141(1):39–51. doi:10.1016/j.cell.2010.03.014
17. Gordon S, Taylor PR. Monocyte and macrophage heterogeneity. *Nat Rev Immunol* (2005) 5(12):953–64. doi:10.1038/nri1733
18. Mantovani A, Germano G, Marchesi F, Locatelli M, Biswas SK. Cancer-promoting tumor-associated macrophages: new vistas and open questions. *Eur J Immunol* (2011) 41(9):2522–5. doi:10.1002/eji.201141894
19. Mantovani A, Sica A, Sozzani S, Allavena P, Vecchi A, Locati M. The chemokine system in diverse forms of macrophage activation and polarization. *Trends Immunol* (2004) 25(12):677–86. doi:10.1016/j.it.2004.09.015
20. Qian BZ, Pollard JW. New tricks for metastasis-associated macrophages. *Breast Cancer Res* (2012) 14(4):316. doi:10.1186/bcr3143
21. Sica A, Mantovani A. Macrophage plasticity and polarization: in vivo veritas. *J Clin Invest* (2012) 122(3):787–95. doi:10.1172/JCI59643
22. Takeda N, O'Dea EL, Doedens A, Kim JW, Weidemann A, Stockmann C, et al. Differential activation and antagonistic function of HIF-{alpha} isoforms in macrophages are essential for NO homeostasis. *Genes Dev* (2010) 24(5):491–501. doi:10.1101/gad.1881410
23. Ying H, Kang Y, Zhang H, Zhao D, Xia J, Lu Z, et al. MiR-127 modulates macrophage polarization and promotes lung inflammation and injury by activating the JNK pathway. *J Immunol* (2015) 194(3):1239–51. doi:10.4049/jimmunol.1402088
24. Wang N, Liang H, Zen K. Molecular mechanisms that influence the macrophage m1-m2 polarization balance. *Front Immunol* (2014) 5:614. doi:10.3389/fimmu.2014.00614
25. Huang C, Liu XJ, QunZhou, Xie J, Ma TT, Meng XM, et al. MiR-146a modulates macrophage polarization by inhibiting Notch1 pathway in RAW264.7 macrophages. *Int Immunopharmacol* (2016) 32:46–54. doi:10.1016/j.intimp.2016.01.009
26. Murray PJ, Allen JE, Biswas SK, Fisher EA, Gilroy DW, Goerdt S, et al. Macrophage activation and polarization: nomenclature and experimental guidelines. *Immunity* (2014) 41(1):14–20. doi:10.1016/j.immuni.2014.06.008
27. Mantovani A, Allavena P. The interaction of anticancer therapies with tumor-associated macrophages. *J Exp Med* (2015) 212(4):435–45. doi:10.1084/jem.20150295
28. Komohara Y, Fujiwara Y, Ohnishi K, Takeya M. Tumor-associated macrophages: potential therapeutic targets for anti-cancer therapy. *Adv Drug Deliv Rev* (2016) 99(Pt B):180–5. doi:10.1016/j.addr.2015.11.009
29. Lehenkari PP, Kellinsalmi M, Napankangas JP, Ylitalo KV, Monkkonen J, Rogers MJ, et al. Further insight into mechanism of action of clodronate: inhibition of mitochondrial ADP/ATP translocase by a nonhydrolyzable, adenine-containing metabolite. *Mol Pharmacol* (2002) 61(5):1255–62. doi:10.1124/mol.61.5.1255
30. Galletti G, Scielzo C, Barbaglio F, Rodriguez TV, Riba M, Lazarevic D, et al. Targeting macrophages sensitizes chronic lymphocytic leukemia to apoptosis and inhibits disease progression. *Cell Rep* (2016) 14(7):1748–60. doi:10.1016/j.celrep.2016.01.042
31. Zeisberger SM, Odermatt B, Marty C, Zehnder-Fjallman AH, Ballmer-Hofer K, Schwendener RA. Clodronate-liposome-mediated depletion of tumour-associated macrophages: a new and highly effective antiangiogenic therapy approach. *Br J Cancer* (2006) 95(3):272–81. doi:10.1038/sj.bjc.6603240
32. Fritz JM, Tennis MA, Orlicky DJ, Lin H, Ju C, Redente EF, et al. Depletion of tumor-associated macrophages slows the growth of chemically induced mouse lung adenocarcinomas. *Front Immunol* (2014) 5:587. doi:10.3389/fimmu.2014.00587
33. Prakash H, Klug F, Nadella V, Mazumdar V, Schmitz-Winnenthal H, Umansky L. Low doses of gamma irradiation potentially modifies immunosuppressive tumor microenvironment by retuning tumor-associated macrophages: lesson from insulinoma. *Carcinogenesis* (2016) 37(3):301–13. doi:10.1093/carcin/bgw007
34. Zhang W, Zhu XD, Sun HC, Xiong YQ, Zhuang PY, Xu HX, et al. Depletion of tumor-associated macrophages enhances the effect of sorafenib in metastatic liver cancer models by antimetastatic and antiangiogenic effects. *Clin Cancer Res* (2010) 16(13):3420–30. doi:10.1158/1078-0432.CCR-09-2904
35. Melani C, Sangaletti S, Barazzetta FM, Werb Z, Colombo MP. Amino-biphosphonate-mediated MMP-9 inhibition breaks the tumor-bone marrow axis responsible for myeloid-derived suppressor cell expansion and macrophage infiltration in tumor stroma. *Cancer Res* (2007) 67(23):11438–46. doi:10.1158/0008-5472.CAN-07-1882
36. Liang W, Kujawski M, Wu J, Lu J, Herrmann A, Loera S, et al. Antitumor activity of targeting SRC kinases in endothelial and myeloid cell compartments of the tumor microenvironment. *Clin Cancer Res* (2010) 16(3):924–35. doi:10.1158/1078-0432.CCR-09-1486
37. Germano G, Frapolli R, Belgiovine C, Anselmo A, Pesce S, Liguori M, et al. Role of macrophage targeting in the antitumor activity of trabectedin. *Cancer Cell* (2013) 23(2):249–62. doi:10.1016/j.ccr.2013.01.008
38. Mirandola P, Ponti C, Gobbi G, Sponzilli I, Vaccarezza M, Cocco L, et al. Activated human NK and CD8+ T cells express both TNF-related apoptosis-inducing ligand (TRAIL) and TRAIL receptors but are resistant to TRAIL-mediated cytotoxicity. *Blood* (2004) 104(8):2418–24. doi:10.1182/blood-2004-04-1294
39. Bak SP, Walters JJ, Takeya M, Conejo-Garcia JR, Berwin BL. Scavenger receptor-A-targeted leukocyte depletion inhibits peritoneal ovarian tumor progression. *Cancer Res* (2007) 67(10):4783–9. doi:10.1158/0008-5472.CAN-06-4410
40. Nagai T, Tanaka M, Tsuneyoshi Y, Xu B, Michie SA, Hasui K, et al. Targeting tumor-associated macrophages in an experimental glioma model with a recombinant immunotoxin to folate receptor beta. *Cancer Immunol Immunother* (2009) 58(10):1577–86. doi:10.1007/s00262-009-0667-x
41. Galmbacher K, Heisig M, Hotz C, Wischhusen J, Galmiche A, Bergmann B, et al. Shigella mediated depletion of macrophages in a murine breast cancer model is associated with tumor regression. *PLoS One* (2010) 5(3):e9572. doi:10.1371/journal.pone.0009572
42. Shen L, Li H, Shi Y, Wang D, Gong J, Xun J, et al. M2 tumour-associated macrophages contribute to tumour progression via legumain remodelling the extracellular matrix in diffuse large B cell lymphoma. *Sci Rep* (2016) 6:30347. doi:10.1038/srep30347
43. Smahel M, Duskova M, Polakova I, Musil J. Enhancement of DNA vaccine potency against legumain. *J Immunother* (2014) 37(5):293–303. doi:10.1097/CJI.0000000000000040
44. Roca H, Varsos ZS, Sud S, Craig MJ, Ying C, Pienta KJ. CCL2 and interleukin-6 promote survival of human CD11b+ peripheral blood mononuclear cells and induce M2-type macrophage polarization. *J Biol Chem* (2009) 284(49):34342–54. doi:10.1074/jbc.M109.042671
45. Soria G, Ben-Baruch A. The inflammatory chemokines CCL2 and CCL5 in breast cancer. *Cancer Lett* (2008) 267(2):271–85. doi:10.1016/j.canlet.2008.03.018

46. Zhang J, Patel L, Pienta KJ. CC chemokine ligand 2 (CCL2) promotes prostate cancer tumorigenesis and metastasis. *Cytokine Growth Factor Rev* (2010) 21(1):41–8. doi:10.1016/j.cytogfr.2009.11.009
47. Kitamura T, Qian BZ, Soong D, Cassetta L, Noy R, Sugano G, et al. CCL2-induced chemokine cascade promotes breast cancer metastasis by enhancing retention of metastasis-associated macrophages. *J Exp Med* (2015) 212(7):1043–59. doi:10.1084/jem.20141836
48. Pienta KJ, Machiels JP, Schrijvers D, Alekseev B, Shkolnik M, Crabb SJ, et al. Phase 2 study of carlumab (CNTO 888), a human monoclonal antibody against CC-chemokine ligand 2 (CCL2), in metastatic castration-resistant prostate cancer. *Invest New Drugs* (2013) 31(3):760–8. doi:10.1007/s10637-012-9869-8
49. Brana I, Calles A, LoRusso PM, Yee LK, Puchalski TA, Seetharam S, et al. Carlumab, an anti-C-C chemokine ligand 2 monoclonal antibody, in combination with four chemotherapy regimens for the treatment of patients with solid tumors: an open-label, multicenter phase 1b study. *Target Oncol* (2015) 10(1):111–23. doi:10.1007/s11523-014-0320-2
50. Zollo M, Di Dato V, Spano D, De Martino D, Liguori L, Marino N, et al. Targeting monocyte chemotactic protein-1 synthesis with bindarit induces tumor regression in prostate and breast cancer animal models. *Clin Exp Metastasis* (2012) 29(6):585–601. doi:10.1007/s10585-012-9473-5
51. Gazzaniga S, Bravo AI, Guglielmotti A, van Rooijen N, Maschi F, Vecchi A, et al. Targeting tumor-associated macrophages and inhibition of MCP-1 reduce angiogenesis and tumor growth in a human melanoma xenograft. *J Invest Dermatol* (2007) 127(8):2031–41. doi:10.1038/sj.jid.5700827
52. D'Incalci M, Badri N, Galmarini CM, Allavena P. Trabectedin, a drug acting on both cancer cells and the tumour microenvironment. *Br J Cancer* (2014) 111(4):646–50. doi:10.1038/bjc.2014.149
53. D'Incalci M, Zambelli A. Trabectedin for the treatment of breast cancer. *Expert Opin Investig Drugs* (2016) 25(1):105–15. doi:10.1517/13543784.2016.1124086
54. Larsen AK, Galmarini CM, D'Incalci M. Unique features of trabectedin mechanism of action. *Cancer Chemother Pharmacol* (2016) 77(4):663–71. doi:10.1007/s00280-015-2918-1
55. Pyonteck SM, Gadea BB, Wang HW, Gocheva V, Hunter KE, Tang LH, et al. Deficiency of the macrophage growth factor CSF-1 disrupts pancreatic neuroendocrine tumor development. *Oncogene* (2012) 31(11):1459–67. doi:10.1038/onc.2011.337
56. Strachan DC, Ruffell B, Oei Y, Bissell MJ, Coussens LM, Pryer N, et al. CSF1R inhibition delays cervical and mammary tumor growth in murine models by attenuating the turnover of tumor-associated macrophages and enhancing infiltration by CD8+ T cells. *Oncoimmunology* (2013) 2(12):e26968. doi:10.4161/onci.26968
57. Pradel LP, Ooi CH, Romagnoli S, Cannarile MA, Sade H, Ruttinger D, et al. Macrophage susceptibility to emactuzumab (RG7155) treatment. *Mol Cancer Ther* (2016) 15(12):3077–86. doi:10.1158/1535-7163.MCT-16-0157
58. Zhu Y, Knolhoff BL, Meyer MA, Nywening TM, West BL, Luo J, et al. CSF1/CSF1R blockade reprograms tumor-infiltrating macrophages and improves response to T-cell checkpoint immunotherapy in pancreatic cancer models. *Cancer Res* (2014) 74(18):5057–69. doi:10.1158/0008-5472.CAN-13-3723
59. Stafford JH, Hirai T, Deng L, Chernikova SB, Urata K, West BL, et al. Colony stimulating factor 1 receptor inhibition delays recurrence of glioblastoma after radiation by altering myeloid cell recruitment and polarization. *Neuro Oncol* (2016) 18(6):797–806. doi:10.1093/neuonc/nov272
60. Butowski N, Colman H, De Groot JF, Omuro AM, Nayak L, Wen PY, et al. Orally administered colony stimulating factor 1 receptor inhibitor PLX3397 in recurrent glioblastoma: an Ivy Foundation Early Phase Clinical Trials Consortium phase II study. *Neuro Oncol* (2016) 18(4):557–64. doi:10.1093/neuonc/nov245
61. Edwards JP, Emens LA. The multikinase inhibitor sorafenib reverses the suppression of IL-12 and enhancement of IL-10 by PGE(2) in murine macrophages. *Int Immunopharmacol* (2010) 10(10):1220–8. doi:10.1016/j.intimp.2010.07.002
62. Hussain SF, Kong LY, Jordan J, Conrad C, Madden T, Fokt I, et al. A novel small molecule inhibitor of signal transducers and activators of transcription 3 reverses immune tolerance in malignant glioma patients. *Cancer Res* (2007) 67(20):9630–6. doi:10.1158/0008-5472.CAN-07-1243
63. Sun L, Chen B, Jiang R, Li J, Wang B. Resveratrol inhibits lung cancer growth by suppressing M2-like polarization of tumor associated macrophages. *Cell Immunol* (2017) 311:86–93. doi:10.1016/j.cellimm.2016.11.002
64. Dong R, Gong Y, Meng W, Yuan M, Zhu H, Ying M, et al. The involvement of M2 macrophage polarization inhibition in fenretinide-mediated chemopreventive effects on colon cancer. *Cancer Lett* (2017) 388:43–53. doi:10.1016/j.canlet.2016.11.029
65. Sakurai M, Nishio M, Yamamoto K, Okuda T, Kawano K, Ohnuki T. TMC-264, a novel inhibitor of STAT6 activation produced by Phoma sp. TC 1674. *J Antibiot (Tokyo)* (2003) 56(6):513–9. doi:10.7164/antibiotics.56.513
66. Miljkovic D, Samardzic T, Mostarica Stojkovic M, Stosic-Grujicic S, Popadic D, Trajkovic V. Leflunomide inhibits activation of inducible nitric oxide synthase in rat astrocytes. *Brain Res* (2001) 889(1–2):331–8. doi:10.1016/S0006-8993(00)03181-4
67. Chiba Y, Todoroki M, Nishida Y, Tanabe M, Misawa M. A novel STAT6 inhibitor AS1517499 ameliorates antigen-induced bronchial hypercontractility in mice. *Am J Respir Cell Mol Biol* (2009) 41(5):516–24. doi:10.1165/rcmb.2008-0163OC
68. De Meyer I, Martinet W, Schrijvers DM, Timmermans JP, Bult H, De Meyer GR. Toll-like receptor 7 stimulation by imiquimod induces macrophage autophagy and inflammation in atherosclerotic plaques. *Basic Res Cardiol* (2012) 107(3):269. doi:10.1007/s00395-012-0269-1
69. Dewan MZ, Vanpouille-Box C, Kawashima N, DiNapoli S, Babb JS, Formenti SC, et al. Synergy of topical toll-like receptor 7 agonist with radiation and low-dose cyclophosphamide in a mouse model of cutaneous breast cancer. *Clin Cancer Res* (2012) 18(24):6668–78. doi:10.1158/1078-0432.CCR-12-0984
70. Kawai T, Akira S. The role of pattern-recognition receptors in innate immunity: update on toll-like receptors. *Nat Immunol* (2010) 11(5):373–84. doi:10.1038/ni.1863
71. Kumagai Y, Takeuchi O, Akira S. TLR9 as a key receptor for the recognition of DNA. *Adv Drug Deliv Rev* (2008) 60(7):795–804. doi:10.1016/j.addr.2007.12.004
72. Hemmi H, Takeuchi O, Kawai T, Kaisho T, Sato S, Sanjo H, et al. A toll-like receptor recognizes bacterial DNA. *Nature* (2000) 408(6813):740–5. doi:10.1038/35047123
73. Chen N, Wei M, Sun Y, Li F, Pei H, Li X, et al. Self-assembly of poly-adenine-tailed CpG oligonucleotide-gold nanoparticle nanoconjugates with immunostimulatory activity. *Small* (2014) 10(2):368–75. doi:10.1002/smll.201300903
74. Buhtoiarov IN, Sondel PM, Wigginton JM, Buhtoiarova TN, Yanke EM, Mahvi DA, et al. Anti-tumour synergy of cytotoxic chemotherapy and anti-CD40 plus CpG-ODN immunotherapy through repolarization of tumour-associated macrophages. *Immunology* (2011) 132(2):226–39. doi:10.1111/j.1365-2567.2010.03357.x
75. Shi Y, Felder MA, Sondel PM, Rakhmilevich AL. Synergy of anti-CD40, CpG and MPL in activation of mouse macrophages. *Mol Immunol* (2015) 66(2):208–15. doi:10.1016/j.molimm.2015.03.008
76. Jordan M, Waxman DJ. CpG-1826 immunotherapy potentiates chemotherapeutic and anti-tumor immune responses to metronomic cyclophosphamide in a preclinical glioma model. *Cancer Lett* (2016) 373(1):88–96. doi:10.1016/j.canlet.2015.11.029
77. Zippelius A, Schreiner J, Herzig P, Muller P. Induced PD-L1 expression mediates acquired resistance to agonistic anti-CD40 treatment. *Cancer Immunol Res* (2015) 3(3):236–44. doi:10.1158/2326-6066.CIR-14-0226
78. Lum HD, Buhtoiarov IN, Schmidt BE, Berke G, Paulnock DM, Sondel PM, et al. Tumoristatic effects of anti-CD40 mAb-activated macrophages involve nitric oxide and tumour necrosis factor-alpha. *Immunology* (2006) 118(2):261–70. doi:10.1111/j.1365-2567.2006.02366.x
79. Johnson EE, Buhtoiarov IN, Baldeshwiler MJ, Felder MA, Van Rooijen N, Sondel PM, et al. Enhanced T-cell-independent antitumor effect of cyclophosphamide combined with anti-CD40 mAb and CpG in mice. *J Immunother* (2011) 34(1):76–84. doi:10.1097/CJI.0b013e318200b28a
80. Weiss JM, Ridnour LA, Back T, Hussain SP, He P, Maciag AE, et al. Macrophage-dependent nitric oxide expression regulates tumor cell detachment and metastasis after IL-2/anti-CD40 immunotherapy. *J Exp Med* (2010) 207(11):2455–67. doi:10.1084/jem.20100670
81. Vonderheide RH, Flaherty KT, Khalil M, Stumacher MS, Bajor DL, Hutnick NA, et al. Clinical activity and immune modulation in cancer

patients treated with CP-870,893, a novel CD40 agonist monoclonal antibody. *J Clin Oncol* (2007) 25(7):876–83. doi:10.1200/JCO.2006.08.3311
82. Georgoudaki AM, Prokopec KE, Boura VF, Hellqvist E, Sohn S, Ostling J, et al. Reprogramming tumor-associated macrophages by antibody targeting inhibits cancer progression and metastasis. *Cell Rep* (2016) 15(9):2000–11. doi:10.1016/j.celrep.2016.04.084
83. Dunn GP, Koebel CM, Schreiber RD. Interferons, immunity and cancer immunoediting. *Nat Rev Immunol* (2006) 6(11):836–48. doi:10.1038/nri1961
84. Jassar AS, Suzuki E, Kapoor V, Sun J, Silverberg MB, Cheung L, et al. Activation of tumor-associated macrophages by the vascular disrupting agent 5,6-dimethylxanthenone-4-acetic acid induces an effective CD8+ T-cell-mediated antitumor immune response in murine models of lung cancer and mesothelioma. *Cancer Res* (2005) 65(24):11752–61. doi:10.1158/0008-5472.CAN-05-1658
85. Kaneda MM, Messer KS, Ralainirina N, Li H, Leem CJ, Gorjestani S, et al. PI3Kgamma is a molecular switch that controls immune suppression. *Nature* (2016) 539(7629):437–42. doi:10.1038/nature19834
86. Rolny C, Mazzone M, Tugues S, Laoui D, Johansson I, Coulon C, et al. HRG inhibits tumor growth and metastasis by inducing macrophage polarization and vessel normalization through downregulation of PlGF. *Cancer Cell* (2011) 19(1):31–44. doi:10.1016/j.ccr.2010.11.009
87. Ding L, Liang G, Yao Z, Zhang J, Liu R, Chen H, et al. Metformin prevents cancer metastasis by inhibiting M2-like polarization of tumor associated macrophages. *Oncotarget* (2015) 6(34):36441–55. doi:10.18632/oncotarget.5541
88. Hachiya M, Shimizu S, Osawa Y, Akashi M. Endogenous production of tumour necrosis factor is required for manganese superoxide dismutase expression by irradiation in the human monocytic cell line THP-1. *Biochem J* (1997) 328(Pt 2):615–23. doi:10.1042/bj3280615
89. Wong GH. Protective roles of cytokines against radiation: induction of mitochondrial MnSOD. *Biochim Biophys Acta* (1995) 1271(1):205–9. doi:10.1016/0925-4439(95)00029-4
90. Meng Y, Beckett MA, Liang H, Mauceri HJ, van Rooijen N, Cohen KS, et al. Blockade of tumor necrosis factor alpha signaling in tumor-associated macrophages as a radiosensitizing strategy. *Cancer Res* (2010) 70(4):1534–43. doi:10.1158/0008-5472.CAN-09-2995
91. Sugino N, Karube-Harada A, Sakata A, Takiguchi S, Kato H. Nuclear factor-kappa B is required for tumor necrosis factor-alpha-induced manganese superoxide dismutase expression in human endometrial stromal cells. *J Clin Endocrinol Metab* (2002) 87(8):3845–50. doi:10.1210/jcem.87.8.8771
92. Chung YW, Kim HK, Kim IY, Yim MB, Chock PB. Dual function of protein kinase C (PKC) in 12-O-tetradecanoylphorbol-13-acetate (TPA)-induced manganese superoxide dismutase (MnSOD) expression: activation of CREB and FOXO3a by PKC-alpha phosphorylation and by PKC-mediated inactivation of Akt, respectively. *J Biol Chem* (2011) 286(34):29681–90. doi:10.1074/jbc.M111.264945
93. Niu Y, Shen H, Epperly M, Zhang X, Nie S, Cao S, et al. Protection of esophageal multi-lineage progenitors of squamous epithelium (stem cells) from ionizing irradiation by manganese superoxide dismutase-plasmid/liposome (MnSOD-PL) gene therapy. *In Vivo* (2005) 19(6):965–74.
94. Epperly MW, Sikora CA, DeFilippi SJ, Gretton JE, Bar-Sagi D, Archer H, et al. Pulmonary irradiation-induced expression of VCAM-I and ICAM-I is decreased by manganese superoxide dismutase-plasmid/liposome (MnSOD-PL) gene therapy. *Biol Blood Marrow Transplant* (2002) 8(4):175–87. doi:10.1053/bbmt.2002.v8.pm12014807
95. Epperly MW, Guo HL, Jefferson M, Nie S, Gretton J, Bernarding M, et al. Cell phenotype specific kinetics of expression of intratracheally injected manganese superoxide dismutase-plasmid/liposomes (MnSOD-PL) during lung radioprotective gene therapy. *Gene Ther* (2003) 10(2):163–71. doi:10.1038/sj.gt.3301852
96. Klug F, Prakash H, Huber PE, Seibel T, Bender N, Halama N, et al. Low-dose irradiation programs macrophage differentiation to an iNOS(+)/M1 phenotype that orchestrates effective T cell immunotherapy. *Cancer Cell* (2013) 24(5):589–602. doi:10.1016/j.ccr.2013.09.014
97. Xu J, Escamilla J, Mok S, David J, Priceman S, West B, et al. CSF1R signaling blockade stanches tumor-infiltrating myeloid cells and improves the efficacy of radiotherapy in prostate cancer. *Cancer Res* (2013) 73(9):2782–94. doi:10.1158/0008-5472.CAN-12-3981
98. Morganti JM, Jopson TD, Liu S, Gupta N, Rosi S. Cranial irradiation alters the brain's microenvironment and permits CCR2+ macrophage infiltration. *PLoS One* (2014) 9(4):e93650. doi:10.1371/journal.pone.0093650
99. Kalbasi A, Komar C, Tooker GM, Liu M, Lee JW, Gladney WL, et al. Tumor-derived CCL2 mediates resistance to radiotherapy in pancreatic ductal adenocarcinoma. *Clin Cancer Res* (2017) 23(1):137–48. doi:10.1158/1078-0432.CCR-16-0870
100. Rodel F, Frey B, Gaipl U, Keilholz L, Fournier C, Manda K, et al. Modulation of inflammatory immune reactions by low-dose ionizing radiation: molecular mechanisms and clinical application. *Curr Med Chem* (2012) 19(12):1741–50. doi:10.2174/092986712800099866
101. Crittenden MR, Cottam B, Savage T, Nguyen C, Newell P, Gough MJ. Expression of NF-kappaB p50 in tumor stroma limits the control of tumors by radiation therapy. *PLoS One* (2012) 7(6):e39295. doi:10.1371/journal.pone.0039295
102. Okubo M, Kioi M, Nakashima H, Sugiura K, Mitsudo K, Aoki I, et al. M2-polarized macrophages contribute to neovasculogenesis, leading to relapse of oral cancer following radiation. *Sci Rep* (2016) 6:27548. doi:10.1038/srep27548
103. Seifert L, Werba G, Tiwari S, Giao Ly NN, Nguy S, Alothman S, et al. Radiation therapy induces macrophages to suppress T-cell responses against pancreatic tumors in mice. *Gastroenterology* (2016) 150(7):1659–72.e5. doi:10.1053/j.gastro.2016.02.070
104. Teresa Pinto A, Laranjeiro Pinto M, Patricia Cardoso A, Monteiro C, Teixeira Pinto M, Filipe Maia A, et al. Ionizing radiation modulates human macrophages towards a pro-inflammatory phenotype preserving their pro-invasive and pro-angiogenic capacities. *Sci Rep* (2016) 6:18765. doi:10.1038/srep18765
105. Hildebrandt G, Radlingmayr A, Rosenthal S, Rothe R, Jahns J, Hindemith M, et al. Low-dose radiotherapy (LD-RT) and the modulation of iNOS expression in adjuvant-induced arthritis in rats. *Int J Radiat Biol* (2003) 79(12):993–1001. doi:10.1080/09553000310001636639
106. Parker JJ, Jones JC, Strober S, Knox SJ. Characterization of direct radiation-induced immune function and molecular signaling changes in an antigen presenting cell line. *Clin Immunol* (2013) 148(1):44–55. doi:10.1016/j.clim.2013.03.008
107. Wu Q, Allouch A, Paoletti A, Leteur C, Mirjolet C, Martins I, et al. NOX2-dependent ATM kinase activation dictates pro-inflammatory macrophage phenotype and improves effectiveness to radiation therapy. *Front Immunol* (2017) 26(8):613. doi:10.3389/fimmu.2017.00613
108. Pinto AT, Pinto ML, Velho S, Pinto MT, Cardoso AP, Figueira R, et al. Intricate macrophage-colorectal cancer cell communication in response to radiation. *PLoS One* (2016) 11(8):e0160891. doi:10.1371/journal.pone.0160891
109. Tsukimoto M, Homma T, Mutou Y, Kojima S. 0.5 Gy gamma radiation suppresses production of TNF-alpha through up-regulation of MKP-1 in mouse macrophage RAW264.7 cells. *Radiat Res* (2009) 171(2):219–24. doi:10.1667/RR1351.1
110. Lodermann B, Wunderlich R, Frey S, Schorn C, Stangl S, Rodel F, et al. Low dose ionising radiation leads to a NF-kappaB dependent decreased secretion of active IL-1beta by activated macrophages with a discontinuous dose-dependency. *Int J Radiat Biol* (2012) 88(10):727–34. doi:10.3109/09553002.2012.689464
111. Frey B, Hehlgans S, Rodel F, Gaipl US. Modulation of inflammation by low and high doses of ionizing radiation: implications for benign and malign diseases. *Cancer Lett* (2015) 368(2):230–7. doi:10.1016/j.canlet.2015.04.010
112. Wunderlich R, Ernst A, Rodel F, Fietkau R, Ott O, Lauber K, et al. Low and moderate doses of ionizing radiation up to 2 Gy modulate transmigration and chemotaxis of activated macrophages, provoke an anti-inflammatory cytokine milieu, but do not impact upon viability and phagocytic function. *Clin Exp Immunol* (2015) 179(1):50–61. doi:10.1111/cei.12344
113. Shin SC, Lee KM, Kang YM, Kim K, Kim CS, Yang KH, et al. Alteration of cytokine profiles in mice exposed to chronic low-dose ionizing radiation. *Biochem Biophys Res Commun* (2010) 397(4):644–9. doi:10.1016/j.bbrc.2010.05.121
114. Ren H, Shen J, Tomiyama-Miyaji C, Watanabe M, Kainuma E, Inoue M, et al. Augmentation of innate immunity by low-dose irradiation. *Cell Immunol* (2006) 244(1):50–6. doi:10.1016/j.cellimm.2007.02.009
115. Ibuki Y, Goto R. Contribution of inflammatory cytokine release to activation of resident peritoneal macrophages after in vivo low-dose gamma-irradiation. *J Radiat Res* (1999) 40(3):253–62. doi:10.1269/jrr.40.253

116. Song KH, Kim MH, Kang SM, Jung SY, Ahn J, Woo HJ, et al. Analysis of immune cell populations and cytokine profiles in murine splenocytes exposed to whole-body low-dose irradiation. *Int J Radiat Biol* (2015) 91(10):795–803. doi:10.3109/09553002.2015.1068461
117. Shan YX, Jin SZ, Liu XD, Liu Y, Liu SZ. Ionizing radiation stimulates secretion of pro-inflammatory cytokines: dose-response relationship, mechanisms and implications. *Radiat Environ Biophys* (2007) 46(1):21–9. doi:10.1007/s00411-006-0076-x
118. Nowosielska EM, Cheda A, Wrembel-Wargocka J, Janiak MK. Effect of low doses of low-let radiation on the innate anti-tumor reactions in radioresistant and radiosensitive mice. *Dose Response* (2012) 10(4):500–15. doi:10.2203/dose-response.12-018.Nowosielska
119. Hoesel B, Schmid JA. The complexity of NF-kappaB signaling in inflammation and cancer. *Mol Cancer* (2013) 12:86. doi:10.1186/1476-4598-12-86
120. Rackov G, Hernandez-Jimenez E, Shokri R, Carmona-Rodriguez L, Manes S, Alvarez-Mon M, et al. p21 mediates macrophage reprogramming through regulation of p50-p50 NF-kappaB and IFN-beta. *J Clin Invest* (2016) 126(8):3089–103. doi:10.1172/JCI83404
121. Tsukimoto M, Tamaishi N, Homma T, Kojima S. Low-dose gamma-ray irradiation induces translocation of Nrf2 into nuclear in mouse macrophage RAW264.7 cells. *J Radiat Res* (2010) 51(3):349–53. doi:10.1269/jrr.10002
122. Fukuchi K, Hagiwara T, Nakamura K, Ichimura S, Tatsumi K, Gomi K. Identification of the regulatory region required for ubiquitination of the cyclin kinase inhibitor, p21. *Biochem Biophys Res Commun* (2002) 293(1):120–5. doi:10.1016/S0006-291X(02)00198-5
123. Fukuchi K, Tomoyasu S, Nakamaki T, Tsuruoka N, Gomi K. DNA damage induces p21 protein expression by inhibiting ubiquitination in ML-1 cells. *Biochim Biophys Acta* (1998) 1404(3):405–11. doi:10.1016/S0167-4889(98)00089-5
124. Yang J, Xu ZP, Huang Y, Hamrick HE, Duerksen-Hughes PJ, Yu YN. ATM and ATR: sensing DNA damage. *World J Gastroenterol* (2004) 10(2):155–60. doi:10.3748/wjg.v10.i2.155
125. Huang TT, Wuerzberger-Davis SM, Wu ZH, Miyamoto S. Sequential modification of NEMO/IKKgamma by SUMO-1 and ubiquitin mediates NF-kappaB activation by genotoxic stress. *Cell* (2003) 115(5):565–76. doi:10.1016/S0092-8674(03)00895-X
126. Hayden MS, Ghosh S. Shared principles in NF-kappaB signaling. *Cell* (2008) 132(3):344–62. doi:10.1016/j.cell.2008.01.020
127. Ibuki Y, Mizuno S, Goto R. gamma-Irradiation-induced DNA damage enhances NO production via NF-kappaB activation in RAW264.7 cells. *Biochim Biophys Acta* (2003) 1593(2–3):159–67. doi:10.1016/S0167-4889(02)00385-3
128. Brune B, Dehne N, Grossmann N, Jung M, Namgaladze D, Schmid T, et al. Redox control of inflammation in macrophages. *Antioxid Redox Signal* (2013) 19(6):595–637. doi:10.1089/ars.2012.4785
129. Zhang Y, Choksi S, Chen K, Pobezinskaya Y, Linnoila I, Liu ZG. ROS play a critical role in the differentiation of alternatively activated macrophages and the occurrence of tumor-associated macrophages. *Cell Res* (2013) 23(7):898–914. doi:10.1038/cr.2013.75
130. Covarrubias A, Byles V, Horng T. ROS sets the stage for macrophage differentiation. *Cell Res* (2013) 23(8):984–5. doi:10.1038/cr.2013.88
131. Qin L, Liu Y, Wang T, Wei SJ, Block ML, Wilson B, et al. NADPH oxidase mediates lipopolysaccharide-induced neurotoxicity and proinflammatory gene expression in activated microglia. *J Biol Chem* (2004) 279(2):1415–21. doi:10.1074/jbc.M307657200
132. Kohchi C, Inagawa H, Nishizawa T, Soma G. ROS and innate immunity. *Anticancer Res* (2009) 29(3):817–21.
133. Kang JL, Go YH, Hur KC, Castranova V. Silica-induced nuclear factor-kappaB activation: involvement of reactive oxygen species and protein tyrosine kinase activation. *J Toxicol Environ Health A* (2000) 60(1):27–46. doi:10.1080/009841000156574
134. Taetzsch T, Levesque S, McGraw C, Brookins S, Luqa R, Bonini MG, et al. Redox regulation of NF-kappaB p50 and M1 polarization in microglia. *Glia* (2015) 63(3):423–40. doi:10.1002/glia.22762
135. Choi SH, Aid S, Kim HW, Jackson SH, Bosetti F. Inhibition of NADPH oxidase promotes alternative and anti-inflammatory microglial activation during neuroinflammation. *J Neurochem* (2012) 120(2):292–301. doi:10.1111/j.1471-4159.2011.07572.x
136. Xu Q, Choksi S, Qu J, Jang J, Choe M, Banfi B, et al. NADPH oxidases are essential for macrophage differentiation. *J Biol Chem* (2016) 291(38):20030–41. doi:10.1074/jbc.M116.731216
137. He C, Carter AB. The metabolic prospective and redox regulation of macrophage polarization. *J Clin Cell Immunol* (2015) 6(6):371–7. doi:10.4172/2155-9899.1000371
138. He C, Ryan AJ, Murthy S, Carter AB. Accelerated development of pulmonary fibrosis via Cu,Zn-superoxide dismutase-induced alternative activation of macrophages. *J Biol Chem* (2013) 288(28):20745–57. doi:10.1074/jbc.M112.410720
139. Gunthner R, Anders HJ. Interferon-regulatory factors determine macrophage phenotype polarization. *Mediators Inflamm* (2013) 2013:731023. doi:10.1155/2013/731023
140. Singh S, Gupta AK. Nitric oxide: role in tumour biology and iNOS/NO-based anticancer therapies. *Cancer Chemother Pharmacol* (2011) 67(6):1211–24. doi:10.1007/s00280-011-1654-4
141. Ryu YK, Lee MH, Lee J, Lee JW, Jang SJ, Kang JH, et al. gamma-Irradiated cancer cells promote tumor growth by activation of toll-like receptor 1-mediated inducible nitric oxide synthase in macrophages. *J Leukoc Biol* (2015) 97(4):711–21. doi:10.1189/jlb.3A0114-055R
142. De Ridder M, Verellen D, Verovski V, Storme G. Hypoxic tumor cell radiosensitization through nitric oxide. *Nitric Oxide* (2008) 19(2):164–9. doi:10.1016/j.niox.2008.04.015
143. Ghosh S, Maurya DK, Krishna M. Role of iNOS in bystander signaling between macrophages and lymphoma cells. *Int J Radiat Oncol Biol Phys* (2008) 72(5):1567–74. doi:10.1016/j.ijrobp.2008.08.006
144. Cargnello M, Roux PP. Activation and function of the MAPKs and their substrates, the MAPK-activated protein kinases. *Microbiol Mol Biol Rev* (2011) 75(1):50–83. doi:10.1128/MMBR.00031-10
145. Kim HS, Asmis R. Mitogen-activated protein kinase phosphatase 1 (MKP-1) in macrophage biology and cardiovascular disease. A redox-regulated master controller of monocyte function and macrophage phenotype. *Free Radic Biol Med* (2017) 109:75–83. doi:10.1016/j.freeradbiomed.2017.03.020
146. Kim HS, Tavakoli S, Piefer LA, Nguyen HN, Asmis R. Monocytic MKP-1 is a sensor of the metabolic environment and regulates function and phenotypic fate of monocyte-derived macrophages in atherosclerosis. *Sci Rep* (2016) 6:34223. doi:10.1038/srep34223
147. Salojin KV, Owusu IB, Millerchip KA, Potter M, Platt KA, Oravecz T. Essential role of MAPK phosphatase-1 in the negative control of innate immune responses. *J Immunol* (2006) 176(3):1899–907. doi:10.4049/jimmunol.176.3.1899
148. Chi H, Barry SP, Roth RJ, Wu JJ, Jones EA, Bennett AM, et al. Dynamic regulation of pro- and anti-inflammatory cytokines by MAPK phosphatase 1 (MKP-1) in innate immune responses. *Proc Natl Acad Sci U S A* (2006) 103(7):2274–9. doi:10.1073/pnas.0510965103
149. Narang H, Krishna M. Effect of nitric oxide donor and gamma irradiation on MAPK signaling in murine peritoneal macrophages. *J Cell Biochem* (2008) 103(2):576–87. doi:10.1002/jcb.21429
150. Kobayashi EH, Suzuki T, Funayama R, Nagashima T, Hayashi M, Sekine H, et al. Nrf2 suppresses macrophage inflammatory response by blocking proinflammatory cytokine transcription. *Nat Commun* (2016) 7:11624. doi:10.1038/ncomms11624
151. Chen W, Sun Z, Wang XJ, Jiang T, Huang Z, Fang D, et al. Direct interaction between Nrf2 and p21(Cip1/WAF1) upregulates the Nrf2-mediated antioxidant response. *Mol Cell* (2009) 34(6):663–73. doi:10.1016/j.molcel.2009.04.029
152. Kalbasi A, June CH, Haas N, Vapiwala N. Radiation and immunotherapy: a synergistic combination. *J Clin Invest* (2013) 123(7):2756–63. doi:10.1172/JCI69219
153. Gupta A, Probst HC, Vuong V, Landshammer A, Muth S, Yagita H, et al. Radiotherapy promotes tumor-specific effector CD8+ T cells via dendritic cell activation. *J Immunol* (2012) 189(2):558–66. doi:10.4049/jimmunol.1200563
154. Lee Y, Auh SL, Wang Y, Burnette B, Wang Y, Meng Y, et al. Therapeutic effects of ablative radiation on local tumor require CD8+ T cells: changing strategies for cancer treatment. *Blood* (2009) 114(3):589–95. doi:10.1182/blood-2009-02-206870

155. Hodge JW, Guha C, Neefjes J, Gulley JL. Synergizing radiation therapy and immunotherapy for curing incurable cancers. Opportunities and challenges. *Oncology (Williston Park)* (2008) 22(9):1064–84.
156. Shiao SL, Ruffell B, DeNardo DG, Faddegon BA, Park CC, Coussens LM. TH2-polarized CD4(+) T cells and macrophages limit efficacy of radiotherapy. *Cancer Immunol Res* (2015) 3(5):518–25. doi:10.1158/2326-6066.CIR-14-0232
157. Lee S, Kivimae S, Dolor A, Szoka FC. Macrophage-based cell therapies: the long and winding road. *J Control Release* (2016) 240:527–40. doi:10.1016/j.jconrel.2016.07.018
158. Hellweg CE, Baumstark-Khan C, Schmitz C, Lau P, Meier MM, Testard I, et al. Carbon-ion-induced activation of the NF-kappaB pathway. *Radiat Res* (2011) 175(4):424–31. doi:10.1667/RR2423.1

Conflict of Interest Statement: The authors declare that the research was conducted in the absence of any commercial or financial relationships that could be construed as a potential conflict of interest.

The reviewer, BB, and handling editor declared their shared affiliation, and the handling editor states that the process nevertheless met the standards of a fair and objective review.

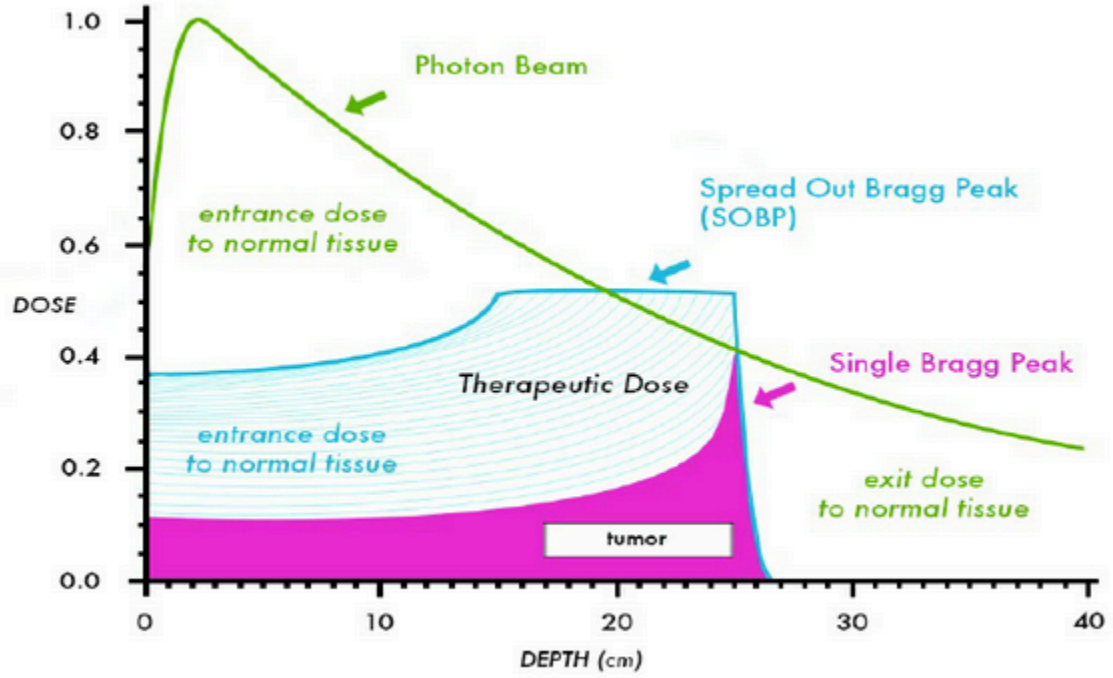

Figure I.29– Depth dose profile for photons and protons.
Comparison of depth dose profile for a 10 MV photon beam and a 200 MeV proton beam. For photons, the maximal dose is delivered within few centimeters. The dose decreases when photons get through the matter, thus irradiating normal tissue upstream (entrance dose) and downstream (exit dose) the tumor. Protons travel through the matter with minimal interactions until they reach a given depth, where the energy is deposited. This high-dose region is called the Bragg Peak. As the width of the Bragg Peak is not large enough to cover the entire targeted tumor volume, multiple peaks of different initial energy must be superimposed to obtain a plateau, so-called the spread-out Bragg peak (SOBP). With the use of protons, healthy tissues are more preserved upstream the tumor and are completely spared downstream the tumor *(Ladra and Yock 2014).*

Chapter 4: Conventional radiotherapy versus hadrontherapy

Nowadays, radiotherapy remains one of the most effective treatment for killing cancer cells and is used to treat up to 50% of cancer patients alone or in combination with other treatments *(Good and Harrington, 2013; Newhauser and Zhang, 2015)*. The therapeutic effect of radiotherapy depends on several factors gathered under the 5Rs of radiobiology. The 5Rs include the differential *repair* of cancer and normal cells between radiotherapy fractions, the *redistribution* of cancer cells into radiosensitive or radioresistant phases of the cell cycle, the *repopulation* of tumors during treatment, the *reoxygenation* of tumors between radiotherapy fractions and the *intrinsic radiosensitivy* of cancer cells. These five rules may all modulate the success or the failure of localized radiotherapy *(Harrington et al., 2007)*. In this system, we could add another "R" for the *reaction of the tumor microenvironment* to radiotherapy, notably explaining the distant effect of radiotherapy on unirradiated site, called the abscopal effect. The improvement of conventional radiotherapy (X-rays or γ-rays) with new technologies (such as intensity modulated radiotherapy (IMRT) and volumetric modulated arc therapy (VMAT)) or the use of high energy charged particles (e.g. protons, carbon ions and alpha particles) has enhanced the success of radiotherapy *(Harrington et al., 2007; Newhauser and Zhang, 2015)*. In the following sections, the physical aspects and radiobiological concepts are described to compare conventional radiotherapy and particle therapy (also named hadrontherapy), and more specifically proton therapy.

1. Physical aspects of radiotherapy

The main advantage for the use of particle therapy over conventional therapy is the spatial dose distribution that spares normal tissues (***figure I.29***) *(Newhauser and Zhang, 2015).* Photons are quanta of electromagnetic field that have neither rest mass nor charge. When they interact with the target material electrons (e.g. the body), there is an initial increase in energy deposition, known as the maximal dose. This maximal dose is then delivered within a few centimeters when the photons get through the matter and is called the dose accumulation effect. The dose subsequently decreases through the body, thus irradiating normal tissues upstream and downstream the tumor. In order to improve the dose distribution, different options are available. For example, with the use of multiple fields, the deposition dose in the entry and exit fields tends to be significantly smaller. Another alternative to achieve a good dose distribution and conformity, and then to avoid the deposition of high doses at organs at risk (OAR) is the use of charged particles. Charged particles, such as protons, carbon ions, oxygen ions or alpha particles, slow down when travelling through the tissues. This slow down is explained by the fact that accelerated ions continuously interact with the matter, leading to small energy deposition. At a given depth, where the velocity is reduced, large interactions occur and most of the energy is released *(Schiller et al., 2016)*. Therefore, the dose deposition of charged particles is characterized by a depth-dose profile distribution with a low entrance dose, followed by a high dose region at a precise depth, called the Bragg peak, and finally a steep fall-off to zero-dose *(Weber et al., 2006)*. The localization of the Bragg peak depends on the initial energy of the particles. Therefore, as the width of the Bragg Peak is not large enough to cover the entire

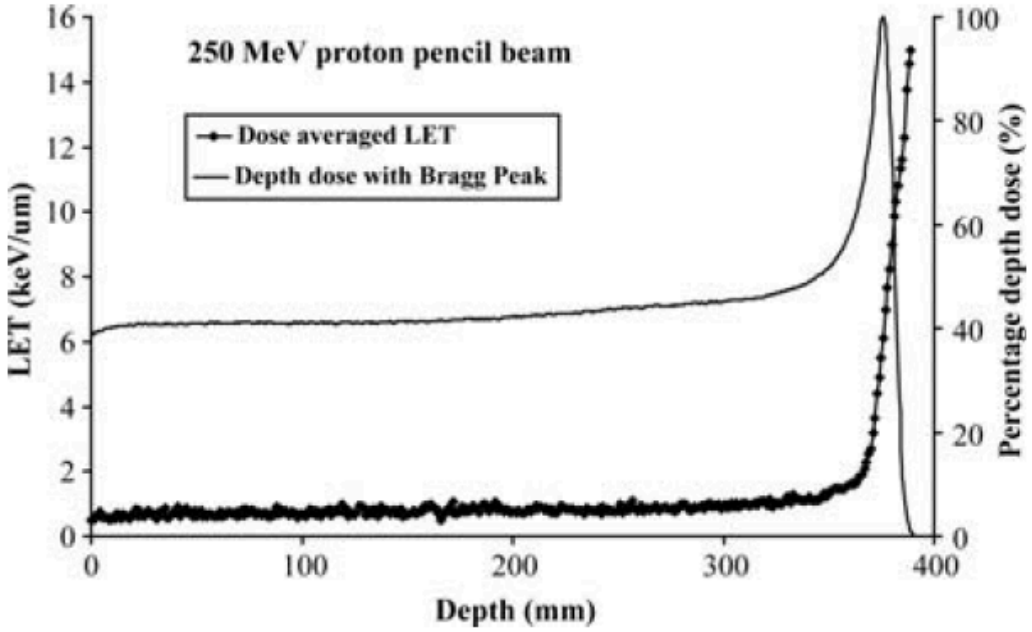

Figure I.30 – Dose average LET and depth dose profile for a 250 MeV proton pencil beam
Simulated dose-averaged LET for 250 MeV proton beam in water showing a steep increase of up to 15keV/μm around 400 mm in the phatom. The Bragg Peak region correlates with the highest LET values and the maximal depth dose *(Chen and Ahmad 2012).*

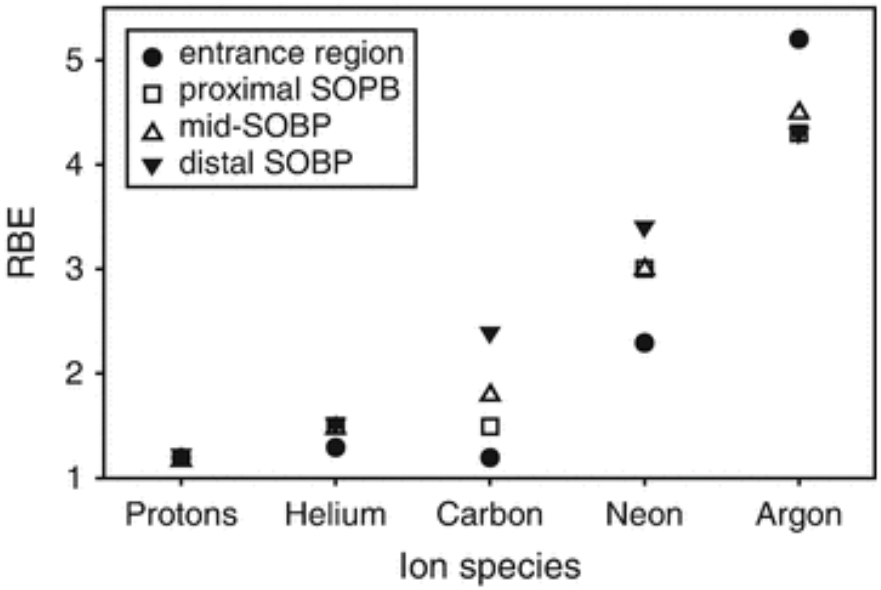

Figure I.31 – Relative biological effectiveness (RBE) for several charged particles in fractionated irradiation of mouse cells
RBE values for a series of ion beams (protons, helium, carbon, neon and argon) for different regions of the beam (entrance region, proximal SOBP, mid-SOBP and distal SOBP). Protons showed a same RBE for all region of the beam. Carbon and neon ions displayed an increased RBE at the proximal and mid- SOBP region. Ions with higher mass (Argon) exhibit a higher RBE at the entrance region and outside the SOBP, due to fragmentation and could thus be more deleterious for healthy tissues *(Jakel 2009).*

targeted tumor volume, multiple peaks of different initial energy must be superimposed to obtain a plateau, so-called the spread-out Bragg peak (SOBP) *(Schiller et al., 2016).* Most clinical treatments are performed with protons and carbon ions, while the use of heavy particles (such as oxygen, iron and alpha particles) is still largely under experimental testing. In clinic, proton therapy is far more used than carbon ion beam mainly because of the treatment expensiveness *(Schiller et al., 2016).* In comparison to protons, carbon ions describe a higher peak-to-plateau ratio in depth dose profile and a steeper lateral fall-off around the target. In order words, carbon ions display a sharper Bragg Peak and a smaller penumbra, thus delivering a more accurate dose *(Shioyama et al., 2015)*. Compared to photons, the depth-dose profile for protons reveals a reduction of 60% in the integral dose delivered to the body for the same delivered dose. The depth-dose profile of charged particle thus allows the use of higher doses and the reduction of fractions, a regimen described as hypofractionnation *(Schiller et al., 2016).*

2. Radiobiological concepts of radiotherapy

2.1. Linear energy transfer (LET)

When going through the matter, the charged particles travel with minimal interactions. They thus transfer a low kinetic energy to the medium, quantified as the linear energy transfer (LET). This energy is deposited along the track of the particle and increases as the particle comes to rest (***Figure I.30***) *(Mohamad et al., 2017)*. Therefore, the LET of the particle is low at the entrance tissues and it increases as the speed of the particle is reduced. Charged particles display low or high LET, depending on their velocity and their charge *(Allen et al., 2011; Mohamad et al., 2017)*. For instance, LET of carbon ions can reach more than 200 keV/μm at the Bragg Peak while the maximal LET of protons can reach 80 keV/μm. For comparison sake, photons are associated to low LET dose to 0.2 keV/μm *(Allen et al., 2011)*. The maximal LET corresponds to the Bragg Peak region and thus to the maximal dose *(Chen and Ahmad, 2012).*

2.2. Radiobiological effectiveness (RBE)

In order to compare the biological effects of different radiation types, the relative biological effectiveness (RBE) is used in radiobiology. RBE is a ratio of the amount of dose from a test radiation required to generate the same biological endpoint (e.g. cell killing, DNA damage, chromosome aberrations), relative to a reference radiation that is usually a beam of 250 kVp X-rays or ^{60}Co γ-rays *(Mohamad et al., 2017)*. For example, the RBE used in clinics for protons equals 1.1, meaning that there is an additional gain of 10% on cancer cell killing compared to photons when analyzing the survival fraction. For carbon ions, the RBE reaches 2 or 3, depending on the examined biological endpoint. However, only few studies are randomized controlled trials that compare protons directly to photons *(Miller et al., 2013).* Therefore, these ratios should be re-evaluated in the next few years with the emergence of randomized controlled trials *(Mohamad et al., 2017; Schiller et al., 2016)*. The RBE depends on several factors, including the LET, the dose per fraction, the tissue, the cell type, the radiosensitivity, the oxygen concentration, the cell cycle phase and the biological endpoint chosen to compare the beams. In addition, the RBE of charged particles varies along the track and is significantly higher near the

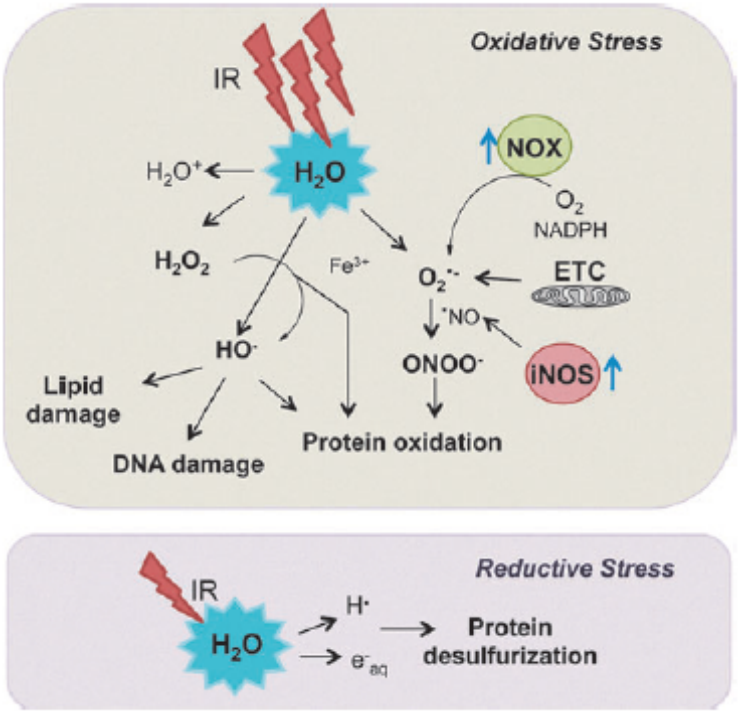

Figure I.32 – Intracellular oxidative and reductive stress generated by ionizing radiation
Irradiation induces intracellular oxidative molecules such as H_2O_2 (hydrogen peroxide), $^{\bullet}OH$ (hydroxyl radical), $O_2^{\bullet-}$ (superoxide), $^{\bullet}NO$ (nitric oxide) and $ONOO^-$ (peroxynitrite anion). The endogenous pool of ROS is generated by mitochondrial electron transport chain (ETC) and oxidative enzymes such as iNOS. In contrast, irradiation may also lead to reductive stress through the loss of sulfur in proteins that generates e_{aq} (hydrated electron) and $H^{\bullet}$ (hydrogen radical) *(Reisz, Bansal et al. 2014)*

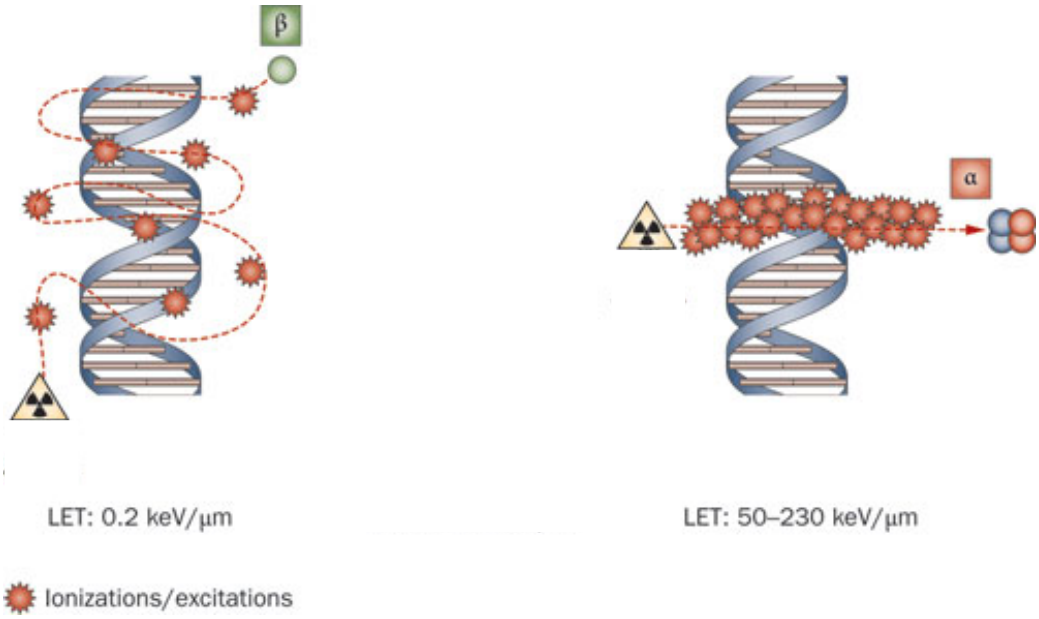

Figure I.33 – Pattern of DNA damage caused by low and high LET radiation
Low LET radiation (*left*) produces sparse ionization and excitations within DNA along the tracks, resulting in DNA damage that are easily repaired. High LET radiation (*right*) such as α-particles produce densely localized ionizations and excitations along a linear track that result in multiple and complex DNA damage, poorly repairable. Modified from Pouget et al. *(Pouget, Navarro-Teulon et al. 2011).*

fall-off portion of the Bragg peak (***Figure I.31***). However, the LET of particle is not sufficient for predicting RBE *(Ilicic et al., 2018).*

2.3. DNA damage

Ionizing radiation releases enough energy to eject one or more orbital electrons from an atom, leading to the ionization of the molecule. The dose (Gy) delivered to tissues is defined by the amount of energy absorbed by mass unit (kJ/kg). When ionizing radiations travel through the cells, the deposited energy promotes the ionization of multiple molecules, mainly including DNA but also proteins, mRNA or lipids. While some of these molecules exist in multiple copies and are continuously replaced, limiting the deleterious effects in the cells, other molecules such as DNA exist in few copies and are central for cell functions. Therefore, the induction of cell death with ionizing radiation is essentially caused by DNA damage and more specifically is related to the complexity of these DNA damage. As the complexity of DNA damage is directly correlated to the LET, low LET radiation induces DNA damage that are easily repaired while high LET radiation generates complex damage *(Joiner and Kogel, 2009)*. In the case of photons, the radiolysis of water produces ROS that interact with proteins and DNA (***Figure I.32***). Most of DNA damage are then indirectly produced and are thus dispersed along the DNA strands. These DNA damage mainly include base modifications and single-strand breaks (SSBs) *(Mohamad et al., 2017)*. It was also noticed that SSBs can give rise to DSBs by collapsing during the DNA replication fork formation *(Khanna, 2015)*. As an example, a photon beam of 1 Gy induces about 10^5 ionizations that are responsible for about 2000 base modifications, 1000 SSBs and 35 DSBs per cell *(Roos and Kaina, 2013)*. It was predicted, in our laboratory, that 25 keV/µm proton irradiation (1 Gy) induces around 1525 base modifications, 940 SSBs and 97 DSBs. However, until now, there is no clear evidence for differences in DSB number between high energy proton- and photon-irradiated cells. Among DNA damage, the DSBs are the most lethal for the cells as they are less easily repaired and they can favor chromosomal aberrations (deletions, translocations or duplications) *(Joiner and Kogel, 2009)*.

In addition to generate indirect DNA damage through the interaction of ROS with DNA backbone, charged particles may directly affect DNA molecules by removing electron, resulting in DNA damage. The complexity of these damage increases with the LET of particles. Therefore, with heavy ions, DNA damage occur relatively close one to each other, resulting in complex DNA damage that are difficult to repair. Indeed, the spatial distribution of DNA damage (at least 2 to 5 ionizations) within one or two turns of the DNA helix makes them more complex (***Figure I.33***) *(Ilicic et al., 2018)*. Only 30% of the deposited energy results in clustered damage site with low LET radiation (e.g. photons), while 90% of the energy deposited generates this type of damage for high LET radiation *(Lomax et al., 2013)*. According to the "local effect model", used to predict RBE for cell killing with heavy ions, the spatial DNA DSB distribution and their local density within the nucleus are the most relevant factors that influence the cell fate following irradiation *(Ilicic et al., 2018)*.

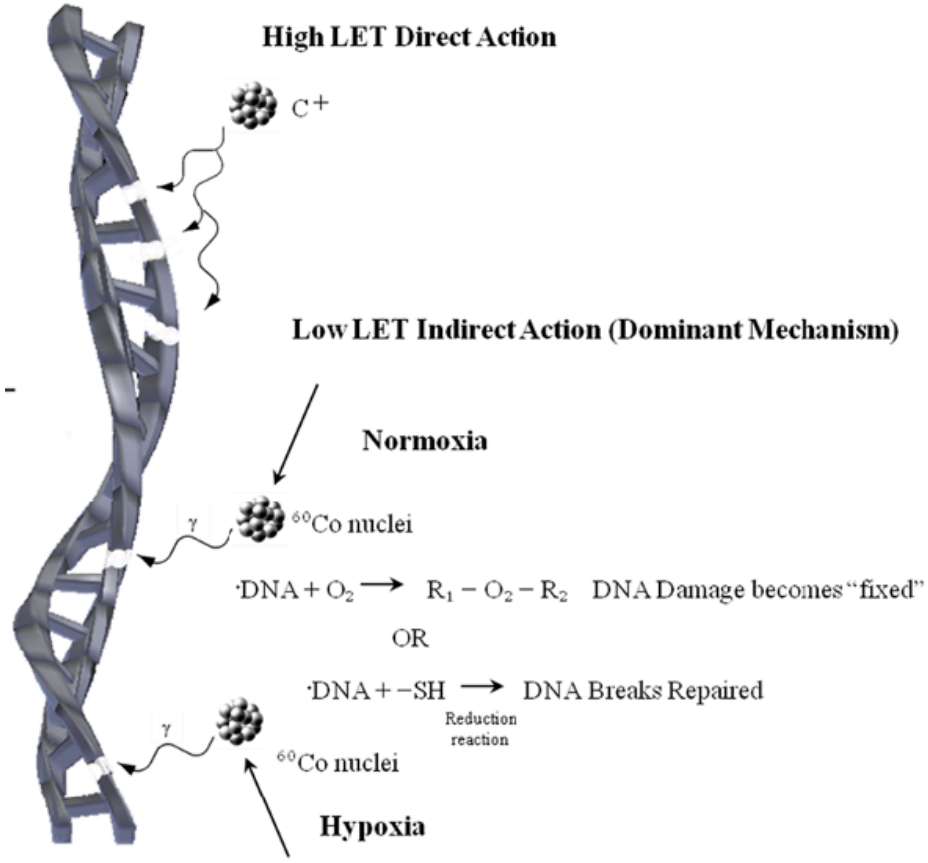

Figure I.34 – Influence of oxygen level on DNA damage caused by different radiation species

Low LET photons produce simple DNA damage by indirect action. Under normoxic conditions, low LET photons hydrolyze water and generate simple DNA damage (breaks in the phosphodiester bonds of DNA). These DNA damage are fixed in the presence of oxygen. Under hypoxic conditions, DNA radicals are modified by sulfhydryl groups, leading to DNA repair. In addition to generate indirect DNA damage through the interaction of ROS with DNA backbone, carbon ions induce direct DNA damage that are close to each other, generating clustered DNA damage *(Schlaff, Krauze et al. 2014).*

2.4. The oxygen enhancement ratio (OER)

The presence of oxygen is important for ROS production and also for fixing DNA damage (***Figure I.34***). Under hypoxic conditions, DNA radicals are reduced by sulfhydryl groups (SH groups), making less severe DNA damage *(Schlaff et al., 2014)*. Therefore, there is more efficient cell killing in oxygenated area than in hypoxic sites upon X-ray or γ-ray irradiation. In contrast, as DNA damage are directly created in the case of high-LET charged particle therapy, the absence of oxygen has less or no effect on the cell killing. Consequently, the oxygen enhancement ratio (OER), or in other words, the amounts of dose necessary to result in an equivalent biological endpoint with or without the presence of oxygen, is less elevated for carbon ions than for protons or photons (***Figure I.35***). Indeed, this ratio is close to 3 for photons and protons, while it is comprised between 2.5 and 1 for carbon ions, depending on the biological endpoint. A ratio of 3 means that photons or protons kill 3 times more cells in normoxic condition compared to hypoxic conditions. This higher efficacy of high LET particle under hypoxic conditions is linked to the induction of direct damage to the DNA molecules and to the formation of clustered DSBs that do not require oxygen *(Mohamad et al., 2017).*

2.5. The DNA repair machinery

Quite similar numbers of DSBs are induced by photons and low LET protons but the repair mechanism involved after DNA damage are different because the nature of the damage is different *(Ilicic et al., 2018)*. The DNA damage response (DDR) includes several effector pathways that once activated phosphorylates p53. p53 interacts with other proteins and activates the transcription of genes involved in cell cycle arrest, DNA repair, cell death or senescence. Only DSBs are difficult to repair and need a sophisticated repair system. The repair of DSBs is extremely important, as the unrepaired or misrepaired sites promote genomic instability and cell death *(Mohamad et al., 2017).* These DSBs are quickly associated with histone modifications, inducing the activation and the access of the DNA repair machinery. In more details, the phosphorylation of the minor histone H2A variant (H_2AX) at serine 139 is performed by ATM. This phosphorylation generates γH_2AX, which is recognized by DDR proteins, promoting the DNA repair. Indeed, γH_2AX generation promotes chromatin relaxation and may then occur at any phase of the cell cycle, even when chromatin is more condensed. The recognition of DSBs and the recruitment of effectors lead to further phosphorylation of ATM and H_2AX, creating foci. In addition to ATM, which is activated by autophosphorylation in the presence of DSBs, other kinases are also responsible for the phosphorylation of H_2AX, such as DNA PKcs (DNA dependent protein kinase catalytic subunit) and ATR (ATM- and Rad3-related) *(Mah et al., 2010).*

Two major DNA repair pathways take care of DSBs: the non-homologous end joining (NHEJ) and the homologous recombination (HR) (***Figure I.36***). NHEJ uses no or little homology to join ends and is thus an error-prone process. The advantage of this repair mechanism is the rapid intervention at any phase of the cell cycle *(Asaithamby and Chen, 2011)*. This DNA repair process consists in the cut or the modification of the ends at the break site. Specifically, by its binding to the DSB ends, the Ku70/Ku80 heterodimer protects the DNA damage from degradation by exonucleases and prevents the activation of the HR repair mechanism. The Ku heterodimer also

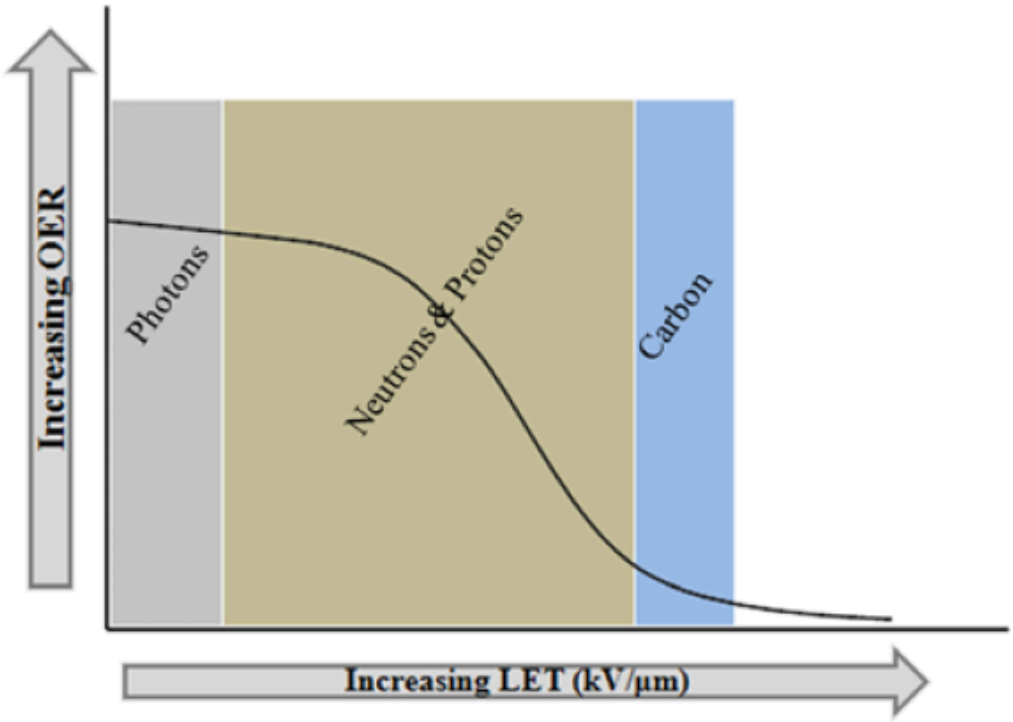

Figure I.35 – The oxygen enhancement ratio (OER) for different radiation species
The OER exhibits an inverse correlation with the LET: low LET beams correlate with a high OER and inversely. The cell killing of low-LET photons (grey) and low-LET particles (protons, neutrons) is poorly efficient in the absence of oxygen and thus explains the cell killing differences between normoxic and hypoxic conditions. Inversely, the cell killing efficiency is high for carbon ions due to their similar effect in normoxic and hypoxic conditions *(Schlaff, Krauze et al. 2014).*

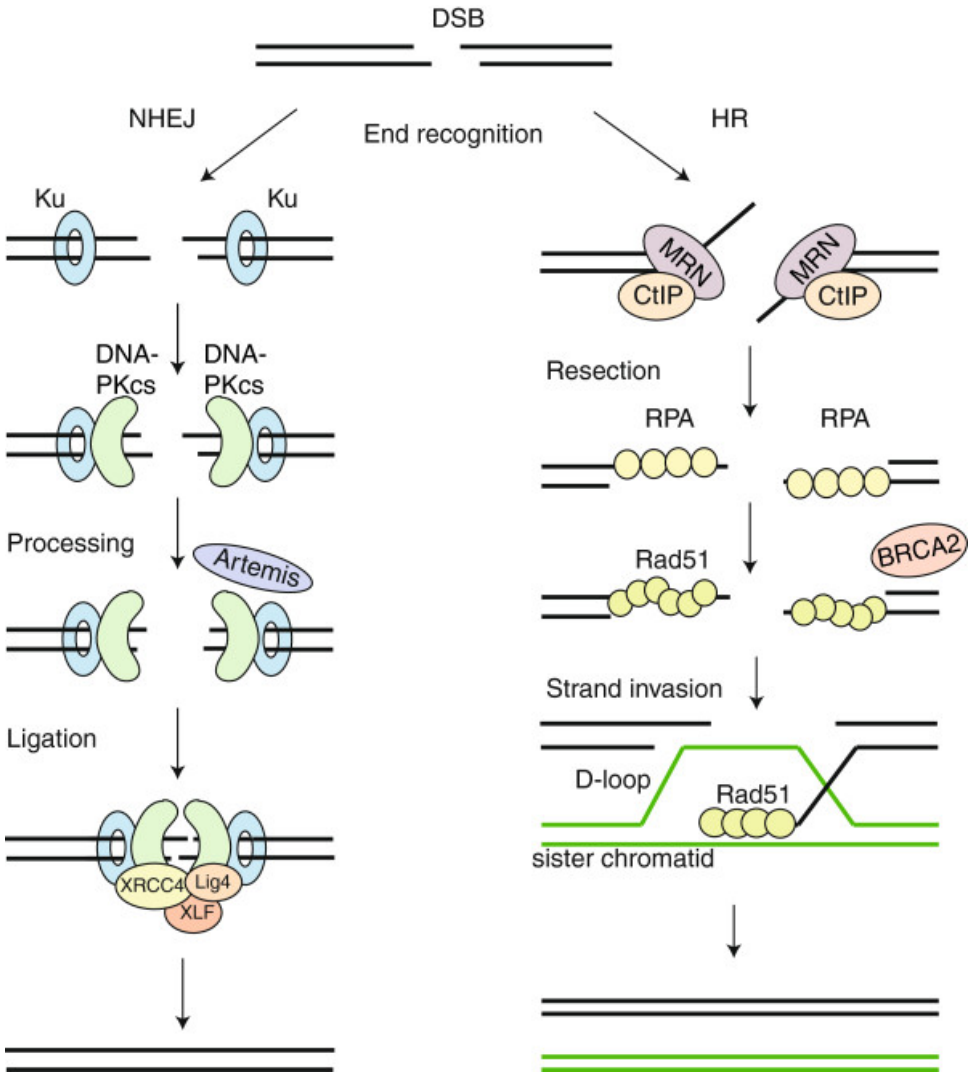

Figure I.36 – DNA repair machinery

In NHEJ (*left),* the KU70/KU80 heterodimer interacts with the DSB, protecting it from degradation by exonucleases. This heterodimer recruits and activates the DNA-PKcs (DNA dependent protein kinase catalytic subunit) and KU70 interacts with XRCC4 (X-ray repair cross-complementing protein 4). In addition, KU heterodimer interacts with the DNA ligase IV and with the contribution of Artemis, the ligation of DNA ends is carried out.

In the HR (*right*) pathway the MRN complex (Mre11 – Rad50 – Nbs1) is recruited at the DSB ends and subsequently enrolls CtIP (RBBP8; retinoblastoma binding protein 8), then creating single strand segments at the borders of the DSB. Another complex formed by hSSB1 (human single-strand DNA binding protein 1) and RPA (Replication protein A) protects free ends against degradation until the recruitment of RAD51 and BRCA2 (breast cancer 2). RAD51 invades the homologues sequences, from sister chromatid, to form a Holliday junction. The sister chromatids are joined by cohesin proteins and DNA is synthetized by the DNA polymerase δ, using the homologous chromatid sequence as template. Finally, DNA ends are joined by DNA ligase I *(Brandsma and Gent 2012)*.

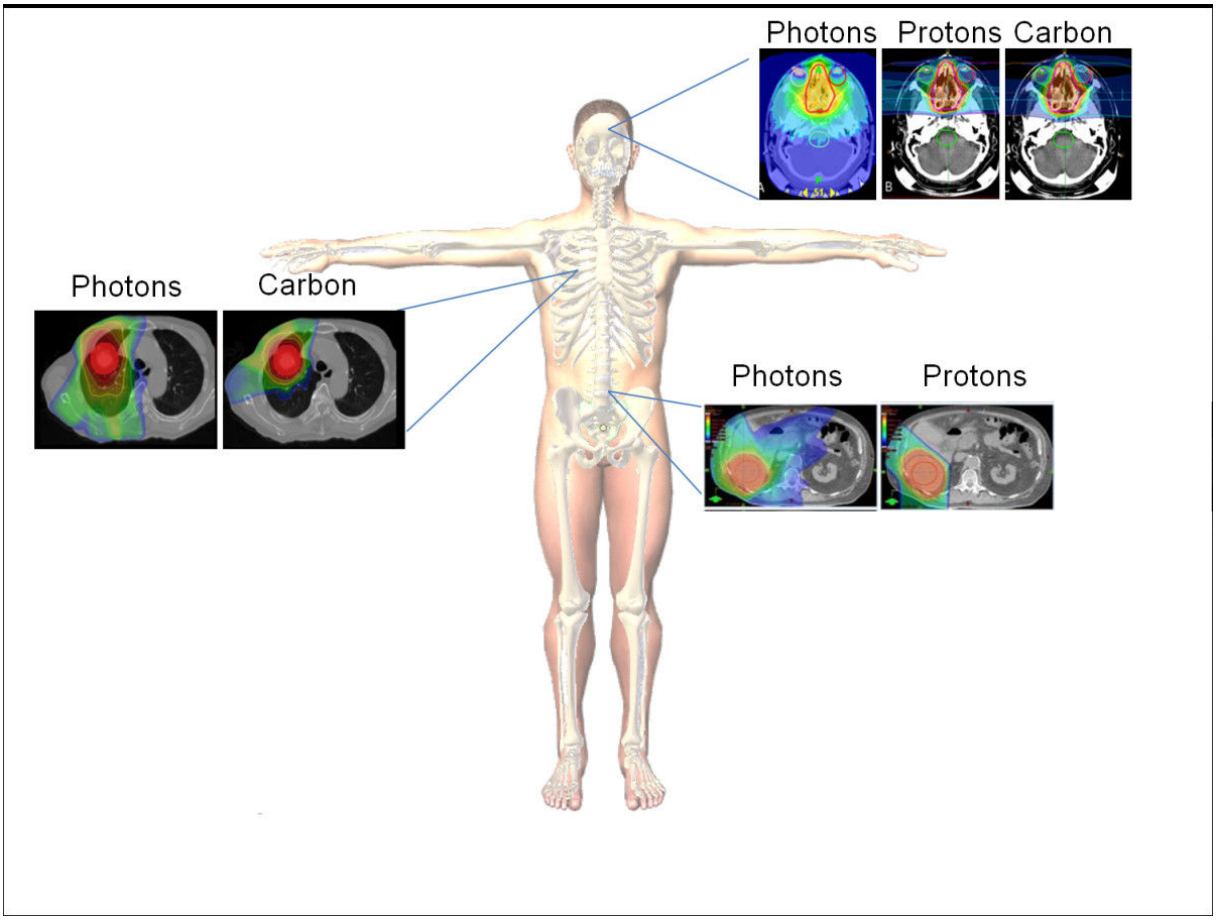

Figure I.37 – The use of proton and carbon therapies to overcome irradiation of healthy tissues during treatment

Examples of treatment planning for the irradiation of intracranial (glioblastoma multiforme), thoracic (lung carcinoma) and pelvic (rectal carcinoma) regions. Compared to photons, carbon ions and protons allow a more accurate targeting of the tumor while limiting irradiation of healthy tissues surrounding the tumor *(Schlaff, Krauze et al. 2014).*

recruits downstream effectors, including DNA PKcs. In addition, it interacts with XRCC4 (X-ray repair cross-complementing protein 4), the DNA ligase IV and Artemis to facilitate the ligation of the DNA ends. Therefore, this mechanism more likely introduces or deletes bases during its process, generating mutations *(Borrego-Soto et al., 2015)*. The second major pathway involved in DNA repair is the HR, a more precise and slower mechanism, that uses the sister chromatid as template. This process is thus error-free but is only effective during the S and G2 phases, i.e. when the sister chromatid is available *(Asaithamby and Chen, 2011)*. This pathway is usually activated in case of complex DNA damage and requires the recruitment of Mre11 – Rad50 – Nbs1 (MRN) complex. This complex allows the binding of CtIP (RBBP8; retinoblastoma binding protein 8), an exonuclease that processes the DNA to create single strand segments at DSB sites. DNA segments are then extended at the DSB site by an exonuclease, the exo 3' – 5'. Another complex comprising hSSB1 (human single-strand DNA binding protein 1) and RPA (replication protein A), protects free ends until the recruitment of Rad51 and BRAC2 (breast cancer 2), that allow the formation of the interconnection between the two sister chromatids, named the Holliday junction. After the joining of sister chromatids by cohesion proteins, DNA is synthetized by the DNA polymerase δ, using the homologous chromatid sequence as template. DNA ends are finally joined by the ligase I *(Borrego-Soto et al., 2015).*

The choice of a DNA repair mechanism over the other is function of the cell cycle phase in which the cell is stopped after DNA damage induction. Furthermore, it depends on the complexity of DNA damage. It was shown that low LET radiation, like X-rays or γ-rays, induces the activation of both NHEJ and HR. Consequently, the inhibition of NHEJ pathway generates a radiosensitivity of irradiated cells *(Asaithamby and Chen, 2011)*. In contrast, the inhibition of NHEJ upon high LET radiation or proton irradiation induces a slight radiosensitivity. Interestingly, the inhibition of HR upon high LET radiation led to high radiosensitivity, indicating that an intact HR is required for the repair of more complex DNA damage *(Zafar et al., 2010)*. These differences are explained by the presence of small DNA fragments generated by charged particle radiation that impede the binding of Ku70/Ku80 heterodimer, thus preventing the activation of NHEJ. It is why the inhibition of HR factors, such as RAD51, makes cancer cells sensitive to particle radiation *(Mohamad et al., 2017)*.

3. Clinical evidences

The first advantage of charged particles over photons is their high accuracy of deposited dose so that the dose distribution of protons makes them less susceptible to induce secondary malignancies (***Figure I.37***). It is why photon beams are less appropriate for the elimination of tumor located at a great depth within the body, despite of the improvement of technologies such as leaf collimators, intensity modulated radiotherapy (IMRT) or image-guided IMRT.

Furthermore, charged particle therapy also induces more severe DNA damage and thus induces more efficient cell killing compared to photons.

Another advantage of charged particles over photons is the magnetic steering of ion beams. As photons lack electric charges, the focus cannot be magnetically or electrically modified but requires the use of collimators to shape the beam laterally *(Mohamad et al., 2017)*. Despite collimators, scattering interactions cause lateral spread outside the collimated field, a zone called penumbra. Conversely, ion beams can be precisely focused on target with magnets. As heavy ions have a sharper lateral penumbra, because of the reduced scattering as they come through the body, they can be used for the irradiation of tumor located near organ at risk (OAR)

(Mohamad et al., 2017) and with a regimen of hypofractionation.
Finally, nuclear interaction of charged particles produce positrons that could be detected by positron emission tomography (PET) scanners in order to verify the dose delivery during the treatment. These measurements should be made during dose delivery but still require further developments. This kind of real-time imagery is not possible with photon beams.

Unfortunately, the adoption of proton therapy and other charged particle therapies has been slowed by technical difficulties, a higher cost and lack of evidences for cost-competitiveness *(Newhauser and Zhang, 2015)*. Until now, the cost effectiveness for protontherapy is higher compared to X-rays. Indeed, the cost for a proton beam center is 40 times higher than for a photon beam center. However, the cost could be reduced by routinely using protontherapy for many types of cancers, such as prostate cancers *(Schiller et al., 2016)*.
In addition, no real differences about toxicities have been evidenced between photon and proton beams *(Newhauser and Zhang, 2015)*. Furthermore, some areas in the body have an extreme variation of density that can modify the energy distribution of the beam. For example, bones reduce the particle energy while an air cavity extends the physical range of the particles, when compared to water. It is thus important to choose beam angles, in order to go through homogeneous tissues *(Kosaki et al., 2012).* Finally, sufficient margins are essential to avoid the location of the Bragg peak in normal tissues, which could decrease the advantages of particle therapy. For the same reasons, patient positioning must be highly precise and the patient motions must be highly controlled *(Schiller et al., 2016)*. Therefore, a better control of these parameters will allow to re-evaluate the efficacy of proton irradiation compared to photons.

High LET radiation is recommended for slowly proliferating tumors, later responding, with high capacity for sublethal damage repair, with a low radiosensitivity and highly resistant to conventional radiotherapy *(Schlaff et al., 2014)*. In practice, charged particle therapy is currently used in clinic to treat tumors near OAR, such as the brain, the spinal cord or the optic nerve. For example, protontherapy is a standard treatment for uveal melanoma and is recommended for chondromas and chondrosarcomas located at the skull base. In addition, the probability to develop radiation-induced cancers for children is higher than for adults and requires a more precise method for the irradiation treatment. Even if there are a lot of uncertainties regarding secondary tumors induced by protons or other charged particles, the depth dose profile of these particles guaranties a more accurate dose delivery, and then the sparing of healthy tissues. It is why protontherapy is usually recommended for pediatric tumors *(Durante and Loeffler, 2010).*

4. Conclusion

Numerous studies are still required to understand the effects of charged particle therapy on tumors, as well as to relieve the remaining questions on its efficacy and on radiation-induced malignancies. Furthermore, it is now well known that extrinsic factors may also influence the effects of irradiation, such as the presence of stem cells, the glucose metabolism, the tumor microenvironment and the angiogenesis *(Schlaff et al., 2014)*. As the number of proton and carbon ion centers is growing *(Ilicic et al., 2018)*, *in vitro*, *in vivo* and randomized clinical studies will allow to unravel the effects of charged particle therapy on tumors and drive the choice of a radiation type over another for every patient.

Radiotherapy remains one of the most effective treatments for cancer, as more than half of all patients receive radiotherapy during their treatment *(Joiner and Kogel, 2009)*. This therapy is constantly improving thanks to new modalities, including new imagery technologies and the use of charged particle therapy *(Harrington et al., 2007; Newhauser and Zhang, 2015)*. Particle therapy presents the main advantage to more precisely target tumors due to a spatial dose distribution that spares normal tissues *(Newhauser and Zhang, 2015)*. In addition to its physical properties, charged particles therapy is also characterized by a higher relative biological effectiveness *(Joiner and Kogel, 2009)*. This efficiency is brought by a decreased radioresistance compared to conventional radiotherapy. Indeed, the resistance to radiotherapy may be intrinsic to cancer cells, notably through beneficial alterations of cell cycle phases and DNA repair machinery activity or by taking advantage of pro-survival mutations *(Schlaff et al., 2014)*. However, often treated as a monocellular area, tumors revealed many strategies to elude cytotoxic therapies *(Palucka and Coussens, 2016),* leading to reconsider the tumor as a complex tissue. Therefore, radioresistance may also be driven by extrinsic factors, such as hypoxia, the tumor vasculature, the extracellular matrix or the cells from the tumor microenvironment *(Barker et al., 2015; Schlaff et al., 2014)*. In this context, TAMs represent a key feature of the microenvironment and frequently antagonize the antitumor efficacy of therapies *(De Palma and Lewis, 2013)*.

TAMs represent a heterogenic population that is usually associated to an oversimplified M2 phenotype with anti-inflammatory and pro-tumoral properties. This phenotype contrasts with the M1 one, that exhibits pro-inflammatory, phagocytic and anti-tumoral roles *(Biswas and Mantovani, 2010; Mittal et al., 2014)*. Owing the high plasticity of macrophages to environmental cues and the poor prognosis associated to TAM infiltration, M2-like TAM reprogramming seems to be a promising strategy to reverse the fate of tumors. In the last few years, chemotherapies and immunotherapies have successfully reprogrammed TAMs towards a M1-like phenotype and were concomitantly associated to tumor regression. However, as these therapies are not localized and could thus trigger a systemic inflammatory response, local radiotherapy is an attractive alternative. Studies on macrophage reprogramming with local conventional radiotherapy revealed that moderate doses (1 – 10 Gy) were able to educate unpolarized macrophages toward a M1 phenotype. However, to our knowledge, none of these researches have demonstrated a reprogramming of M2-like macrophages toward a M1 phenotype *(See Chapter 3)*.

Therefore, the overall objective of this thesis was to examine the effects of proton irradiation on macrophages, and more specifically on their reprogramming. The first part of this work consisted in the evaluation of macrophage responses to proton irradiation. The aim was double: firstly, we attempted to characterize the sensitivity of *in vitro* unpolarized (M0) and polarized macrophages (M1 and M2) to proton irradiation and secondly, we examined the effect of proton and X-ray irradiation on macrophage reprogramming in differentiated (M0) and polarized (M1 and M2) macrophages. In the second part of this work, the effects of cancer cells on proton-induced macrophage reprogramming were investigated. To this aim, we set-up a new co-culture system that allows the irradiation of either M2 macrophages or cancer cells, or both together.

Altogether, the results obtained during this thesis allowed to highlight differential radioresistance according to the macrophage phenotype. Furthermore, we evidenced the influence of proton irradiation on macrophage reprogramming. By understanding the way by which protontherapy promotes macrophage reprogramming, these findings open new perspectives for the use of particle therapy. Further investigations on macrophage reprogramming induced by ion beams are of great importance for future approaches in the treatment of cancer patients.

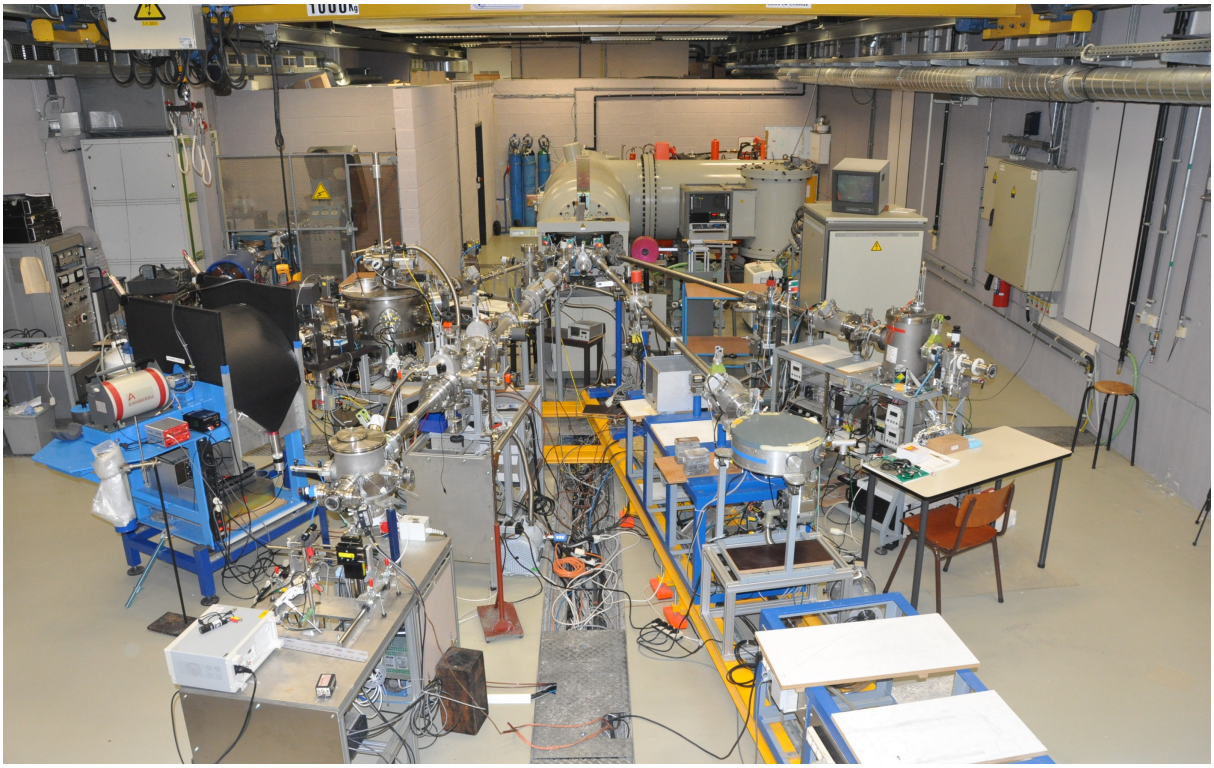

Figure III.1. Picture of the accelerator

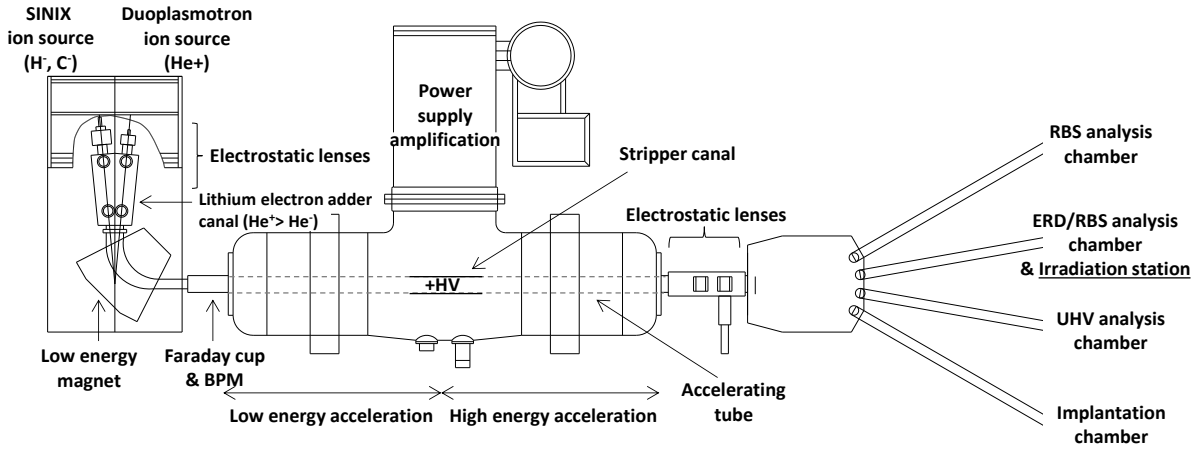

Figure III.2 – Schematic representation of the accelerator "ALTAIS" (Accélérateur Linéaire Tandétron pour l'Analyse et l'Implantation des Solides)

1. Proton irradiation: the particle accelerator and the irradiation chambers

In order to irradiate the cells, the irradiation chambers containing the cells were placed on one of the four exit lines of the 2MV tandem accelerator (High Voltage Engineering Europa, ALTAIS), available at the LARN laboratory (University of Namur) (***Figure III.1***). ALTAIS (for "Accélérateur linéaire Tandétron pour l'Analyse et l'Implantation des Solides") allows the acceleration of ions from light weight (such as hydrogen) to heavy ones (such as uranium). In the following experiments, we used a H^+ homogenous broad beam produced from the sputtering of a TiH_2 860 source powder. Briefly, negative ions are extracted from the plasma are then selected with a low energy magnet and accelerated through a Tandetron accelerator (tandem acceleration). This accelerator setup allows a two step acceleration. Indeed, negative ions are attracted by a high positive tension localized at the middle of the accelerator tube and undergo a first acceleration. In the middle of the accelerator tube, nitrogen, released by a stripper canal, produces charge changes, making positive ions. H+ ions are then repulsed by the high positive tension and undergo a second acceleration. Finally, the accelerated ions are deflected with a high-energy magnet to the desire beam line. In our experiments, the left 10° beam line was used (***Figure III.2***).

Thanks to tools such as Beam Profile Monitor (BPM), the shape and the intensity of the beam were adjusted before and after the acceleration of particles, by playing on parameters such as the position of electrostatic lenses. Once the shape of the beam was adjusted, the homogeneity was tuned with camera and detectors localized in the cell irradiation station (***Figure III.3***), placed at the end of the beam line. The cell irradiation station consists of vacuum chamber with a charge-coupled device (CCD) camera that was used to shape the beam and to acquire a quite homogeneous beam. Passivated Implanted Planar Silicon (PIPS) detectors were placed before and after the cell irradiation station. They were used to tune the dose rate and to help ensuring the homogeneity and the stability of the proton beam (***Figure III.4***) *(Wéra et al., 2011)*. The H+ broad beam irradiation field was delimited using a 8 mm diameter collimator. The homogeneous beam over 0.8 cm^2 went through a 1 μm thick Si_3N_4 exit foil. All these adjustments require several hours of settings before cell irradiation. The LET of particles was set-up to 25 keV/μm in order to obtain the maximal RBE in cell nucleus. The dose rate was fixed to 2 Gy/min for the irradiation of macrophages alone and to 10 Gy/min for the co-culture experiments. This difference will be explained and described in the second part of the « Results » section.

The irradiation chambers are composed of two stainless steel pieces, covered by a 3 μm thick mylar foil. The bottom and top parts make a sealed irradiation chamber thanks to a sealing joint. The filling of the irradiation chambers (2 ml) is made by one of the two holes located on the side, using a syringe (***Figure III.5***).

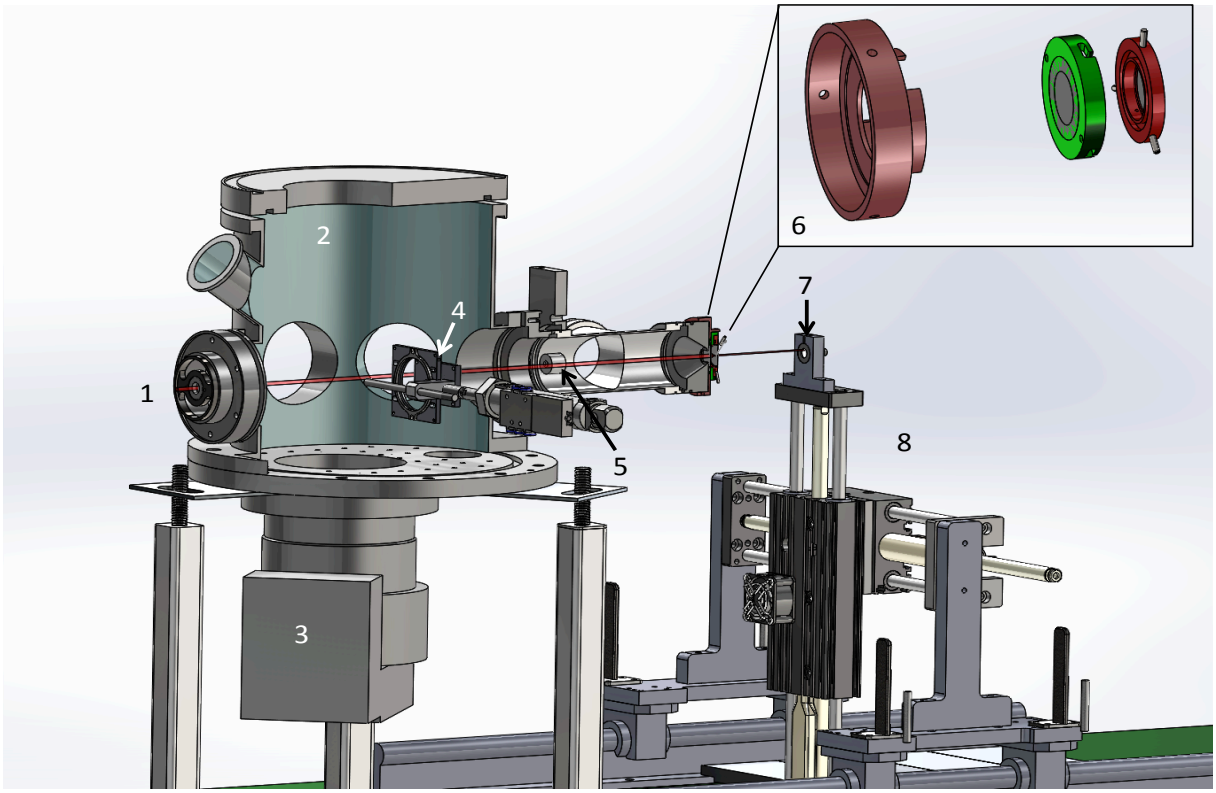

Figure III.3 – Cell irradiation station

The cell irradiation station is equipped with a charged-couple device (CDD) camera, a passivated implanted planar silicon (PIPS) detector and a plastic scintillator BC-400. The XY motorized table allows the cartography of the beam in order to evaluate its homogeneity. (1) H^+, He^{2+} or C^{4+} broad beam; (2) vacuum chamber; (3) pumping system; (4) BC400 scintillator + CCD camera fixed on a pneumatic jack; (5) PIPS detector placed on the left side of the beam for the dose-rate monitoring; (6) irradiation head and irradiation chamber; (7) movable PIPS detector; (8) XY motor *(Wéra A.-C. 2011)*.

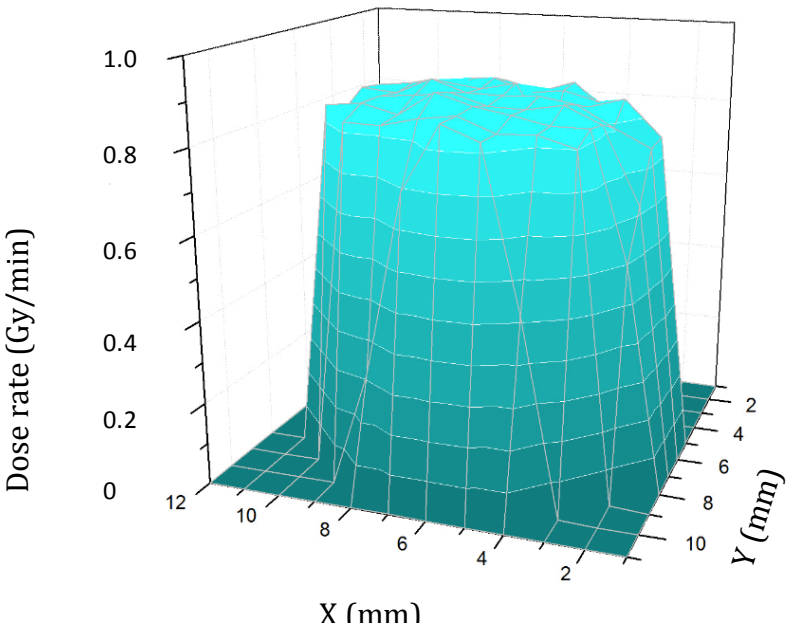

Figure III.4 – Homogeneity cartography for a 1.3 MeV proton beam

The incident flow was measured every millimeter on a 1 cm^2 surface with the PIPS detector. The dose rate (Gy/min) is then calculated based on LET (25 keV/µm) and the incident flow.

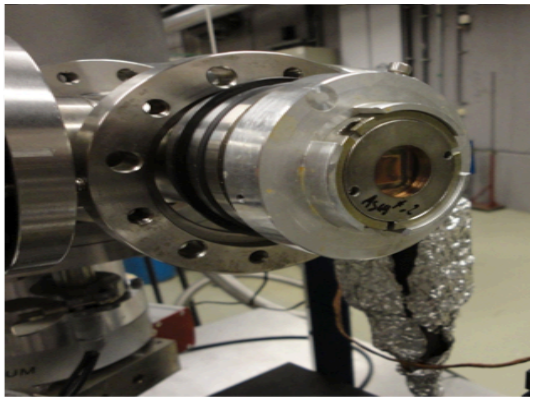

Figure III.5 – Irradiation chamber
The irradiation chambers are composed of two stainless steel pieces covered by a mylar foil. The irradiation chamber is placed on an aluminum support that fits together with the Si_3N_4 exit window.

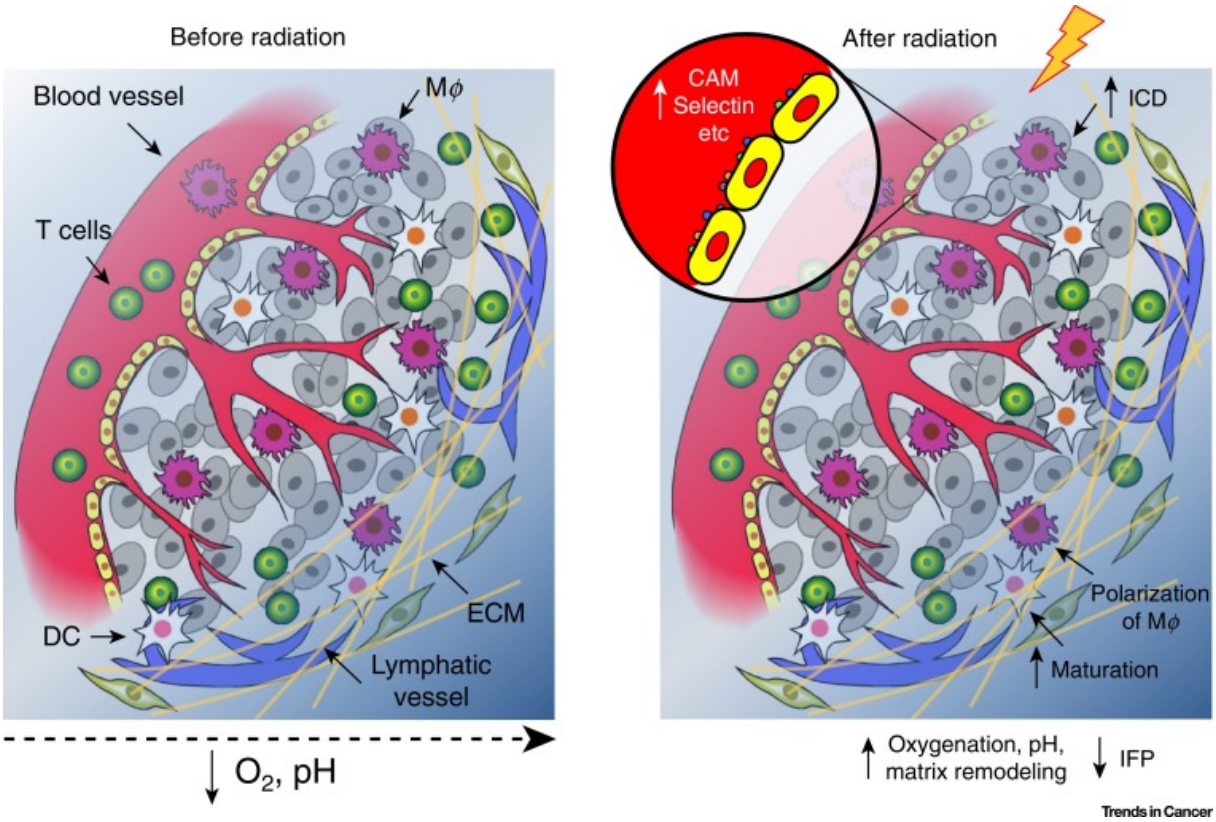

Figure III.6 – Immunomodulation of the tumor microenvironment after radiotherapy
Irradiation modifies the tumor microenvironment by increasing the intratumoral oxygenation and pH, by promoting immunogenic cell death (ICD) and by remodeling the extracellular matrix (ECM) and the tumor vasculature. In addition, radiotherapy also modulates the recruitment of immune effectors into the tumor. Mϕ, macrophages; IFP, interstitial fluid pressure; CAM, cell adhesion molecules *(Jiang, Chan et al. 2016)*.

2. PART 1: Effects of proton irradiation on human macrophages

2.1. Objectives

Nowadays, radiotherapy is used to treat up to 50% of cancer patients alone or in combination with other treatments *(Good and Harrington, 2013; Newhauser and Zhang, 2015)*. Unfortunately, the efficacy of this treatment is often limited by toxicity to healthy tissues and by radioresistance *(Barker et al., 2015)*. In order to palliate all these drawbacks, new modalities have emerged, including the improvement of conventional radiotherapy and the use of charged particle therapy. Indeed, the interest for proton irradiation is currently increasing given its accurate dose distribution and the sparing of healthy tissues *(Durante and Loeffler, 2010).*

For a long time, researches had been focused on the effect of radiotherapy on cancer cells themselves, ignoring the tumor microenvironment components and their biological interactions with cancer cells *(Barker et al., 2015)*. The resistance to radiotherapy may be intrinsic to cancer cells (cell cycle phases, DNA repair machinery activity…) but may also be caused by extrinsic factors, such as oxygen levels, the tumor vasculature, the stromal constituents or the cells from the tumor microenvironment *(Barker et al., 2015; Schlaff et al., 2014)*. In the past few years, the influence of the immune system on tumor fate has been largely studied, revealing opposite functions of immune cells. Similarly, the response of the tumor immune cells to radiotherapy is ambivalent (***Figure III.6***). It is shown that radiotherapy promotes an inflammatory environment by stimulating the innate immune system, as well as induces the recruitment of immune cells into tumors. This immune activation is generated through the release of DAMPs by damaged cells or dead cells and leads to the immunogenic cell death (ICD) of cancer cells, or in other words to the cell death of cancer cells triggered by the activation of DAMPs-PRR signaling in immune cells. In contrast, radiotherapy also elevates the number of immunosuppressive cells that are related to a poor prognosis for cancer patients. These suppressive cells include Tregs, MDSCs and M2-like TAMs, which are less radiosensitive than other immune cells *(Barker et al., 2015).*

Regarding the high plasticity of macrophages, an increasing interest has been made for re-educating TAMs to an antitumor phenotype. Therefore, a lot of efforts were made to find chemotherapeutic agents, immunotherapies or other compounds that reprogram TAMs towards an anti-tumor phenotype, usually associated with an elevation of the expression of M1 markers and a reduced expression of M2 markers. However, most of these agents have a systemic distribution and may influence the function of out-of-target cells. These last years, several studies with localized conventional radiotherapy have shown interesting effects on macrophage polarization. Interestingly, moderate doses (1 – 10 Gy) of X-ray or γ-ray radiation drive M1 polarization in unpolarized macrophages. Unfortunately, local conventional radiotherapy alone has not succeeded to induce a reprogramming of M2-like TAMs or *in vitro* M2 macrophages into M1 ones *(See Chapter 3).* As compared to photons, the biology associated with exposure to protons still remains largely unknown. Therefore, the aim of the first part of this work was to evaluate the effects of proton irradiation on unpolarized (M0) or polarized (M1 and M2) macrophages.

A **B**

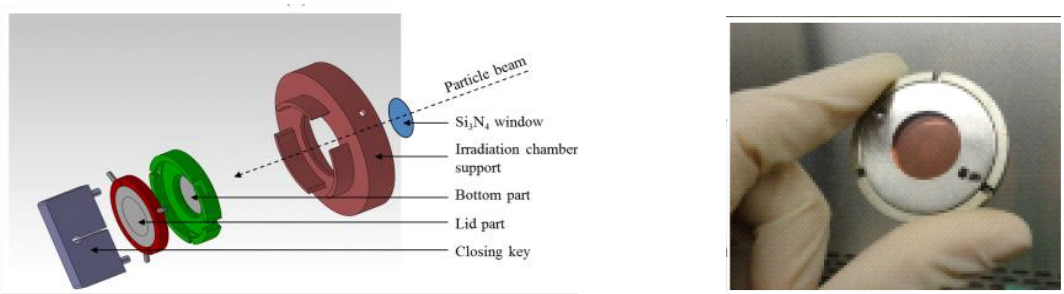

Figure III.7 – Irradiation chamber

(A) Irradiation chamber scheme and **(B)** irradiation chamber containing cells and culture medium

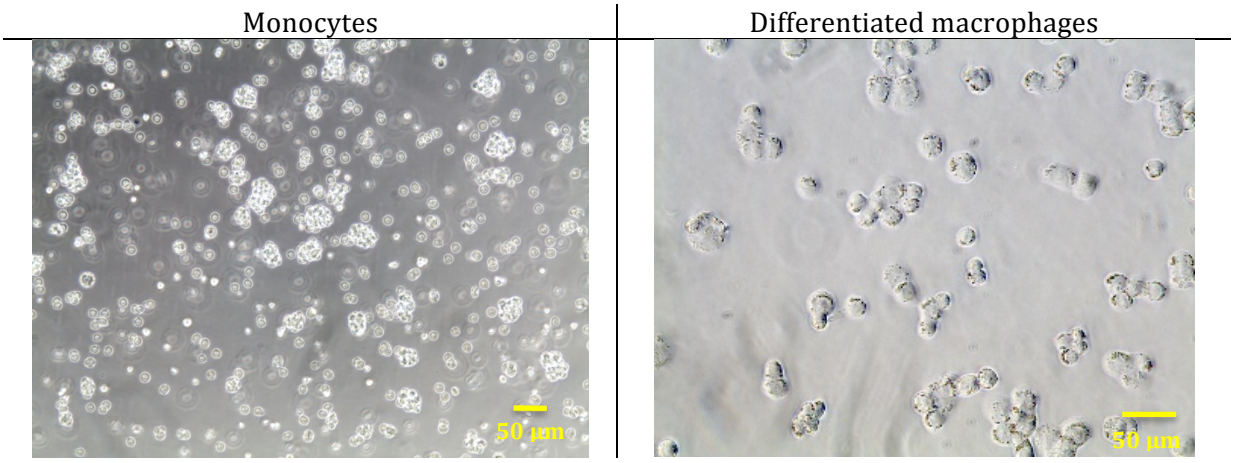

Figure III.8 – Monocytes versus macrophages

Pictures in phase contrast microscopy of THP-1 monocytes (*left*) and PMA-differentiated THP-1 macrophages (*right*).

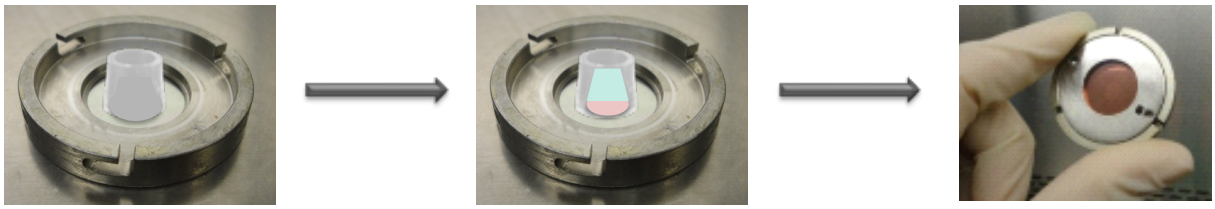

Figure III.9 – Cloning cylinder in irradiation chamber

A cloning cylinder was deposited at the center of the irradiation chamber and was filled with 50 µl of Cell Tak (5 µg/cm²) diluted in bisphosphonate solution (0.1 M, pH 8) for 1h. After rinsing with milli Q water, the cloning cylinder was filled with 190 µl of medium containing 50,000 THP-1 monocytes, 150 nM PMA and penicillin streptomycin 10,000 U/ml for 24h. The day after, the cloning cylinder was removed and the chamber was closed and filled with RPMI medium without PMA.

2.2. Experimental model

In order to study the effect of proton irradiation on macrophages, we used differentiated (M0) and polarized (M1 and M2) THP-1 macrophages, a model of macrophage polarization optimized by Marie Genin *(Genin et al., 2015)* and adapted to the irradiation chambers at the beginning of this project. The THP-1 cell line was isolated from peripheral blood of a 1-year old male patient suffering from acute monocytic leukemia and is a monocyte/macrophage model frequently used in research.

The irradiation procedure allowed the production of a homogeneous broad beam of 1 cm^2, placed at the center of the irradiation chamber (2 cm diameter) (***Figure III.7***). Therefore, the cells were seeded as a 32 µl-drop at the center of the irradiation chambers. In order to differentiate non-adherent THP-1 monocytes into adherent macrophages (***Figure III.8***), we used phorbol-12-myristate-13-acetate (PMA). This step required an incubation time of 24h with 150 nM PMA and could not be performed in a small drop. Consequently, a cloning cylinder was deposited at the center of the irradiation chamber, allowing PMA differentiation in a total volume of 190 µl (***Figure III.9***). The incubation of monocytes with PMA is known to mediate the activation of protein kinase C (PKC), a ubiquitous cellular enzyme. In more details, PMA mimics diacylglycerol (DAG), which is required for PKC activation. Once translocated from cytosol to plasma membrane, PKC phosphorylates different target substrates, including different transcription factors, such as STAT, NFκB, AP-1 or MAPK. By playing a crucial role in diverse signaling pathways, PKC activation promotes cytoskeletal remodeling, cell adherence, loss of proliferation, differentiation and phagocytosis *(Richter et al., 2016; Schwende et al., 1996)*. For the irradiation step, it is important to have a homogeneous monolayer of cells because the initial energy (1.3 MeV) of particles is not high enough to go through several layers of cells. This initial energy was determined to obtain a LET of 25 keV/µm along the proton path into the cells, a monolayer allowing to have the same LET at the entrance and the exit of the cells. The irradiation field is limited using collimator, therefore, cells outside the field would not be irradiated. Despite a good adherence to the mylar foil, differentiated THP-1 cells tended to form clusters when seeded on Mylar foil. Different coatings were thus tested to circumvent this problem (***Figure III.10***). Only Cell Tak allowed a homogenous monolayer of cells while the use of other coatings has not succeded to impact the cell distribution. Cell Tak was thus used for the following experiments. After 24h incubation with PMA, the cloning cylinder was removed and a 24h rest period in supplemented RMPI medium without PMA was required before polarization. At the end of this period, macrophages were polarized in M1 or M2 macrophages as described in *(Genin et al., 2015)*. Briefly, macrophages were incubated with 10 pg/ml LPS and 20 ng/ml recombinant human IFNγ (rhIFNγ) medium in order to obtain M1 macrophages. For M2 macrophages, irradiation chambers were filled with RPMI medium containing 20 ng/ml rhIL4 and 20 ng/ml rhIL-13 medium.

Morphological changes were observed after polarization in M1 and M2 macrophages (***Figure III.11***). Indeed, M1 macrophages exhibited a spread shape and were individualized while M2 macrophages fused to form multinucleated giant cells with some prominent cytoplasmic processes. Cell fusion and giant cell formation are caused by an elevation of integrin and E-cadherin expression on cell membrane, elicited by IL-4 *(Aghbali et al., 2017)*. These morphological differences were accentuated in the irradiation chamber as compared to well

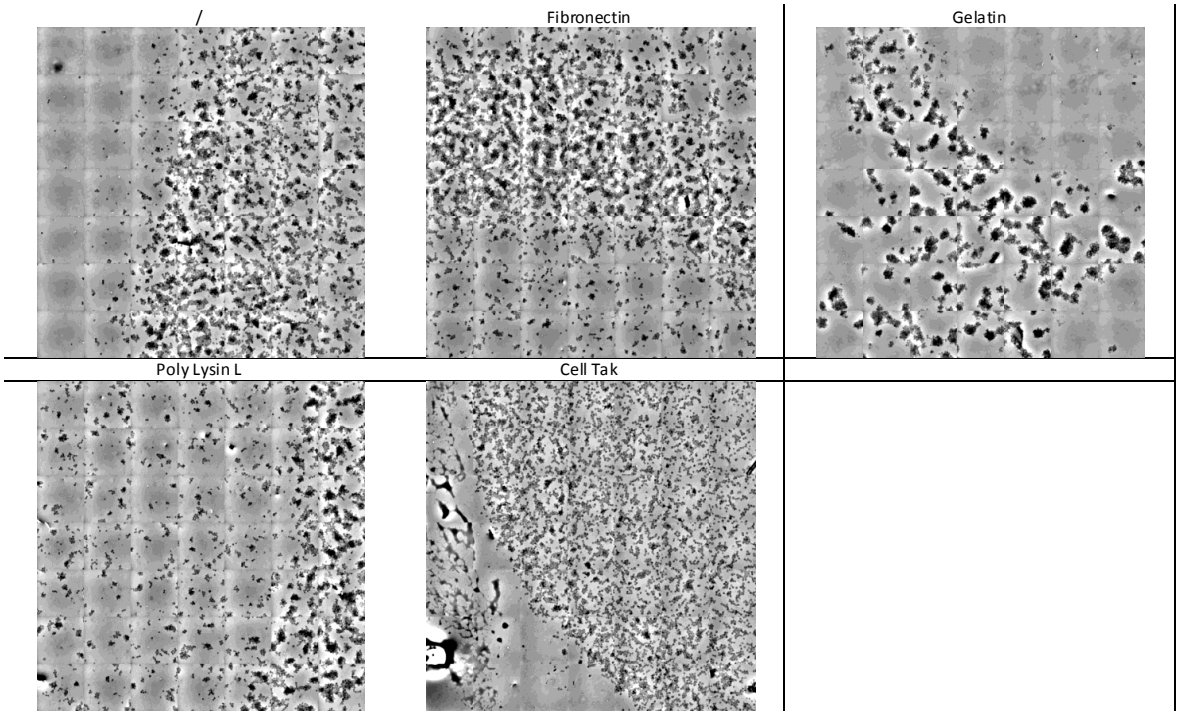

Figure III.10 – Effect of coatings on macrophage clustering
As the irradiation step requires a homogenous monolayer of cells, the cell distribution was evaluated. 49 pictures were captured with a digital holographic microscope (objective 20X) for each condition and were assembled to have an overview. Cell clusters were observed when macrophages were seeded directly on mylar or when fibronectin, gelatin or poly L-lysin coatings were used. In contrast, the use of Cell Tak allowed a homogenous monolayer of cells.

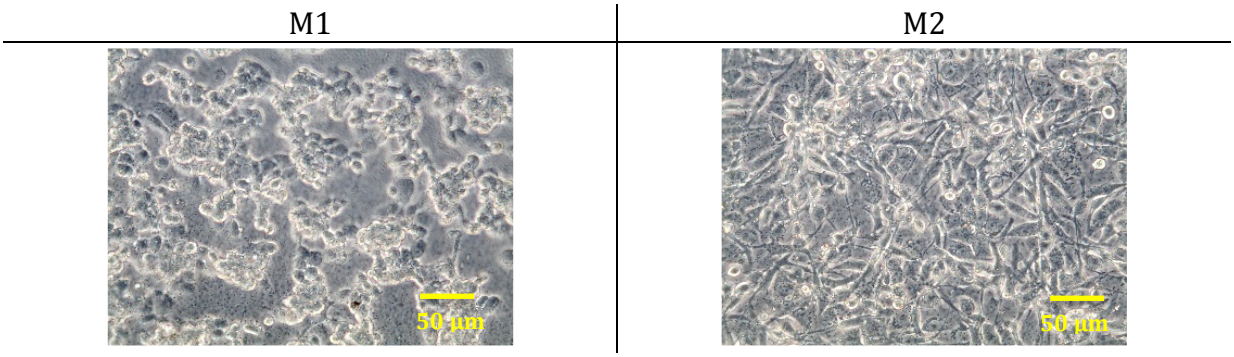

Figure III.11 – Morphological changes after macrophage polarization in irradiation chambers
Pictures of M1 (*left*) and M2 (*right*) macrophages in phase contrast microscopy.

M1	M2
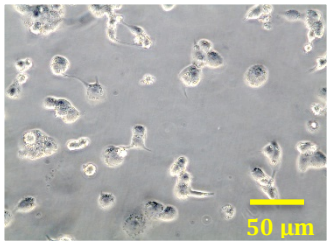	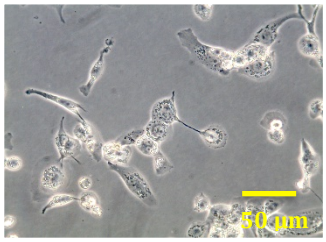

Figure III.12 – Morphological changes after macrophage polarization in 6-well plates
Pictures of M1 (*left*) and M2 (*right*) macrophages in phase contrast microscopy.

plate (***Figure III.12***). However, the expression of M1 and M2 markers was similar in well plates and in irradiation chambers after macrophage polarization (***cfr supplementary figure S4 of the research article p. 81***).

2.3. Limitations

The choice of a technique over another to analyze viability and mRNA or protein expression was determined by the limitations of our system. Indeed, we have been confronted to several constraints that impeded the proper use of some techniques, such as western blot or flow cytometry. The first constraint we have met was the limited number of seeded cells. As cells must be plated at the center of the irradiation chamber on a small surface, only 50 000 cells were seeded in each irradiation chamber. Therefore, the experiments for RT-qPCR required pooling the material of three irradiation chambers. Even with three irradiation chambers, small quantities of RNA were collected (1300 ng – 3500 ng per sample) and restricted the expression analysis of multiple target genes. The small number of seeded cells made also impossible to perform western blot experiments due to too small protein quantities. The second constraint was the difficulty to detach the cells once seeded on the mylar foil. This problem was probably caused by the use of Cell Tak, without which it is impossible to obtain a homogeneous monolayer of differentiated macrophages (M0). Hence, the use of Cell Tak prevented for instance the analysis of apoptosis by flow cytometry.

2.4. Research article: "Proton irradiation orchestrates macrophage reprogramming through NFκB signaling"

Submitted on the 1st of February 2018 in Cell Death & Disease – Nature. The reviewing was received on the 27th of February 2018.

Reviewer's comments:

The current study examines the impact of heavy particles irradiation using protons on tumor associated macrophages phenotypes, particularly in the context of the anti tumor M1 subtype and the protumorigenic M2 subtype.
The authors suggest a NF-κB - associated M2 to M1 reprogramming following proton IR.
This is quite an interesting study as the number of proton irradiators in clinical oncology is steadily increasing and the biology associated with exposure to protons as compared to gamma irradiation is still at large unknown.
Before publication, the authors need to follow with several points:

1. The authors are using M0, M1 and M2 cells derived from THP-1 monocytic line. I think it would be useful when they start the results section to give a small description of the system. They should also explain why they do not use additional cell lines as well, which could make the data more valid.
2. Please explain why the study does not include as control the same cellular systems exposed to gamma/X IR.
3. Figure 2 shows impact of 10Gy on γH_2AX status. It was not very clear how the quantification was made. Normally γH_2AX foci are counted and not overall fluoresensce. In that respect, I would suggest in addition to the microscopy data to provide results of γH_2AX on cell lysates under same experimental conditions using Western blotting. Additionally, the data would be stronger if an additional marker of DSBs is examined as well, for example foci of 53BP1 could be quite appropriate.
4. The English throughout the paper must be improved. I suggest to have the paper extensively edited for a revised version.

The edited and revised version of the article was re-submitted on the 26th of May in Cell Death & Disease (Nature publishing group).

Proton irradiation orchestrates macrophage reprogramming through NFκB signaling

GENARD Géraldine [1], WERA Anne-Catherine [1], HUART Camille [1] LE CALVE Benjamin [1], PENNINCKX Sébastien [2], FATTACCIOLI Antoine [1], TABARRANT Tijani [2], DEMAZY Catherine [1], NINANE Noëlle [1], HEUSKIN Anne-Catherine [2], LUCAS Stéphane [2], MICHIELS Carine [1*]

1. Cellular Biology Research Unit (URBC) - NARILIS, University of Namur, Namur, Belgium.
2. Laboratory of Analysis by Nuclear Reaction (LARN / PMR) - NARILIS, University of Namur, Namur, Belgium.

Running title: Macrophage reprogramming by proton irradiation

Géraldine Genard is a recipient of a Télévie grant (National Fund for Scientific Research (FNRS)). Anne-Catherine Wéra and Benjamin Le Calvé benefit from a Postdoctoral Move-in-Louvain-Marie Curie grant. Camille Huart is a recipient of a FSR (fonds special de la recherche) grant from the University of Namur. Sébastien Penninckx is supported by FNRS (PhD grant).

* corresponding author: URBC-NARILIS, University of Namur, 61 rue de Bruxelles, 5000 NAMUR, Belgium tel +32-81-724131, fax +32-81-724135 Email: carine.michiels@unamur.be

Abstract

Tumor-associated macrophages (TAMs) represent potential targets for anti-cancer treatments as these cells play critical roles in tumor progression and frequently antagonize the response to treatments. TAMs are usually associated to a M2-like phenotype, characterized by anti-inflammatory and protumoral properties. This phenotype contrasts with the M1-like macrophages, which exhibits pro-inflammatory, phagocytic and antitumoral functions. As macrophages hold a high plasticity, strategies to orchestrate the reprogramming of M2-like TAMs towards a M1 antitumor phenotype offer potential therapeutic benefits. One of the most used anti-cancer treatments is the conventional X-ray radiotherapy (RT), but this therapy failed to reprogram TAMs towards a M1 phenotype. While protontherapy is more and more used in clinic to circumvent the side effects of conventional RT, the effects of proton irradiation on macrophages have not been investigated yet. Here we showed that M1 macrophages (THP-1 cell line) were more resistant to proton irradiation than unpolarized (M0) and M2 macrophages, which correlated with differential DNA damage detection. Moreover, proton irradiation induced macrophage reprogramming from M2 to a mixed M1/M2 phenotype. This reprogramming required the nuclear translocation of NFκB p65 subunit as the inhibition of IκBα phosphorylation completely reverted the macrophage re-education. Altogether, the results suggest that proton irradiation promotes NFκB-mediated macrophage polarization towards M1 and opens new perspectives for macrophage targeting with charged particle therapy.

Keywords: *Inflammation and tumor development – molecular target of radiation response, radiation-activated signaling pathways – tumor microenvironment and modification* **OR** Macrophages, proton irradiation, nuclear factor kappa B, polarization, reprogramming.

Introduction

The immune system takes part in both cancer elimination and tumor development, especially through its activation and then its adaption to cancer cells (1). This process is called the cancer immunoediting and it perfectly illustrates the ambivalent function of the immune system in cancer. In addition, the effectiveness of treatments such as X-ray or γ-ray radiotherapy (RT) is partially conditioned by the presence of immune cells into the tumor. For example, ablative radiation (20 Gy) on local tumor significantly reduced the tumor volume in wild-type (WT) but not in nude (T-cell deficient) mice bearing a melanoma (B16 melanoma cells) (2). In line with this observation, local RT produces an abscopal response, which is an antitumor effect on distant unirradiated tumors (metastases), by triggering systemic immune responses (3). Another example is the systemic immune activation in mice previously treated by local RT and immune checkpoint inhibitors that prevented the tumor growth in mice rechallenged with the same tumor (4). However, the number of infiltrating tumor-associated macrophages (TAMs) is known to limit radiotherapy efficiency and is directly correlated to a poor prognosis (5). Inside the tumor, TAMs represent up to 50 % of the host infiltrating cells (6, 7), meaning that these cells are highly recruited at the tumor site and play critical roles in tumor development. It has been shown that RT promotes the recruitment of macrophages into the tumor, favoring tumor relapse after treatment (8). Indeed, TAM depletion or inhibition of monocyte recruitment into the tumor site combined to RT induce tumor regression in mouse cancer models and increase the survival of cancer patients (9, 10). Another attractive and effective strategy is the re-education of TAMs towards an antitumoral phenotype.

Macrophages display a remarkable plasticity allowing them to fulfill a multiple range of functions. These multi-task skills rely on two opposite phenotypes, M1 versus M2. These two subpopulations are classified as two extremes of a linear scale between which exists a multitude of intermediate states (11). Pro-inflammatory M1 macrophages, also called classically activated macrophages, exhibit enhanced pathogen phagocytosis, promote inflammation and activate immune system. On the opposite, anti-inflammatory M2 macrophages, referred to as alternatively activated macrophages, contribute to tissue repair, matrix remodeling and angiogenesis, and also repress the immune system. It is well accepted that M1 macrophages exert anti-tumor functions while M2 macrophages show pro-tumoral activity and, unfortunately, are usually the most representative TAM population into the tumor (12). M2-like TAMs display their harmful actions by promoting genetic instability, stem cell nurturing, angiogenesis, metastasis spreading and local immunosuppression (8). The polarization of macrophages towards a M1 or a M2 phenotype is driven by the activity of diverse transcription factors and miRNAs. Among transcription factors, NFκB plays a central role to influence the inflammatory macrophage status. While the active heterodimer NFκB (p50 – p65) promotes the transcription of pro-inflammatory genes, such as TNFα, IL-6, and IL1β, the inactive homodimer NFκB (p50 – p50) prevents the transcription of pro-inflammatory genes and confers the anti-inflammatory status to M2 macrophages (13).

The plasticity of TAMs and their ability to be reprogrammed, especially from M2 to M1 phenotype, make them an attractive target for anticancer therapies. Conventional radiotherapy (X-rays or γ-rays) initiated the polarization of differentiated but unpolarized (M0) macrophages towards M1 when exposed to moderate doses (1 – 10 Gy) (for a review, see

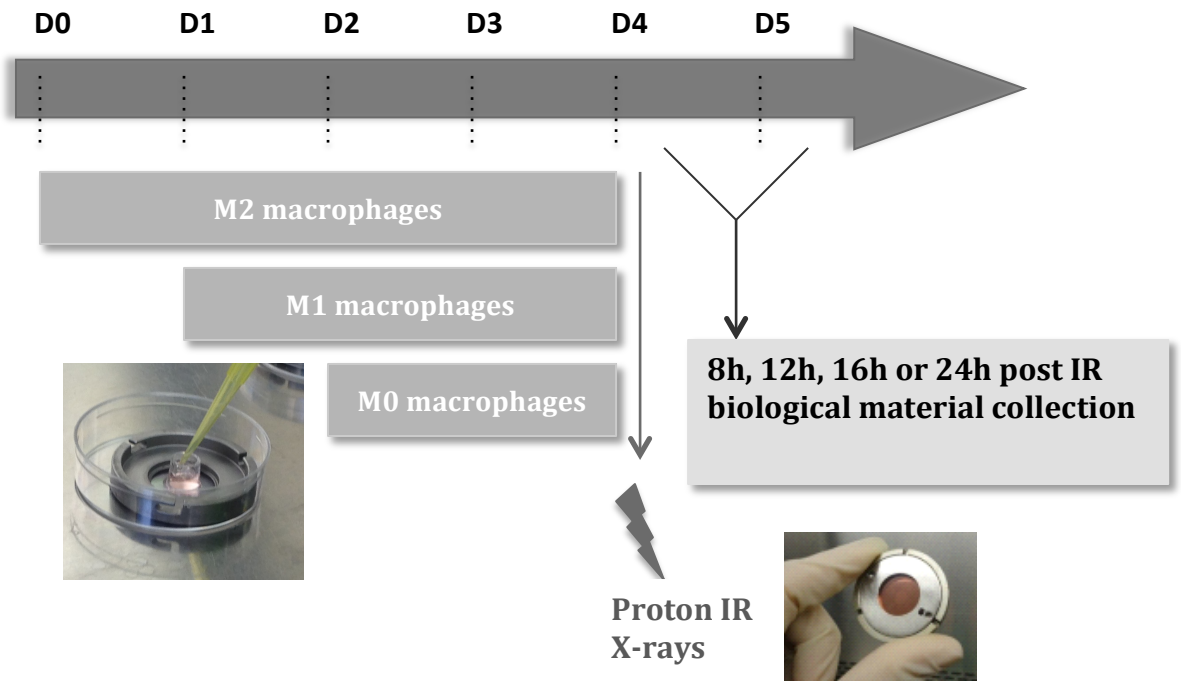

Figure 1. Schematic outline of the irradiation procedure for macrophages.
THP-1 monocytes were differentiated into macrophages (M0) with 150 nM PMA in cloning cylinder, placed at the center of the irradiation chamber. Macrophages were polarized in M1 phenotype with 10 pg/ml LPS and 20 ng/ml IFN-γ during 24h incubation or were polarized in M2 phenotype with 20 ng/ml IL-4 and IL-13 during 48h incubation. THP-1 monocytes were differentiated on the appropriate day, in order to obtain the three phenotypes on day 4. Following the experiment that was performed, the biological material was collected 8h, 12h, 16h or 24h after proton irradiation.

(14)). In addition, the combination of $CD8^+$ T cell transfer and γ-ray used at moderate doses (2 Gy) re-educated TAMs towards a M1 phenotype in a pancreatic tumor mice model (10). Other studies also reported TAM reprogramming after low dose of whole body irradiation (15, 16). However, no study has established the reprogramming of M2 into M1 macrophages with local conventional RT only. This suggests that RT alone is not sufficient to reverse macrophage polarization.

Last decades, efforts aimed to improve the delivery of conventional RT using image guidance. Despite these improvements, side effects associated to this treatment have remained severe. To spare surrounding healthy tissues, protontherapy presents an increasing interest thanks to the charged nature of the particles and its depth dose profile. In more details, the one-shot energy release at the end of the charged particle track allows the improvement of dose conformation. This is added to the fact that the track of charged particles can be easily deviated by a magnetic field to precisely target the tumor. As for X-ray irradiation, the deposited energy by charged particle beam promotes the ionization of DNA through ROS production. In addition to these indirect DNA damage, charged particles also directly interact with DNA, resulting in more complex DNA damage (17). Our work demonstrated the ability of protontherapy to induce macrophage reprogramming. By using THP-1-derived M0, M1 and M2 macrophages, we evidenced that proton irradiation, but not X-ray irradiation, induced a partial switch from M2 to M1 macrophages. This macrophage reprogramming is orchestrated, at least in part, by a NFκB activation.

Results

To address these goals, THP-1 cells were differentiated (M0) and polarized (M1 or M2) in irradiation chambers (**Fig. 1**). These special devices were placed at the end of the accelerator-produced proton beam and the effects on macrophages were then analyzed.

M1 macrophages are more resistant to moderate doses of proton irradiation than M0 and M2 macrophages

In order to evaluate the cell viability after proton irradiation, ethidium bromide - acridine orange staining was performed (**Fig. 2A**) and the number of dead cells (orange) and viable cells (green) was counted (**Fig. 2B**). The cell viability slightly decreased 8h (**Fig 2B**) after moderate proton irradiation doses (0 – 10 Gy), as indicated by a survival of 82% for M0 macrophages, 82% for M1 macrophages and 78% for M2 macrophages when irradiated with a dose of 10 Gy. Proton irradiation at 10 Gy further lowered the viability of M0 and M2 macrophages respectively to 42% and 50% after 16h (**Fig. 2B**). Surprisingly, the viability of M1 macrophages was only slightly affected (92%) 16h after proton irradiation at doses as high as 10 Gy. These results suggest an early radioresistance of the M1 phenotype to moderate proton irradiation doses compared to the two other phenotypes.

M1 radioresistance correlates with more intense γH_2AX and 53BP1 labeling

In order to further examine the influence of proton irradiation on macrophages, phosphorylated H_2AX (Ser 139) (γH_2AX), a sensitive marker for DNA double-strand breaks (DSBs), was evaluated by immunofluorescence labeling (**Fig. 3A**). Quantifications of γH_2AX

A

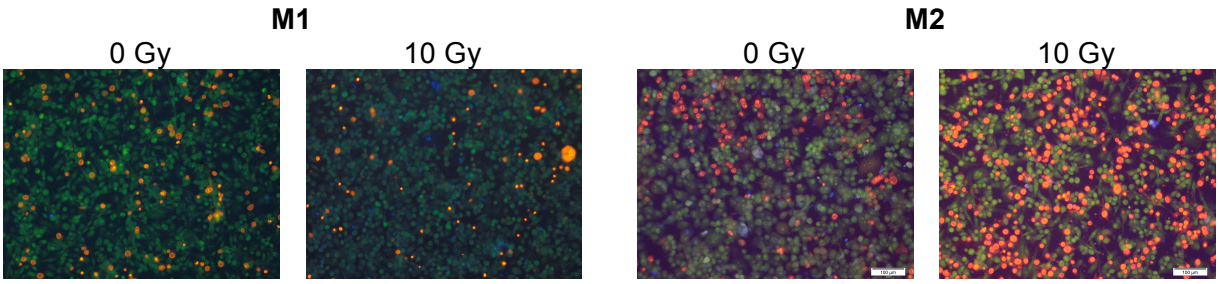

B

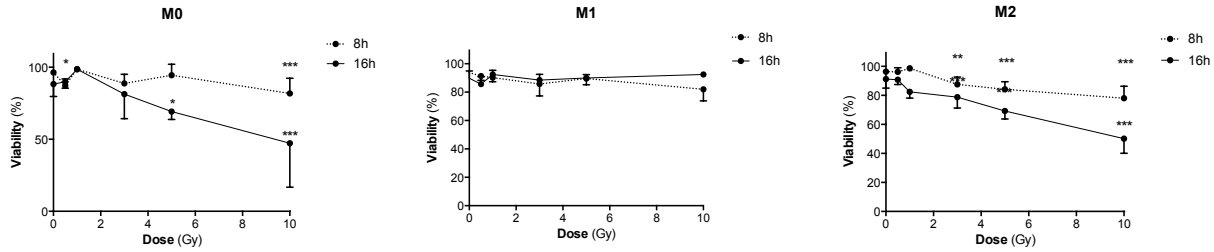

Figure 2. Early radioresistance of M1 macrophages after moderate doses of proton irradiation

M0, M1 and M2 macrophages were irradiated with different doses of protons. **A**, Viability was assessed by ethidium bromide - acridine orange at different times post-irradiation. **A,** Representative ethidium bromide - acridine orange staining images of M1 and M2 macrophages 16h after proton irradiation (0 Gy and 10 Gy). Lived cells appeared in green while dead cells are stained in orange. **B,** Quantification of viability (%) in M0, M1 and M2 macrophages, 8h or 16h after proton irradiation. N=3 for each dose (mean ± SD). One-way ANOVA analyses followed by Dunnett's multiple comparisons post-tests were performed on data; * $p \leq 0.05$; ** $p < 0.01$; *** $p < 0.001$.

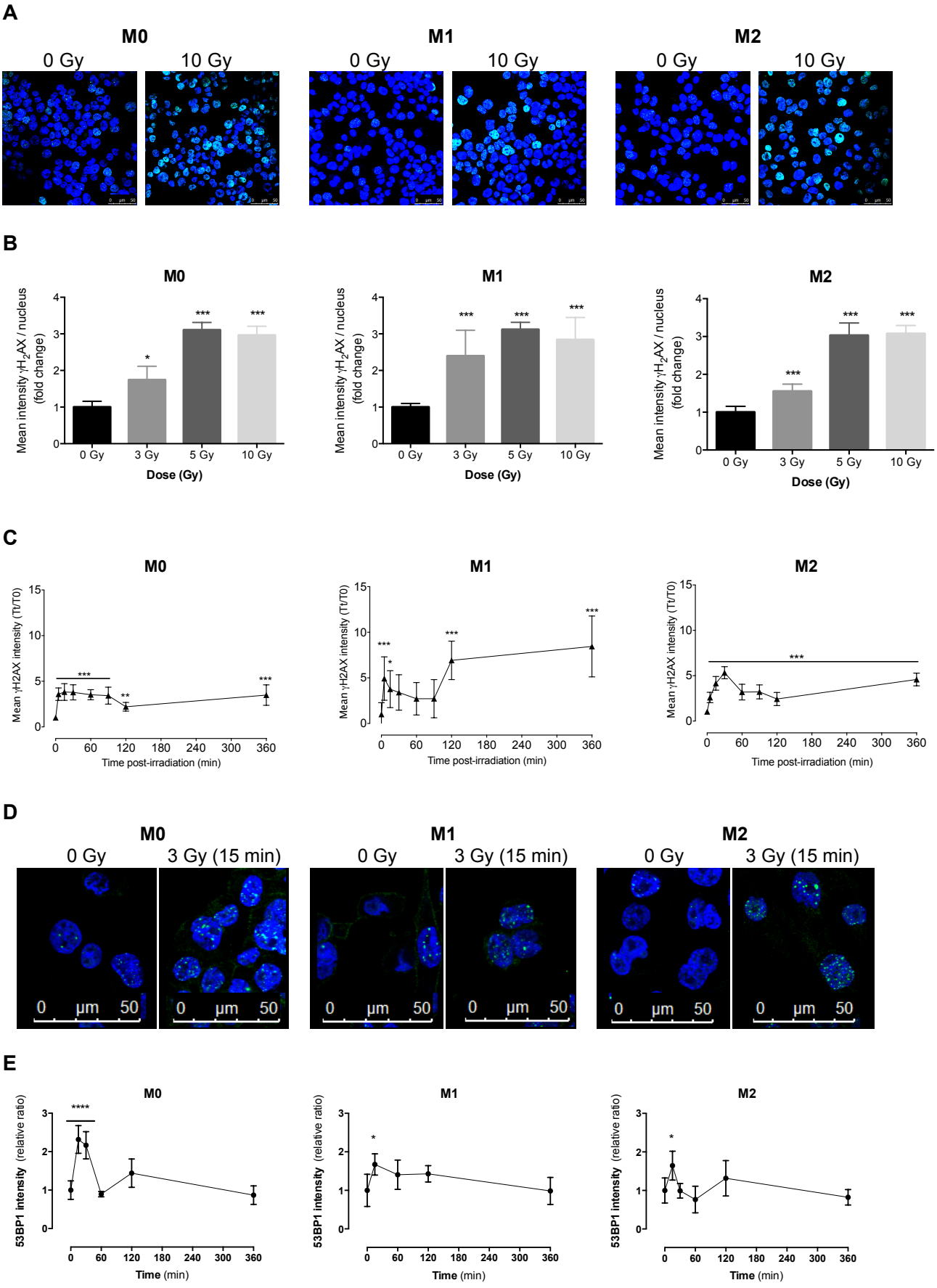
A
M0
M1
M2
0 Gy
10 Gy
B
M0
M1
M2
Mean intensity γH2AX / nucleus (fold change)
0 Gy
3 Gy
5 Gy
10 Gy
Dose (Gy)
C
M0
M1
M2
Mean γH2AX intensity (Tt/T0)
Time post-irradiation (min)
D
M0
M1
M2
0 Gy
3 Gy (15 min)
0 µm 50
E
M0
M1
M2
53BP1 intensity (relative ratio)
Time (min)

Figure 3. M1 resistance to proton irradiation correlates with a higher γH_2AX and 53BP1 labeling

M0, M1 and M2 macrophages were irradiated with different doses of protons. The evaluation of DNA damage following proton irradiation was performed by phosphorylated H_2AX (γH_2AX) or 53BP1 labeling **A,** Representative immunofluorescence labeling of γH_2AX for M0, M1 and M2 macrophages 15 minutes after proton irradiation. γH_2AX labeling appears in green and nuclei are stained in blue (To-pro) **B**, Quantification of the mean γH_2AX intensity per nucleus 15 minutes after proton irradiation. Results are expressed in mean pixel intensity value and are normalized to the non-irradiated condition (fold change). Quantifications were performed on minimum 5 images per condition; representative experiment (N=3, mean ± SD). **C,** Mean γH_2AX intensity after proton irradiation (3 Gy), several times post-irradiation. Each point corresponds to the mean γH_2AX intensity at time t (Tt) normalized to time 0 (T0). Quantifications were performed on minimum 10 images per condition; representative experiment, N=3 (mean ± SD). One-way ANOVA analyses were performed on data, followed by Dunnett's post-tests; * $p \leq 0.05$; ** $p < 0.01$; *** $p < 0.001$. **D**, Representative immunofluorescence labeling of 53BP1 for M0, M1 and M2 macrophages 15 minutes after proton irradiation. 53BP1 labeling appears in green and nuclei are stained in blue (To-pro). **E**, Quantification of the 53BP1 intensity per nucleus after proton irradiation (3 Gy), several time post-irradiation. Each point corresponds to the mean numbers of 53BP1 intensity at time t (Tt), normalized to time 0 (T0). Quantifications were performed on 5 images per condition; N=1 (mean ± SD). On-way ANOVA analyses were performed on data, followed by Dunnett's post-tests; * $p \leq 0.05$; ** $p < 0.01$; *** $p < 0.001$.

labeling (**Fig. 3B**) 15 minutes after irradiation indicated a similar profile for the three macrophage phenotypes when irradiated at different doses (3, 5 and 10 Gy). However, the quantifications of γH_2AX labeling (**Fig. 3C**) over the time post irradiation (0 – 360 min) indicated a similar profile for M0 and M2 macrophages while M1 phenotype exhibited a higher level of phosphorylated H_2AX. In more details, γH_2AX labeling increased 5 minutes after proton irradiation (3 Gy) in M0 and M2 phenotypes and was mostly decreased 2h after irradiation. In contrast, the γH_2AX labeling was increased and plateaued as long as 6h after irradiation in M1 macrophages, indicating an increasing and prolonged detection of DSBs in this phenotype. In order to confirm these data, 53BP1 intensity were also assessed by immunofluorescence labeling (**Fig. 2D**). 53BP1 is known for its role in DNA repair machinery. Similarly to γH_2AX labeling, the quantification of 53BP1 intensity revealed a sustained labeling over the time in M1 macrophages, while 53BP1 intensity was decreased 1h after proton irradiation in M0 and M2 macrophages. As chromatin conformation could influence the detection and the repair of DSBs, we evaluated the heterochromatin content by MNAse I assay in the three different phenotypes. The radioresistance of M1 macrophages was not linked to a higher level of DNA condensation before irradiation since there was no difference in the heterochromatin content in the three phenotypes (**Fig. S1**). In addition to a differential γH2AX labeling, the analysis of ROS content by flow cytometry revealed that M1 macrophages better managed H_2O_2 treatment (**Fig. S2**). Taken together, these results indicated that the radioresistance of M1 macrophages to proton irradiation could be related to higher DSB detection and/or to better efficiency of DNA repair machinery in this phenotype, and also correlates with a better elimination of ROS.

Proton irradiation induces macrophage reprogramming

Proton irradiation of M0, M1 and M2 macrophages with moderate doses promotes the reprogramming of M0 and M2 macrophages towards a M1 phenotype (**Fig. 4**). mRNA levels of several M1 markers (IL-6 and IL-8) increased significantly in M0 macrophages (**Fig. 4A**, *left panel*) exposed to 10 Gy. At the same time, we observed a significant reduction of the mRNA expression of EGF, a specific marker of M2 population. Consistent with these results, the secretion of TNFα was also significantly higher (**Fig. 4B**, *left panel*) in this macrophage phenotype after 5 Gy of proton irradiation. Taken together, these results indicated a polarization of M0 macrophages towards a M1 phenotype after moderate doses of proton irradiation. The irradiation of M1 macrophages (**Fig. 4A**, *middle panel*) did not exhibit any change in mRNA expression for M1 (TNFα, IL-6 and IL-8) and M2 (CCL22, IL-10 and EGF) markers. The secretion of IL-6 and TNFα was then quantified after moderate doses of irradiation (**Fig. 4B**, *middle panel*). The results revealed a strengthening of the M1 phenotype in M1 macrophages. The proton irradiation of M2 macrophages (**Fig 4A**, *right panel*) led to a significant decrease in EGF mRNA expression at 5 and 10 Gy while the expression of other M2 markers remained unchanged. The mRNA level of M1 markers was not affected by proton irradiation. However, the irradiation of M2 macrophages generated a significant increase in TNFα secretion (**Fig. 4B**, *right panel*). As a whole, proton irradiation (5 and 10 Gy) initiated the polarization of M2 macrophages towards the M1 phenotype, thus generating an intermediate phenotype. Similarly to other studies, X-ray irradiation did not succeed to induce a reprogramming of M2 macrophages towards a M1 phenotype in our model (**Fig. S3**). The mRNA expression of M1 and M2 markers was not affected by X-ray irradiation in M0 and M2 macrophages, while the mRNA level of EGF was reduced in irradiated M1

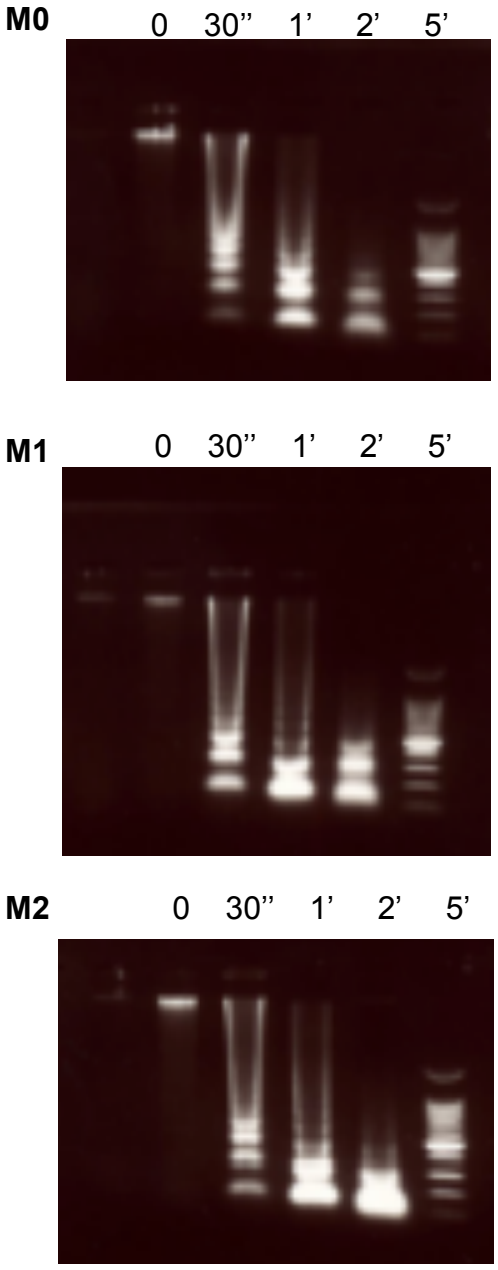

Figure S1. Heterochromatin content in M0, M1 and M2 macrophages
Heterochromatin content was evaluated by MNAse assay. DNA was extracted from M0, M1 and M2 macrophages and then exposed to MNAse enzyme for 30 seconds, 1, 2 or 5 minutes. Resulting fragments were separated by electrophoresis. Representative images show the migration profile of fragmented DNA in M0, M1 and M2 macrophages after MNAse treatment (N=5).

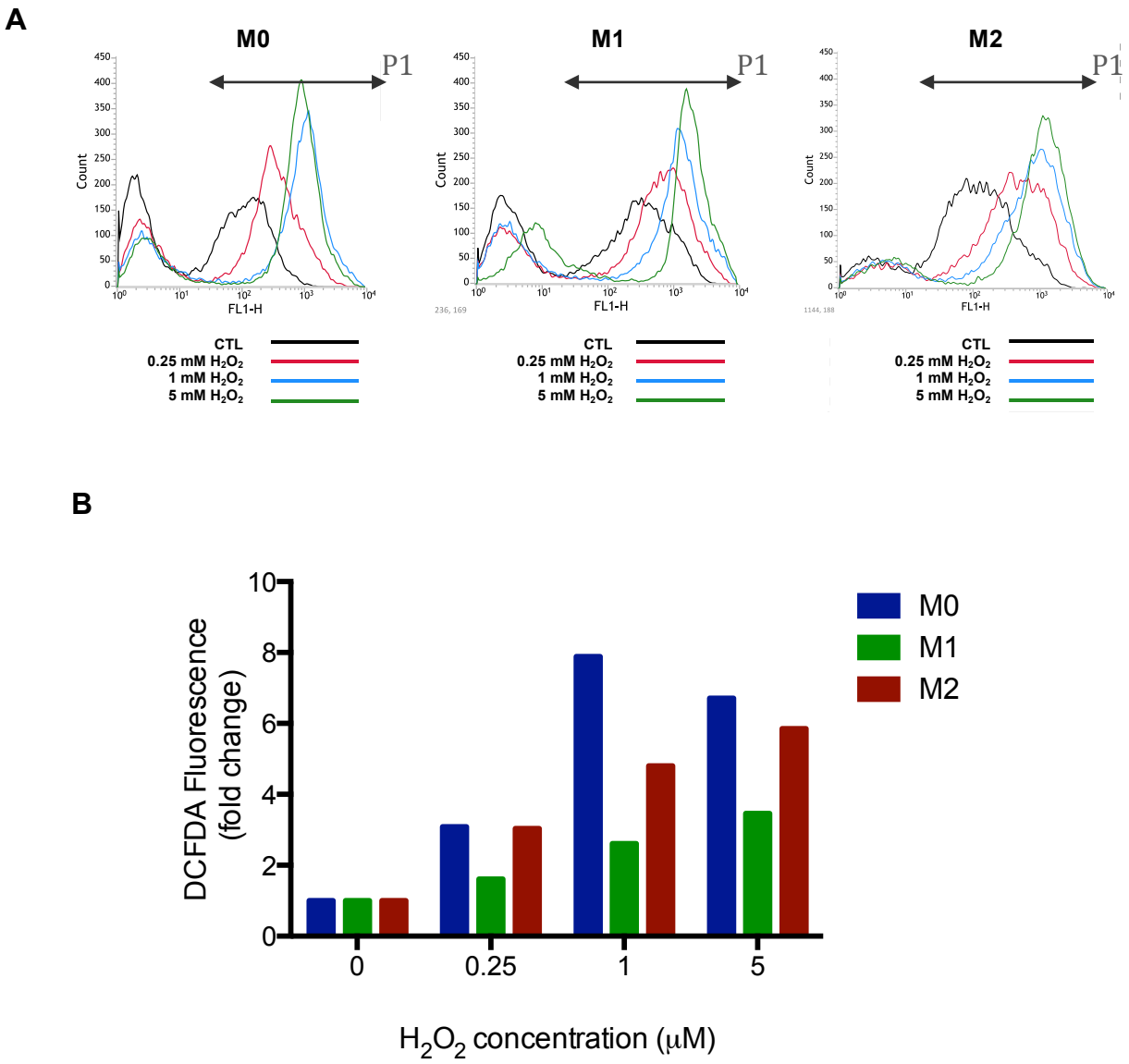

Figure S2. Differential ROS management in M0, M1 and M2 macrophages
M0, M1 and M2 macrophages were treated with different H_2O_2 concentrations (0, 0.25, 1 and 5 μM) and ROS content was detected by flow cytometry (DCFDA fluorescence). **A**, Evaluation of ROS content in M0, M1 and M2 macrophages after exposure to different H_2O_2 concentrations. **B**, Quantification of the mean fluorescence (ROS level) in macrophages in gated population (P1). Results are normalized to the untreated condition (N=1).

A

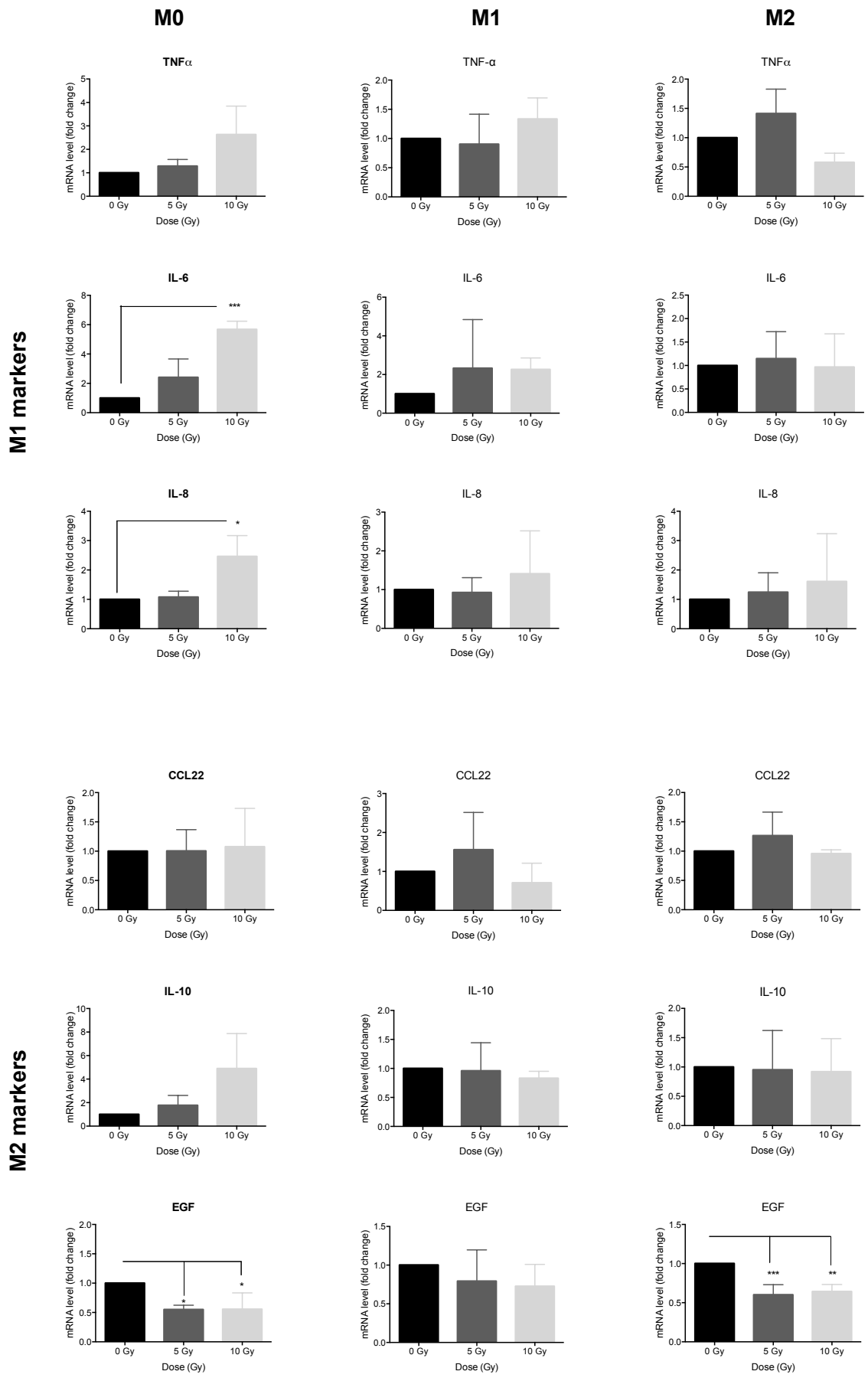
M0
M1
M2
M1 markers
M2 markers
TNFα
TNF-α
TNFα
IL-6
IL-6
IL-6
IL-8
IL-8
IL-8
CCL22
CCL22
CCL22
IL-10
IL-10
IL-10
EGF
EGF
EGF
mRNA level (fold change)
0 Gy
5 Gy
10 Gy
Dose (Gy)
*
**
***

B

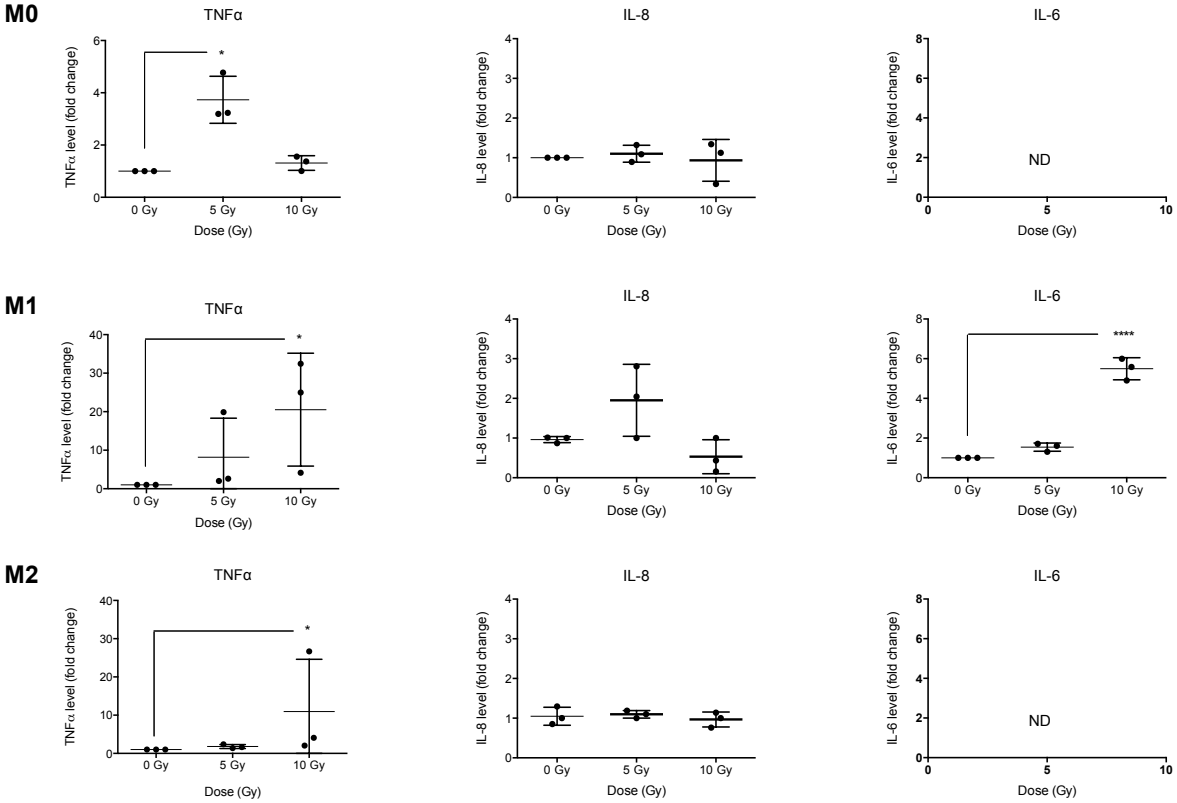

Figure 4. Proton irradiation induces macrophage reprogramming

M0, M1 and M2 macrophages were irradiated with different doses of protons **A,** 24h after proton irradiation, mRNA levels of M1 (TNFα, IL-6, IL-8) and M2 (CCL22, IL-10, EGF) markers were assessed by RTqPCR (N=3, mean ± SD). One-way ANOVA analyses followed by Dunnett's multiple comparison tests were performed to evaluate the significance (* $p \leq 0.05$; ** $p < 0.01$; *** $p < 0.001$). **B,** 24h after proton irradiation, TNFα, IL-8 and IL-6 secretion was evaluated by ELISA. Results are expressed in pg/ng of proteins and are normalized to the non-irradiated condition (fold change) for each macrophage phenotype; ND was used for not detected (N=3, mean ± SD). One-way ANOVA analyses followed by Kruskal Wallis multiple comparison tests were performed on data (* $p \leq 0.05$; ** $p < 0.01$; *** $p < 0.001$).

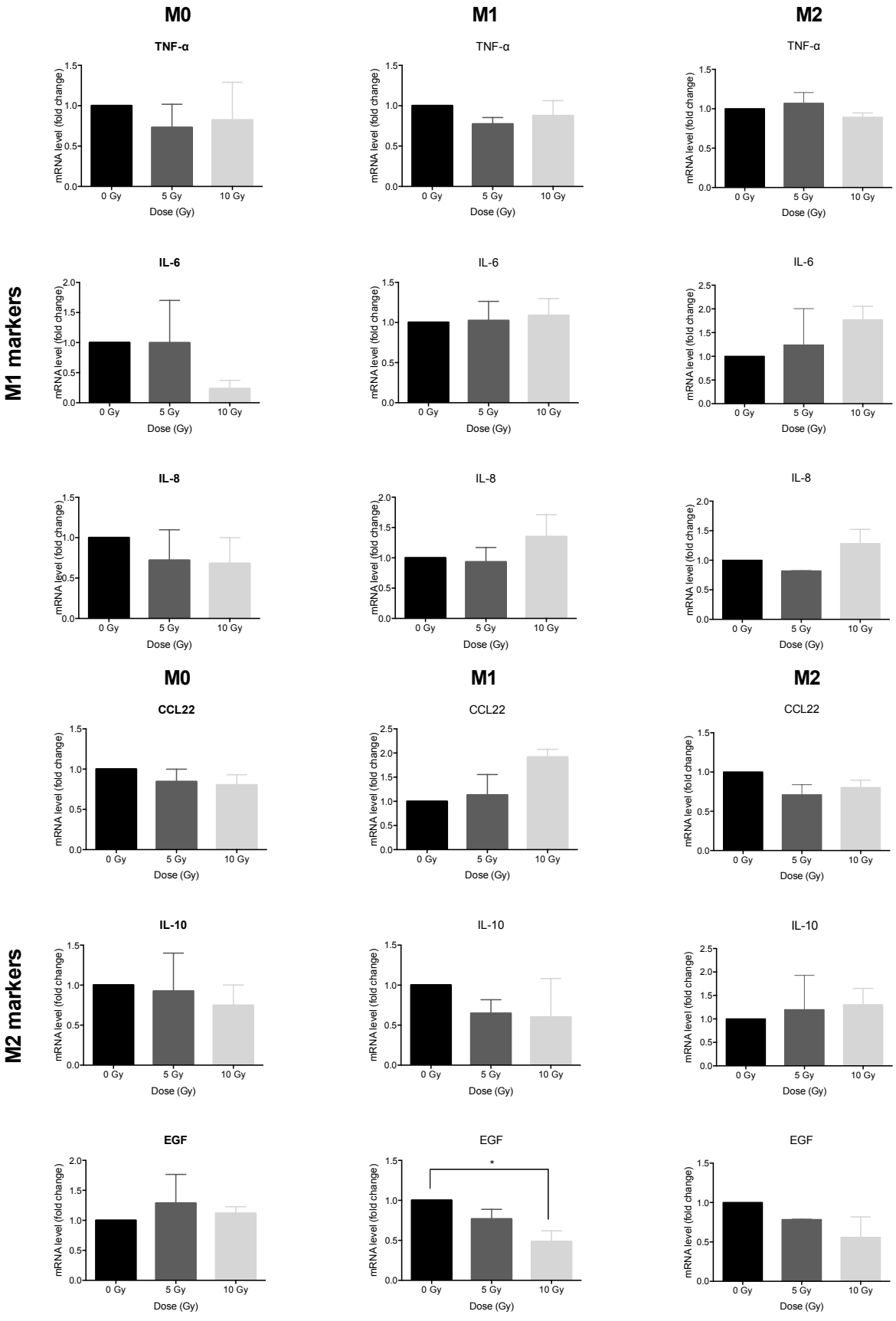
M0
M1
M2
M1 markers
M2 markers
TNF-α
IL-6
IL-8
CCL22
IL-10
EGF
mRNA level (fold change)
0 Gy
5 Gy
10 Gy
Dose (Gy)
*

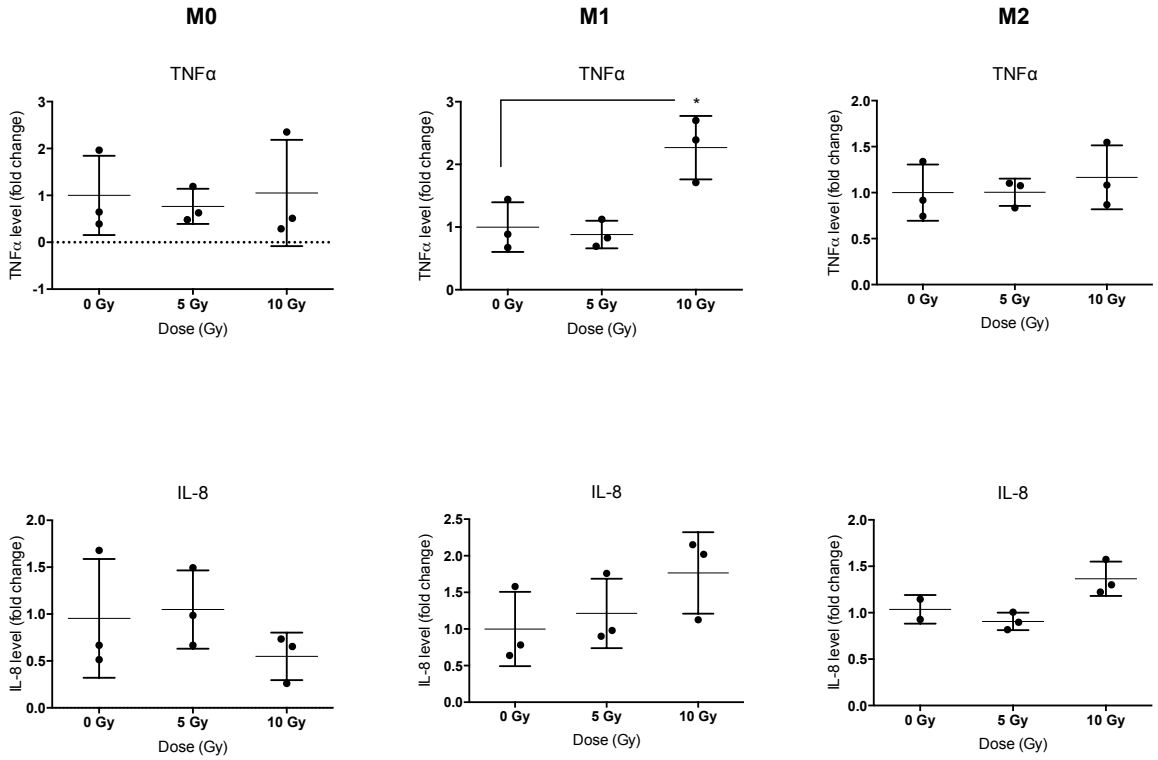

Figure S3. **X-ray irradiation does not induce macrophage reprogramming**
M0, M1 and M2 macrophages were irradiated with different doses of X-rays (0, 5 and 10 Gy) **A,** 24h after X-ray irradiation, mRNA levels of M1 (TNFα, IL-6, IL-8) and M2 (CCL22, IL-10, EGF) markers were assessed by RT-qPCR (N=3, mean ± SD). One-way ANOVA analyses followed by Dunnett's multiple comparison tests were performed to evaluate the significance (* $p \leq 0.05$; ** $p < 0.01$; *** $p < 0.001$). **B,** 24h after X-ray irradiation, TNFα and IL-8 secretion was evaluated by ELISA. Results are expressed in pg/ng of proteins and are normalized to the non-irradiated condition (fold change) for each macrophage phenotype (N=3, mean ± SD). One-way ANOVA analyses followed by Kruskal Wallis multiple comparison tests were performed on data (* $p \leq 0.05$; ** $p < 0.01$; *** $p < 0.001$).

A

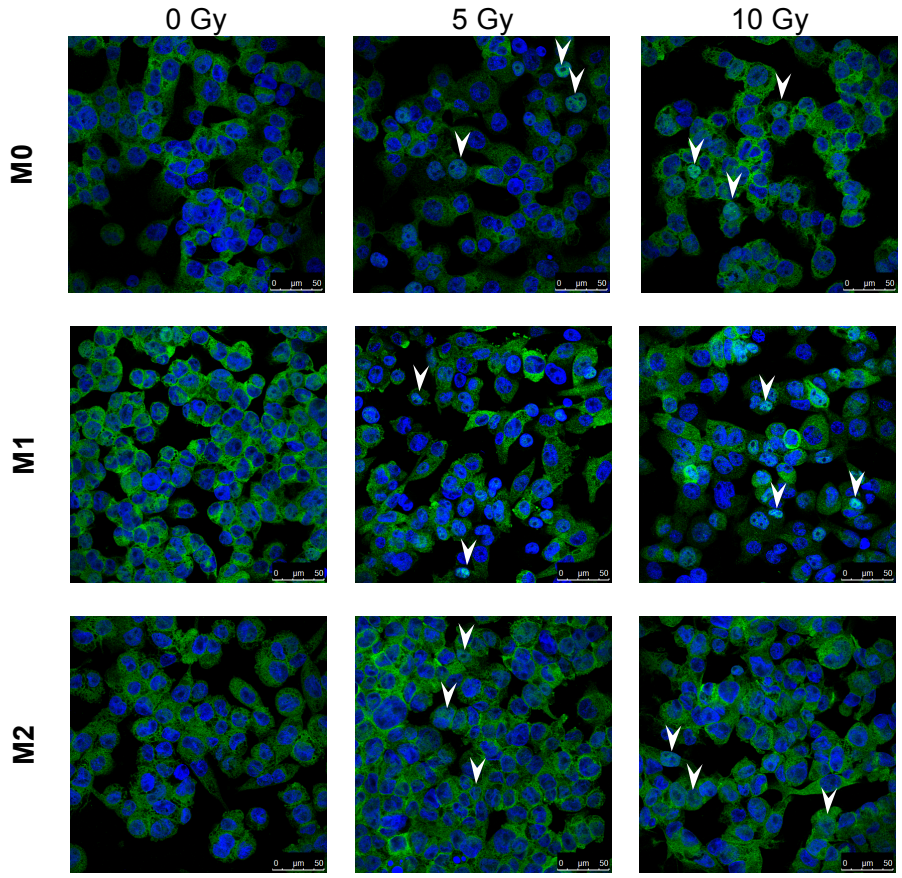

B

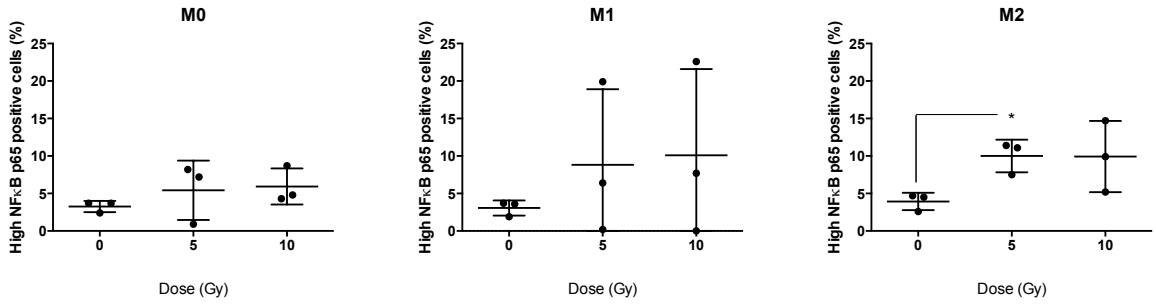

Figure 5. Proton irradiation induces nuclear translocation of p65 (NFκB)
M0, M1 and M2 macrophages were irradiated by different doses of protons. 2h after the irradiation, the nuclear translocation of p65 was evaluated by NFκB p65 immunofluorescence labeling. NFκB p65 is stained in green and nucleus appears in blue. **A**, Nuclear translocation of NFκB p65 is indicated (arrow) on representative immunofluorescence labeling images for M0 macrophages, M1 macrophages and M2 macrophages after irradiation. **B**, Quantification of the mean NFκB p65 intensity per nucleus 2h after proton irradiation. Results are expressed in percentage of high NFκB p65 positive cells. Quantifications were performed on minimum 5 images per condition (N=3, mean ± SD). An unpaired t-test was performed on data (* $p \leq 0.05$; ** $p < 0.01$; *** $p < 0.001$).

macrophages. In addition, the secretion of TNFα was elevated in irradiated M1 macrophages, consistent with a strengthening of the M1 phenotype in M1 macrophages.

Proton irradiation orchestrates NFκB p65 nuclear translocation in macrophages

To investigate the mechanism underlying macrophage reprogramming after moderate doses of proton irradiation, the nuclear translocation of NFκB p65 subunit was evaluated after the irradiation. This translocation was analyzed in M0, M1 and M2 macrophages at different times post-irradiation (0, 5, 15, 30, 60, 90, 120 and 360 minutes) (data not shown) and was observed in the three phenotypes 2h after the irradiation (**Fig 5A**). The quantification of highly positive cells for NFκB p65 suggested a nuclear translocation of NFκB p65 in M0, M1 and M2 macrophages after proton irradiation (5 and 10 Gy) (**Fig. 5B**).

NFκB inhibition reverts macrophage reprogramming induced by proton irradiation

To study the role of NFκB in proton beam mediated – macrophage reprogramming, we assessed the mRNA level of M1 and M2 markers in M0 and M2 macrophages 12h after Bay 11-7082 (IKK inhibitor) treatment combined with proton irradiation (**Fig. 6**). Based on preliminary results, we chose to treat macrophages during 12h with 5 µM of Bay 11-7082 inhibitor. Indeed, for longer incubation time and for higher concentrations, we observed a cell death higher than 20% (data not shown). In accordance with the results from **Fig 4A**, the proton irradiation (10 Gy) of M0 macrophages displayed a non-significant increase in M1 marker mRNA levels (TNFα, IL-6 and IL-8) 12h after irradiation while the mRNA expression of M2 markers were not influenced by the irradiation (**Fig. 6A**). The combination of the IKK inhibitor with the proton irradiation completely inhibited the programming of M0 into M1 phenotype and induced a non-significant increase in M2 marker expression (CCL22, IL-10 and EGF). Although Bay 11-8072 treatment alone drove the expression of IL-10 and EGF, the combination of the inhibitor with proton irradiation induced a much higher expression of these genes. The same experiment has been performed for M2 macrophages (**Fig. 6B**). As it was aforementioned, the irradiation of M2 macrophages had no effect on the M1 marker mRNA levels after 24h (**Fig. 4A**) and we detected no change in the TNFα and IL-8 mRNA expression after 12h (**Fig. 6B**). However, a decrease in IL-6 expression was noticed in the same condition. When proton irradiation was combined to NFκB inhibition, diverse effects were observed on the expression of M1 markers. No effect was observed on TNFα expression, while the expression of IL-8 surprisingly increased when proton irradiation was combined to Bay 11-7082 treatment. As the activation of NFκB regulates the expression of IL-8, it is surprising to observe an elevation of the IL-8 mRNA level in M2 macrophages irradiated in the presence of Bay 11-7082. However, the transcription of IL-8 is also regulated by other transcription factors, such as the activator protein 1 (AP-1), that could be also activated when NFκB is inhibited in proton-irradiated M2 macrophages (18). On the other hand, IL-6 expression was strongly decreased by the IKK inhibitor: its expression decreased by four times with Bay 11-7082 alone and by five times with the combination. For M2 markers, proton irradiation alone did not alter the expression of these markers after 24h (**Fig 4A**). In the same line, 10 Gy of irradiation did not change the expression of M2 markers after 12h (**Fig. 6B**). However, the combination of NFκB inhibitor to proton irradiation induced a

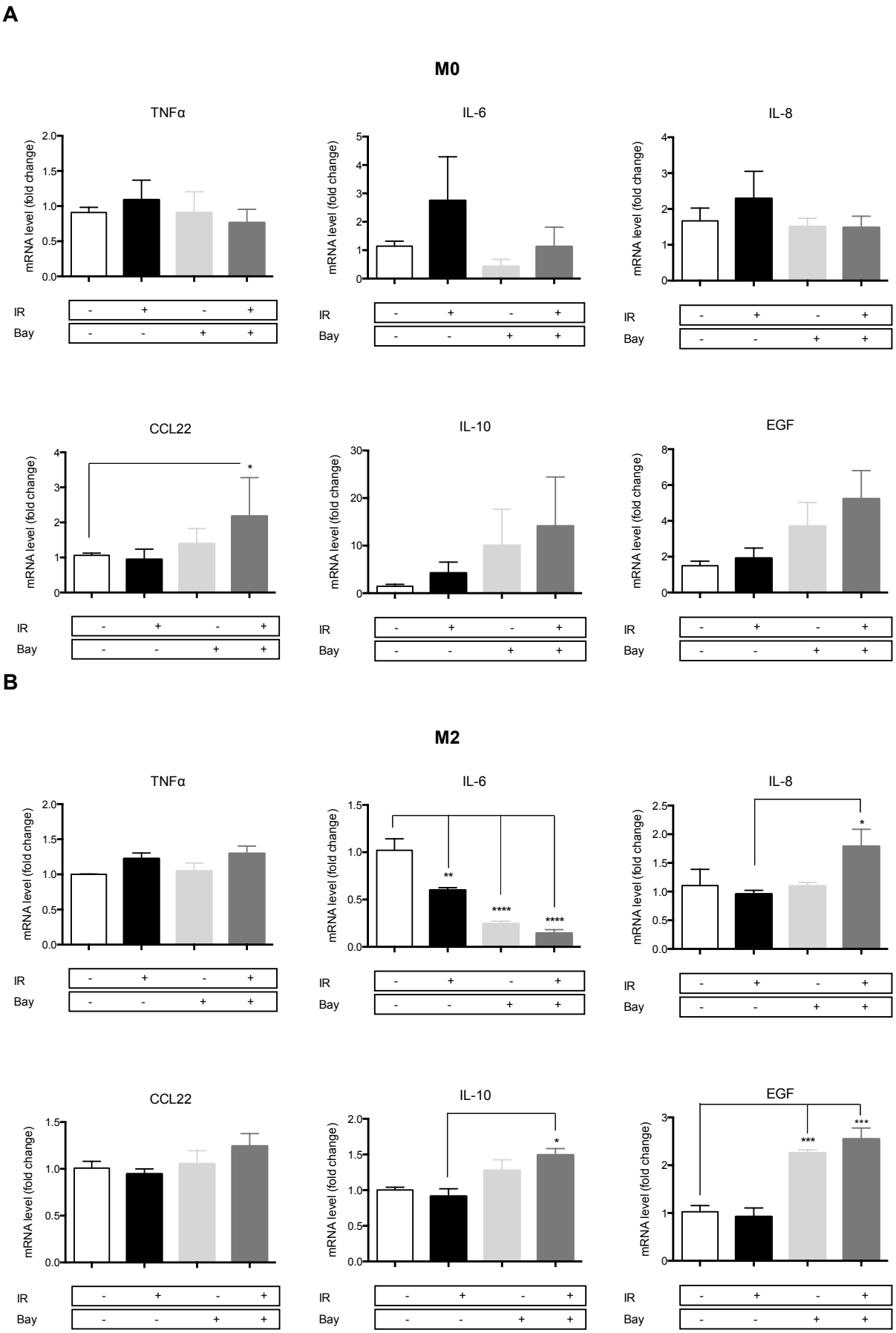
A
M0
TNFα
IL-6
IL-8
CCL22
IL-10
EGF
mRNA level (fold change)
IR
Bay
B
M2
TNFα
IL-6
IL-8
CCL22
IL-10
EGF
mRNA level (fold change)
IR
Bay

Figure 6. NFκB inhibition reverts proton irradiation-induced macrophage reprogramming

M0 and M2 macrophages were irradiated (IR) using protons (10 Gy) with or without NFκB inhibitor (Bay 11-7082 – 5μM). The inhibitor was added 1h before irradiation for the following 12h. Macrophage polarization was evaluated by RTqPCR 12h after proton irradiation by the analysis of M1 (TNFα, IL-6, IL-8) and M2 (CCL22, IL-10, EGF) marker mRNA level in **A**, M0 macrophages (N=3, mean ± SD) and **B**, M2 macrophages (N=4, mean ± SD). Two-way ANOVA analyses followed by Tukey's multiple comparison tests were performed on data; * $p \leq 0.05$; ** $p < 0.01$; *** $p < 0.001$.

higher expression of M2 markers. The elevation of M2 marker expression was higher in M2 macrophages exposed to the combined treatment than for macrophages treated with the inhibitor alone. In conclusion, the NFκB inhibitor combined to proton irradiation completely prevented the programming of M0 macrophages towards a M1 phenotype. On the contrary, it promoted the programming of M0 macrophages towards a M2 phenotype. In addition, M2 macrophages reinforce their M2 phenotype when exposed to proton irradiation in combination with Bay 11-7082.

Discussion

As M2-like TAMs play an important role in tumor promotion and treatment failure, the reprogramming of these cells has been shown to be an efficient way to promote tumor regression. It is already known that macrophages are more radioresistant compared to other cell types (19). Indeed, the fusion of macrophages with breast cancer cell line (MCF7) resulted in hybrids developing the abilities to resist high radiation doses and to repair DNA damage faster than the parental MCF7 cells (20). In the present study, we demonstrated the radioresistance of M1 macrophages compared to M0 and M2 phenotypes. Several evidences highlighted the radioresistance of M1 macrophages in the literature. For example, BALB/c mice naturally exhibiting a T_H1/M1 (T_H1 lymphocytes and M1 macrophages) response were more radioresistant than C57BL/6 mice naturally exhibiting a T_H2/M2 response (16). TNFα play key roles in macrophage radioresistance since an intact TNFα signaling is needed for radioresistance. Indeed, the deletion of tumor necrosis factor receptor 1 or 2 (TFNR1 or TNFR2) in mice rendered macrophages radiosensitive (21). In contrast to our observations, a recent *in vitro* study indicated that unpolarized (M0) and M1 macrophages were more sensitive to X-ray irradiation than M2 macrophages. The divergent results could be explained by the use of higher LPS concentration (100 ng/ml instead of 10 pg/ml in the present study) for the polarization process before the irradiation (22).

The resistance of M1 macrophages to proton irradiation correlated with a higher level of phosphorylated H_2AX, possibly indicating either more DSBs, or a higher activity of DNA damage repair. Another explanation could rely on the ability of macrophages to detoxify irradiation-induced radicals formed upon H_2O radiolysis. It is well established that the radioresistance of macrophages is conferred by a high production of anti-oxidative molecules, such as manganese superoxide dismutase (MnSOD). Higher MnSOD expression is associated to a resistance against damaging effects from ROS and reactive nitrogen species (RNS) (23). Indeed, the scavenging of ROS by N-acetyl-l-tryptophan glucopyranoside (NATG) in J774A.1 macrophages provided a protection against radiation-dependent apoptosis (24). Furthermore, another *in vitro* study revealed that mouse peritoneal macrophages polarized towards the M1 phenotype with methionine displayed increased SOD activity and decreased ROS production (25). In our experiments, the analysis of reactive oxygen species (ROS) management revealed a more efficient elimination of ROS in M1 macrophages when challenged with H_2O_2 compared to M0 and M2 macrophages (**Fig. S2**). In conclusion, the radioresistance of M1 macrophages to proton irradiation is related to a higher DNA damage detection. Several causes like a larger antioxidant pool, a more active DNA repair machinery and the differential promoter methylation of genes involved in DNA repair should be taken in considerations for future studies.

Macrophage re-education represents a promising approach to reverse the fate of tumor and generates tumor regression. To our knowledge, this is the first observation of *in vitro* macrophage reprogramming with particle therapy. Previous studies with conventional radiotherapy (X-rays or γ-rays) revealed an efficient programming of unpolarized macrophages (M0) towards the M1 phenotype but not M2 reprogramming towards M1-like phenotype (for a review, see (14)). For example, the irradiation of monocyte-derived macrophages with fractionated doses (2Gy 5x/week) induced the polarization towards M1-like macrophages as evidenced by a higher expression of pro-inflammatory genes and a downregulation of anti-inflammatory genes (26). Another study also revealed the programming of unpolarized macrophages towards a pro-inflammatory profile after moderate dose of γ-irradiation (2 or 4 Gy) (27). In the last study, the authors also reported an increased expression of IL-6, IL-8 and TNFα in γ-irradiated (4 Gy) human monocyte-derived macrophages. While the use of X-ray irradiation induced a M1 polarization of unpolarized human monocyte-derived macrophages, Raw 264.7 cells, PMA-differentiated THP-1 cells and peritoneal macrophages *(14),* our results indicated that X-ray irradiation failed to program PMA-differentiated THP-1 macrophages in our experimental settings. In our experiments, a resting time period of 24h allowed a decrease in NFκB gene cluster expression, upregulated during PMA induced – differentiation (28). This may explain the discrepancy with previously reported results The release of TNFα by M0, M1 and M2 macrophages after proton irradiation confirms the reprogramming of macrophages to a M1-like phenotype. Indeed, TNFα is a potent anti-M2 polarization factor and strongly correlates with a M1-like phenotype (29). Inversely, a decrease mRNA expression of EGF was shown for the three phenotypes upon irradiation. EGF is well known to be involved in both angiogenesis and cell migration, two roles fulfilled by M2 macrophages (30)**.**

Our results demonstrated the implication of NFκB p65 subunit in macrophage reprogramming after moderate doses of proton irradiation. In addition, the combination of proton irradiation to an IKK complex inhibitor (Bay 11-7082) completely aborted the re-education towards a M1 phenotype in M0 and M2 macrophages. In general, NFκB is activated in irradiated cancer cells when doses are comprised in the range of 7-10 Gy (31-33). The active heterodimer NFκB p50 – p65 is predominant for M1 activation, leading to a pro-inflammatory profile while the induction of the inactive homodimer NFκB p50 – p50 inhibits the expression of pro-inflammatory genes in M2 macrophages (12, 13)**.** In a previous study, the X-ray irradiation of monocyte-derived macrophages also induced the upregulation of total and phosphorylated p65, from 1h to 6h after irradiation at 2 Gy and 10 Gy. This was correlated to the reduced expression of anti-inflammatory genes (26). Furthermore, the whole-body irradiation of RT5 insulinoma bearing mice increased NFκB p65 phosphorylation in tumors, partially explaining the TAM reprogramming after γ-irradiation (15). Proton irradiation is also more likely to induce more severe DNA damage and higher ROS production compared to photons (34). These damages activate the DNA repair system, including ATM (ataxia-telangiectasia mutated) kinase, notably responsible for the translocation of NFκB p65 into the nucleus (35). Hence, ROS production and double DNA strand breaks are strongly linked to NFκB p65 activation (14, 36). In addition, other studies have demonstrated the activation of NFκB p65 in cancer cells after high LET charged particle irradiation. Indeed, heavy ions with a LET of 100 – 300keV/μm showed an up to nine times higher potential to activate the NFκB pathway compared to X-rays (37) while carbon ions

with a LET under 73 keV/μm induced a NFκB p65 activation twice as high as the one induced by conventional radiotherapy (38). For future studies, the use of high LET radiation should be considered, as it can potentiate the activation of NFκB in macrophages and induce apoptosis in cancer cells. However, further investigations are needed to clarify if charged particle therapy may be used for all cancer types. Indeed, constitutive activation of NFκB is associated to tumor growth for several human cancer cells such as breast cancer, colon cancer, prostate cancer and lymphoid cancer. In cancer cells, NFκB plays key roles in cell survival, notably by regulating the expression of genes involved in cell survival and cell cycle (38). For conventional radiotherapy, the use of NFκB inhibitors increased the radiosensitivity of many cancer cells (39). However, no study has been performed yet to assess the balance between NFκB-mediated survival and apoptosis in high LET radiation context. Also, the activation of the immune system by particle therapy could overcome the activation of NFκB in cancer cells. These questions reveal a need for further investigations regarding the use of charged particle therapy in cancer.

Our study provides direct evidences that there could be a selection of M1 macrophages in tumors with proton irradiation, since this phenotype is more radioresistant. Furthermore, we showed that 10 Gy of proton irradiation is able to program M0 macrophages towards M1 phenotype, to enhance the M1 phenotype in M1 macrophages and to initiate a M1 phenotype in M2 macrophages. This re-education is due, at least in part, to NFκB p65 activation. Therefore, our data open new perspectives for macrophage clinical targeting with charged particle therapy. In the future, these results need to be confirmed by *in vivo* experiments, as other cell types are present in the tumor microenvironment and could influence the response to proton irradiation. It has to be noted that macrophage reprogramming after proton irradiation may not be exclusively associated to NFκB activation. Indeed, the interaction between several pathways (NFκB, MAPK and IRF/STAT pathways) may be involved in this process and needs to be further investigated. Moreover, metabolism reprogramming has been demonstrated to influence macrophage polarization (40, 41) and should be taken into account in the further studies.

Materials and Methods

Differentiation of monocytes to macrophages and macrophage polarization

Human monocytic cell line (THP-1 – ATCC TIB-202) were grown in Roswell Park Memorial Institute (RPMI 1640, Gibco #21875034) culture medium containing 10% of heat inactivated fetal bovine serum (Gibco) and supplemented with 10 mM Hepes (Gibco, #15630-056), 2 mM pyruvate (Gibco, #11360-039), 2.5 g/L D-glucose (Merck) and 50 pM β-mercaptoethanol (Gibco, #31350-010). As the proton accelerator used in this study produces a horizontal beam, cells were plated in suitable irradiation chambers, composed of two stainless steel rings with the central holes covered by 3 μm Mylar foils (Goodfellow). THP-1 monocytes were seeded at the center of irradiation chambers, on the mylar foil, and differentiated into macrophages with 150 nM phorbol 12-myristate 13-acetate (PMA, Sigma P8139). For this step, a cloning cylinder (6.4 mm diameter size, Sigma C3983-50EA) was placed at the center

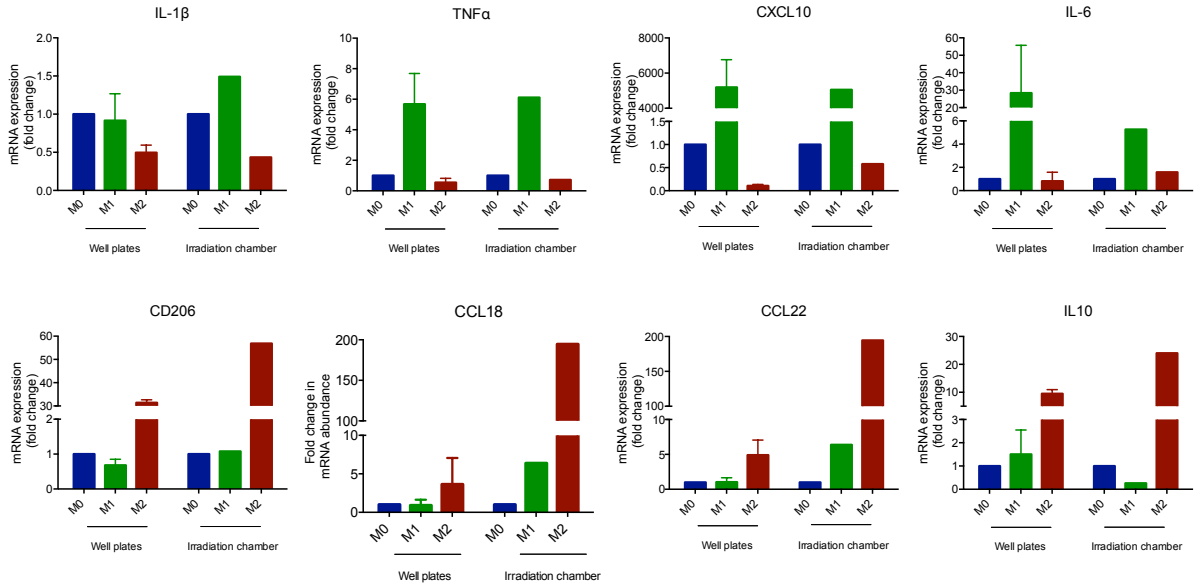

Figure S4. Evaluation of macrophage phenotype after differentiation and polarization in the irradiation chambers

THP-1 cells were differentiated and polarized into M0, M1 and M2 macrophages in conventional well plates and irradiation chambers. mRNA levels of M1 (IL-1β, TNFα, CXCL10 and IL-6) and M2 (CD206, CL18, CCL22 and IL-10) markers were assessed by RT-qPCR in M0 (blue), M1 (green) and M2 (red) macrophages (N=2 for well plate; N=1 for irradiation chamber).

of the chamber and filled with Cell Tak (VWR #354240) for coating. Differentiated THP-1 cells tend to form clusters when seeded on Mylar foil and Cell tak allowed a homogenous monolayer. The cloning cylinders were rinsed with milli Q water and were filled with 190 µl of medium containing 50,000 THP-1 monocytes, penicillin streptomycin 10,000 U/ml (Fisher, #15140122) and PMA for 24h incubation. The differentiation medium was replaced with RPMI medium for a further 24h incubation. Macrophages were polarized in M1 phenotype with 10 pg/ml lipopolysaccharides (LPS, Sigma; #8630) and 20 ng/ml interferon γ (IFN-γ, R&D system, #285-IF) during 24h incubation or were polarized in M2 phenotype with 20 ng/ml interleukin 4 (IL-4, R&D systems, #204-IL) and 20 ng/ml interleukin 13 (IL-13, R&D systems, #213-ILB) during 48h incubation as described in (42). The gene expression of M1 (IL-1β, TNFα, CXCL10 and IL-6) and M2 (CCL18, CCL22, CD206 and IL-10) markers were analyzed to verify the macrophage phenotype of M0, M1 and M2 macrophages in the irradiation chambers (**Fig. 4S**).

Proton irradiation

Four days before irradiation, THP-1 monocytes were differentiated in the irradiation chambers to generate M2 macrophages. To obtain M1 or M0 macrophages, cells were seeded three or two days respectively before irradiation. Just before proton irradiation, culture medium was changed by CO_2 independent medium (Gibco #18045054) supplemented with 2 mM L-glutamine and 3.75 g/L of D-glucose. The irradiation chambers were placed at the end of a 2 MV Tandem accelerator (High Voltage Engineering Europa) available at the University of Namur. The experimental set-up and irradiation procedure are described elsewhere (43, 44). Briefly, a H^+ homogenous 1 cm ² broad beam went through a 1 µm thick Si_3N_4 exit foil. The chambers were placed vertically at 3 mm from the exit window of the accelerator. The linear energy transfer (LET) of protons was set to 25 keV/µm and the dose rate fixed to 2 Gy/min. After irradiation, the chambers were replaced in the CO_2 incubator until the experiments were performed.

Determination of cell viability

Because of the Cell Tak, the cells could not be detached from the Mylar foil. Ethidium bromide (1mg/ml Sigma E8751) - acridin orange (0.3 mg/ml, Sigma A6014) (EBAO) was used at 1:100 dilution in PBS to analyze viability. The cells were stained with EBAO for 5 minutes, 8h or 16h after irradiation. Cells were then rinsed with PBS and were observed with Olympus stream microscope beyond UV light. Lived cells are stained in green while dead cells are stained in orange. Quantifications were performed with Aphelion Lab ® software on approximately 1000 cells.

Immunofluorescence labeling

Cells were fixed for 10 minutes with paraformaldehyde 4% in PBS, and then permeabilized with triton 0.1% for 5 minutes. The cells were rinsed three times with PBS – BSA 2% (bovine serum albumin) and incubated overnight at 4°C with primary antibody in the irradiation chambers. Primary antibodies were 1:800 (γH2AX, BioKe 2577), 1:400 (NFκB p65, Cell Signaling D14E12) or 1:1500 (53BP1, Novus NB100-304) diluted in PBS – BSA 2%. Cells were rinsed three times with PBS – BSA 2% and then incubated for 1h with secondary antibody 1:1000 diluted (Alexa Fluor 488 conjugated anti rabbit IgG antibody; Molecular probes, #A11034) at room temperature. After washing the cells three times with PBS, nuclei

Gene	Forward	Reverse
CCL22	CACTTCTACTGGACCTCAGAC	AGTAGGCTCTTCATTGGCTCA
EGF	ATGTCCTGCCCTCAACC	GGTTGCATTGACCCATCTGC
IL-6	CCTGAACCTTCCAAAGATGGC	CACCAGGCAAGTCTCCTCATT
IL-8	TCTGTGTGAAGGTGCAGTTTT	GGGGTGGAAAGGTTTGGAGTA
IL-10	TTCCCTGTGAAAACAAGAGCAA	GTAGATGCCTTTCTCTTGGAGCTTA
RPS9	CTGGATGAGGGCAAGATGAAG	GTCTGCAGGCGTCTCTCTAAGAA
TNFα	CTGCACTTTGGAGTGATCGG	TCAGCTTGAGGGTTTGCTAC

Table S1. Primers used for RT-qPCR

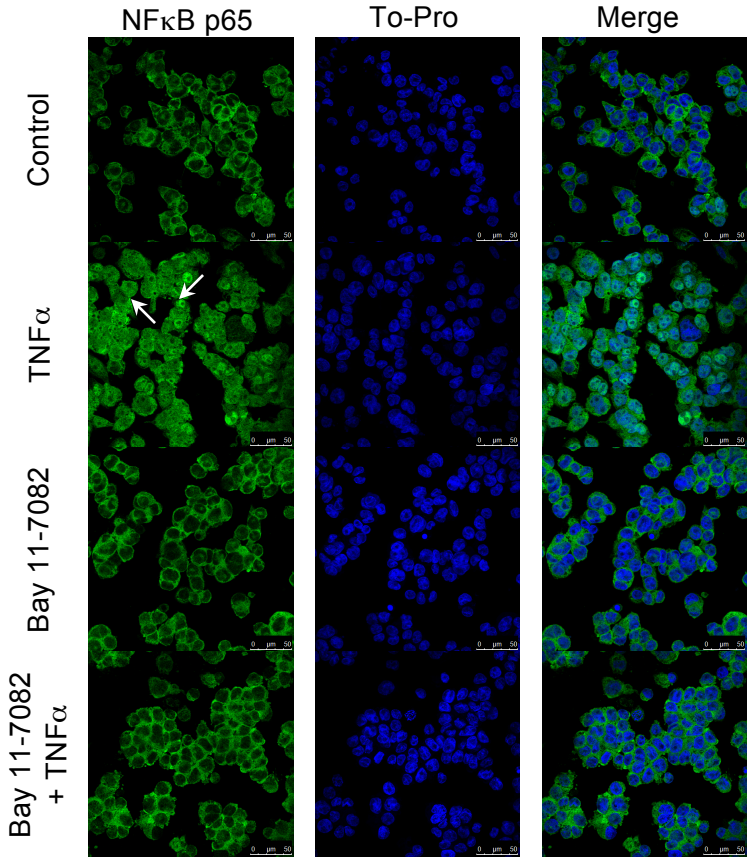

Figure S5. Inhibition of nuclear NFκB p65 translocation after Bay 11-7082 exposure
M0 macrophages were exposed to TNFα (20 ng/ml) or to Bay 11-7082 inhibitor (5 μM) as well as to the combination of both TNFα and Bay 11-7082 for 12h. The nuclear translocation of NFκB p65 was evaluated by immunofluorescence staining. Representative immunofluorescence staining images display NFκB p65 in green and nuclei in blue (N=1).

were stained with TOPRO-3 (1:80 diluted in RNase solution). Cells were then washed three times with PBS and the Mylar foil was cut around the cell drop and was deposited on a microscope slide, cells on top. A coverslip was mounted using Mowiol (Sigma) above the cells and the cells were observed with a confocal microscope (SP5, Leica). A constant photomultiplier gain value and a constant laser power were used to take the pictures. Quantifications for γH_2AX intensity or 53BP1 foci were performed using Aphelion Lab ® software on approximately 1000 cells. For γH_2AX, the quantification was performed as followed: mean of (Number of green pixels X intensity of each pixel) / nucleus. Usually, the quantification of γH_2AX labeling is performed by counting γH_2AX foci. However, as high doses were used in this study, large numbers of foci were observed and it was impossible to discriminate foci at high doses. Therefore, we choose to quantify the mean intensity of γH_2AX per nucleus. Apoptotic cells were not taken into account for the quantification. Quantification for 53BP1 was performed by counting 53BP1 foci per nucleus. Quantification for NFκB p65 was performed as followed: number of cells with higher pixel numbers than mean + 2 standard deviations, representative of cells with high translocation of NFκB p65.

Relative quantification of mRNA levels

Total RNA was extracted from cells in irradiation chambers with RNeasy micro kit and DNAse protocol (QIAGEN # 74004). Reverse transcription was performed on 1 μg using Transcriptor first strand cDNA synthesis kit (Roche #4309155). The quantitative Real Time PCR was performed using Viia 7 (Thermo Fisher Scientific) with SYBRGreen PCR Master Mix (Applied Biosystem, #4309155) and primers (IDT, 300 nM). 40S ribosomal protein S9 (RPS9) was selected as the housekeeping gene for normalization, based on its constant expression within all samples. The primers used for RT-qPCR are summarized in supplementary information (**table S1**).

Cytokine quantification

Secreted cytokine (IL-6, CXCL-8/IL-8 and TNFα) analysis was assessed using ELISA kit, according to the manufacturer recommendations (Quantikine, R&D systems D6050, D8000C and DTA00C). Culture media were diluted in CO_2 independent medium 5 and 50 times for TNFα and IL-8, respectively, while the culture medium was not diluted for IL-6. For all samples, concentrations were normalized by total protein (μg proteins/ml) determined by Folin method.

IKK inhibition

Bay 11-7082 inhibitor (3-((4-methylphenyl)sulfonyl)-(2E)-propenenitrile - Selleckchem S2913) selectively and irreversibly inhibits the phosphorylation of IκB-α and then prevents the NFκB activation. This inhibitor was added at 5 μM in CO_2 independent medium 1h before irradiation and the cells were incubated for 12h after irradiation in the presence of the inhibitor. TNFα (20 ng/ml, R&D Systems #210-TA-020) was used as a positive control to verify the nuclear translocation of NFκB p65. In order to validate the inhibition of p65 nuclear translocation in our model, cells were incubated with TNFα and Bay 11-7082 (**Fig. 5S**).

Statistical analysis

Statistical analyses were performed using Graph Pad Prism software. Data are reported as mean ± 1 SD of *N* independent experiments. A *p* value of < 0.05 was considered as significant.

Conflict of interest

The authors declare no potential conflicts of interest

Acknowledgment

The authors thank Denis Mottet (PhD.) for advices on the MNAse assay. We would like to acknowledge Romain Tonneau for the computational method. We are thankful to the technological platforms SIAM and Morph-In (University of Namur).

Authors' contributions

GG carried out the experiments and wrote the manuscript. ACW, CH and SP helped for the experiments. TT, AF, CD and NN contributed to the acquisition of data. BL and ACW reviewed the manuscript. CM, SL and ACH conceived of the study, participated in its design and coordination, and revised the manuscript. All authors read and approved the final manuscript.

1. Mittal D, Gubin MM, Schreiber RD, Smyth MJ. New insights into cancer immunoediting and its three component phases--elimination, equilibrium and escape. Curr Opin Immunol. 2014;27:16-25.

2. Lee Y, Auh SL, Wang Y, Burnette B, Wang Y, Meng Y, et al. Therapeutic effects of ablative radiation on local tumor require CD8+ T cells: changing strategies for cancer treatment. Blood. 2009;114(3):589-95.

3. Weichselbaum RR, Liang H, Deng L, Fu YX. Radiotherapy and immunotherapy: a beneficial liaison? Nat Rev Clin Oncol. 2017;14(6):365-79.

4. Dovedi SJ, Adlard AL, Lipowska-Bhalla G, McKenna C, Jones S, Cheadle EJ, et al. Acquired resistance to fractionated radiotherapy can be overcome by concurrent PD-L1 blockade. Cancer Res. 2014;74(19):5458-68.

5. Lewis CE, Pollard JW. Distinct role of macrophages in different tumor microenvironments. Cancer Res. 2006;66(2):605-12.

6. van Ravenswaay Claasen HH, Kluin PM, Fleuren GJ. Tumor infiltrating cells in human cancer. On the possible role of CD16+ macrophages in antitumor cytotoxicity. Lab Invest. 1992;67(2):166-74.

7. Gentles AJ, Newman AM, Liu CL, Bratman SV, Feng W, Kim D, et al. The prognostic landscape of genes and infiltrating immune cells across human cancers. Nat Med. 2015;21(8):938-45.

8. Mantovani A, Marchesi F, Malesci A, Laghi L, Allavena P. Tumour-associated macrophages as treatment targets in oncology. Nat Rev Clin Oncol. 2017;14(7):399-416.

9. Pienta KJ, Machiels JP, Schrijvers D, Alekseev B, Shkolnik M, Crabb SJ, et al. Phase 2 study of carlumab (CNTO 888), a human monoclonal antibody against CC-chemokine ligand 2 (CCL2), in metastatic castration-resistant prostate cancer. Invest New Drugs. 2013;31(3):760-8.

10. Klug F, Prakash H, Huber PE, Seibel T, Bender N, Halama N, et al. Low-dose irradiation programs macrophage differentiation to an iNOS(+)/M1 phenotype that orchestrates effective T cell immunotherapy. Cancer Cell. 2013;24(5):589-602.

11. Mosser DM, Edwards JP. Exploring the full spectrum of macrophage activation. Nat Rev Immunol. 2008;8(12):958-69.

12. Biswas SK, Mantovani A. Macrophage plasticity and interaction with lymphocyte subsets: cancer as a paradigm. Nat Immunol. 2010;11(10):889-96.

13. Wang N, Liang H, Zen K. Molecular mechanisms that influence the macrophage m1-m2 polarization balance. Front Immunol. 2014;5:614.

14. Genard G, Lucas S, Michiels C. Reprogramming of Tumor-Associated Macrophages with Anticancer Therapies: Radiotherapy versus Chemo- and Immunotherapies. Front Immunol. 2017;8:828.

15. Prakash H, Klug F, Nadella V, Mazumdar V, Schmitz-Winnenthal H, Umansky L. Low doses of gamma irradiation potentially modifies immunosuppressive tumor microenvironment by retuning tumor-associated macrophages: lesson from insulinoma. Carcinogenesis. 2016;37(3):301-13.

16. Nowosielska EM, Cheda A, Wrembel-Wargocka J, Janiak MK. Effect of low doses of low-let radiation on the innate anti-tumor reactions in radioresistant and radiosensitive mice. Dose Response. 2012;10(4):500-15.

17. Ilicic K, Combs SE, Schmid TE. New insights in the relative radiobiological effectiveness of proton irradiation. Radiat Oncol. 2018;13(1):6.

18. Roebuck KA. Regulation of interleukin-8 gene expression. J Interferon Cytokine Res. 1999;19(5):429-38.

19. Tsai CS, Chen FH, Wang CC, Huang HL, Jung SM, Wu CJ, et al. Macrophages from irradiated tumors express higher levels of iNOS, arginase-I and COX-2, and promote tumor growth. Int J Radiat Oncol Biol Phys. 2007;68(2):499-507.

20. Lindstrom A, Midtbo K, Arnesson LG, Garvin S, Shabo I. Fusion between M2-macrophages and cancer cells results in a subpopulation of radioresistant cells with enhanced DNA-repair capacity. Oncotarget. 2017;8(31):51370-86.

21. Meng Y, Beckett MA, Liang H, Mauceri HJ, van Rooijen N, Cohen KS, et al. Blockade of tumor necrosis factor alpha signaling in tumor-associated macrophages as a radiosensitizing strategy. Cancer Res. 2010;70(4):1534-43.

22. Leblond MM, Peres EA, Helaine C, Gerault AN, Moulin D, Anfray C, et al. M2 macrophages are more resistant than M1 macrophages following radiation therapy in the context of glioblastoma. Oncotarget. 2017;8(42):72597-612.

23. Hachiya M, Shimizu S, Osawa Y, Akashi M. Endogenous production of tumour necrosis factor is required for manganese superoxide dismutase expression by irradiation in the human monocytic cell line THP-1. Biochem J. 1997;328 (Pt 2):615-23.

24. Malhotra P, Adhikari M, Singh SK, Kumar R. N-acetyl tryptophan glucopyranoside (NATG) provides radioprotection to murine macrophage J774A.1 cells. Free Radic Res. 2015;49(12):1488-98.

25. Dos Santos LM, da Silva TM, Azambuja JH, Ramos PT, Oliveira PS, da Silveira EF, et al. Methionine and methionine sulfoxide treatment induces M1/classical macrophage polarization and modulates oxidative stress and purinergic signaling parameters. Mol Cell Biochem. 2017;424(1-2):69-78.

26. Teresa Pinto A, Laranjeiro Pinto M, Patricia Cardoso A, Monteiro C, Teixeira Pinto M, Filipe Maia A, et al. Ionizing radiation modulates human macrophages towards a pro-inflammatory phenotype preserving their pro-invasive and pro-angiogenic capacities. Sci Rep. 2016;6:18765.

27. Wu Q, Allouch A, Paoletti A, Leteur C, Mirjolet C, Martins I, et al. NOX2-dependent ATM kinase activation dictates pro-inflammatory macrophage phenotype and improves effectiveness to radiation therapy. Cell Death Differ. 2017;24(9):1632-44.

28. Chanput W, Mes JJ, Wichers HJ. THP-1 cell line: an in vitro cell model for immune modulation approach. Int Immunopharmacol. 2014;23(1):37-45.

29. Murray PJ. Macrophage Polarization. Annu Rev Physiol. 2017;79:541-66.

30. Sasaki T, Hiroki K, Yamashita Y. The role of epidermal growth factor receptor in cancer metastasis and microenvironment. Biomed Res Int. 2013;2013:546318.

31. Hellweg CE. The Nuclear Factor kappaB pathway: A link to the immune system in the radiation response. Cancer Lett. 2015;368(2):275-89.

32. Schaue D, Kachikwu EL, McBride WH. Cytokines in radiobiological responses: a review. Radiat Res. 2012;178(6):505-23.

33. Formenti SC, Demaria S. Combining radiotherapy and cancer immunotherapy: a paradigm shift. J Natl Cancer Inst. 2013;105(4):256-65.

34. Alan Mitteer R, Wang Y, Shah J, Gordon S, Fager M, Butter PP, et al. Proton beam radiation induces DNA damage and cell apoptosis in glioma stem cells through reactive oxygen species. Sci Rep. 2015;5:13961.

35. Hayden MS, Ghosh S. Shared principles in NF-kappaB signaling. Cell. 2008;132(3):344-62.

36. Huang TT, Wuerzberger-Davis SM, Wu ZH, Miyamoto S. Sequential modification of NEMO/IKKgamma by SUMO-1 and ubiquitin mediates NF-kappaB activation by genotoxic stress. Cell. 2003;115(5):565-76.

37. Hellweg CE, Baumstark-Khan C, Schmitz C, Lau P, Meier MM, Testard I, et al. Activation of the nuclear factor kappaB pathway by heavy ion beams of different linear energy transfer. Int J Radiat Biol. 2011;87(9):954-63.

584 38. Hellweg CE, Baumstark-Khan C, Schmitz C, Lau P, Meier MM, Testard I, et al. Carbon-ion-
585 induced activation of the NF-kappaB pathway. Radiat Res. 2011;175(4):424-31.

586 39. Criswell T, Leskov K, Miyamoto S, Luo G, Boothman DA. Transcription factors activated in
587 mammalian cells after clinically relevant doses of ionizing radiation. Oncogene.
588 2003;22(37):5813-27.

589 40. Liu PS, Wang H, Li X, Chao T, Teav T, Christen S, et al. alpha-ketoglutarate orchestrates
590 macrophage activation through metabolic and epigenetic reprogramming. Nat Immunol.
591 2017;18(9):985-94.

592 41. Kelly B, O'Neill LA. Metabolic reprogramming in macrophages and dendritic cells in
593 innate immunity. Cell Res. 2015;25(7):771-84.

594 42. Genin M, Clement F, Fattaccioli A, Raes M, Michiels C. M1 and M2 macrophages derived
595 from THP-1 cells differentially modulate the response of cancer cells to etoposide. BMC Cancer.
596 2015;15:577.

597 43. Riquier H, Abel D, Wera AC, Heuskin AC, Genard G, Lucas S, et al. Effects of Alpha Particle
598 and Proton Beam Irradiation as Putative Cross-Talk between A549 Cancer Cells and the
599 Endothelial Cells in a Co-Culture System. Cancers (Basel). 2015;7(1):481-502.

600 44. Wéra A.-C. RH, Heuskin A.-C., Michiels C., Lucas S. *In vitro* irradiation station for broad
601 beam radiobiological experiments. Nuclear Instruments and Methods in Physics Research.
602 2011;B 269:3120 - 4.

603

2.5. Perspectives

In the first part of this study, a higher viability of M1 macrophages was observed after proton irradiation, compared to the M0 and M2 phenotypes. In order to further identify the actors involved in this resistance, it would be interesting to study DNA and histone methylation and the chromatin condensation after proton irradiation. These experiments may evidence changes in DNA remodeling after irradiation in the three macrophage phenotypes. These analyses could be performed by labeling methylated histones: H3K36me3 for uncondensed DNA and H3k9me3 for condensed DNA for example. The use of enzymatic assay, such as MNAse I assay or DNAse assay after proton irradiation would complete this analysis. Furthermore, the study of DNA repair proteins by western blot analysis or immunofluorescence labeling would bring more information on the higher survival of M1 macrophages to proton irradiation. Finally, the investigation of ROS management during and after proton irradiation by using different fluorescent probes for detecting ROS and RNS, coupled to the use of antioxidants, could help to identify the effect of ROS management on macrophage survival.

As the actual standard for radiotherapy is the use of X-rays or γ-rays, we initiated the comparison regarding the effects of proton and photon irradiation on macrophage polarization. While in other studies the use of X-ray radiation induced a M1 polarization of unpolarized human monocyte-derived macrophages, Raw 264.7 cells, PMA-differentiated THP-1 cells and peritoneal macrophages (see Chapter 3), our results indicated that X-ray radiation failed to program PMA-differentiated macrophages. These differences could rely on the use of different cell lines and different protocols for THP-1 differentiation. In contrast to our study, Wu and his colleagues differentiated THP-1 monocytes into macrophages with 320 nM PMA for 24h and the differentiation step was not followed by a 24h rest period *(Wu et al., 2017)*. This resting time allows a decrease in NFκB gene cluster expression, upregulated during differentiation, as well as increases the expression of macrophage markers *(Chanput et al., 2014).* In order to further characterize the effects of protons compared to X-rays, it would be interesting to assess the effect of both irradiation types on NFκB p65 nuclear translocation by western blot analysis or immunofluorescence labeling. Previously, it has been shown that charged particle irradiation is more likely to induce NFκB p65 activation in cancer cells compared to X-rays *(Hellweg et al., 2011a)*. It would also be interesting to identify the role of ROS and DNA damage in macrophage reprogramming. In order to perform these analyses, it would be worth to combine antioxidant (e.g. N-acetyl cysteine, butylated hydroxyanisole or ebselen) to proton or photon irradiation and to observe the effects on macrophage reprogramming. In addition, the combination of RNA sequencing analysis and proteomic profiling would bring a lot of information on the effects of proton and X-ray irradiation of macrophages. Functional analyses would also help to further characterize the effects of proton irradiation on macrophage reprogramming. Moreover, as M1 macrophages are notably identified by their high phagocytosis activity, the use of fluorescent E. *Coli*, fluoresceine isothiocyanate (FITC)-labeled *Staphylococcus aureus* particles or fluorescent beads would confirm proton irradiation mediated - macrophage reprogramming. In the same line, by studying the expression of HLA-DR in irradiated macrophages, it would be possible to examine the antigen - presenting functions of irradiated macrophages. The ability of macrophages to present antigen to CD8+ T cells is another experiment that could be performed. This study requires the stimulation of macrophages with antigenic peptide to be presented to peptide-specific CD8+ T cell line *(Short et al., 2013)*. In contrast to M1, M2 macrophages are

identified by a high capacity to induce angiogenesis and invasion of cancer cells. Therefore by studying the activity of macrophage released-metalloproteinases through gelatin-zymography or by using matrigel invasion assays, it is possible to characterize the effects of irradiated macrophages on cancer cell invasion. To identify the effect of proton irradiation on angiogenesis, the medium of unirradiated or irradiated macrophages could be used in chick embryo angiogenesis assay or endothelial cell (HUVEC-2 cell line) tube formation in matrigel.

2.6. Conclusion

The goal of this study was to examine whether proton irradiation could influence macrophage survival as well as macrophage polarization. By studying cell survival in the first part of this article, we demonstrated that M1 macrophages were more resistant to proton irradiation as compared to M2 and M0 macrophages. This early enhanced radioresistance was related to a higher DNA damage detection. We also revealed a possible implication of a better ROS management in M1 macrophages, which could explain the higher resistance of this phenotype to proton irradiation. In the second part of this work, we evidenced that M0 macrophages, exposed to 10 Gy of proton irradiation, displayed a polarization towards a M1 phenotype. These results confirm that it is possible to polarize unpolarized macrophages with radiotherapy. Actually, it was already demonstrated in other macrophage models that moderate doses (1 – 10 Gy) of X-ray and γ-ray radiation induced M1 polarization in unpolarized macrophages. Surprisingly, X-rays irradiation failed to polarize M0 macrophages into M1 ones in our conditions. However, we demonstrated for the first time that protontherapy is able to re-educate M2 macrophages into a mixed M1/M2 phenotype. Macrophage reprogramming orchestrated by proton irradiation occurred, at least in part, through the activation of NFκB p65, as it was evidenced by a nuclear translocation of this subunit. These results were confirmed by the use of Bay 11-7082, an IKK inhibitor. Indeed, macrophage reprogramming was aborted after proton irradiation by the cytoplasmic sequestration of NFκB p65 generated by the IKK inhibitor. In conclusion, our findings evidenced for the first time the radioresistance of M1 macrophages and a reprogramming of M2 macrophages after proton irradiation. Although these results require additional experiments to further characterize the effects of proton irradiation on macrophages, our study opens new perspectives for the targeting of macrophages with proton irradiation.

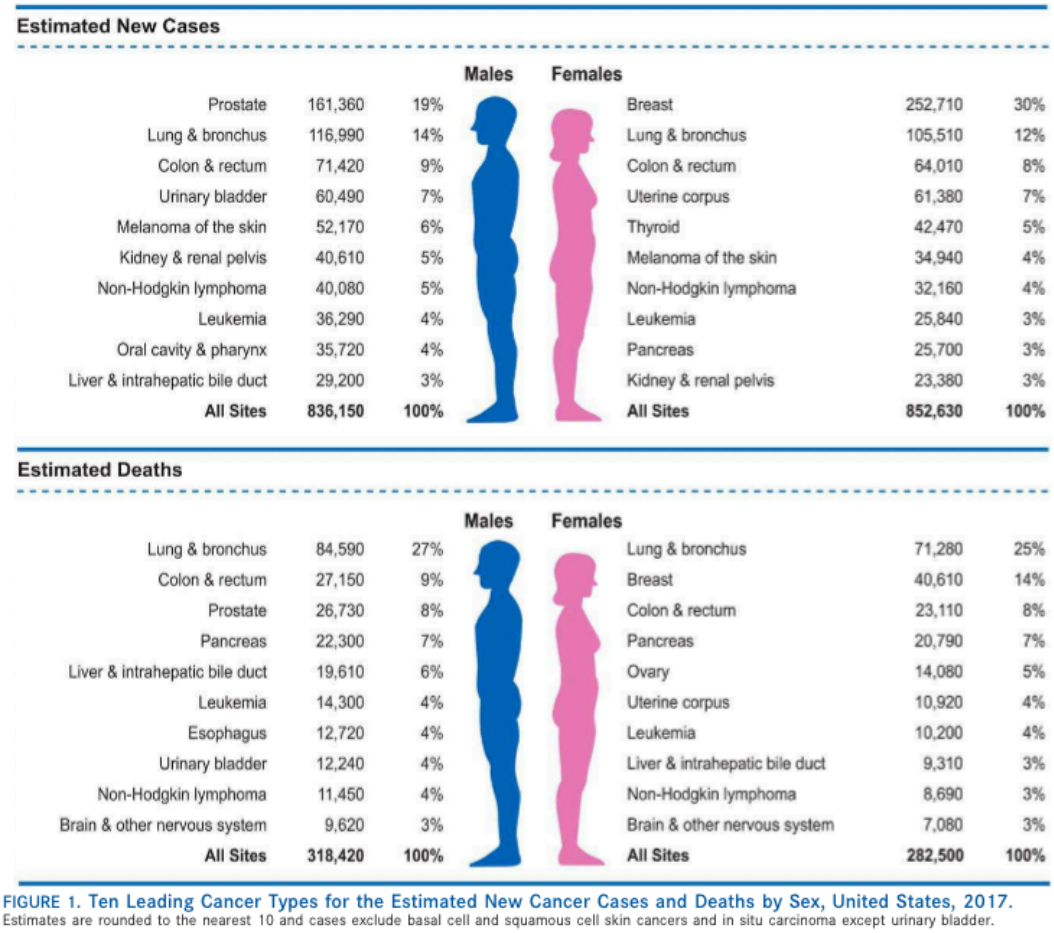

Estimated New Cases

Males			Females		
Prostate	161,360	19%	Breast	252,710	30%
Lung & bronchus	116,990	14%	Lung & bronchus	105,510	12%
Colon & rectum	71,420	9%	Colon & rectum	64,010	8%
Urinary bladder	60,490	7%	Uterine corpus	61,380	7%
Melanoma of the skin	52,170	6%	Thyroid	42,470	5%
Kidney & renal pelvis	40,610	5%	Melanoma of the skin	34,940	4%
Non-Hodgkin lymphoma	40,080	5%	Non-Hodgkin lymphoma	32,160	4%
Leukemia	36,290	4%	Leukemia	25,840	3%
Oral cavity & pharynx	35,720	4%	Pancreas	25,700	3%
Liver & intrahepatic bile duct	29,200	3%	Kidney & renal pelvis	23,380	3%
All Sites	**836,150**	**100%**	**All Sites**	**852,630**	**100%**

Estimated Deaths

Males			Females		
Lung & bronchus	84,590	27%	Lung & bronchus	71,280	25%
Colon & rectum	27,150	9%	Breast	40,610	14%
Prostate	26,730	8%	Colon & rectum	23,110	8%
Pancreas	22,300	7%	Pancreas	20,790	7%
Liver & intrahepatic bile duct	19,610	6%	Ovary	14,080	5%
Leukemia	14,300	4%	Uterine corpus	10,920	4%
Esophagus	12,720	4%	Leukemia	10,200	4%
Urinary bladder	12,240	4%	Liver & intrahepatic bile duct	9,310	3%
Non-Hodgkin lymphoma	11,450	4%	Non-Hodgkin lymphoma	8,690	3%
Brain & other nervous system	9,620	3%	Brain & other nervous system	7,080	3%
All Sites	**318,420**	**100%**	**All Sites**	**282,500**	**100%**

FIGURE 1. Ten Leading Cancer Types for the Estimated New Cancer Cases and Deaths by Sex, United States, 2017.
Estimates are rounded to the nearest 10 and cases exclude basal cell and squamous cell skin cancers and in situ carcinoma except urinary bladder.

Figure III.13 – Estimated new cases and estimated deaths for the leading cancer types (United States, 2017)

Statistics for estimated new cases and estimated deaths for the ten leading cancer types, excluding basal cell and squamous skin cancers and *in situ* carcinoma except urinary bladder *(Siegel, Miller et al. 2017)*.

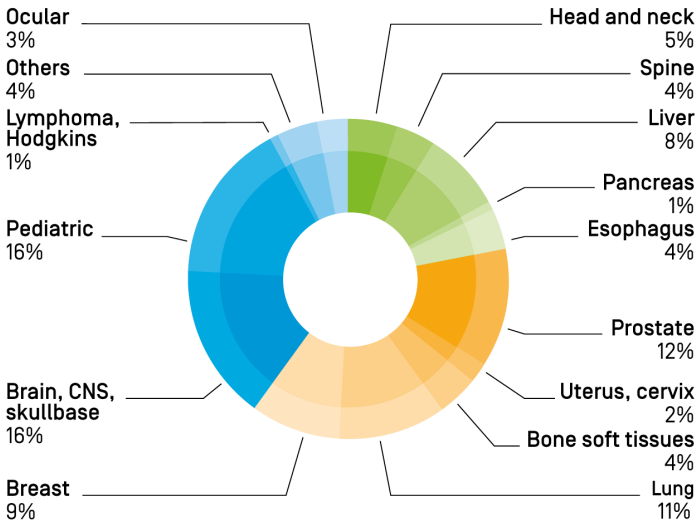

Figure III.14 – Ongoing trials for protontherapy

Graphical representation of cancer types recruited in open trials for protontherapy. Data from clinical trial.gov at the end of December 2016, Yves Jongen

3. PART 2: Effects of proton irradiation on co-cultured macrophages and non-small lung cancer cells

3.1. Objectives

In 2017, lung cancer remained a leading cancer type in terms of estimated new cases (14% for males and 12% for females) and estimated death cases (27% for males and 25% for females) in United States (***Figure III.13***) *(Siegel et al., 2017)*. Indeed, most locally advanced lung tumors are inoperable. It is why the 5-year survival rate for radiotherapy combined with chemotherapy is approximately 5% for these patients *(Joiner and Kogel, 2009)*. The most frequent lung cancer types are small-cell lung cancer (SCLC) and non-small-cell lung cancer (NSCLC), distinguished by histopathological aspects. NSCLCs mainly gather adenocarcinomas, epidermoid carcinomas and large cell carcinomas. While adenocarcinomas and large cell carcinomas are localized in lung periphery, epidermoid carcinomas are usually found in bronchi. Radiotherapy is recommended for 75% of lung cancer cases and is such more indicated in advanced stages: 92% for stage III and 83% for stage IV *(Delaney et al., 2003),* for palliative reasons. Lung cancer is also one of the leading cancer type recruited for trials with proton beam therapy (25 on 187 studies) (***Figure III.14***) (*Clinicaltrial.gov; on March 2018*) and the most indicated for proton therapy (***Figure III.15***) (*data from leading center in US*).

The response of cancer cells to radiotherapy is influenced by intrinsic factors and was intensively studied. These intrinsic modifications include alterations of DNA repair efficiency *(Mohamad et al., 2017)*, enhanced aerobic glycolysis, altered mitochondrial function *(Van den Bossche et al., 2017)*, chromatin modifications *(Natale et al., 2017)* or up-regulation of pro-survival factors *(Hanahan and Weinberg, 2011).* Despite growing evidences suggesting the involvement of tumor microenvironment in tumor progression, only few studies have paid attention to the influence of tumor-associated cells on cancer cells response to radiotherapy, and inversely.

Numerous clinical studies have indicated that TAM infiltration is linked to poor prognosis in many cancers *(Fridman et al., 2017)*. In fact, TAMs are known to influence the fate of tumors, mainly by releasing growth factors and other mediators (e.g. EGF, TGFβ, MMPs) that promote the aggressiveness of cancer cells. Interestingly, previous studies have demonstrated that macrophages enhance invasiveness and matrix degrading activity of cancer cells, facilitating metastasis. In return, cancer cells modulate macrophage activities and their recruitment, through the release of different factors including CSF-1 and CCL2 *(Qian and Pollard, 2010)*. Therefore, it is not surprising that the interactions between cancer cells and macrophages may dictate the response of tumor to radiotherapy.

As we showed in the first part of this thesis, proton irradiation orchestrated M2 macrophage reprogramming. Therefore, we focused our attention on the effect of protontherapy on co-cultured M2 macrophages and on the expression of pro-apoptic proteins in cancer cells. In order to perform these experiments, we choose A549 cells, frequently used as a model of NSCLCs.

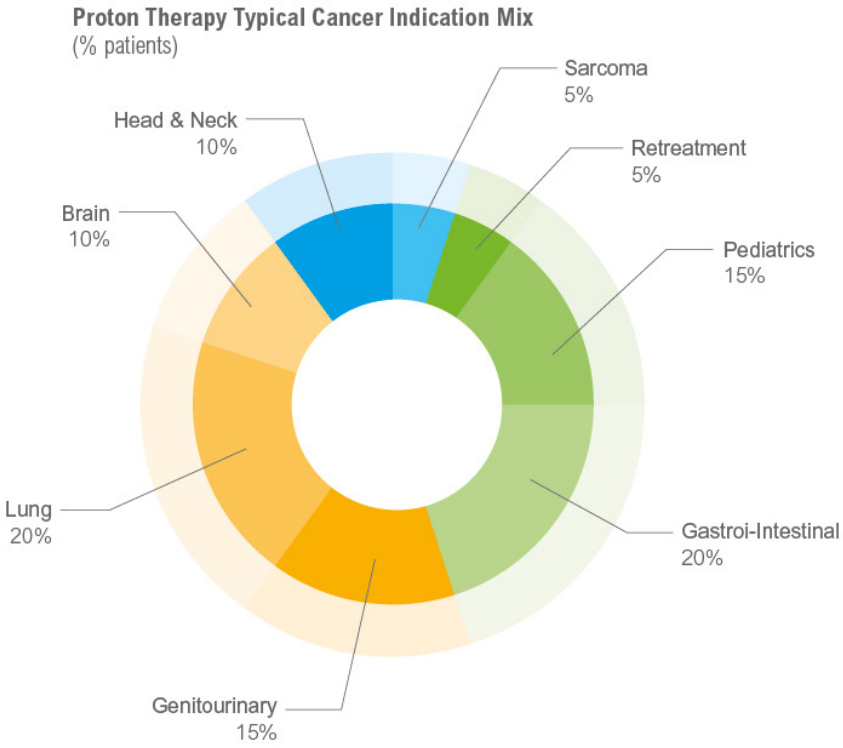

Figure III.15 – Protontherapy indications for several cancer types
Data from Yves Jongen, October 2015

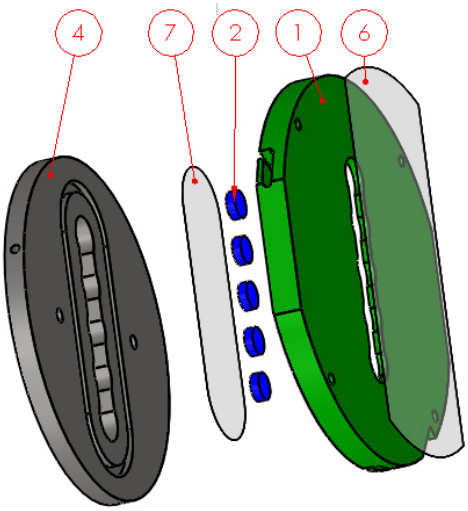

Figure III.16 – Schematic representation of the multiple drop irradiation chamber
The top side (4) is covered by a mylar foil (7) on its internal part while another mylar foil (6) is glued on the bottom side (1). The cells (2) are seeded as drops on mylar foils.

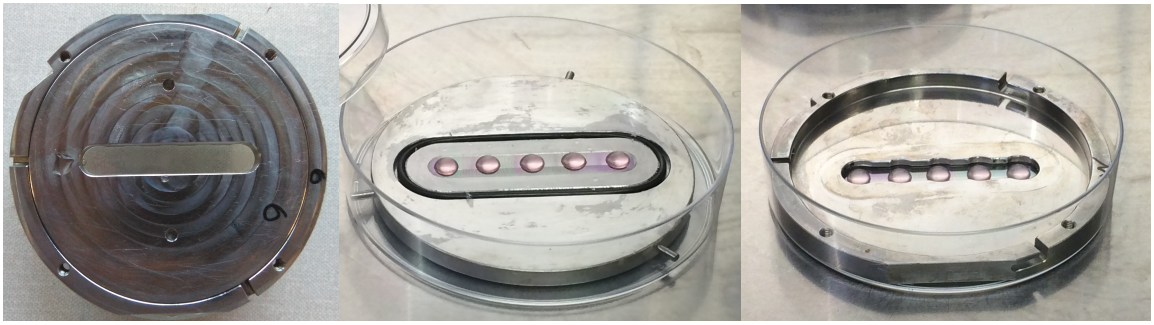

Figure III.17 – Multiple drop irradiation chamber
The multiple drop irradiation chamber (l*eft*) is composed of two stainless steel pieces, covered by a mylar foil on their center. Five cell drops are seeded on each side of these irradiation chambers. The top side (*middle*) was used for A549 cells while the bottom side (*right*) was intended for THP-1 macrophages.

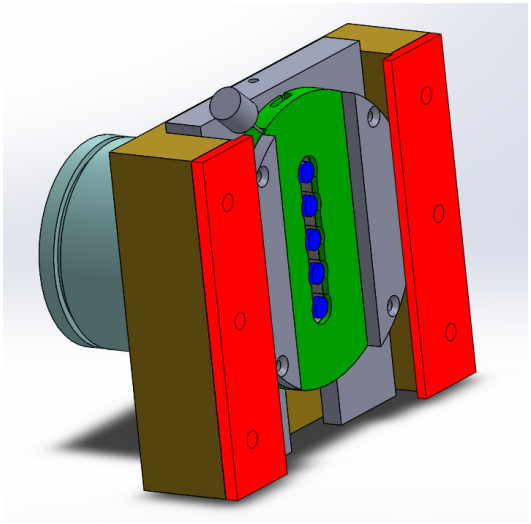

Figure III.18 – Irradiation of co-cultured cells
The multiple drop irradiation chambers are disposed in a support that guides them for the irradiation process. The XY motorized table was used to slip up the irradiation chambers ahead the beam, with a constant speed of 0.133 m/sec.

3.2. Experimental settings and limitations

Because simple irradiation chambers were not adapted for co-cultures of macrophages and cancer cells, new irradiation chambers were designed (***Figure III.16***). There are two main reasons for these modifications. Firstly, the number of cells was increased, aiming to collect higher amounts of biological material (RNA, proteins…). Secondly the volume capacity was reduced to facilitate exchange and communication between the two cell types. The multiple drop irradiation chambers consist of two stainless steel pieces, which are each covered by a mylar foil on their centers. On each side of the irradiation chambers, five drops of cells may be shaped (***Figure III.17***). In our experiments, five drops of 50 000 A549 cells were seeded on the top side while five drops of 50 000 M2 polarized THP-1 macrophages were plated on the bottom side. For the irradiation step, the multiple drop irradiation chambers slipped ahead the beam with a constant speed (0.133 mm/sec) (***Figure III.18***). The cells were irradiated successively on both sides with a constant LET of 25 keV/µm and a dose rate of 10 Gy/min, instead of 2 Gy/min previously used. The dose rate was modified in order to reduce the time during which cells were outside the incubator. Indeed, a dose rate of 2 Gy/min required an irradiation time of more than 30 minutes while a dose rate of 10 Gy/min allowed reducing this time to approximately 7 minutes.

3.3. Validation

3.3.1. Macrophage polarization is similar in simple and multiple drop irradiation chambers

At first, the polarization status of differentiated and polarized macrophages was examined in multiple drop irradiation chambers and compared to the one in simple irradiation chambers. This verification aimed to ensure that the configuration of new chambers (reduced volume and increased cell number) did not alter the activation state of macrophages. In order to make this comparison, the expression of M1 (TNFα, IL-1β, IL-6 and CXCL10) and M2 (CD206, CCL18 and CCL22) markers was evaluated by RT-qPCR 24h after the end of the polarization process (***Figure III.19***). The M1 markers were similarly expressed in M1 macrophages cultured in simple or multiple drop irradiation chambers, while these markers appeared at very low levels in M2 macrophages in both chambers. It has to be noticed that the expression of CXCL10 was 6 times higher in M1 macrophages cultured in multiple drop irradiation chambers as compared to its expression in M1 macrophages cultured in simple chambers. Similarly, the M2 markers were highly expressed in M2 macrophages but not in M1 macrophages whatever the support. For M2 macrophages, the expression of CD206 was also higher in multiple drop irradiation chambers than in simple chamber. Altogether, these results confirm a similar polarization status in both irradiation chamber types.

3.3.2. The use of a higher dose rate does not alter A549 cell survival and macrophage reprogramming after proton irradiation

Due to the use of a different dose rate and a vertical scanning irradiation process, we analyzed the effects of these changes on A549 cell survival and M2 macrophage reprogramming.

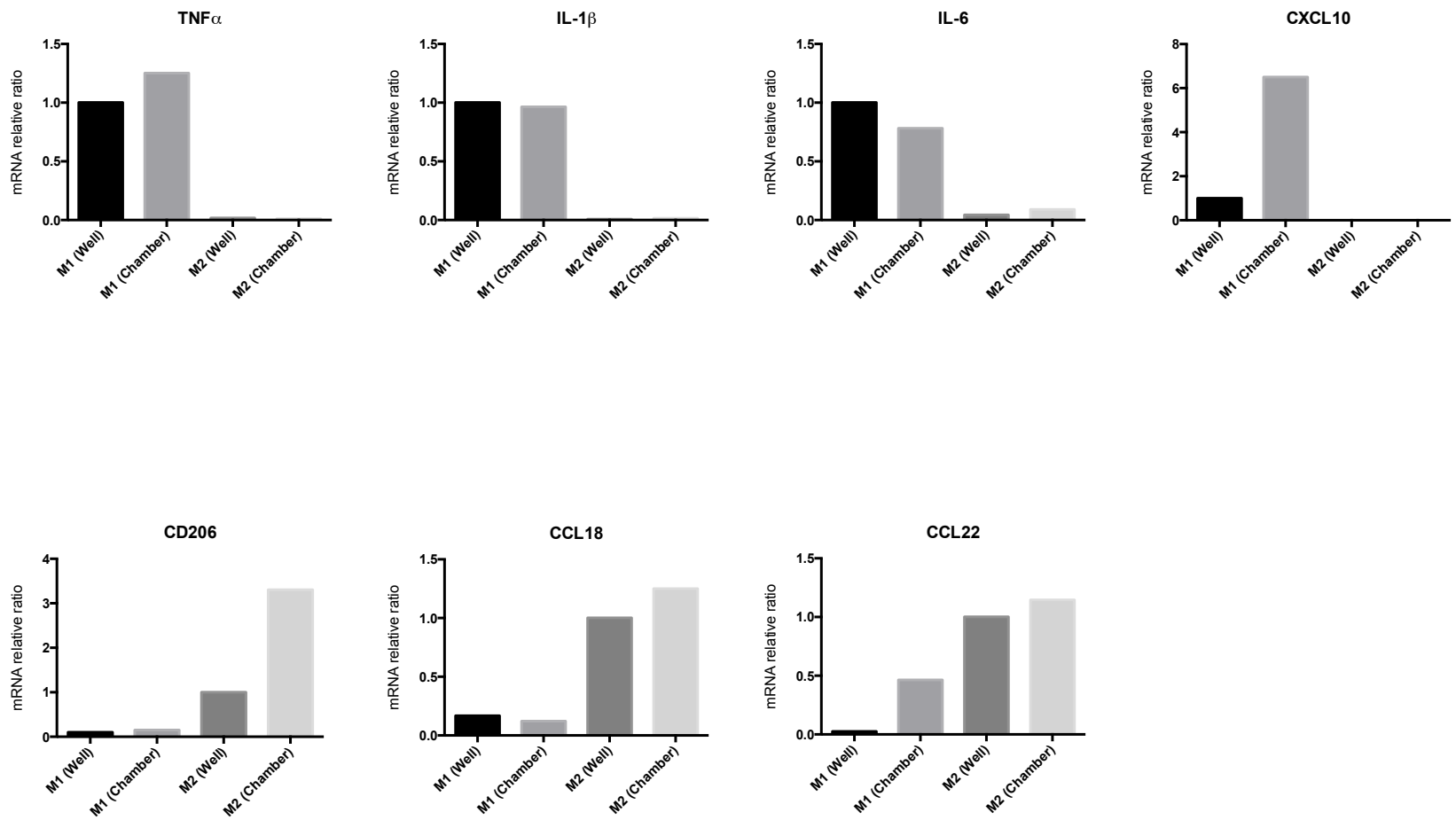

Figure III.19 – Polarization status of M1 and M2 macrophages in simple and multiple drop irradiation chambers

mRNA levels of M1 (TNFα, IL-1β, IL-6 and CXCL10) and M2 (CD206, CCL18 and CCL22) markers were evaluated by RTqPCR in M1 and M2 macrophages cultured in simple irradiation chambers or multiple drop irradiation chambers (N=1).

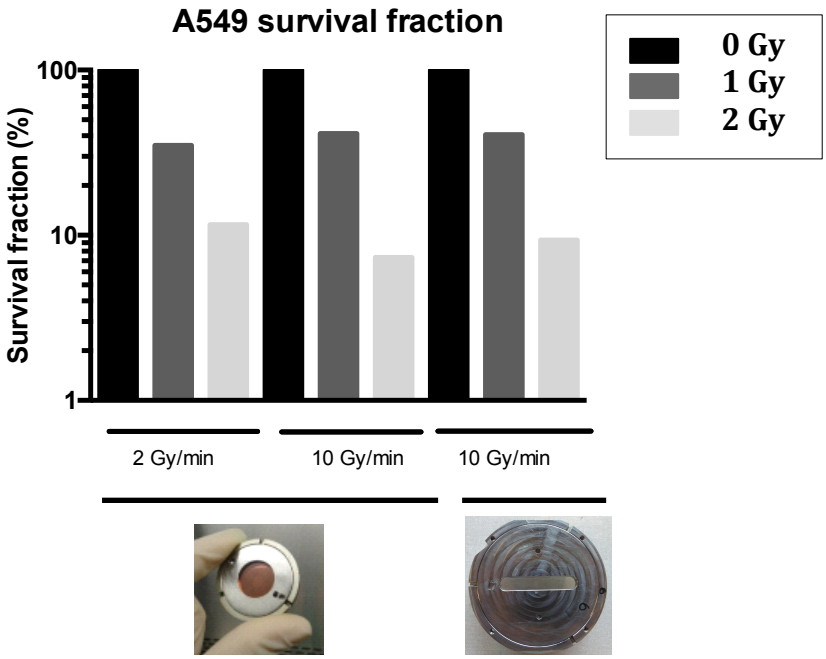

Figure III.20 – Survival fraction of A549 cells after proton irradiation
Survival fraction of A549 cells exposed to proton irradiation (1 or 2 Gy) in simple chambers or multiple drop irradiation chambers. Two dose rates were tested: 2 Gy/min and 10 Gy/min. Survival fractions were calculated using conventional clonogenic assays. The survival fraction of unirradiated A549 cells was set to 100% and the survival fractions of treated A549 cells were normalized with unirradiated A549 cells (N=1).

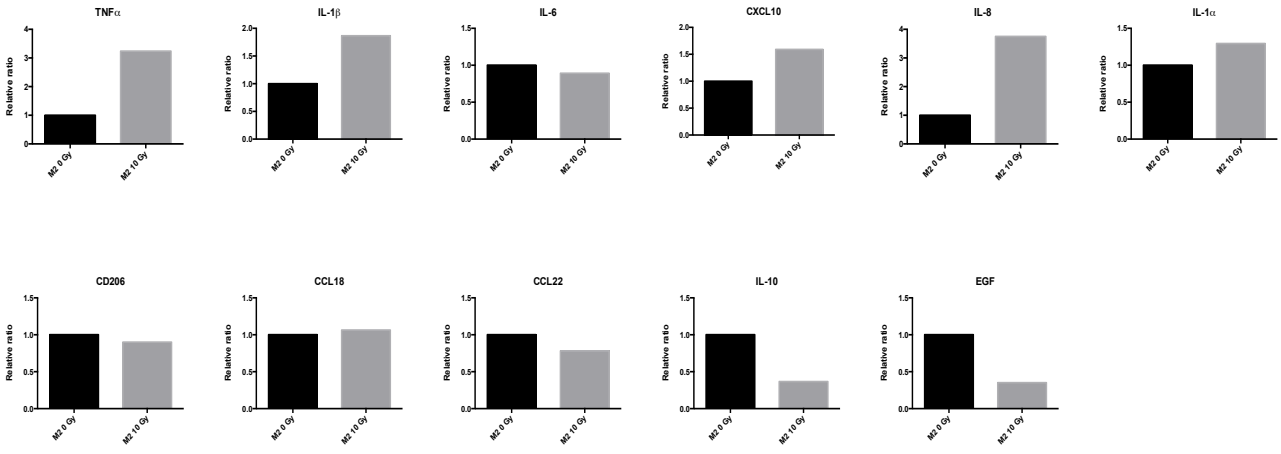

Figure III.21 – M2 macrophage reprogramming after 10 Gy proton irradiation in multiple drop irradiation chambers
M2 macrophages were irradiated with different doses of protons. 24h after proton irradiation, mRNA levels of M1 (TNFα, IL-1β, IL-6, CXCL10, IL-8 and IL-1α) and M2 (CD206, CCL18, CCL22, IL-10 and EGF) markers were assessed by RTqPCR (N=1).

The survival of A549 cells after proton irradiation was assessed by clonogenic assay. This method is a gold standard experiment based on the ability of cells to form colonies within a given growth environment. This *in vitro* experiment enables the study of cell death by plating cells with a low confluence and then allowing the formation of colony from single cells. After several days, only colonies exceeding 50 cells are taken into account. Indeed, a colony formed by 50 cells represents five or six generations of proliferation, hence excluding surviving cells that lost their proliferating ability (differentiated cells or sublethally damaged cells). This test compares the survival rate of treated cells to the one of untreated cells. Following the irradiation, A549 cells were seeded in 6 well plates with different densities according to the dose. After 11 days, the cells were colored with Violet Crystal solution and scored to establish the survival rate. The survival fraction is calculated as the ratio of the plating efficiency of treated cells related to the plating efficiency of control cells.

$$\text{Surviving fraction} = \frac{\text{PE irradiated cells (colonies of minimum 50 cells)}}{\text{PE control cells}}$$

Surviving fractions are usually used for establishing survival curve, a plot of surviving fractions against dose.

Directly after the exposure to a single dose of 1 or 2 Gy of proton irradiation, A549 cells were plated in 6-well plates for conventional clonogenic assay in order to compare the survival fractions of cells irradiated with two different dose rates: 2 Gy/min versus 10 Gy/min (***Figure III.20***). Similar survival fractions were observed for A549 cells irradiated with a dose rate of 2 Gy/min or 10 Gy/min in simple irradiation chambers. Survival rate dropped to 35 % and 41 % after 1 Gy of proton irradiation and to 12 % and 7% after 2 Gy when 2 Gy/min and 10 Gy/min were applied respectively. In addition, the scanning irradiation of A549 cells plated in multiple drop irradiation chambers did not alter the results obtained in simple irradiation chamber as the survival fraction of cancer cells felt off to 41 % after 1 Gy and 9 % after 2 Gy. These results are also comparable to the ones previously obtained by Anne-Catherine Wéra *(Wéra et al., 2011).*

In parallel, the M2 macrophage reprogramming was also studied in multiple drop irradiation chambers following 10 Gy of proton irradiation (***Figure III.21***). The results evidenced a higher expression of almost all M1 markers (TNFα, IL-1β, CXCL10, IL8 and IL-1α) in irradiated M2 macrophages while the mRNA levels of M2 markers in M2 macrophages were unchanged (CD206, CCL18) or reduced (CCL22, IL-10, EGF) 24h after proton irradiation.

In conclusion, these results confirmed that the use of scanning irradiation with a dose rate of 10 Gy/min did neither influence the effect of proton irradiation on cancer cell survival nor on M2 macrophage reprogramming, in multiple drop irradiation chambers.

3.3.3. Set-up of the experimental model for proton-irradiated co-cultures of M2 THP-1 macrophages and A549 cancer cells

After several adjustments, the irradiation protocol for the irradiation of co-cultured macrophages and cancer cells was established as followed (***Figure III.22***): THP-1 cells were

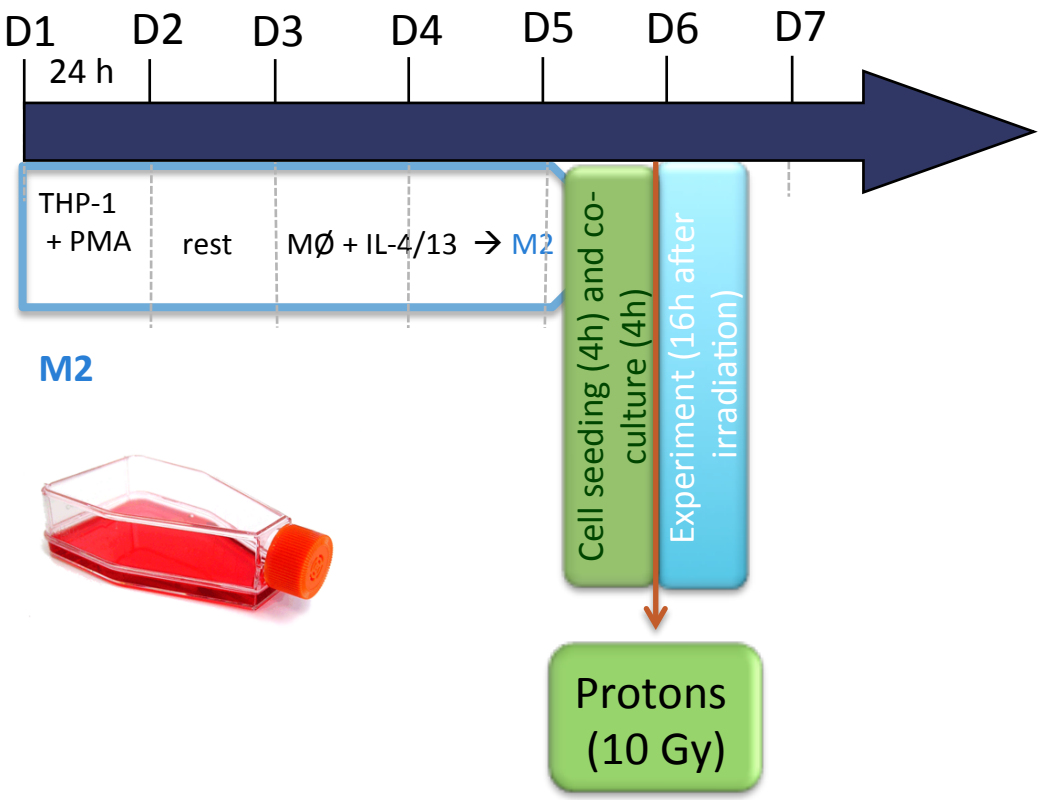

Figure III.22 - Schematic representation of the experimental model of irradiated co-culture

THP-1 monocytes (3.6 x 10^6) were differentiated with 150 nM PMA for 24h in T75 flask. The next day, medium was replaced by supplemented RPMI without PMA for the following 24h. Differentiated macrophages were polarized into M2-like macrophages with 20 ng/ml rhIL-4 and 20 ng/ml rhIL-13 for 48h. 8h before irradiation, A549 cells and M2 macrophages were seeded on the top side or de bottom side of irradiation chambers respectively. 4h after the seeding, irradiation chambers were closed and filled with CO_2 independent medium. A co-culture of both cell types were performed for 4h. The same day, both cell types were exposed to 10 Gy of proton irradiation.

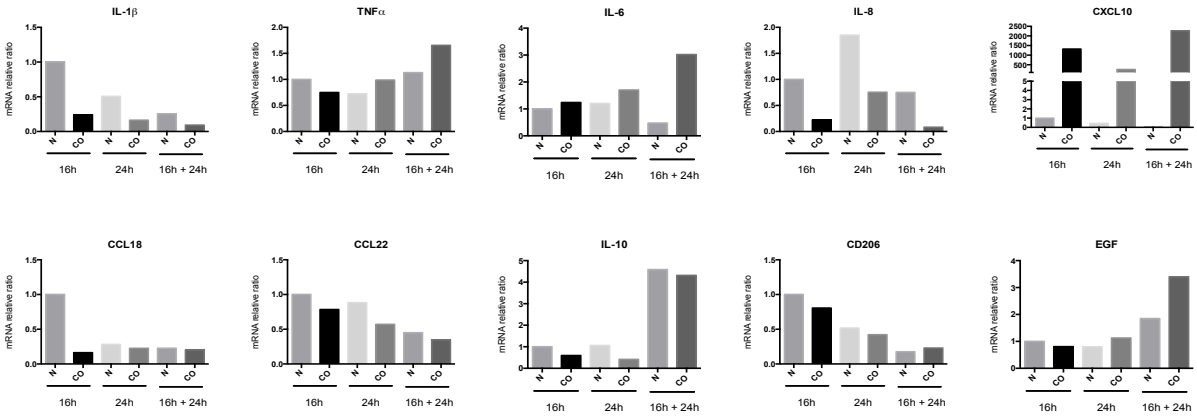

Figure III.23 - Polarization status of co-cultured M2 macrophages after different time points

M2 macrophages were co-cultured with A549 cells for 16h, 24h or 40h (16h + 24h) to mimic the experimental model of co-culture irradiation. mRNA levels of M1 (IL-1β, TNFα, IL-6, IL-8 and CXCL10) and M2 (CCL18, CCL22, IL-10, CD206 and EGF) markers were assessed by RTqPCR (N=1).

Co-cultured M2 macrophages (16h)	Co-cultured M2 macrophages (24h)	Co-cultured M2 macrophages (16h + 24h)
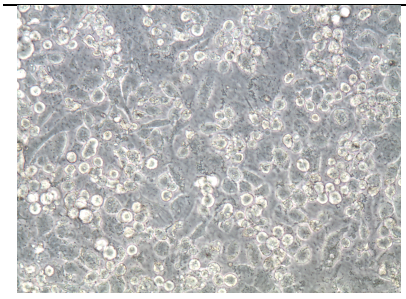	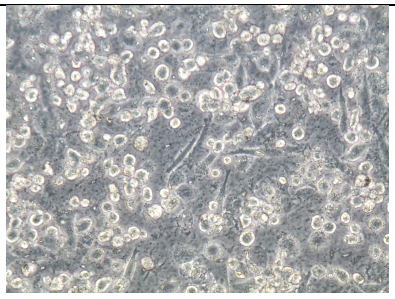	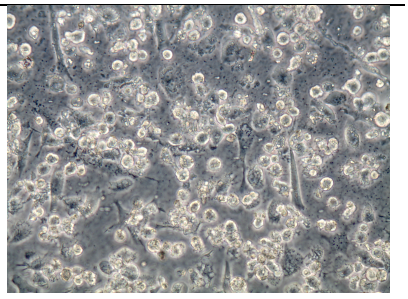

Figure III. 24 – Phenotypic alteration of macrophages co-cultured with A549 cells

M2 macrophages were co-cultured with A549 cells for 16h, 24h or 40h (16h + 24h) to mimic the experimental model of irradiated co-culture. Pictures were captured before performing RNA extraction and revealed the lost of M2 macrophage elongated shape and the acquisition of a round one for long time points (24h and 16h + 24h).

differentiated and polarized into M2 macrophages in T75 flask, 4 days before irradiation. On day 5, M2 macrophages were detached with Triple E and seeded in five 45µl-drops (50 000 cells/drop) on the bottom side of multiple drop irradiation chambers. At the same time, A549 cells were trypsinized and seeded in five 45µl-drops (50 000 cells/drop) on the top side of multiple drop irradiation chambers. Both types of cells were allowed to adhere on their respective chamber side for 4h. After this period, the irradiation chambers were closed and filled with CO_2 independent medium supplemented with 3.75 g/L D-glucose, 2mM L-glutamine and 10 000U/ml penicillin-streptomycin. The cells were then co-cultured for 4h before proton irradiation and analyses were performed 16h after irradiation. These timings were chosen based on previous experiments assessing the mRNA levels of M1 and M2 markers in co-cultured macrophages. Indeed, for longer periods, we observed a decreased expression of M2 marker mRNA levels for long time points (24h and 16h + 24h) (***Figure III.23***). In addition to these molecular changes, phenotypic alterations were noticed in macrophages as they lost their elongated shape and acquired a round one (***Figure III.24***), reflecting a depolarization of macrophages.

3.4. Results

3.4.1. Co-culture with M2 macrophages does not influence the expression of pro-apoptotic proteins in proton-irradiated A549 cells

DNA damage promotes the phosphorylation of ATM and ATR that respectively phosphorylate Chk2 (checkpoint kinase 2) and Chk1. In turn, Chk2 and Chk1 activate the transcription factor p53 by phosphorylation. This event prevents the proteosomal degradation of p53 and thus stabilizes this factor. It was also noticed that ATM and ATR may directly phosphorylate p53. Once activated, this transcription factor regulates the expression of pro- (e.g. BAX, BAK) and anti- (e.g. Bcl-2, MCL1) apoptotic genes *(Roos and Kaina, 2013).* In the established co-cultured conditions, the effects of proton irradiation on the expression of pro-apoptotic proteins were investigated in co-cultured A549 cells. To this aim, an analysis of the expression of three actors involved in the apoptotic pathway (p53, BAX and BAK) was evaluated by western blot analysis (***Figure III.25***).

Our preliminary results revealed that the expression of p53 was increased after proton irradiation (10 Gy) in A549 cells cultured alone. In addition, it seems that the presence of M2 macrophages slightly decreased the expression of p53 exposed to 10 Gy compared to irradiated A549 cells alone. In contrast, the quantification of phosphorylated p53, indicating an activation of this transcription factor, showed a reduction of its expression after the irradiation. This reduction was less significant after the irradiation of co-cultured A549. Under stress, the level of phosphorylated p53 is usually increased and correlates with an identical or increased level of total p53. In our case, it is possible that p53 undergoes other posttranslational modifications than phosphorylation. It is known that p53 may be regulated by a variety of posttranslational modifications, comprising phosphorylation, acetylation, methylation, ubiquitination, sumoylation and neddylation. The acetylation of p53 may lead to p53 activation and is a potential regulator of radiosensitivity. Interestingly, under DNA damage, the acetylation of p53 can lead to different responses. In case of non-lethal DNA damage, unacetylated p53 engages cell

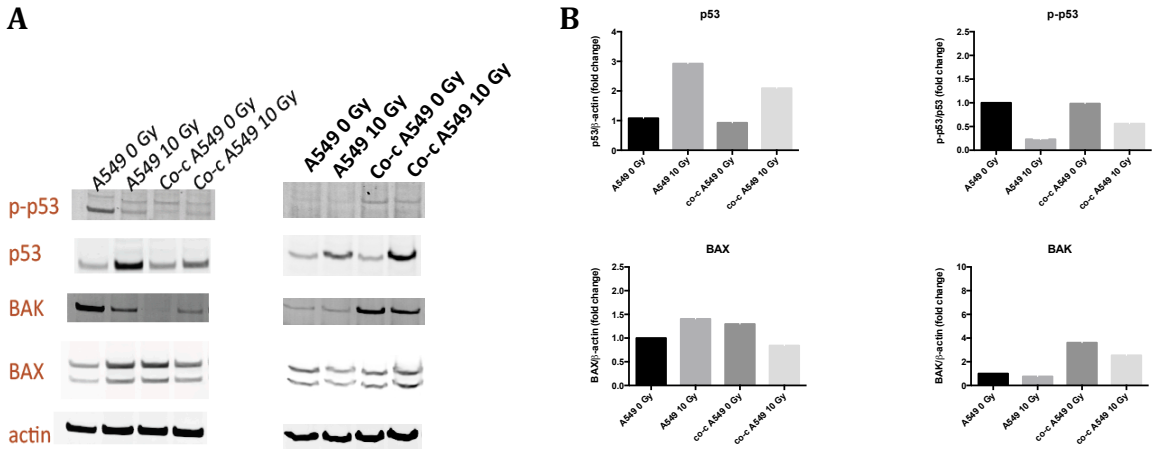

Figure III.25 – Co-culture with M2 macrophages does not influence the expression of pro-apoptotic proteins in proton-irradiated A549 cells

(A) The protein levels of p53, phosphorylated p53 (p-p53), BAK and BAX were assessed by western blotting in A549 cells cultured alone or co-cultured with M2 macrophages (co-c) after proton irradiation (10 Gy). β-actin was used as loading control.

(B) Quantification of protein levels was performed as followed: total p53, BAK and BAX fluorescence intensity was normalized for β-actin fluorescence intensity while p-p53 fluorescence intensity was normalized for p53 fluorescence intensity (N=2; mean).

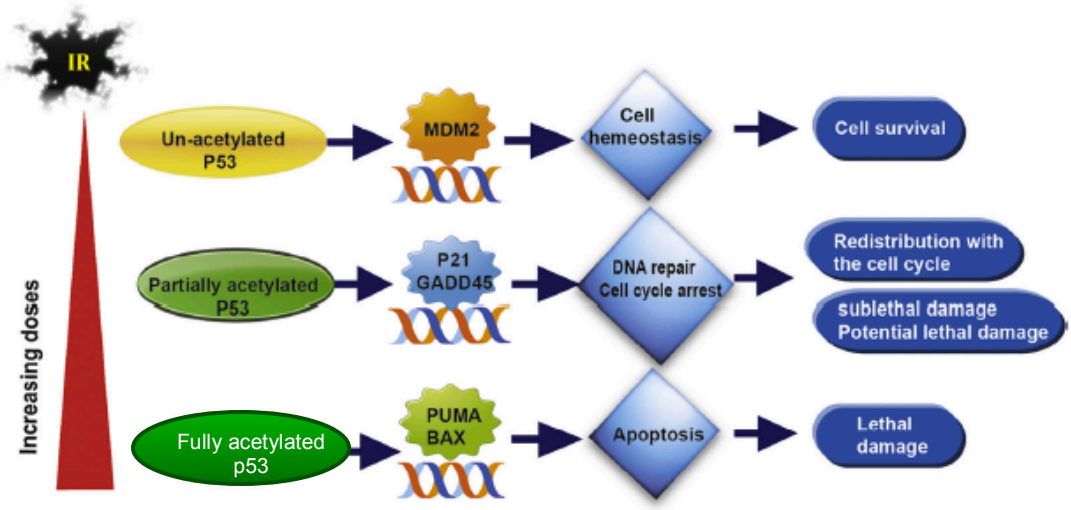

Figure III.26 – Relation between irradiation, p53 acetylation and cell response *(Zhang, Shen et al. 2015)*

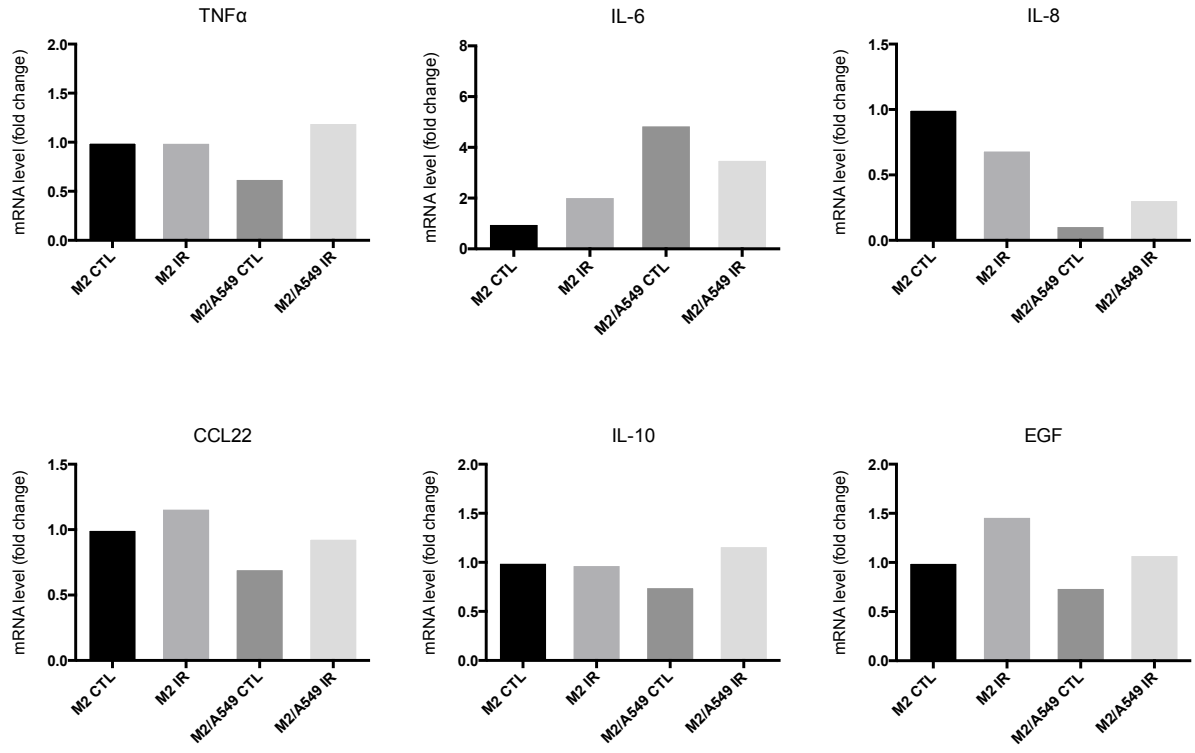

Figure III.27 – Proton irradiation induces macrophage reprogramming in co-cultured M2 macrophages

M2 macrophages cultured alone or with A549 cells were irradiated with 10 Gy of protons. 16h after proton irradiation, mRNA levels of M1 (TNFα, IL-6, IL-8) and M2 (CCL22, IL-10, EGF) markers were assessed by RTqPCR (N=2, mean).

survival. Potential lethal or sublethal DNA damage leads to partially acetylated p53 that induces DNA repair and cell cycle arrest. Finally, lethal damage favors the acetylation of p53 on specific residues (fully acetylated p53) and cells undergo apoptosis (***Figure III.26***) *(Zhang et al., 2015)*. Besides, the quantification did not reveal any effect of proton irradiation on BAK and BAX expression in A549 cells cultured alone or in co-culture with M2 macrophages. It was however noticed that there was a huge variability from an experiment to another. Therefore, our results suggest that the expression of pro-apoptotic proteins was not triggered in A549 cells 16h after irradiation. Interestingly, in another study, the presence of human peripheral blood monocyte-derived macrophages (hPBMC, M0 macrophages) protected a colorectal cancer cell line (SW1463) against radiation – induced apoptosis. Indeed, the authors observed a lower level of cleaved PARP and cleaved caspase 3 protein after X-ray radiation in co-cultured SW1463 cell line. This protection was generated by the elevation of the pro-survival gene expression (Bcl-2 and MCL1) in colorectal cancer cells. The expression of these genes was further increased in irradiated cancer cells, which were co-cultured with human M0 macrophages *(Pinto et al., 2016)*. In line with these observations, Marie Genin reported that cell death triggered by etoposide was reduced in A549 or HepG2 cells co-cultured with M2 macrophages. Interestingly, this protection was not noticed in A549 cells or HepG2 cells co-cultured with M0 or M1 macrophages *(Genin et al., 2015)*. Altogether, these results suggest that p53 expression would be impacted quite similarly in proton-irradiated A549 cells cultured alone or co-cultured with M2 macrophages.

3.4.2. Macrophage reprogramming in co-cultured macrophages after proton irradiation

In our co-cultured conditions, macrophage reprogramming was assessed by RT-qPCR 16h after the irradiation (***Figure III.27***). Neither the presence of A549 cells, nor the irradiation seem to influence the mRNA levels of CCL22 and IL-10 (M2 markers) in M2 macrophages. However, the expression of EGF (M2 marker) tended to be slightly increased in M2 macrophages exposed to proton irradiation but not in irradiated M2 macrophages co-cultured with A549 cells. Although the mRNA expression of TNFα (M1 marker) was not altered by 10 Gy of proton irradiation in macrophage cultured alone or in the presence of A549 cells, the expression of IL-6 and IL-8 (M1 markers) tended to be respectively higher and lower in co-culture conditions. Interestingly, the TNFα release (***Figure III.28***) in medium from M2 macrophages cultured alone was higher after irradiation compared to control cells. These experiments corroborate the macrophage reprogramming previously observed after 10 Gy of proton irradiation (***Figure 4 article***). The same trend was observed when M2 macrophages were co-cultured with A549 cells, as the irradiation of both cells also induced an increased secretion of TNFα compared to the unirradiated co-cultured cells. To ensure that TNFα was not released by irradiated A549 cells, the secretion of TNFα was also evaluated in irradiated and unirradiated A549 cells cultured alone. The contribution of A549 cells to the release of TNFα in the extracellular medium was very low and should not be responsible for the high TNFα release observed in medium from irradiated co-cultured cells. As a whole, these results confirmed that moderate doses of proton irradiation orchestrate M2 macrophage reprogramming towards a mixed M1/M2 phenotype and showed that the presence of cancer cells did not influence this reprogramming 16h after proton irradiation.

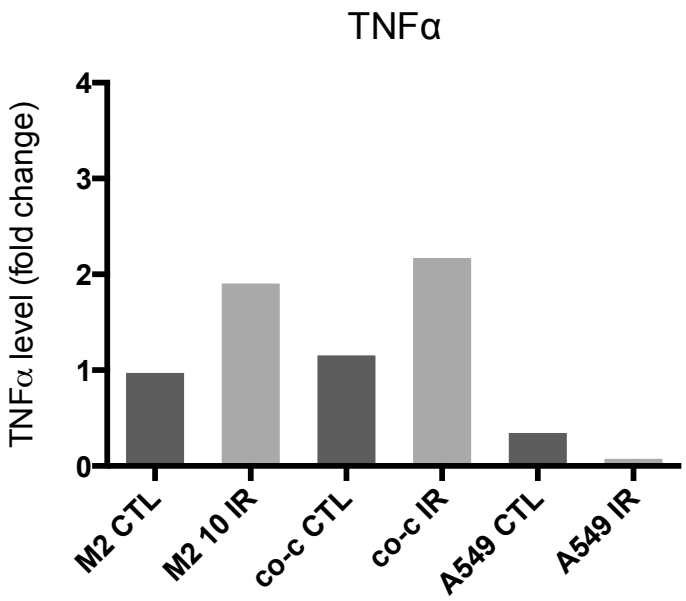

Figure III.28 – TNFα release after proton irradiation in co-cultured M2 macrophages
M2 macrophages cultured alone or with A549 cells were irradiated with 10 Gy of protons. 16h after proton irradiation, TNFα secretion was evaluated by ELISA. Results are expressed in pg/ng of proteins and are normalized to the corresponding non-irradiated M2 macrophage (fold change) (N=2, mean).

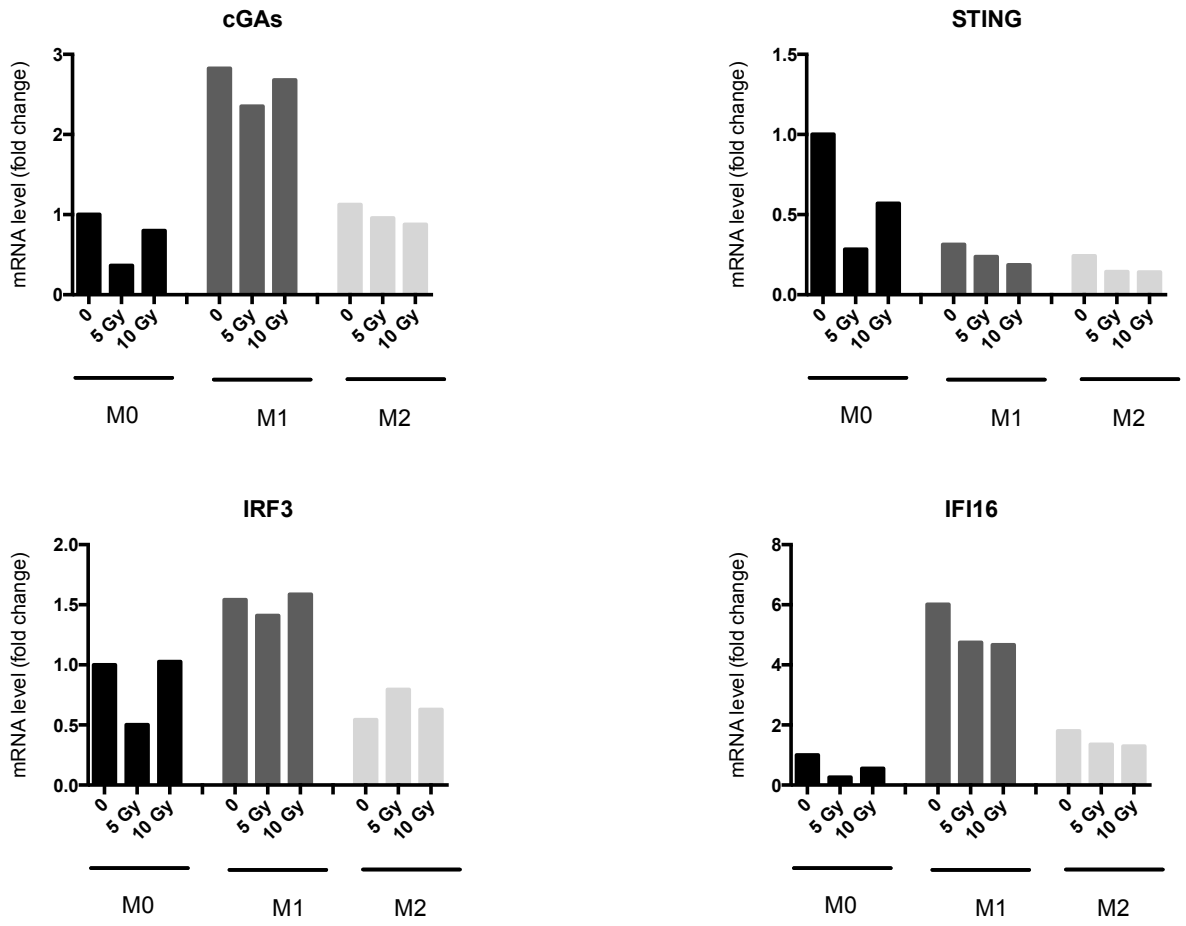

Figure III.29 – Proton irradiation does not influence the mRNA level of genes involved in the cGAS/STING pathway in M0, M1 and M2 macrophages

M0, M1 and M2 macrophages were irradiated with different doses of protons (5 and 10 Gy). 24h after proton irradiation, mRNA levels of cGAS, STING, IRF3 and IFI16 were assessed by RTqPCR (N=1).

In our laboratory, Marie Genin already showed that co-culture macrophages with HepG2 cells did not alter the mRNA levels of M1 and M2 markers in M0, M1 and M2 macrophages *(Genin et al., 2015)*. In contrast with our results, another study revealed that colorectal cancer cells (SW1463 or RKO cell lines) promoted a pro-inflammatory phenotype in differentiated human macrophages (M0). In the same study, the pro-inflammatory phenotype of co-cultured macrophages was maintained after X-ray irradiation (5 x 2 Gy over 5 days) *(Pinto et al., 2016).*

3.4.3. cGAS/STING pathway activation in macrophages

As described in chapter 2, cytosolic recognition of microbial DNA *(Jonsson et al., 2017)* or cancer cell DNA in immune cells promotes pro-inflammatory cytokine production through the activation of cyclic GMP/AMP synthase (cGAS) and the stimulator of interferon genes (STING). The release of these pro-inflammatory factors is mediated by the nuclear activation of transcription factors such as IRF3 and NFκB *(Cai et al., 2014).* The inducible factor 16 (IFI16) also contributes to cGAS/STING pathway by promoting the production of cGAMP and by recruiting and activating the TANK-binding kinase 1 (TBK1) in STING complex *(Jonsson et al., 2017)*. Interestingly, the expression of STING in macrophages is associated with spontaneous rejection of immunogenic or partially allogenic tumors *(Chen et al., 2016a)*. Moreover, it was recently shown that the activation of host STING by radiotherapy triggered the death of immunogenic cancer cells *(Deng et al., 2014)*. As the combination of X-ray radiation (10 Gy) to cyclic dinucleotides (CDNs), known to activate STING pathway, generated a reprogramming of macrophages *(Baird et al., 2016)*, we sought whether the cGAS/STING pathway could be required for M2 reprogramming in co-cultured macrophages. For this preliminary study, we analyzed the effect of proton irradiation on the mRNA expression of four factors of the DNA sensor pathway (cGAS, STING, IRF3 and IFI16) in co-cultured macrophages.

We first evaluated the influence of proton irradiation on the expression of this pathway in M0, M1 and M2 macrophages. Although these results must be confirmed by other replicates, we observed that the expression of cGAS, IRF3 and IFI16 was higher in M1 macrophages while the expression of STING was similar between the three phenotypes (***Figure III.29***). These results were not surprising as M1 macrophages are associated with phagocytosis and microbial elimination *(Qian and Pollard, 2010)*. Furthermore, proton irradiation (5 or 10 Gy) did not influence the expression of these genes in M0, M1 or M2 macrophages.

A significant increase of the cGAS mRNA level was observed in proton - irradiated M2 macrophages co-cultured with A549 cells (***Figure III.30***). The irradiation of macrophages cultured alone or the presence of A549 cells did not alter the expression of this factor. Although the expression of IRF3 did not seem to be influenced by proton irradiation (5 or 10 Gy) after 24h (***Figure III.29***), the irradiation of M2 macrophages induced a slight decrease in IRF3 mRNA level 16h after proton irradiation (10 Gy). However, the effect of proton irradiation on IRF3 expression was abrogated when M2 macrophages were co-cultured with A549 cells (***Figure III.30***). As we showed in irradiated M0, M1 or M2 macrophages, STING expression was not influenced by the irradiation (***Figure III.29***) or by the polarization. The irradiation of co-cultured macrophages neither influenced the mRNA expression of STING (***Figure III.30***). Regarding IFI16, the mRNA expression of this gene was significantly increased in co-cultured

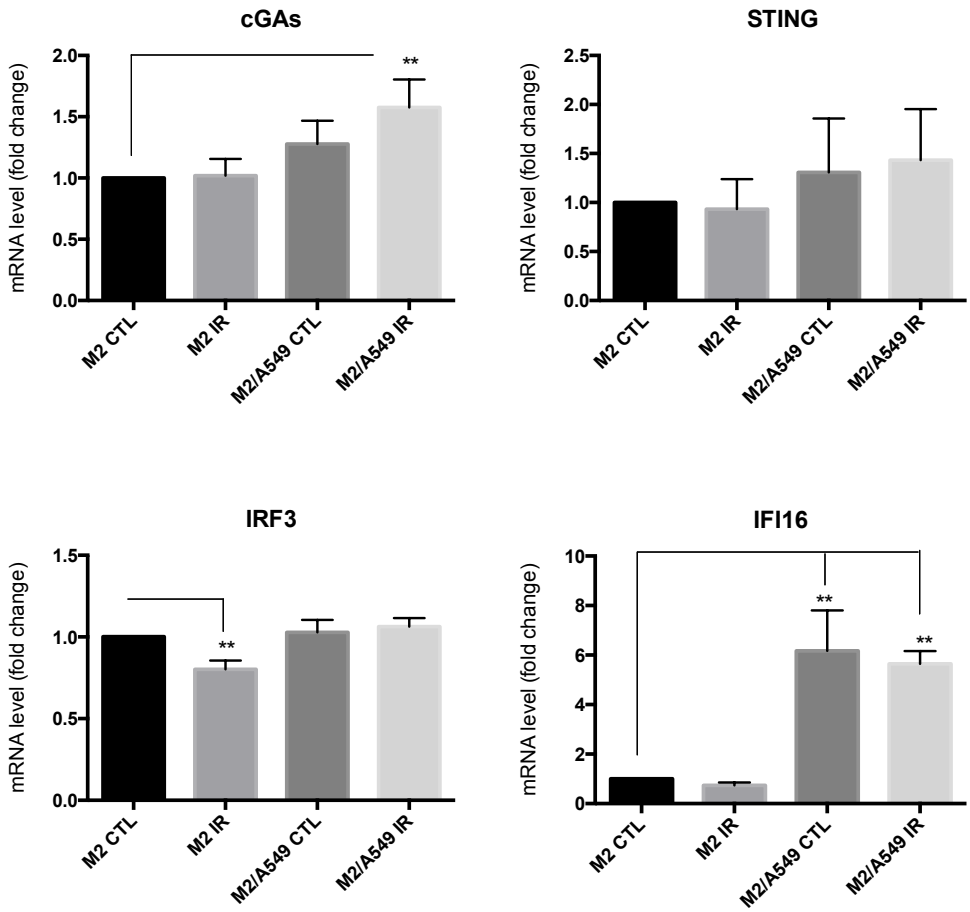

Figure III.30 – Proton irradiation promotes cGAS/STING pathway activation in M2 macrophages co-cultured with A549 cancer cells.

M0, M1 and M2 macrophages were irradiated with different doses of protons (5 and 10 Gy). 24h after proton irradiation, mRNA levels of cGAS, STING, IRF3 and IFI16 were assessed by RTqPCR (N=3, mean ± SD). One-way ANOVA analyses followed by Dunnett's multiple comparison tests were performed to evaluate the significance (* $p \leq 0.05$; ** $p < 0.01$; *** $p < 0.001$).

macrophages but proton irradiation had no additional effect on its expression. IFI16 is well known for its role in DNA sensing *(Jonsson et al., 2017)*. However, the increased expression of this factor in unirradiated co-cultured macrophages suggests a regulation of its expression via another pathway. Similarly to our study, the expression of IFI16 was upregulated in the supernatant from co-culture of normal bone marrow cells and human primary myeloma cells that *(Bam et al., 2015)*. It is well established that an activation loop exists between cancer cells and macrophages: cancer cells release CSF1 that recruits macrophages into the tumor and in turn, recruited macrophages secrete endothelial growth factor (EGF), activating the migratory capability of cancer cells *(Wyckoff et al., 2004; Wyckoff et al., 2007).* In response to M-CSF, it was shown that p204, the mouse orthologue of IFI16, was activated in macrophages, inducing macrophage differentiation *(Dauffy et al., 2006)*. Therefore, it would be interesting to investigate the role of the EGF – CSF1 axis in the elevated IFI16 expression in co-cultured macrophages. Once activated, IFI16 fulfils multiple functions, ranging from DNA damage response, apoptosis and senescence promotion, cell growth, and cell differentiation regulation *(Dell'Oste et al., 2015)*. Interestingly, in tumors, IFI16 inhibits cell growth and angiogenesis, but it induces macrophage recruitment, thus exerting an antitumoral activity *(Mazibrada et al., 2010)*.

Although these results need to be confirmed at protein level, it suggests that cGAS/STING pathway is partially activated in co-cultured macrophages and that proton irradiation affects the expression of cGAS in co-cultured macrophages. The analysis of this pathway at different time points post-irradiation could allow to evaluate the effect of dead cancer cells on the activation of cGAS/STING pathway in macrophages. Furthermore, in order to evaluate the impact on this pathway on macrophage reprogramming, it could be interesting to analyze the activation of IRF3 and NFκB, as well as the expression of IFNα/β in co-cultured macrophages exposed to proton irradiation.

3.5. Conclusions and perspectives

In the second part of this thesis, we set up co-culture experiments in order to study the impact of proton irradiation on the interactions between cancer cells and M2 macrophages. Our preliminary results indicated that the expression of pro-apoptotic proteins was not trigerred in proton-irradiated A549 cells cultured alone or co-cultured with M2 macrophages. It also suggested that the presence of cancer cells (A549 cell line) did not alter the proton irradiation – induced macrophage reprogramming 16h after treatment. Finally, proton irradiation could also trigger the activation of cGAS/STING signaling pathway in M2 macrophages. This signaling axis is involved in immunogenic cell death of cancer cells and is implied in macrophage reprogramming.

However, these preliminary results should be completed with the investigation of some important matters and by performing major experiments.

First, despite the developments performed to set-up the co-culture experiments, some improvements are still required. As we observed that the co-culture of macrophages and A549 cells could not be extended longer than 24h with the actual multiple drop chambers, new chambers were designed with a volume capacity of 1 ml instead of 200 µl. In fact, phenotypic

alterations of macrophages, caused by a depolarization, were noticed when cells were co-cultured in the same medium for 24h or longer. These changes were probably related to a depletion of glucose and other nutrients in the medium shared by macrophages and cancer cells. This hypothesis is strengthened by the fact that Marie Genin did not observe macrophage depolarization when M2 macrophages were co-cultured with A549 cells for 40h in 6-well plate *(Genin et al., 2015)*. In the actual configuration, 250 000 A549 cells (50 000 x 5 drops) and 250 000 M2 macrophages (50 000 x 5 drops) were seeded on their respective sides of the chamber and chambers were filled with 200 µl. This setting was decided to favorize cytokine exchange and interactions between both cell types. An increase in volume capacity should allow prolonging the time of co-culture before and after proton irradiation, in order to perform analyses 24h or 48h after irradiation.
Another limitation we have met is the impossibility to obtain homogeneous monolayer of M0 macrophages. As we encountered seeding problems for A549 cells on the top side of irradiation chambers when macrophages were differentiated and polarized in irradiation chambers, the , differentiation and polarization of macrophages was performed in T75. After the detachment of M0 macrophages and their seeding in irradiation chambers, the cells tend to form clusters. The polarization of M0 macrophages into M1 or M2 macrophages induces the spreading of cells, thus preventing this problem. Although the use of M0 macrophages has brought an additional and complementary support to study the effect of proton irradiation, this phenotype is rarely found in tumors, due to the presence of multiple cytokines and mediators that rapidly polarize macrophages in tumors. If the use of M0 macrophages is required for future experiments, a solution would be to use two different steel stainless top sides: the first one during macrophage differentiation (using cloning cylinders and Cell Tak) and the second one for the seeding of A549 cells.

The first results obtained after proton irradiation of co-cultured cells indicated an elevation of p53 expression in irradiated A549 cells alone or in co-culture with M2 macrophages. However, our results did not reveal the expression of pro-apoptotic proteins in A549 cells, 16h after 10 Gy of proton irradiation. The gold standard for studying cell death after irradiation is the clonogenic assay. In our case, a dose of 10 Gy would kill a lot of cells, hence generating a very small survival fraction and thus a high variability. In addition, as A549 cells are co-cultured with M2 macrophages during 16h after the irradiation, and as early apoptosis may occur during this time, a clonogenic assay at this time would underestimate the cell death.
In order to better understand the effect of proton irradiation on co-cultured A549 cells, it would be interesting to analyze cell death with other methods, such as flow cytometry or western blot. For instance, the Annexin V/propidium iodide staining would bring useful information about cell death type (apoptosis, necrosis…) and cell cycle arrest. These experiments should be performed at different time points post-irradiation. Another experiment that could be performed is the quantification of cleaved caspase 3/7 and cleaved PARP by western blot analysis at different time points post-irradiation. It is well known that the vast majority of cancer cells die through late cell death after irradiation. The kinetic study of cell death should thus include late time points. In fact, irradiated cells cease proliferationg after attempting mitosis one or more times *(Joiner and Kogel, 2009)* and progress to mitotic catastrophe and senescence, that are both non-lethal mechanism *(Galluzzi et al., 2018)*. Mitotic catastrophe is characterized by nuclear changes, including multinucleation, macronucleation and micronucleation. This mechanism mainly involves the activation of p53 and caspase 2, and is characterized by a prolonged cell cycle

arrest. Eventually, cells undergo intrinsic apoptosis or enter cellular senescence *(Galluzzi et al., 2018)*. Therefore, the analysis of nuclear morphology with DAPI labeling, as well as the quantification of cleaved caspase 2 levels would allow evaluating the impact of proton irradiation on mitotic catastrophe in co-cultured A549 cells.

Secondly, we have demonstrated that M2 macrophage reprogramming occurred after moderate doses of proton irradiation, even when co-cultured with A549 cancer cells. The new configuration of multiple drop irradiation chambers should allow the analysis of macrophage reprogramming after longer time points, such as 24h or 48h after irradiation. Furthermore, the study of additional markers such as IL-1α, IL-12 (M1 markers) and TGFβ (M2 markers) would also consolidate our results. Finally, a classical feature of M1 macrophages is bacterial phagocytosis. Therefore, it could be interesting to analyze phagocytosis activity of irradiated M2 macrophages in order to further characterize their reprogramming towards a M1 phenotype. These experiments can be performed by using fluorescent beads or fluorescent *E. coli*.

Finally, we evaluated the activation of cGAS/STING pathway at mRNA levels. Interestingly, we noticed an elevation of cGAS expression in M2 macrophages co-cultured with A549 cells 16h after proton irradiation. This pathway should be evaluated at protein levels by western blot analyses as well as by immunofluorescence labeling at different time points post-irradiation. Indeed, Jonsson and his collaborators have shown that STING dimerization occurred between 4h and 6h after dsDNA stimulation in THP-1 cells. In addition, the assessment of IRF3 levels and the study of NFκB phosphorylation would also bring more information about the activation of this signaling pathway. Therefore, we suggest measuring the NFκB nuclear translocation and the phosphorylation level of IRF3 in macrophages co-cultured with cancer cells, after proton irradiation. The analysis of IFNα/β release, as the final endpoint, would also help to characterize the effect of proton irradiation on this pathway in co-cultured M2 macrophages. If an activation of this pathway is confirmed in irradiated M2 macrophages co-cultured with A549 cells, the effects of the invalidation of cGAS or STING on macrophage reprogramming after proton irradiation would finally consolidate the results obtained in this second part.

Additionally, these experiments should be confirmed with TAMs isolated from tumor-bearing mice and with an *in vivo* model in order to study the effect of proton irradiation on macrophage reprogramming and tumor regression.

In conclusion, these preliminary results revealed macrophage reprogramming in the presence of cancer cells after proton irradiation. This reprogramming could be partly generated by the activation of NFκB, as observed in the first part of this project, as well as by the activation of cGAS/STING pathway. However, the analysis of macrophage phenotype 16h after proton irradiation did not reveal any differences between irradiated M2 macrophages alone or in co-cultured with A549 cells. Despite some experimental improvements and the need for additional experiments, our preliminary results would suggest that proton irradiation activate antitumor functions in M2 macrophages co-cultured with A549 cells.

1. Discussion and perspectives

1.1. Reprogramming of tumor-associated macrophages, a therapeutic strategy for cancer elimination

Tumor formation has long been considered as a multistep process where only genetic alterations drive the progressive transformation of normal cells into highly malignant cells *(Foulds, 1954)*. Often treated as a homogeneous monocellular tissue, tumors revealed many strategies to elude cytotoxic therapies *(Palucka and Coussens, 2016)*. In the last decades, emerging evidences have led to redefine the tumor as a complex heterogenic tissue constituted by neoplastic cells themselves and by a tumor microenvironment gathering an extracellular matrix, a vascular network and a diversity of normal resident and recruited accessory cells, that fuels tumorigenesis and tumor dissemination *(Hanahan and Coussens, 2012)*. Therefore, more and more therapeutic strategies have been focused on the elimination of cancer cells themselves, as well as have targeted cells from the tumor microenvironment *(Van der Jeught et al., 2015)*. In this context, we choose to focus on one of the most representative cells in tumors: the tumor-associated macrophages. TAMs represent a key feature of this microenvironment by playing different roles through their interactions with cancer cells and tumor invading cells. These roles mainly include tumor initiation, tumor promotion, tumor invasion and metastasis. TAMs also hold a particular interaction with endothelial cells and immune cells that favor the angiogenesis and the immunosuppression in tumors. All these functions are each associated to a specific phenotype, influenced by a specific local microenvironment, which triggers specific signaling pathways *(Qian and Pollard, 2010)*. However, all these TAM phenotypes are usually gathered under an oversimplified M2 phenotype with anti-inflammatory and pro-tumoral properties. This alternative activation state of macrophages contrasts with the classical activation state, also termed as the M1 phenotype, that is associated to pro-inflammatory, phagocytic and anti-tumoral roles. However, M1-like TAMs are usually few represented in settled tumors *(Biswas and Mantovani, 2010; Mittal et al., 2014)*.

Regarding the ability of macrophages to switch from a phenotype to another in function of the local microenvironment, M2-like TAM reprogramming seems to be a promising strategy to reverse the fate of tumors. In the last few years, a lot of researches have been focused on a way to target the reprogramming of pro-tumoral TAMs toward M1-like antitumoral macrophages. Different chemotherapies and immunotherapies, most of them already existing, have successfully triggered a re-education of TAMs with a concomitant tumor regression. However, as these therapies are not localized and could thus trigger a systemic inflammatory response, local radiotherapy is an attractive alternative. For a long time, studies have focused on the effect of radiotherapy on cancer cells. More recently, more and more researches in the field of radiobiology have integrated the microenvironment, and more precisely the immune system, in their studies *(Barker et al., 2015)*. Studies on macrophage reprogramming with local conventional radiotherapy revealed that moderate doses (1 – 10 Gy) were able to educate

unpolarized macrophages toward a M1 phenotype. However, to our knowledge, none of these researches have demonstrated a reprogramming of M2-like macrophages toward a M1 phenotype (See *Chapter 3*). As protontherapy presents several physical advantages over conventional radiotherapy and has demonstrated a different radiobiological response, understanding the effect of proton irradiation on macrophages, and more specifically on their reprogramming, could imply to re-evaluate the use of protontherapy for all kind of tumors.

1.2. M1 macrophage radioresistance to proton irradiation

Macrophages represent one of the more resistant cells of the immune system to irradiation. It was already shown that fusion of cancer cells with macrophages creates a population of radioresistant cells. This radioresistance is brought by ROS scavengers that neutralize ROS and prevent the radiation-induced cell death *(Lindstrom et al., 2017)*. Among these anti-oxidative mediators, the manganese superoxide dismutase (MnSOD) has already been demonstrated to confer radioresistance to several myelocytic cell lines *(Hachiya et al., 1997; Wong, 1995)*. As little is known about the effect of proton irradiation on macrophages, we first decided to analyze the effect of different doses of proton irradiation (1 – 10 Gy) on macrophage survival. In this work, the viability of differentiated and polarized THP-1 macrophages was differently influenced in the three phenotypes 16h after high doses (5 and 10 Gy) of proton irradiation.

1.2.1. Heterochromatin regions: a role in radioresistance?

By using ethidium bromide acridine orange, we analyzed the viability of M0, M1 and M2 THP-1 macrophages after proton irradiation and we found that M1 macrophages better survived to 5 and 10 Gy early after proton irradiation (16h), while M0 and M2 macrophages were more sensitive. In the literature, only few studies have analyzed the viability of macrophage phenotype to irradiation. Similarly to our results, a higher radioresistance to X-rays was observed in BALB/c mice naturally exhibiting a T_H1/M1 (T_H1 lymphocytes and M1 macrophages) response compared to C57BL/6 mice naturally exhibiting a T_H2/M2 response *(Nowosielska et al., 2012)*.

As DNA is the prominent target of ionizing radiation, the cell survival is directly correlated to DNA damage. Indeed, upon sensing DNA damage, the DNA damage response (DDR) is rapidly activated and triggers multiple pathways, including DNA repair machinery, cell cycle arrest, senescence or apoptosis. Among DNA damage, double strand-breaks (DSBs) are the most lethal forms due to their ability to induce genomic instability. The early cellular response to these DSBs is the phosphorylation of H2AX variant *(Mah et al., 2010)*. Once DNA damage are tagged by the phosphorylation of H2AX, ATM and DNA-PK amplify the DDR by creating large chromatin domains of γH2AX around the DSBs or in other words γH2AX foci. In this context, chromatin remodeling is important for the amplification of the response to DNA damage. Interestingly, chromatin condensation is required for triggering ATM/ATR signaling and is a potent mean to increase the signal around a single DSB. Subsequently, the chromatin relaxation is essential for promoting the downstream signaling and repair *(Burgess et al., 2014)*. γH2AX assay is a useful tool to detect the presence of DSBs after radiation. In order to further investigate the early

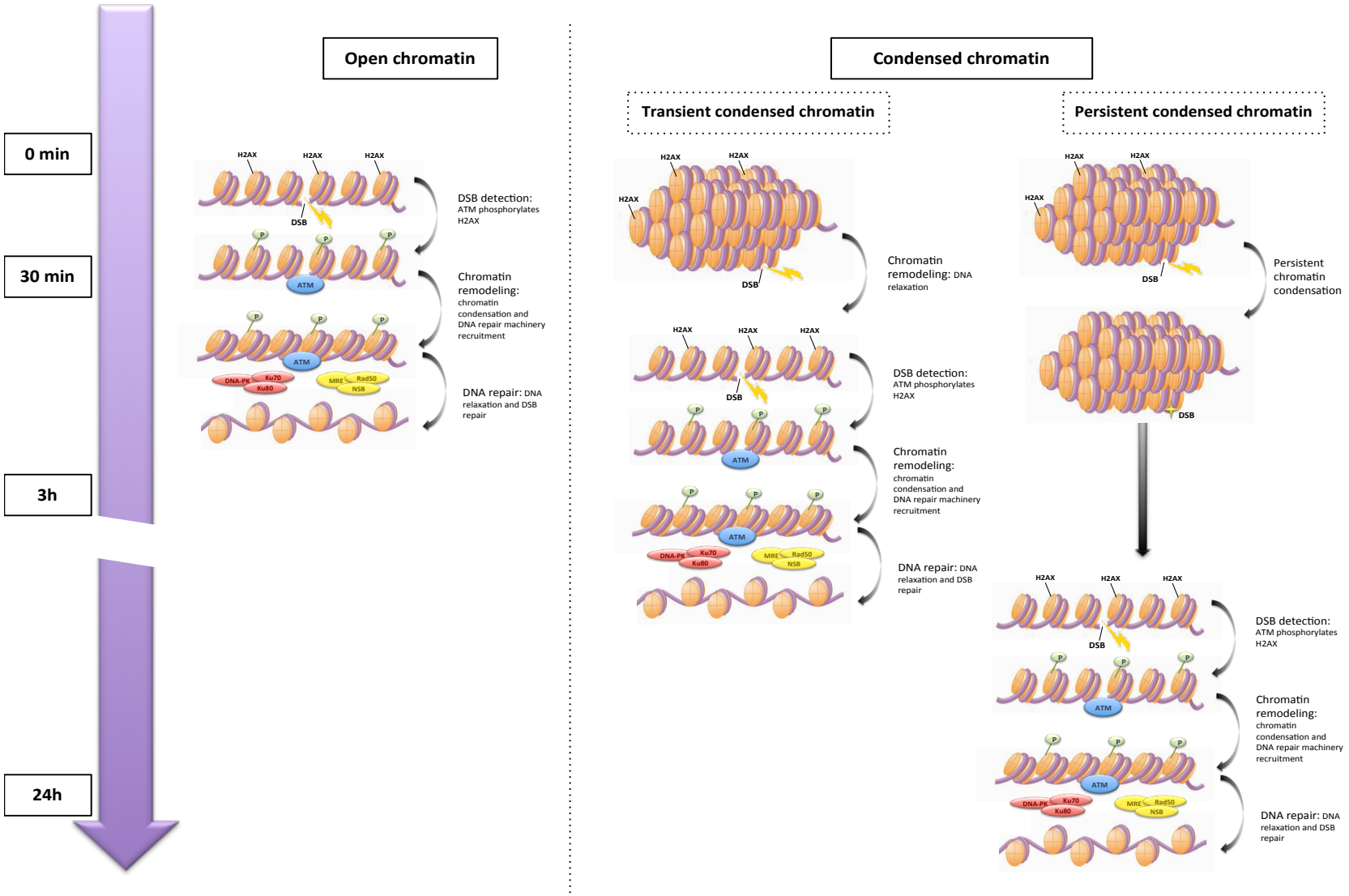

Figure IV.1 – Hypothetical mechanism for DSB detection after proton irradiation of macrophages

radioresistance of M1 macrophages to proton irradiation, we performed an immunofluorescence labeling of γH2AX 15 minutes after the irradiation. Quantification of γH2AX indicated a similar profile for M0, M1 and M2 macrophages early after being exposed to different doses (3, 5 or 10 Gy) of proton irradiation. With this γH2AX assay, it is possible to follow the DSB detection, while the link between the disappearance of γH2AX and DSB repair is less evident *(Bouquet et al., 2006)*. In order to follow the DSB detection, the γH2AX foci are labeled using specific antibodies along the time. The quantification of γH2AX over the time evidenced a decreased in the level of γH2AX 2h after irradiation in M0 and M2 macrophages while the level of DNA damage further increased in M1 macrophages 2h after irradiation. These results indicated a different kinetic of DNA damage detection in M1 macrophages compared to the M0 and M2 phenotypes.

Other studies have shown that the phosphorylation of H2AX is delayed in condensed chromatin regions. Indeed, there is a strong correlation at early time (30 minutes) post irradiation between γH2AX and euchromatic features while in the heterochromatic regions, this correlation appeared later (3h – 24h). It also means that the DSB repair may be affected by the chromatin state (***Figure IV. 1***). When the chromatin region is already in an open state before irradiation, it would be repaired earlier compared to compact chromatin regions. Indeed, these condensed chromatin regions require further structural remodeling before the DNA repair machinery could eventually exert its activity *(Natale et al., 2017)*. For this reason, we hypothesized that compaction of chromatin could be differently regulated in M0, M1 and M2 macrophage, thus influencing the response to irradiation. However, the evaluation of the heterochromatin content in unirradiated macrophages, using MNAse I assay, did not reveal any difference between M0, M1 and M2 macrophages. These results indicated that the radioresistance of M1 macrophages is probably not linked to the presence of higher level of condensed chromatin before irradiation. For the future experiments, it would be interesting to analyze the evolution of condensed and opened chromatin regions following irradiation and correlate these regions with γH2AX appearance. It was already shown that local chromatin condensation promotes ATM- and ATR- dependent activation of upstream DDR signaling. However, a persistent chromatin condensation is associated with a reduced recovery and survival. Indeed, we cannot exclude that chromatin remodeling after irradiation could be differently affected in the three macrophage subtypes. Chromatin remodeling is performed by DNA methylation or by multiple histone posttranslational modifications, comprising acetylation, methylation, phosphorylation and ubiquitination. These modifications require substrates from metabolic intermediates, such as acetyl-CoA or S-adenosylmethionine *(Turgeon et al., 2018)*. As chromatin organization has an impact on DNA repair, it would be not surprising that differential metabolism differently influences the DNA repair pathways, knowing that M1 and M2 macrophages present distinct metabolic status *(Van den Bossche et al., 2017)*. Therefore the analysis of chromatin compaction after irradiation could help to unravel the mechanism beyond different repair kinetics in M0, M1 and M2 macrophage subtypes.

1.2.2. The influence of ROS homeostasis on macrophage survival

Irradiated cells have to face cytotoxicity, generated by oxidative stress as well as DNA damage caused directly by DNA breaks or indirectly through ROS generation . As described above, the

efficacy of charged particle irradiation is usually associated with direct DNA damage. However, a report recently indicated that ROS production was higher in proton-irradiated glioma stem cells compared to the same cell line irradiated with X-rays. Interestingly, the authors showed that ROS levels constantly increased during the first 20h post proton irradiation (5 and 10 Gy) to progressively reach 7-fold increase 3 days post-irradiation. By using a ROS scavenger (TEMPOL), they also demonstrated that the majority of the efficacy associated to proton irradiation was generated by massive ROS production *(Alan Mitteer et al., 2015)*. As we have to deal with some technical constraints for our experiments, we choose to evaluate the ROS management in unirradiated M0, M1 and M2 macrophages, rather than the ROS levels in irradiated macrophages. The results indicated that M0 and M2 macrophages accumulated more ROS than M1 macrophages exposed to the same H_2O_2 concentration, meaning that M1 macrophages better manage ROS than the two other phenotypes. Based on these results, we could thus suggest that M1 macrophages could better survive to high ROS production induced by proton irradiation than the two other phenotypes.

The oxidative stress is defined by a disruption of ROS homeostasis, which is caused by the deregulation of ROS production or ROS elimination and by a missed adaptation to this oxidative stress *(Nathan and Cunningham-Bussel, 2013)*. Indeed, ROS may oxidize proteins, lipids and nucleic acids. In nucleus, ROS and mainly $^{\bullet}OH$, attack the DNA backbone, then generating abasic sites (purine and pyrimidine lesions), oxidized bases, DNA-DNA intrastrand adducts, DNA-protein crosslinks, single strand breaks and DSBs *(Filomeni et al., 2015; Lomax et al., 2013)*. In addition to DNA oxidation, ROS may also oxidize sulphur atoms localized in cysteine or methionine residues in peptides or proteins. Some of these oxidative damage are irreversible and cannot be repaired, leading to proteins that undergo conformational changes. These macromolecules are then degraded by the proteasome or by autophagy, or are sequestered by chaperones *(Nathan and Cunningham-Bussel, 2013)*. Depending on ROS levels, different biological responses are triggered in cells through the activation of distinct redox-sensitive signaling pathways. A low ROS level promotes the induction of antioxidant enzyme. An intermediate ROS levels induces an inflammatory response and a high ROS level leads to apoptosis or necrosis, caused by the disruption of the electron chain in mitochondria *(Gloire et al., 2006)*. At physiological low levels, ROS acts as messengers in different signaling pathways. In response to ROS accumulation, multiple proteins are activated, including tyrosine and serine/threonine phosphatases, tyrosine and serine/threonine kinases, transcription factors, histone deacetylases, metabolic enzymes and others. Moreover, by facilitating phosphorylation, ROS activate transcription factors such as JUN or induce the nuclear translocation of cytosolic factor such as NFκB. In parallel, ROS also trigger metabolic changes in cells by preventing the degradation of HIF1α. In order to respond to ROS accumulation, HIF1α acts by reducing the mitochondrial electron flow, thus reducing ROS production, eventually leading to glycolytic metabolism *(Nathan and Cunningham-Bussel, 2013)*. When ROS levels are too high, it irreversibly impairs cellular functions through the accumulation of damaged macromolecules. The lost of function of proteins promotes cell death mainly through the apoptotic pathway, autophagy and necrosis *(Circu and Aw, 2010; Filomeni et al., 2015).* Beside the ROS level, the fate of cells that encounter oxidative stress is also depending on their ability to reset the intracellular ROS homeostasis. The catabolism of ROS is performed by multiple antioxidant systems, mostly including superoxide dismutase and glutathione redox cycle. These two-coupled mechanisms convert peroxide into water. Additionally, the thioredoxin redox system, the nicotinamide

adenine dinucleotide (NADH/NAD+) and the nicotinamide adenine dinucleotide phosphate (NADPH/NAD+), peroxiredoxins, methionine sulphoxide reductase are other examples of antioxidant systems. Other enzymes involved in the metabolism may also be activated by ROS and shift the metabolism toward the pentose phosphate pathway in order to recover a ROS homeostasis *(Nathan and Cunningham-Bussel, 2013)*.

This gives rise to another question: is there an increased expression of free radical scavenging system in the M1 macrophages? As M1 macrophages are able to produce huge amounts of ROS in order to react against pathogens, it is not surprising that they protect themselves against ROS leaking into cytosol during high oxidative burst *(Ghesquiere et al., 2014)*. M1 macrophages thus use pentose phosphate pathway (PPP) to increase their overall redox potential *(Zhu et al., 2015)*. The investigation of these pathways would allow to elucidate the effect of proton irradiation on macrophage survival. The use of antioxidants, combined to proton irradiation, may also indicate whether ROS are responsible for enhanced cell death in M0 and M2 macrophages.

1.2.3. NFκB plays key roles in radioresistance

NFκB p50 – p65 may be recruited by ATM, downstream the signal transduction generated upon DSB sensing. The heterodimer NFκB p50 - p65, mostly activated in M1 macrophages, increases the transcription of genes encoding for antioxidant enzymes and anti-apoptotic proteins, thus favoring ROS clearance and cell survival respectively *(Gloire et al., 2006)*. Indeed, by targeting pro-survival genes (e.g. Bcl-2, Fas receptor, Fas ligand, A20 and inhibitor of apoptosis (IAP)) and through the inhibition of c-Jun, a pro-apoptotic factor, it was shown that the constitutive NFκB activity prevents apoptosis *(Pahl, 1999; Smirnov et al., 2001)*. In addition, NFκB finely regulates ROS homeostasis by regulating the expression of antioxidant such as MnSOD, heme oxygenase A (HO-1), thioredoxin-1, gluthatione peroxidase and others *(Morgan and Liu, 2011)*.

1.3. Macrophage reprogramming with proton irradiation: the role of NFκB

These last years, diverse therapies attempted to target macrophages in tumors. Rather than to eliminate macrophages from tumors or to inhibit their recruitment, therapies aimed at re-educating or reprogramming TAMs to adopt an antitumor M1-like phenotype, which is characterized by a pro-inflammatory phenotype, phagocytosis and antigen-presenting properties. The presence of pro-inflammatory macrophages in tumors is related to inflammation-induced tumorigenesis at early stage of the disease, or is associated to antitumor functions in settled tumors *(Mittal et al., 2014)*. Among all therapies, conventional radiotherapy demonstrated interesting effects. The response of unpolarized macrophages to conventional radiotherapy was shown to either polarize them to antitumoral M1-like macrophages or to promote a pro-tumoral M2-like phenotype, depending on the doses. While association of radiation to chemotherapies or immunotherapies have succeeded to reprogram M2-like TAMs, X-rays or γ-rays by themselves have not allowed M2 macrophage re-education (See *Chapter 3*).

1.3.1. Proton irradiation promotes an inflammatory phenotype in M0, M1 and M2 macrophages

Similarly to photon irradiation, exposure to moderate doses of protons is able to educate unpolarized macrophages toward a pro-inflammatory phenotype and to sustain this phenotype in M1 macrophages. However, unlike photons, our study revealed for the first time the acquisition of an intermediate M1/M2 phenotype in M2-like macrophages after moderate doses of protons.

We choose to characterize the pro-inflammatory phenotype by evaluating the secretion of TNFα, IL-6 and IL-8 from macrophages. The exposure of M0, M1 and M2 macrophages to 5 or 10 Gy displayed an increased secretion of TNFα. In tumors, the presence of TNFα is associated with an increased NK recruitment, DC maturation and the enrollment of $CD4^+$ and $CD8^+$ T cells, all favoring anti-tumor responses. Regarding cancer cells, TNFα may promote survival or tumor immunogenicity. This bivalent function depends on the subsequent signaling pathway that is activated. The binding of TNFα to TNFR1 may trigger NFκB pathway and thus pro-survival signals, or may activate MAPK pathway, and more specifically JNK, which is related to apoptosis. The apoptosis of cancer cells increases the stimulation of the immune system through the release of cancer cell antigens *(Burkholder et al., 2014)*. Our results also evidenced a higher secretion of IL-6 in proton-irradiated M1 macrophages with a dose of 10 Gy. The role of IL-6 in tumor is still discussed, as pro- and anti- tumoral functions are associated with its presence in tumors. Chronic IL-6 exposure increases cancer cell proliferation, survival and metastasis, promotes angiogenesis and participates to immune suppression. The inhibition of the immune system is performed through MDSC recruitment and the blockade of DC maturation. In contrast, acute IL-6 exposure decreases tumor growth and stimulates anti-tumor immunity, mainly by favoring T and B cell proliferation and survival and by increasing $CD8^+$ T cell trafficking to lymph nodes and tumors *(Burkholder et al., 2014; Fisher et al., 2014)*. Finally, we did not show significant modification of IL-8 secretion in proton-irradiated macrophages. Although this pro-inflammatory cytokine is mostly associated with pro-tumoral functions by promoting neutrophil chemotaxis (associated to angiogenesis), invasion and migration of cancer cells (EMT) and cancer stemness, it is also stimulates immunogenicity of dying cancer cells through the translocation of calreticulin on cell surface *(Nagarsheth et al., 2017)*. While the mRNA expression of IL-10 and CCL22, two immunosuppressive factors associated to M2 macrophages, was not altered by proton irradiation, the mRNA levels of EGF were reduced after irradiation. In tumors, EGF is known to enhance the migratory profile and proliferation of cancer cells and to induce angiogenesis *(Quail and Joyce, 2013)*. Altogether, these results indicated the acquisition of a pro-inflammatory and antitumor phenotype in irradiated macrophages. In order to complete the characterization of macrophage reprogramming after proton irradiation, it would be interesting to assess the extracellular release of IL-12 and TGFβ, involved in immunostimulation or immunosuppression respectively. Indeed, the inhibition of TGFβ in irradiated MMTV/PyVmT transgenic model of metastatic breast cancer restored T cell response and thus reduced the tumor burden *(Deng et al., 2016; Vanpouille-Box et al., 2015).* Furthermore, the study of phagocytosis and antigen presentation after irradiation would also bring more information regarding the acquisition of an antitumor phenotype.

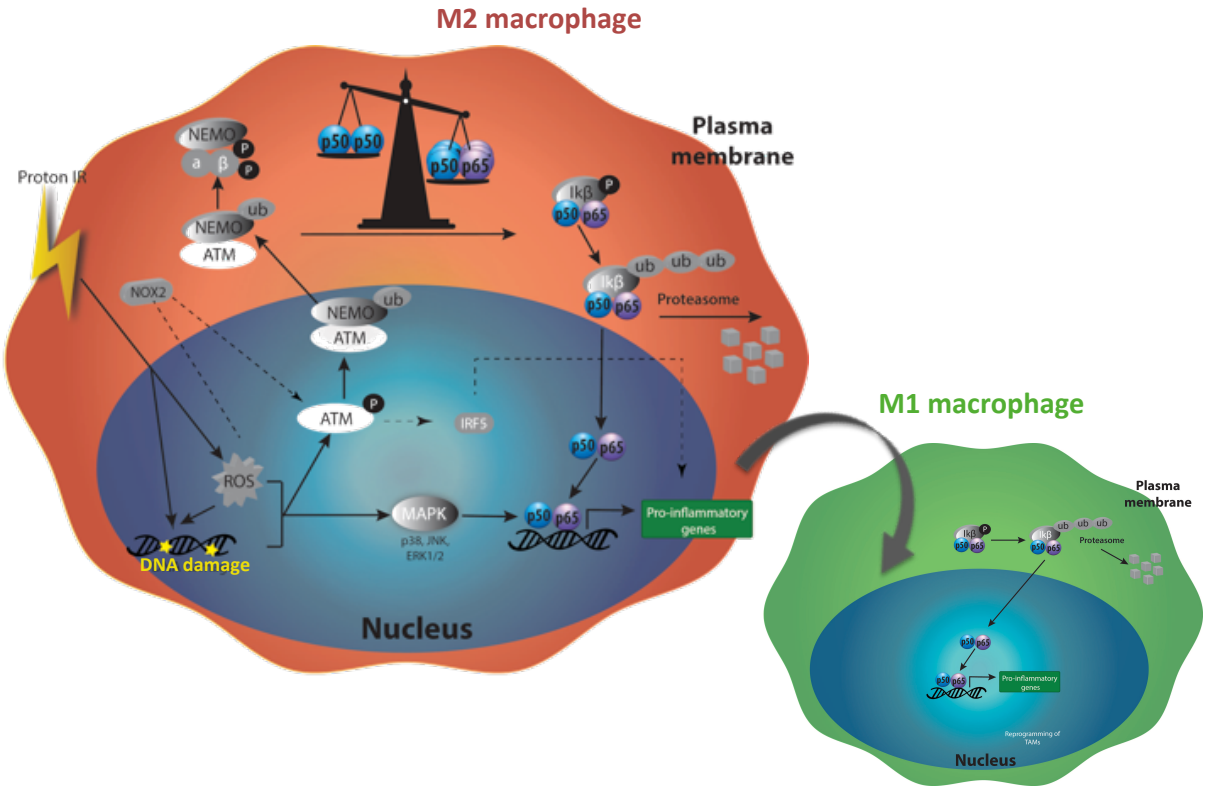

Figure IV.2 – Macrophage reprogramming after proton irradiation

By inducing DNA damage and ROS production, proton irradiation activates the NFκB pathway. Upon DSB detection, recruited ATM phosphorylates and subsequently ubiquitinylates NEMO, which triggers the cytoplasmic activation of IKK complex. In more details, the SUMOylation of NEMO impedes the cytoplasmic localization of NEMO, thus favoring its nuclear distribution. Later, ATM phosphorylates NEMO, a modification that is required for its ubiquitination. The monoubiquitination of NEMO regulates the nuclear export of NEMO associated to ATM. Once exported into the cytoplasm, NEMO is polyubiquitinated, thus allowing the activation of IKK complex and the subsequent release of NFκB p50 – p65 from the inhibitor of NFκB (IκBα). A lot of genes contain NFκB response elements (NREs) binding sites in their promoter/enhancer regions. By regulating the expression of pro-inflammatory chemokines and cytokines such as IL-1α, IL-1β, IL-6, IL8, IL-12, IFNβ or TNFα, this nuclear transcription factor promotes a pro-inflammatory phenotype in macrophages. In addition to induce indirect DNA damage, ROS also directly interact with the NFκB signaling pathway to trigger its activation or inhibition.

1.3.2. NFκB p50 – p65 orchestrates macrophage reprogramming after proton irradiation

Given the increased expression of TNFα and IL6 expression in proton-irradiated macrophages, we suspected that the heterodimer NFκB p50 – p65 might be activated by proton irradiation and would be responsible for macrophage reprogramming. This transcription factor is indeed responsible for the gene transcription of pro-inflammatory cytokines such as TNFα, IL-6 and IL-8 *(Pahl, 1999)*. By analyzing the nuclear translocation of NFκB p65 and the effect of its inhibition on proton radiation-induced macrophage reprogramming, we demonstrated the contribution of this transcription factor for the acquisition of a M1-like phenotype in irradiated M0, M1 and M2 macrophages (***Figure IV.2***). Based on previous results regarding photon-irradiated M2 macrophages (See *Chapter 3*) and the results we obtained with X-ray irradiated M2 THP-1 macrophages, it seems that conventional irradiation (γ-rays or X-rays) fails to re-educate M2 macrophages to adopt a M1 phenotype. This difference could be explained by a stronger NFκB activation in macrophages with protons compared to photons. Interestingly, the activation of NFκB p65, triggered by γ-rays and X-rays mostly requires doses comprised between 5 and 100 Gy. In contrast, high LET radiation targets NFκB p65 activation with doses around 1 Gy *(Hellweg, 2015)*. For example, NFκB activation was triggered in fibroblasts with 0.5 Gy of α-particles (LET 120 keV/μm) *(Ivanov et al., 2010)*. In transformed human epithelial cells (HEK/293 cell line), ^{36}Ar ion beam (LET 272 keV/μm) and ^{13}C ion beam (LET 33 keV/μm) elicited NFκB p65 nuclear translocation with 0.7 Gy and 1.3 Gy respectively *(Hellweg et al., 2011a, b)*. In addition, high LET ^{56}Fe ion beam was shown to activate NFκB p65 in normal human monocytes after 0.7 Gy *(Natarajan et al., 2002)*. More importantly, NFκB activation increased with the LET of charged particles: ^{13}C (LET 33 keV/μm), ^{22}Ne (LET 91 keV/μm) and ^{36}Ar ion beam (LET 272 keV/μm) increased the NFκB expression by 2, 8 and 9 times respectively when a 150 kV X-rays beam was used as reference *(Hellweg et al., 2011a)*. One prominent difference between photons and high LET particles is the complexity of DNA damage. This brings us to wonder how DNA damage may be linked to NFκB activation.

The link between DNA damage and NFκB activation has already been intensively studied and is called the genotoxic-induced pathway *(Hellweg et al., 2016)*. Upon DSB detection, recruited ATM and DNA-PK mobilize multiple factors, inducing the recognition and the repair of DSBs, the cell-cycle arrest and the activation of pro-survival and stress-response pathways. In case of extreme DNA damage, ATM also activates programmed cell death *(Biton and Ashkenazi, 2011; Magne et al., 2006)*. Previous studies suggested that ATM phosphorylates and subsequently ubiquitylates NEMO, which triggers the cytoplasmic activation of IKK complex *(Biton and Ashkenazi, 2011)*. Indeed, directly after DNA damage, a minor proportion of NEMO dissociates from the cytoplasmic IKK complex to migrate into the nucleus *(Wang et al., 2017b)*. Once into the nucleus, poly(ADP-Ribose) polymerase-1 (PARP-1) assembles the nucleoplasmic signalosome comprising SUMO E3 ligase protein inhibitor of activated STATy (PIASy), NEMO, p53-induced protein with a death domain (PIDD), receptor interacting protein 1 (RIP1) and ATM. This complex favors the SUMOylation of NEMO. This transient modification impedes the cytoplasmic localization of NEMO, thus favoring its nuclear distribution. Later, ATM phosphorylates NEMO, a modification that is required for its ubiquitination. The monoubiquitination of NEMO regulates the nuclear export of NEMO associated to ATM. Into the cytoplasm, NEMO phosphorylates TAK1 and activates IKK complex *(Biton and Ashkenazi, 2011)* Once exported into the cytoplasm, NEMO

is polyubiquitinated, thus allowing the activation of IKK complex and the subsequent release of NFκB p50 – p65 from the inhibitor of NFκB (IκBα) *(McCool and Miyamoto, 2012; Wang et al., 2017b)*. More recent work has indicated that ATM may also drive the cytoplasmic ubiquitylation of NEMO *(Biton and Ashkenazi, 2011)*. In fact, upon high genotoxic stress, NEMO may also be monoubiquitinylated in the cytoplasm by a complex composed of ATM and TRAF6 (TNF receptor associated factor 6) *(McCool and Miyamoto, 2012; Wang et al., 2017b)*, thus strengthening the activation of NFκB p50 – p65.

In addition to DNA damage, ROS interact with NFκB signaling pathways at different levels. Reactive radicals act through direct NFκB modifications or indirectly by targeting phosphatases and other enzymes that allow the release of NFκB heterodimer from the IκB complex. By reacting with cysteine, ROS may impede the DNA binding of NFκB. Especially, the cysteine Cys-62 of NFκB p50 is sensitive to oxidation. In contrast, ROS are required for the NFκB p65 phosphorylation on Ser-276 and Ser-536 and thus for its activation. Besides, ROS may also trigger the phosphorylation of IκBα, thus promoting its degradation and the nuclear translocation of NFκB p50 – p65. However, in some case, ROS also inhibit IκBα proteasome degradation, promoting IκBα stability and inhibition NFκB activation. Although ROS mainly inhibit IKKα and IKKβ subunits, ROS favor NEMO dimerization, potentiating NFκB activation *(Morgan and Liu, 2011)*. Therefore, oxidative stress finely regulates NFκB signaling and may activate NFκB in parallel with DNA damage signaling.

All these studies might suggest that the higher proportion of DNA damage and oxidative stress generated by proton irradiation could contribute to a higher NFκB activation. This hypothesis could explain why proton irradiation induces macrophage reprogramming while X-rays seemed not to exert the same effect. The evaluation of NFκB activation in X-ray irradiated and proton-irradiated macrophages would confirm or not this hypothesis. In addition, it might be possible that the contribution of DNA damage to NFκB activation outdoes the effect of oxidative stress, as an increasing complexity of DNA damage (correlated to increasing LET) is associated to a higher NFκB response. The use of antioxidant in combination with proton irradiation should allow to unravel the contribution of ROS to macrophage reprogramming after proton irradiation.

A lot of genes contain NFκB response elements (NREs) binding sites in their promoter/enhancer regions. By regulating the expression of pro-inflammatory chemokines and cytokines such as IL-1α, IL-1β, IL-6, IL8, IL-12, IFNβ or TNFα, this nuclear transcription factor promotes a pro-inflammatory phenotype in macrophages *(Pahl, 1999)*. In our studies, we showed that proton irradiation of macrophages enhanced the production of TNFα in the three macrophage phenotype. As TNFα is an inductor and a target of NFκB *(Magne et al., 2006)*, an amplification loop could therefore favorize the effect of proton irradiation macrophage reprogramming. Indeed, the exposure of HeLa cells to etoposide revealed two waves of NFκB activation: the first one appears rapidly (6h) after DNA damage and the second one arises later (26h) in response to TNFα *(Hellweg, 2015).*

Altogether, these results suggest that the use of high-LET charged particles could potentiate macrophage reprogramming by more strongly activating NFκB p65. In addition, the study of

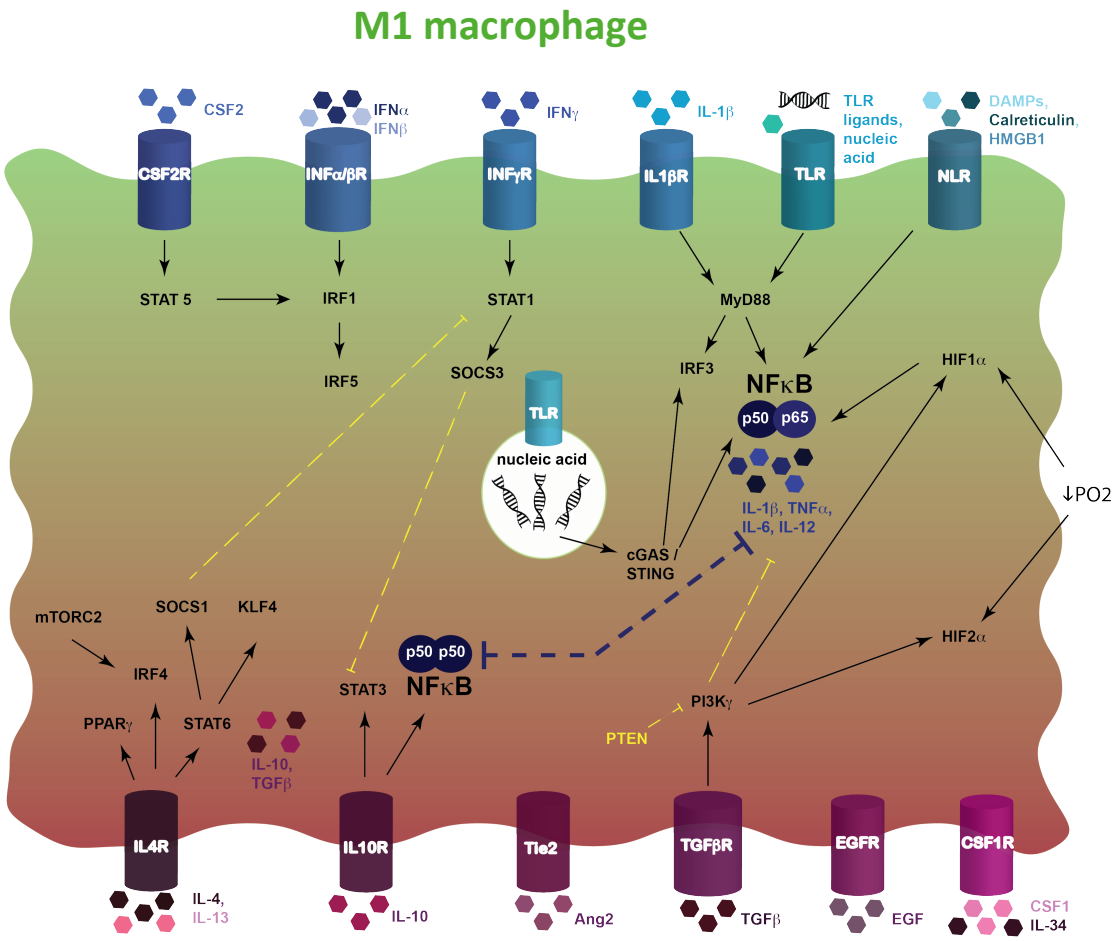

Figure IV.3 – Overview of signaling pathways involved in macrophage polarization

The homodimer NFkB p50 – p50 and the heterodimer p50 – p65 are key players in macrophage polarization: while the heterodimer p50 – p65 is associated with the transcription of pro-inflammatory genes and thus a M1 polarization, the homodimer p50 – p50 is related to a M2 macrophage polarization. IRF/STAT pathway is also a major axis in macrophage polarization as the balance between activated STAT1 and STAT3/STAT6 finely tunes macrophage phenotype. STAT1 and IRF3/5 predominate in M1 macrophage polarization and are associated with pro-inflammatory and cytotoxic functions, while STAT3/STAT6 and IRF4 trigger M2 phenotype and control anti-inflammatory and immunosuppressive functions. In this signaling network, SOCS1 and SOCS3 are both inhibitors of STAT1 and STAT3 respectively, that reinforce one or the other activated IRF/STAT pathway. Other mediators, such as PPARδ, cMyc, c-Maf, also contribute to M2 polarization. Finally, hypoxia is also involved in the activation status of macrophages: HIF1α is associated to M1 phenotype while HIF2α promotes M2 polarization (adapted from *(Wang, Liang et al. 2014)*).

ROS contribution to macrophage reprogramming and the demonstration of ROS production by high-LET charged particles should help to direct future studies.

1.3.3. The role of other factors in macrophage reprogramming

Despite the interesting correlation between NFκB activation and macrophage reprogramming, we cannot exclude the contribution of other factors to macrophage polarization after proton irradiation. It was already shown that conventional radiotherapy might trigger the activation of other pathways involved in macrophage polarization, including IRF/STAT signaling pathway and MAPK (see *Chapter 3*). Moreover, other proteins such as PI3Kγ, AP-1, HIF1, SOCS, KLF4, PPARγ or mTOR are also attributed to the M1 or M2 activation state (***Figure IV. 3***) *(Wang et al., 2014)*. In order to further characterize the effect of proton irradiation on macrophage reprogramming, we have initiated RNA sequencing and secretome meta-analyses in X-ray irradiated and proton-irradiated M1 and M2 macrophages. These experiments will also allow to better discriminate M1 from M2 macrophages by evidencing new markers. Indeed, for our experiments, we selected several M1 and M2 markers to analyze the effects of proton irradiation on macrophage reprogramming. However, we were limited by the quantity of mRNA to perform our analysis. As a high-sensitive technique, RNA sequencing would allow the analysis of the whole transcriptome with only 1 μg of mRNA. Moreover, recent investigations have shown that the metabolic profile of macrophages shapes their activation state *(Geeraerts et al., 2017)*. By using RNA sequencing analyses, it would be possible to associate a specific metabolic profile to each phenotype and to investigate the effects of irradiation on these metabolic pathways. The RNA sequencing would also bring more information on the effects of proton or X-rays irradiation on the expression of pathways involved in the survival and the DNA repair machinery. Thereafter, these large-scale analyses should be confirmed by the invalidation of target genes and target proteins in macrophages and the effects of their invalidation on proton-irradiation-induced macrophage reprogramming should be also assessed. Finally, as miRNAs play key roles in macrophage polarization (See chapter 2, section I.3 Non coding RNA (microRNA and long non-coding RNA), miRNA sequencing analysis would also bring interesting information regarding proton-induced macrophage reprogramming.

1.4. Interaction between M2 macrophages and cancer cells after proton irradiation: intervention of the cGAS/STING pathway

Type I IFNs (IFNα/β) are potent antiviral cytokines, which also intervene in antitumor immunity. IFNα and IFNβ are both able to bridge innate immunity to adaptative response. Secreted by cancer cells themselves, DCs and TAMs upon cytosolic DNA sensing, type I IFNs stimulate DC maturation and activate bone marrow-derived cells to finely handle the process of $CD8^+$ T cell cross-priming against cancer cells. It then triggers T cell expansion, activation, survival and memory formation *(Deng et al., 2016; Vanpouille-Box et al., 2017)*. In this antitumor response, the cytosolic DNA-sensing pathway (cGAS/STING) plays a prominent role. Both genomic and mitochondrial cancer cell-derived DNA may mobilize the cytosolic DNA sensor, cGAS, and the downstream signaling pathway, involving STING, IRF3 and NFκB. Upon radiotherapy, the activation of this pathway is fully potentiated compared to the natural antitumor immunity *(Chen et al., 2016a; Deng et al., 2016)*. It appeared that cGAS/STING pathway has a real impact on

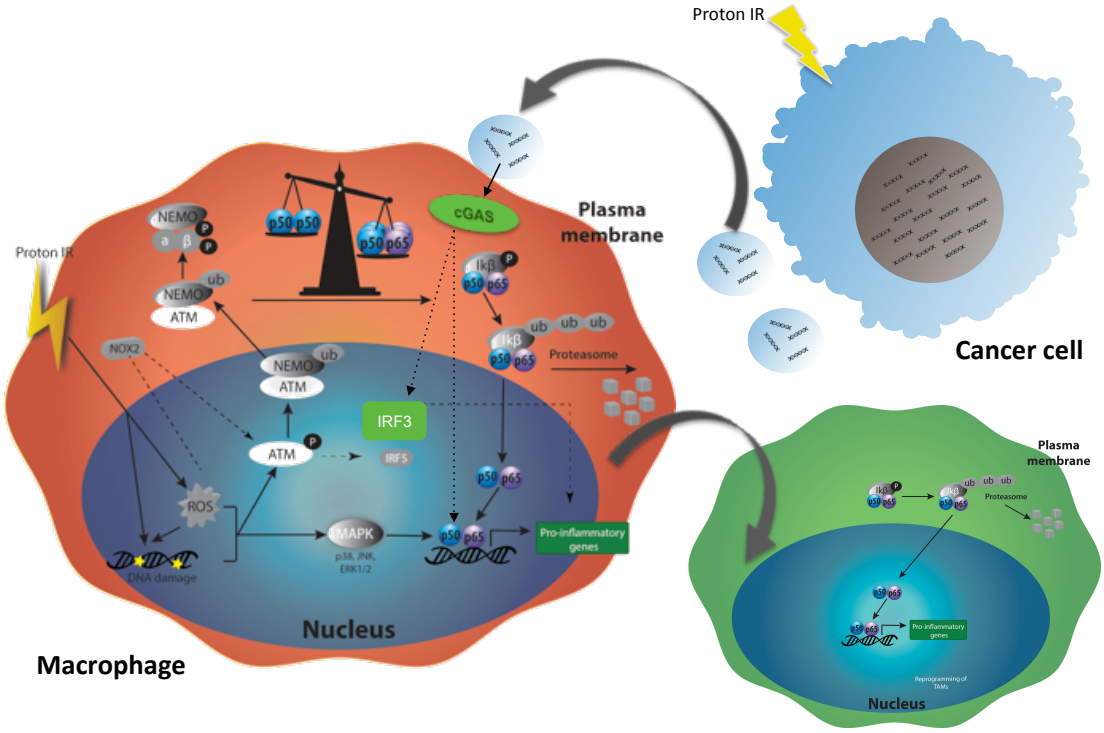

Figure IV.4 – Proposed mechanism for the activation of cGAS/STING pathway in proton-irradiated macrophages

The cGAS/STING pathway plays a prominent role in sensing cytosolic DNA. Upon irradiation, cytosolic recognition of cancer cell DNA by immune cells promotes pro-inflammatory cytokine production through the activation of cyclic GMP/AMP synthase (cGAS) and the stimulator of interferon genes (STING). The release of these pro-inflammatory factors is probably mediated by the nuclear activation of transcription factors such as IRF3 and NFκB.

radiotherapy-mediated therapeutic effects, either on locally irradiated tumors or on distant unirradiated metastasis *(Deng et al., 2014)* and would be mostly triggered in DCs and macrophages *(Baird et al., 2016; Corrales et al., 2015; Deng et al., 2014)*. We thus hypothesized that moderate doses (10 Gy) of proton irradiation could activate this pathway in M2 macrophages, co-cultured with cancer cells. We indeed evidenced that the mRNA expression of cGAS was upregulated in co-cultured macrophages, 16h after exposure to 10 Gy of protons, but not in M2 macrophages irradiated alone (***Figure IV. 4***). The assessment of type I IFN release after proton irradiation of co-culture would bring more information regarding the activation of this pathway and the potential antitumor functions of macrophages. Interestingly, it seems that the activation of cGAS/STING pathway increases with the doses. However, it was shown in a recent study that doses above 10 Gy failed to trigger cGAS/STING pathway due to the activation of the 3' repair exonuclease 1 (Trex1) in cancer cells. The activation of this exonuclease promoted the clearing of cytoplasmic double and single stranded DNA in cancer cells, thus preventing DNA release and sensing by APCs *(Vanpouille-Box et al., 2017)*. It still remains unclear how proton and high LET radiation doses would affect Trex1 and cGAS/STING pathways. However, this issue should be kept in mind for future investigations.

In parallel, we evaluated the influence of cancer cells on M2 macrophage reprogramming mediated by proton irradiation. Our preliminary results indicated a similar effect of proton irradiation in M2 macrophages cultured alone or co-cultured with cancer cells. We could thus hypothesize that the cGAS/STING pathway does not influence macrophage reprogramming in co-culture configuration, 16h after proton irradiation. As we did not observe an effect on the expression of pro-apoptotic proteins in A549 cell 16h after proton irradiation in co-culture configuration, we suggest to evaluate the influence of this DNA-sensing pathway on macrophage reprogramming at later time points. Furthermore, the activation of cGAS/STING pathway after radiation is transient, thus requiring repeated exposure to ionizing radiation to sustain the activation *(Deng et al., 2016; Vanpouille-Box et al., 2017)*. The use of fractionation should thus be considered for future *in vivo* experiments in order to maintain the activation of this pathway in macrophages.

2. Future directions

The present study demonstrated the benefits of protons over photon radiation on *in vitro* macrophage reprogramming. Our results further imply an interesting potential for the treatment of *in vivo* tumors and for future clinical strategies. Therefore, one of the important perspectives to this work is to evaluate the effects of proton irradiation in tumor-bearing mice.

The fate of tumors upon conventional radiotherapy strongly depends on the interaction between the innate immune response and the priming of the adaptative immunity. However, conventional RT engenders either immunostimulative as immunosuppressive responses in tumors. After exposure to radiotherapy, cancer cells may die by immunogenic cell death (ICD). This type of death is a regulated cell death that induces an immune response through antigens expressed by dying cells. Typically, dying and damaged cancer cells respond to radiotherapy via DAMPs, which include protein exposed on cell surface (e.g. calreticulin) or released molecules such as HMGB1 or ATP. Subsequently, ICD influences tumor immune response through DC priming and the subsequent $CD8^+$ T cell activation. Indeed, photon irradiation was shown to

positively influence the recruitment of circulating immune cells, to increase antigen exposure and presentation and thus to re-prime adaptive immune response *(Barker et al., 2015)*. The activation of the immune system after radiotherapy also generates tumor regression in distant unirradiated metastases, called the abscopal effect *(Wennerberg et al., 2017)*. Besides these immunostimulative effects, RT also promotes the activity of local immunosupressive cells, such as TAMs, MDSCs and Tregs, and enhances the expression of checkpoint inhibitors like PD-L1 and CTLA-4 *(Barker et al., 2015; Deng et al., 2016; Ebner et al., 2017)*. As Tregs are the less sensitive lymphocyte subset, there are the ones that easily populated tumors after radiotherapy *(Barker et al., 2015)*. Unfortunately, antitumor immune responses are rarely observed in poorly immunogenic tumors following conventional radiation and in order to reach these antitumor effects, radiotherapy must be synergized by immunotherapy *(Wennerberg et al., 2017)*.

The tumor immunosuppressive activities are widely associated to the presence of TGFβ into the microenvironment. This cytokine regulates cellular differentiation, survival and function of almost all immune cells *(Wennerberg et al., 2017)* and is mainly secreted by TAMs *(Morvan and Lanier, 2016)*. Specifically targeting TAMs in tumors has largely revealed positive effects on tumor regression *(*See *Chapter 3; Komohara et al., 2016)*. However, RT mainly increases TAM recruitment into tumors, favors TAM redistribution between necrotic and hypoxic areas *(Wennerberg et al., 2017)* and fails to re-educate TAMs to adopt a M1-like antitumor phenotype (See *Chapter 3*). As described in chapter 1, TAMs hold many interactions with other cell types and influence their pro-tumoral functions, their maturation or their exclusion from tumors. Inversely, MDSCs and B cells contribute to the acquisition for macrophages of a M2 phenotype, mainly through the release of IL-10. It is however unknown how these cells may influence TAM polarization after radiotherapy. The effect of charged particles on tumor is poorly characterized. It was shown that treatment of tumors with high-LET particle radiation led to a broader immunogenic response *(Durante et al., 2013)*. Interestingly, our *in vitro* experiments indicated the acquisition of a mixed M1/M2 phenotype in M2 macrophages being exposed to 10 Gy of protons. The reprogramming of TAMs into M1-like macrophages has already been demonstrated as an efficient way to induce tumor regression. Indeed, antitumor M1-like TAMs favor an immunostimulatory microenvironment that allows DC maturation, CD8+ cytotoxic T cell recruitment and then the killing of cancer cells. Therefore, it would be interesting to evaluate if a TAM reprogramming is observed in tumor-bearing mice treated with protontherapy. More specifically, as TAMs are characterized by multiple phenotypes depending on their location and their origin, it would be important to examine the effect of proton irradiation on the diversity of macrophage subsets in tumors. Furthermore, to fully understand the effect of proton irradiation on tumor immunosuppression, the effects on MDSCs and Tregs, as well as the incidence on co-stimulatory (CD40) and inhibitory (PD-L1, CTLA-4) checkpoint molecules should also be evaluated. Finally, as dose and dose fractionation were both shown to modify the effect of radiotherapy on the tumor microenvironment, it would be useful to identify the optimal dose schedule to maximize the effect of proton irradiation. Based on our results, we suggest using doses of about 10 Gy.

One important issue that should be taken into account is the impact on NFκB in cancer cells. Some cancer cells present constitutive activation of NFκB, leading to high radioresistance *(Hellweg et al., 2016).* Indeed, NFκB triggers anti-apoptotic and pro-survival pathways in cancer cells. It should be noted that the effect of proton irradiation on the tumor fate would depend on

the balance between the detrimental NFκB activation in cancer cells and the beneficial activation of this transcription factor in the tumor microenvironment. Together, these parameters should drive the choice of a tumor model and the schedule for proton irradiation.

3. General conclusion

Protontherapy represents a good alternative to circumvent the side effects of conventional radiotherapy, as this therapy has the advantage to spare normal tissues while maximizing the dose delivered to the tumor. In addition to these physical properties, we demonstrated *in vitro* that, in contrast to X-rays, proton irradiation efficiently reprograms macrophages towards a pro-inflammatory phenotype, known for its antitumor functions. Thanks to the development of new irradiation chambers, the interactions between cancer cells and M2 macrophages has been studied in this work. The results would suggest the activation of antitumor functions in irradiated M2 macrophages co-cultured with cancer cells. It has been shown that M2-like TAM reprogramming in mice and patients is a promising strategy to reverse the fate of tumors. Interestingly, we demonstrated that macrophage reprogramming induced by proton irradiation is orchestrated by the activation of NFκB p65. As NFκB p65 activation increases with the LET of charged particles, it brings us to consider high-LET particle therapy for macrophage reprogramming. Nowadays, more and more clinical researches have been focused on carbon ions and other experimental studies on oxygen, iron and other ion beams will further shed some more light onto the effects of these particles on the tumor microenvironment. Moreover, as other immunosuppressive cells play an important role in tumor progression and in the radioresistance to conventional radiotherapy, the evaluation of the effect of charged particle therapy on these cells could also position charged particle therapy as a first treatment for poorly immunogenic tumors. Altogether, our results further imply the huge potential of protontherapy for targeting TAMs in tumors and open new perspectives for clinical targeting of macrophages with charged particle therapy.

Achyut, B.R., Angara, K., Jain, M., Borin, T.F., Rashid, M.H., Iskander, A.S.M., Ara, R., Kolhe, R., Howard, S., Venugopal, N.*, et al.* (2017). Canonical NFkappaB signaling in myeloid cells is required for the glioblastoma growth. Sci Rep *7*, 13754.

Afik, R., Zigmond, E., Vugman, M., Klepfish, M., Shimshoni, E., Pasmanik-Chor, M., Shenoy, A., Bassat, E., Halpern, Z., Geiger, T.*, et al.* (2016). Tumor macrophages are pivotal constructors of tumor collagenous matrix. J Exp Med *213*, 2315-2331.

Aghbali, A., Rafieyan, S., Mohamed-Khosroshahi, L., Baradaran, B., Shanehbandi, D., and Kouhsoltani, M. (2017). IL-4 induces the formation of multinucleated giant cells and expression of beta5 integrin in central giant cell lesion. Med Oral Patol Oral Cir Bucal *22*, e1-e6.

Akira, S. (2006). TLR signaling. Curr Top Microbiol Immunol *311*, 1-16.

Alan Mitteer, R., Wang, Y., Shah, J., Gordon, S., Fager, M., Butter, P.P., Jun Kim, H., Guardiola-Salmeron, C., Carabe-Fernandez, A., and Fan, Y. (2015). Proton beam radiation induces DNA damage and cell apoptosis in glioma stem cells through reactive oxygen species. Sci Rep *5*, 13961.

Allen, C., Borak, T.B., Tsujii, H., and Nickoloff, J.A. (2011). Heavy charged particle radiobiology: using enhanced biological effectiveness and improved beam focusing to advance cancer therapy. Mutat Res *711*, 150-157.

Allen, I.C. (2014). Non-Inflammasome Forming NLRs in Inflammation and Tumorigenesis. Front Immunol *5*, 169.

Almendros, I., Wang, Y., Becker, L., Lennon, F.E., Zheng, J., Coats, B.R., Schoenfelt, K.S., Carreras, A., Hakim, F., Zhang, S.X.*, et al.* (2014). Intermittent hypoxia-induced changes in tumor-associated macrophages and tumor malignancy in a mouse model of sleep apnea. Am J Respir Crit Care Med *189*, 593-601.

Amici, S.A., Dong, J., and Guerau-de-Arellano, M. (2017). Molecular Mechanisms Modulating the Phenotype of Macrophages and Microglia. Front Immunol *8*, 1520.

Andreu, P., Johansson, M., Affara, N.I., Pucci, F., Tan, T., Junankar, S., Korets, L., Lam, J., Tawfik, D., DeNardo, D.G.*, et al.* (2010). FcRgamma activation regulates inflammation-associated squamous carcinogenesis. Cancer Cell *17*, 121-134.

Ansell, S.M., and Vonderheide, R.H. (2013). Cellular composition of the tumor microenvironment. Am Soc Clin Oncol Educ Book.

Antoniv, T.T., and Ivashkiv, L.B. (2011). Interleukin-10-induced gene expression and suppressive function are selectively modulated by the PI3K-Akt-GSK3 pathway. Immunology *132*, 567-577.

Armstrong, C.W., Maxwell, P.J., Ong, C.W., Redmond, K.M., McCann, C., Neisen, J., Ward, G.A., Chessari, G., Johnson, C., Crawford, N.T.*, et al.* (2016). PTEN deficiency promotes macrophage infiltration and hypersensitivity of prostate cancer to IAP antagonist/radiation combination therapy. Oncotarget *7*, 7885-7898.

Arwert, E.N., Hoste, E., and Watt, F.M. (2012). Epithelial stem cells, wound healing and cancer. Nat Rev Cancer *12*, 170-180.

Asaithamby, A., and Chen, D.J. (2011). Mechanism of cluster DNA damage repair in response to high-atomic number and energy particles radiation. Mutat Res *711*, 87-99.

Baer, C., Squadrito, M.L., Laoui, D., Thompson, D., Hansen, S.K., Kiialainen, A., Hoves, S., Ries, C.H., Ooi, C.H., and De Palma, M. (2016). Suppression of microRNA activity amplifies IFN-gamma-induced macrophage activation and promotes anti-tumour immunity. Nat Cell Biol *18*, 790-802.

Baird, J.R., Friedman, D., Cottam, B., Dubensky, T.W., Jr., Kanne, D.B., Bambina, S., Bahjat, K., Crittenden, M.R., and Gough, M.J. (2016). Radiotherapy Combined with Novel STING-Targeting Oligonucleotides Results in Regression of Established Tumors. Cancer Res *76*, 50-61.

Balkwill, F., and Mantovani, A. (2001). Inflammation and cancer: back to Virchow? Lancet *357*, 539-545.

Bam, R., Khan, S., Ling, W., Randal, S.S., Li, X., Barlogie, B., Edmondson, R., and Yaccoby, S. (2015). Primary myeloma interaction and growth in coculture with healthy donor hematopoietic bone marrow. BMC Cancer *15*, 864.

Banerjee, S., Halder, K., Bose, A., Bhattacharya, P., Gupta, G., Karmahapatra, S., Das, S., Chaudhuri, S., Bhattacharyya Majumdar, S., and Majumdar, S. (2011). TLR signaling-mediated differential histone modification at IL-10 and IL-12 promoter region leads to functional impairments in tumor-associated macrophages. Carcinogenesis *32*, 1789-1797.

Banerjee, S., Xie, N., Cui, H., Tan, Z., Yang, S., Icyuz, M., Abraham, E., and Liu, G. (2013). MicroRNA let-7c regulates macrophage polarization. J Immunol *190*, 6542-6549.

Barker, H.E., Paget, J.T., Khan, A.A., and Harrington, K.J. (2015). The tumour microenvironment after radiotherapy: mechanisms of resistance and recurrence. Nat Rev Cancer *15*, 409-425.

Bellora, F., Castriconi, R., Dondero, A., Pessino, A., Nencioni, A., Liggieri, G., Moretta, L., Mantovani, A., Moretta, A., and Bottino, C. (2014). TLR activation of tumor-associated macrophages from ovarian cancer patients triggers cytolytic activity of NK cells. Eur J Immunol *44*, 1814-1822.

Bellora, F., Castriconi, R., Dondero, A., Reggiardo, G., Moretta, L., Mantovani, A., Moretta, A., and Bottino, C. (2010). The interaction of human natural killer cells with either unpolarized or polarized macrophages results in different functional outcomes. Proc Natl Acad Sci U S A *107*, 21659-21664.

Beury, D.W., Parker, K.H., Nyandjo, M., Sinha, P., Carter, K.A., and Ostrand-Rosenberg, S. (2014). Cross-talk among myeloid-derived suppressor cells, macrophages, and tumor cells impacts the inflammatory milieu of solid tumors. J Leukoc Biol *96*, 1109-1118.

Beutler, B., Jiang, Z., Georgel, P., Crozat, K., Croker, B., Rutschmann, S., Du, X., and Hoebe, K. (2006). Genetic analysis of host resistance: Toll-like receptor signaling and immunity at large. Annu Rev Immunol *24*, 353-389.

Binnemars-Postma, K., Bansal, R., Storm, G., and Prakash, J. (2018). Targeting the Stat6 pathway in tumor-associated macrophages reduces tumor growth and metastatic niche formation in breast cancer. FASEB J *32*, 969-978.

Biswas, S.K., Gangi, L., Paul, S., Schioppa, T., Saccani, A., Sironi, M., Bottazzi, B., Doni, A., Vincenzo, B., Pasqualini, F.*, et al.* (2006). A distinct and unique transcriptional program expressed by tumor-associated macrophages (defective NF-kappaB and enhanced IRF-3/STAT1 activation). Blood *107*, 2112-2122.

Biswas, S.K., and Lewis, C.E. (2010). NF-kappaB as a central regulator of macrophage function in tumors. J Leukoc Biol *88*, 877-884.

Biswas, S.K., and Mantovani, A. (2010). Macrophage plasticity and interaction with lymphocyte subsets: cancer as a paradigm. Nat Immunol *11*, 889-896.

Biton, S., and Ashkenazi, A. (2011). NEMO and RIP1 control cell fate in response to extensive DNA damage via TNF-alpha feedforward signaling. Cell *145*, 92-103.

Bodduluru, L.N., Kasala, E.R., Madhana, R.M., and Sriram, C.S. (2015). Natural killer cells: the journey from puzzles in biology to treatment of cancer. Cancer Lett *357*, 454-467.

Borrego-Soto, G., Ortiz-Lopez, R., and Rojas-Martinez, A. (2015). Ionizing radiation-induced DNA injury and damage detection in patients with breast cancer. Genet Mol Biol *38*, 420-432.

Bouquet, F., Muller, C., and Salles, B. (2006). The loss of gammaH2AX signal is a marker of DNA double strand breaks repair only at low levels of DNA damage. Cell Cycle *5*, 1116-1122.

Bowman, R.L., Klemm, F., Akkari, L., Pyonteck, S.M., Sevenich, L., Quail, D.F., Dhara, S., Simpson, K., Gardner, E.E., Iacobuzio-Donahue, C.A.*, et al.* (2016). Macrophage Ontogeny Underlies Differences in Tumor-Specific Education in Brain Malignancies. Cell Rep *17*, 2445-2459.

Brown, J.M. (1979). Evidence for acutely hypoxic cells in mouse tumours, and a possible mechanism of reoxygenation. Br J Radiol *52*, 650-656.

Burgess, R.C., Burman, B., Kruhlak, M.J., and Misteli, T. (2014). Activation of DNA damage response signaling by condensed chromatin. Cell Rep *9*, 1703-1717.

Burkholder, B., Huang, R.Y., Burgess, R., Luo, S., Jones, V.S., Zhang, W., Lv, Z.Q., Gao, C.Y., Wang, B.L., Zhang, Y.M.*, et al.* (2014). Tumor-induced perturbations of cytokines and immune cell networks. Biochim Biophys Acta *1845*, 182-201.

Burnet (1970). The concept of immunologic surveillance. Prog Exp Tumor Res *13*, 1 - 27.

Caescu, C.I., Guo, X., Tesfa, L., Bhagat, T.D., Verma, A., Zheng, D., and Stanley, E.R. (2015). Colony stimulating factor-1 receptor signaling networks inhibit mouse macrophage inflammatory responses by induction of microRNA-21. Blood *125*, e1-13.

Cai, X., Chiu, Y.H., and Chen, Z.J. (2014). The cGAS-cGAMP-STING pathway of cytosolic DNA sensing and signaling. Mol Cell *54*, 289-296.

Cai, X., Yin, Y., Li, N., Zhu, D., Zhang, J., Zhang, C.Y., and Zen, K. (2012). Re-polarization of tumor-associated macrophages to pro-inflammatory M1 macrophages by microRNA-155. J Mol Cell Biol *4*, 341-343.

Carmeliet, P., and Jain, R.K. (2011). Molecular mechanisms and clinical applications of angiogenesis. Nature *473*, 298-307.

Castriconi, R., Cantoni, C., Della Chiesa, M., Vitale, M., Marcenaro, E., Conte, R., Biassoni, R., Bottino, C., Moretta, L., and Moretta, A. (2003). Transforming growth factor beta 1 inhibits expression of NKp30 and NKG2D receptors: consequences for the NK-mediated killing of dendritic cells. Proc Natl Acad Sci U S A *100*, 4120-4125.

Chang, C.P., Su, Y.C., Hu, C.W., and Lei, H.Y. (2013). TLR2-dependent selective autophagy regulates NF-kappaB lysosomal degradation in hepatoma-derived M2 macrophage differentiation. Cell Death Differ *20*, 515-523.

Chang, W.J., Du, Y., Zhao, X., Ma, L.Y., and Cao, G.W. (2014). Inflammation-related factors predicting prognosis of gastric cancer. World J Gastroenterol *20*, 4586-4596.

Chanput, W., Mes, J.J., and Wichers, H.J. (2014). THP-1 cell line: an in vitro cell model for immune modulation approach. Int Immunopharmacol *23*, 37-45.

Chen, Q., Sun, L., and Chen, Z.J. (2016a). Regulation and function of the cGAS-STING pathway of cytosolic DNA sensing. Nat Immunol *17*, 1142-1149.

Chen, W., Xu, Y., Zhong, J., Wang, H., Weng, M., Cheng, Q., Wu, Q., Sun, Z., Jiang, H., Zhu, M.*, et al.* (2016b). MFHAS1 promotes colorectal cancer progress by regulating polarization of tumor-associated macrophages via STAT6 signaling pathway. Oncotarget *7*, 78726-78735.

Chen, X., Ying, X., Wang, X., Wu, X., Zhu, Q., and Wang, X. (2017). Exosomes derived from hypoxic epithelial ovarian cancer deliver microRNA-940 to induce macrophage M2 polarization. Oncol Rep *38*, 522-528.

Chen, Y., and Ahmad, S. (2012). Empirical model estimation of relative biological effectiveness for proton beam therapy. Radiat Prot Dosimetry *149*, 116-123.

Chenoweth, M.J., Mian, M.F., Barra, N.G., Alain, T., Sonenberg, N., Bramson, J., Lichty, B.D., Richards, C.D., Ma, A., and Ashkar, A.A. (2012). IL-15 can signal via IL-15Ralpha, JNK, and NF-kappaB to drive RANTES production by myeloid cells. J Immunol *188*, 4149-4157.

Chevrier, S., Levine, J.H., Zanotelli, V.R.T., Silina, K., Schulz, D., Bacac, M., Ries, C.H., Ailles, L., Jewett, M.A.S., Moch, H.*, et al.* (2017). An Immune Atlas of Clear Cell Renal Cell Carcinoma. Cell *169*, 736-749 e718.

Circu, M.L., and Aw, T.Y. (2010). Reactive oxygen species, cellular redox systems, and apoptosis. Free Radic Biol Med *48*, 749-762.

Clawson, G.A., Matters, G.L., Xin, P., Imamura-Kawasawa, Y., Du, Z., Thiboutot, D.M., Helm, K.F., Neves, R.I., and Abraham, T. (2015). Macrophage-tumor cell fusions from peripheral blood of melanoma patients. PLoS One *10*, e0134320.

Coffelt, S.B., Chen, Y.Y., Muthana, M., Welford, A.F., Tal, A.O., Scholz, A., Plate, K.H., Reiss, Y., Murdoch, C., De Palma, M.*, et al.* (2011). Angiopoietin 2 stimulates TIE2-expressing monocytes to suppress T cell activation and to promote regulatory T cell expansion. J Immunol *186*, 4183-4190.

Colegio, O.R., Chu, N.Q., Szabo, A.L., Chu, T., Rhebergen, A.M., Jairam, V., Cyrus, N., Brokowski, C.E., Eisenbarth, S.C., Phillips, G.M.*, et al.* (2014). Functional polarization of tumour-associated macrophages by tumour-derived lactic acid. Nature *513*, 559-563.

Colotta, F., Allavena, P., Sica, A., Garlanda, C., and Mantovani, A. (2009). Cancer-related inflammation, the seventh hallmark of cancer: links to genetic instability. Carcinogenesis *30*, 1073-1081.

Comito, G., Giannoni, E., Segura, C.P., Barcellos-de-Souza, P., Raspollini, M.R., Baroni, G., Lanciotti, M., Serni, S., and Chiarugi, P. (2014). Cancer-associated fibroblasts and M2-polarized macrophages synergize during prostate carcinoma progression. Oncogene *33*, 2423-2431.

Condeelis, J., and Pollard, J.W. (2006). Macrophages: obligate partners for tumor cell migration, invasion, and metastasis. Cell *124*, 263-266.

Connelly, L., Barham, W., Onishko, H.M., Chen, L., Sherrill, T.P., Zabuawala, T., Ostrowski, M.C., Blackwell, T.S., and Yull, F.E. (2011). NF-kappaB activation within macrophages leads to an anti-tumor phenotype in a mammary tumor lung metastasis model. Breast Cancer Res *13*, R83.

Corrales, L., Glickman, L.H., McWhirter, S.M., Kanne, D.B., Sivick, K.E., Katibah, G.E., Woo, S.R., Lemmens, E., Banda, T., Leong, J.J.*, et al.* (2015). Direct Activation of STING in the Tumor Microenvironment Leads to Potent and Systemic Tumor Regression and Immunity. Cell Rep *11*, 1018-1030.

Corrales, L., McWhirter, S.M., Dubensky, T.W., Jr., and Gajewski, T.F. (2016). The host STING pathway at the interface of cancer and immunity. J Clin Invest *126*, 2404-2411.

Dannenmann, S.R., Thielicke, J., Stockli, M., Matter, C., von Boehmer, L., Cecconi, V., Hermanns, T., Hefermehl, L., Schraml, P., Moch, H.*, et al.* (2013). Tumor-associated macrophages subvert T-cell function and correlate with reduced survival in clear cell renal cell carcinoma. Oncoimmunology *2*, e23562.

Dauffy, J., Mouchiroud, G., and Bourette, R.P. (2006). The interferon-inducible gene, Ifi204, is transcriptionally activated in response to M-CSF, and its expression favors macrophage differentiation in myeloid progenitor cells. J Leukoc Biol *79*, 173-183.

De Palma, M. (2016). Origins of Brain Tumor Macrophages. Cancer Cell *30*, 832-833.

De Palma, M., and Lewis, C.E. (2013). Macrophage regulation of tumor responses to anticancer therapies. Cancer Cell *23*, 277-286.

De Palma, M., and Naldini, L. (2011). Angiopoietin-2 TIEs up macrophages in tumor angiogenesis. Clin Cancer Res *17*, 5226-5232.

Delaney, G., Barton, M., Jacob, S., and Jalaludin, B. (2003). A model for decision making for the use of radiotherapy in lung cancer. Lancet Oncol *4*, 120-128.

Dell'Oste, V., Gatti, D., Giorgio, A.G., Gariglio, M., Landolfo, S., and De Andrea, M. (2015). The interferon-inducible DNA-sensor protein IFI16: a key player in the antiviral response. New Microbiol *38*, 5-20.

Deng, L., Liang, H., Fu, S., Weichselbaum, R.R., and Fu, Y.X. (2016). From DNA Damage to Nucleic Acid Sensing: A Strategy to Enhance Radiation Therapy. Clin Cancer Res *22*, 20-25.

Deng, L., Liang, H., Xu, M., Yang, X., Burnette, B., Arina, A., Li, X.D., Mauceri, H., Beckett, M., Darga, T.*, et al.* (2014). STING-Dependent Cytosolic DNA Sensing Promotes Radiation-Induced Type I Interferon-Dependent Antitumor Immunity in Immunogenic Tumors. Immunity *41*, 843-852.

Ding, H., Cai, J., Mao, M., Fang, Y., Huang, Z., Jia, J., Li, T., Xu, L., Wang, J., Zhou, J.*, et al.* (2014). Tumor-associated macrophages induce lymphangiogenesis in cervical cancer via interaction with tumor cells. APMIS *122*, 1059-1069.

Ding, M., Fu, X., Tan, H., Wang, R., Chen, Z., and Ding, S. (2012). The effect of vascular endothelial growth factor C expression in tumor-associated macrophages on lymphangiogenesis and lymphatic metastasis in breast cancer. Mol Med Rep *6*, 1023-1029.

Dunn, G.P., Old, L.J., and Schreiber, R.D. (2004). The immunobiology of cancer immunosurveillance and immunoediting. Immunity *21*, 137-148.

Durante, M., and Loeffler, J.S. (2010). Charged particles in radiation oncology. Nat Rev Clin Oncol *7*, 37-43.

Durante, M., Reppingen, N., and Held, K.D. (2013). Immunologically augmented cancer treatment using modern radiotherapy. Trends Mol Med *19*, 565-582.

Dvorak, H.F. (1986). Tumors: wounds that do not heal. Similarities between tumor stroma generation and wound healing. N Engl J Med *315*, 1650-1659.

Ebner, D.K., Tinganelli, W., Helm, A., Bisio, A., Yamada, S., Kamada, T., Shimokawa, T., and Durante, M. (2017). The Immunoregulatory Potential of Particle Radiation in Cancer Therapy. Front Immunol *8*, 99.

El Kasmi, K.C., and Stenmark, K.R. (2015). Contribution of metabolic reprogramming to macrophage plasticity and function. Semin Immunol *27*, 267-275.

Escribese, M.M., Casas, M., and Corbi, A.L. (2012). Influence of low oxygen tensions on macrophage polarization. Immunobiology *217*, 1233-1240.

Fabbri, M., Paone, A., Calore, F., Galli, R., Gaudio, E., Santhanam, R., Lovat, F., Fadda, P., Mao, C., Nuovo, G.J.*, et al.* (2012). MicroRNAs bind to Toll-like receptors to induce prometastatic inflammatory response. Proc Natl Acad Sci U S A *109*, E2110-2116.

Fan, Q.M., Jing, Y.Y., Yu, G.F., Kou, X.R., Ye, F., Gao, L., Li, R., Zhao, Q.D., Yang, Y., Lu, Z.H.*, et al.* (2014). Tumor-associated macrophages promote cancer stem cell-like properties via transforming growth factor-beta1-induced epithelial-mesenchymal transition in hepatocellular carcinoma. Cancer Lett *352*, 160-168.

Fang, L.Y., Izumi, K., Lai, K.P., Liang, L., Li, L., Miyamoto, H., Lin, W.J., and Chang, C. (2013). Infiltrating macrophages promote prostate tumorigenesis via modulating androgen receptor-mediated CCL4-STAT3 signaling. Cancer Res *73*, 5633-5646.

Filomeni, G., De Zio, D., and Cecconi, F. (2015). Oxidative stress and autophagy: the clash between damage and metabolic needs. Cell Death Differ *22*, 377-388.

Fisher, D.T., Appenheimer, M.M., and Evans, S.S. (2014). The two faces of IL-6 in the tumor microenvironment. Semin Immunol *26*, 38-47.

Forget, M.A., Voorhees, J.L., Cole, S.L., Dakhlallah, D., Patterson, I.L., Gross, A.C., Moldovan, L., Mo, X., Evans, R., Marsh, C.B.*, et al.* (2014). Macrophage colony-stimulating factor augments Tie2-expressing monocyte differentiation, angiogenic function, and recruitment in a mouse model of breast cancer. PLoS One *9*, e98623.

Foulds, L. (1954). The experimental study of tumor progression: a review. Cancer Res *14*, 327-339.

Franklin, R.A., Liao, W., Sarkar, A., Kim, M.V., Bivona, M.R., Liu, K., Pamer, E.G., and Li, M.O. (2014). The cellular and molecular origin of tumor-associated macrophages. Science *344*, 921-925.

Fridman, W.H., Zitvogel, L., Sautes-Fridman, C., and Kroemer, G. (2017). The immune contexture in cancer prognosis and treatment. Nat Rev Clin Oncol *14*, 717-734.

Gajewski, T.F., Schreiber, H., and Fu, Y.X. (2013). Innate and adaptive immune cells in the tumor microenvironment. Nat Immunol *14*, 1014-1022.

Galluzzi, L., Vitale, I., Aaronson, S.A., Abrams, J.M., Adam, D., Agostinis, P., Alnemri, E.S., Altucci, L., Amelio, I., Andrews, D.W.*, et al.* (2018). Molecular mechanisms of cell death: recommendations of the Nomenclature Committee on Cell Death 2018. Cell Death Differ *25*, 486-541.

Gao, Z., Li, Y., Wang, F., Huang, T., Fan, K., Zhang, Y., Zhong, J., Cao, Q., Chao, T., Jia, J.*, et al.* (2017). Mitochondrial dynamics controls anti-tumour innate immunity by regulating CHIP-IRF1 axis stability. Nat Commun *8*, 1805.

Garcia, S., Krausz, S., Ambarus, C.A., Fernandez, B.M., Hartkamp, L.M., van Es, I.E., Hamann, J., Baeten, D.L., Tak, P.P., and Reedquist, K.A. (2014). Tie2 signaling cooperates with TNF to promote the pro-inflammatory activation of human macrophages independently of macrophage functional phenotype. PLoS One *9*, e82088.

Geeraerts, X., Bolli, E., Fendt, S.M., and Van Ginderachter, J.A. (2017). Macrophage Metabolism As Therapeutic Target for Cancer, Atherosclerosis, and Obesity. Front Immunol *8*, 289.

Genard, G., Lucas, S., and Michiels, C. (2017). Reprogramming of Tumor-Associated Macrophages with Anticancer Therapies: Radiotherapy versus Chemo- and Immunotherapies. Front Immunol *8*, 828.

Genin, M., Clement, F., Fattaccioli, A., Raes, M., and Michiels, C. (2015). M1 and M2 macrophages derived from THP-1 cells differentially modulate the response of cancer cells to etoposide. BMC Cancer *15*, 577.

Gentles, A.J., Newman, A.M., Liu, C.L., Bratman, S.V., Feng, W., Kim, D., Nair, V.S., Xu, Y., Khuong, A., Hoang, C.D.*, et al.* (2015). The prognostic landscape of genes and infiltrating immune cells across human cancers. Nat Med *21*, 938-945.

Ghesquiere, B., Wong, B.W., Kuchnio, A., and Carmeliet, P. (2014). Metabolism of stromal and immune cells in health and disease. Nature *511*, 167-176.

Gloire, G., Legrand-Poels, S., and Piette, J. (2006). NF-kappaB activation by reactive oxygen species: fifteen years later. Biochem Pharmacol *72*, 1493-1505.

Go, Y., Tanaka, H., Tokumoto, M., Sakurai, K., Toyokawa, T., Kubo, N., Muguruma, K., Maeda, K., Ohira, M., and Hirakawa, K. (2016). Tumor-Associated Macrophages Extend Along Lymphatic Flow in the Pre-metastatic Lymph Nodes of Human Gastric Cancer. Ann Surg Oncol *23 Suppl 2*, S230-235.

Gomez Perdiguero, E., Klapproth, K., Schulz, C., Busch, K., Azzoni, E., Crozet, L., Garner, H., Trouillet, C., de Bruijn, M.F., Geissmann, F.*, et al.* (2015). Tissue-resident macrophages originate from yolk-sac-derived erythro-myeloid progenitors. Nature *518*, 547-551.

Good, J.S., and Harrington, K.J. (2013). The hallmarks of cancer and the radiation oncologist: updating the 5Rs of radiobiology. Clin Oncol (R Coll Radiol) *25*, 569-577.

Gordon, S.R., Maute, R.L., Dulken, B.W., Hutter, G., George, B.M., McCracken, M.N., Gupta, R., Tsai, J.M., Sinha, R., Corey, D.*, et al.* (2017). PD-1 expression by tumour-associated macrophages inhibits phagocytosis and tumour immunity. Nature *545*, 495-499.

Gosselin, D., Link, V.M., Romanoski, C.E., Fonseca, G.J., Eichenfield, D.Z., Spann, N.J., Stender, J.D., Chun, H.B., Garner, H., Geissmann, F.*, et al.* (2014). Environment drives selection and function of enhancers controlling tissue-specific macrophage identities. Cell *159*, 1327-1340.

Goubau, D., Romieu-Mourez, R., Solis, M., Hernandez, E., Mesplede, T., Lin, R., Leaman, D., and Hiscott, J. (2009). Transcriptional re-programming of primary macrophages reveals distinct apoptotic and anti-tumoral functions of IRF-3 and IRF-7. Eur J Immunol *39*, 527-540.

Greten, F.R., Eckmann, L., Greten, T.F., Park, J.M., Li, Z.W., Egan, L.J., Kagnoff, M.F., and Karin, M. (2004). IKKbeta links inflammation and tumorigenesis in a mouse model of colitis-associated cancer. Cell *118*, 285-296.

Grivennikov, S.I., Greten, F.R., and Karin, M. (2010). Immunity, inflammation, and cancer. Cell *140*, 883-899.

Guiducci, C., Vicari, A.P., Sangaletti, S., Trinchieri, G., and Colombo, M.P. (2005). Redirecting in vivo elicited tumor infiltrating macrophages and dendritic cells towards tumor rejection. Cancer Res *65*, 3437-3446.

Gunderson, A.J., Kaneda, M.M., Tsujikawa, T., Nguyen, A.V., Affara, N.I., Ruffell, B., Gorjestani, S., Liudahl, S.M., Truitt, M., Olson, P.*, et al.* (2016). Bruton Tyrosine Kinase-Dependent Immune Cell Cross-talk Drives Pancreas Cancer. Cancer Discov *6*, 270-285.

Hachiya, M., Shimizu, S., Osawa, Y., and Akashi, M. (1997). Endogenous production of tumour necrosis factor is required for manganese superoxide dismutase expression by irradiation in the human monocytic cell line THP-1. Biochem J *328 (Pt 2)*, 615-623.

Hagemann, T., Biswas, S.K., Lawrence, T., Sica, A., and Lewis, C.E. (2009). Regulation of macrophage function in tumors: the multifaceted role of NF-kappaB. Blood *113*, 3139-3146.

Hagemann, T., Lawrence, T., McNeish, I., Charles, K.A., Kulbe, H., Thompson, R.G., Robinson, S.C., and Balkwill, F.R. (2008). "Re-educating" tumor-associated macrophages by targeting NF-kappaB. J Exp Med *205*, 1261-1268.

Hanahan, D., and Coussens, L.M. (2012). Accessories to the crime: functions of cells recruited to the tumor microenvironment. Cancer Cell *21*, 309-322.

Hanahan, D., and Weinberg, R.A. (2000). The hallmarks of cancer. Cell *100*, 57-70.

Hanahan, D., and Weinberg, R.A. (2011). Hallmarks of cancer: the next generation. Cell *144*, 646-674.

Harney, A.S., Arwert, E.N., Entenberg, D., Wang, Y., Guo, P., Qian, B.Z., Oktay, M.H., Pollard, J.W., Jones, J.G., and Condeelis, J.S. (2015). Real-Time Imaging Reveals Local, Transient Vascular Permeability, and Tumor Cell Intravasation Stimulated by TIE2hi Macrophage-Derived VEGFA. Cancer Discov *5*, 932-943.

Harrington, K., Jankowska, P., and Hingorani, M. (2007). Molecular biology for the radiation oncologist: the 5Rs of radiobiology meet the hallmarks of cancer. Clin Oncol (R Coll Radiol) *19*, 561-571.

Hashimoto, D., Chow, A., Noizat, C., Teo, P., Beasley, M.B., Leboeuf, M., Becker, C.D., See, P., Price, J., Lucas, D*., et al.* (2013). Tissue-resident macrophages self-maintain locally throughout adult life with minimal contribution from circulating monocytes. Immunity *38*, 792-804.

He, Y., Qian, H., Liu, Y., Duan, L., Li, Y., and Shi, G. (2014). The roles of regulatory B cells in cancer. J Immunol Res *2014*, 215471.

Hellweg, C.E. (2015). The Nuclear Factor kappaB pathway: A link to the immune system in the radiation response. Cancer Lett *368*, 275-289.

Hellweg, C.E., Baumstark-Khan, C., Schmitz, C., Lau, P., Meier, M.M., Testard, I., Berger, T., and Reitz, G. (2011a). Activation of the nuclear factor kappaB pathway by heavy ion beams of different linear energy transfer. Int J Radiat Biol *87*, 954-963.

Hellweg, C.E., Baumstark-Khan, C., Schmitz, C., Lau, P., Meier, M.M., Testard, I., Berger, T., and Reitz, G. (2011b). Carbon-ion-induced activation of the NF-kappaB pathway. Radiat Res *175*, 424-431.

Hellweg, C.E., Spitta, L.F., Henschenmacher, B., Diegeler, S., and Baumstark-Khan, C. (2016). Transcription Factors in the Cellular Response to Charged Particle Exposure. Front Oncol *6*, 61.

Hoeffel, G., and Ginhoux, F. (2015). Ontogeny of Tissue-Resident Macrophages. Front Immunol *6*, 486.

Hoesel, B., and Schmid, J.A. (2013). The complexity of NF-kappaB signaling in inflammation and cancer. Mol Cancer *12*, 86.

Huang, C., Liu, X.J., QunZhou, Xie, J., Ma, T.T., Meng, X.M., and Li, J. (2016a). MiR-146a modulates macrophage polarization by inhibiting Notch1 pathway in RAW264.7 macrophages. Int Immunopharmacol *32*, 46-54.

Huang, F., Zhao, J.L., Wang, L., Gao, C.C., Liang, S.Q., An, D.J., Bai, J., Chen, Y., Han, H., and Qin, H.Y. (2017). miR-148a-3p Mediates Notch Signaling to Promote the Differentiation and M1 Activation of Macrophages. Front Immunol *8*, 1327.

Huang, S.C., Smith, A.M., Everts, B., Colonna, M., Pearce, E.L., Schilling, J.D., and Pearce, E.J. (2016b). Metabolic Reprogramming Mediated by the mTORC2-IRF4 Signaling Axis Is Essential for Macrophage Alternative Activation. Immunity *45*, 817-830.

Huang, Z., Gan, J., Long, Z., Guo, G., Shi, X., Wang, C., Zang, Y., Ding, Z., Chen, J., Zhang, J*., et al.* (2016c). Targeted delivery of let-7b to reprogramme tumor-associated macrophages and tumor infiltrating dendritic cells for tumor rejection. Biomaterials *90*, 72-84.

Huang, Z., Luo, Q., Yao, F., Qing, C., Ye, J., Deng, Y., and Li, J. (2016d). Identification of Differentially Expressed Long Non-coding RNAs in Polarized Macrophages. Sci Rep *6*, 19705.

Hui, L., and Chen, Y. (2015). Tumor microenvironment: Sanctuary of the devil. Cancer Lett *368*, 7-13.

Ibberson, M., Bron, S., Guex, N., Faes-van't Hull, E., Ifticene-Treboux, A., Henry, L., Lehr, H.A., Delaloye, J.F., Coukos, G., Xenarios, I*., et al.* (2013). TIE-2 and VEGFR kinase activities drive immunosuppressive function of TIE-2-expressing monocytes in human breast tumors. Clin Cancer Res *19*, 3439-3449.

Ilicic, K., Combs, S.E., and Schmid, T.E. (2018). New insights in the relative radiobiological effectiveness of proton irradiation. Radiat Oncol *13*, 6.

Ivanov, V.N., Zhou, H., Ghandhi, S.A., Karasic, T.B., Yaghoubian, B., Amundson, S.A., and Hei, T.K. (2010). Radiation-induced bystander signaling pathways in human fibroblasts: a role for interleukin-33 in the signal transmission. Cell Signal *22*, 1076-1087.

Jeannin, P., Paolini, L., Adam, C., and Delneste, Y. (2017). The roles of CSFs on the functional polarization of tumor-associated macrophages. FEBS J.

Ji, H., Cao, R., Yang, Y., Zhang, Y., Iwamoto, H., Lim, S., Nakamura, M., Andersson, P., Wang, J., Sun, Y.*, et al.* (2014). TNFR1 mediates TNF-alpha-induced tumour lymphangiogenesis and metastasis by modulating VEGF-C-VEGFR3 signalling. Nat Commun *5*, 4944.

Jia, X., Li, X., Shen, Y., Miao, J., Liu, H., Li, G., and Wang, Z. (2016). MiR-16 regulates mouse peritoneal macrophage polarization and affects T-cell activation. J Cell Mol Med *20*, 1898-1907.

Jiang, X., Zhou, T., Xiao, Y., Yu, J., Dou, S., Chen, G., Wang, R., Xiao, H., Hou, C., Wang, W.*, et al.* (2016). Tim-3 promotes tumor-promoting M2 macrophage polarization by binding to STAT1 and suppressing the STAT1-miR-155 signaling axis. Oncoimmunology *5*, e1211219.

Jimenez-Sanchez, A., Memon, D., Pourpe, S., Veeraraghavan, H., Li, Y., Vargas, H.A., Gill, M.B., Park, K.J., Zivanovic, O., Konner, J.*, et al.* (2017). Heterogeneous Tumor-Immune Microenvironments among Differentially Growing Metastases in an Ovarian Cancer Patient. Cell *170*, 927-938 e920.

Joiner, M., and Kogel, A.v.d. (2009). Basic clinical radiobiology, 4th edn (London: Hodder Arnold ;).

Jonsson, K.L., Laustsen, A., Krapp, C., Skipper, K.A., Thavachelvam, K., Hotter, D., Egedal, J.H., Kjolby, M., Mohammadi, P., Prabakaran, T.*, et al.* (2017). IFI16 is required for DNA sensing in human macrophages by promoting production and function of cGAMP. Nat Commun *8*, 14391.

Joshi, S., Singh, A.R., Zulcic, M., and Durden, D.L. (2014). A macrophage-dominant PI3K isoform controls hypoxia-induced HIF1alpha and HIF2alpha stability and tumor growth, angiogenesis, and metastasis. Mol Cancer Res *12*, 1520-1531.

Joyce, J.A., and Fearon, D.T. (2015). T cell exclusion, immune privilege, and the tumor microenvironment. Science *348*, 74-80.

Junttila, M.R., and de Sauvage, F.J. (2013). Influence of tumour micro-environment heterogeneity on therapeutic response. Nature *501*, 346-354.

Kaneda, M.M., Messer, K.S., Ralainirina, N., Li, H., Leem, C.J., Gorjestani, S., Woo, G., Nguyen, A.V., Figueiredo, C.C., Foubert, P.*, et al.* (2016). PI3Kgamma is a molecular switch that controls immune suppression. Nature *539*, 437-442.

Karin, M., and Ben-Neriah, Y. (2000). Phosphorylation meets ubiquitination: the control of NF-[kappa]B activity. Annu Rev Immunol *18*, 621-663.

Kee, J.Y., Ito, A., Hojo, S., Hashimoto, I., Igarashi, Y., Tsuneyama, K., Tsukada, K., Irimura, T., Shibahara, N., Takasaki, I.*, et al.* (2014). CXCL16 suppresses liver metastasis of colorectal cancer by promoting TNF-alpha-induced apoptosis by tumor-associated macrophages. BMC Cancer *14*, 949.

Kerbel, R.S., Lagarde, A.E., Dennis, J.W., and Donaghue, T.P. (1983). Spontaneous fusion in vivo between normal host and tumor cells: possible contribution to tumor progression and metastasis studied with a lectin-resistant mutant tumor. Mol Cell Biol *3*, 523-538.

Kerkar, S.P., and Restifo, N.P. (2012). Cellular constituents of immune escape within the tumor microenvironment. Cancer Res *72*, 3125-3130.

Khanna, A. (2015). DNA damage in cancer therapeutics: a boon or a curse? Cancer Res *75*, 2133-2138.

Kim, R., Emi, M., and Tanabe, K. (2007). Cancer immunoediting from immune surveillance to immune escape. Immunology *121*, 1-14.

Kitamura, T., Kometani, K., Hashida, H., Matsunaga, A., Miyoshi, H., Hosogi, H., Aoki, M., Oshima, M., Hattori, M., Takabayashi, A*., et al.* (2007). SMAD4-deficient intestinal tumors recruit CCR1+ myeloid cells that promote invasion. Nat Genet *39*, 467-475.

Klug, F., Prakash, H., Huber, P.E., Seibel, T., Bender, N., Halama, N., Pfirschke, C., Voss, R.H., Timke, C., Umansky, L*., et al.* (2013). Low-dose irradiation programs macrophage differentiation to an iNOS(+)/M1 phenotype that orchestrates effective T cell immunotherapy. Cancer Cell *24*, 589-602.

Komohara, Y., Fujiwara, Y., Ohnishi, K., and Takeya, M. (2016). Tumor-associated macrophages: Potential therapeutic targets for anti-cancer therapy. Adv Drug Deliv Rev *99*, 180-185.

Komohara, Y., Jinushi, M., and Takeya, M. (2014). Clinical significance of macrophage heterogeneity in human malignant tumors. Cancer Sci *105*, 1-8.

Kono, Y., Kawakami, S., Higuchi, Y., Yamashita, F., and Hashida, M. (2014). In vitro evaluation of inhibitory effect of nuclear factor-kappaB activity by small interfering RNA on pro-tumor characteristics of M2-like macrophages. Biol Pharm Bull *37*, 137-144.

Kosaki, K., Ecker, S., Habermehl, D., Rieken, S., Jakel, O., Herfarth, K., Debus, J., and Combs, S.E. (2012). Comparison of intensity modulated radiotherapy (IMRT) with intensity modulated particle therapy (IMPT) using fixed beams or an ion gantry for the treatment of patients with skull base meningiomas. Radiat Oncol *7*, 44.

Kubo, H., Mensurado, S., Goncalves-Sousa, N., Serre, K., and Silva-Santos, B. (2017). Primary Tumors Limit Metastasis Formation through Induction of IL15-Mediated Cross-Talk between Patrolling Monocytes and NK Cells. Cancer Immunol Res *5*, 812-820.

Kumar, V., Patel, S., Tcyganov, E., and Gabrilovich, D.I. (2016). The Nature of Myeloid-Derived Suppressor Cells in the Tumor Microenvironment. Trends Immunol *37*, 208-220.

Laoui, D., Van Overmeire, E., Di Conza, G., Aldeni, C., Keirsse, J., Morias, Y., Movahedi, K., Houbracken, I., Schouppe, E., Elkrim, Y*., et al.* (2014). Tumor hypoxia does not drive differentiation of tumor-associated macrophages but rather fine-tunes the M2-like macrophage population. Cancer Res *74*, 24-30.

Lavin, Y., Winter, D., Blecher-Gonen, R., David, E., Keren-Shaul, H., Merad, M., Jung, S., and Amit, I. (2014). Tissue-resident macrophage enhancer landscapes are shaped by the local microenvironment. Cell *159*, 1312-1326.

Leblond, M.M., Gerault, A.N., Corroyer-Dulmont, A., MacKenzie, E.T., Petit, E., Bernaudin, M., and Valable, S. (2016). Hypoxia induces macrophage polarization and re-education toward an M2 phenotype in U87 and U251 glioblastoma models. Oncoimmunology *5*, e1056442.

Lewis, C.E., De Palma, M., and Naldini, L. (2007). Tie2-expressing monocytes and tumor angiogenesis: regulation by hypoxia and angiopoietin-2. Cancer Res *67*, 8429-8432.

Lewis, C.E., Harney, A.S., and Pollard, J.W. (2016). The Multifaceted Role of Perivascular Macrophages in Tumors. Cancer Cell *30*, 18-25.

Li, N., Qin, J., Lan, L., Zhang, H., Liu, F., Wu, Z., Ni, H., and Wang, Y. (2015a). PTEN inhibits macrophage polarization from M1 to M2 through CCL2 and VEGF-A reduction and NHERF-1 synergism. Cancer Biol Ther *16*, 297-306.

Li, Y., Zhao, L., Shi, B., Ma, S., Xu, Z., Ge, Y., Liu, Y., Zheng, D., and Shi, J. (2015b). Functions of miR-146a and miR-222 in Tumor-associated Macrophages in Breast Cancer. Sci Rep *5*, 18648.

Lin, E.Y., Nguyen, A.V., Russell, R.G., and Pollard, J.W. (2001). Colony-stimulating factor 1 promotes progression of mammary tumors to malignancy. J Exp Med *193*, 727-740.

Lin, L., Lin, H., Wang, L., Wang, B., Hao, X., and Shi, Y. (2015). miR-130a regulates macrophage polarization and is associated with non-small cell lung cancer. Oncol Rep *34*, 3088-3096.

Lindstrom, A., Midtbo, K., Arnesson, L.G., Garvin, S., and Shabo, I. (2017). Fusion between M2-macrophages and cancer cells results in a subpopulation of radioresistant cells with enhanced DNA-repair capacity. Oncotarget *8*, 51370-51386.

Liu, B., Sun, L., Liu, Q., Gong, C., Yao, Y., Lv, X., Lin, L., Yao, H., Su, F., Li, D.*, et al.* (2015). A cytoplasmic NF-kappaB interacting long noncoding RNA blocks IkappaB phosphorylation and suppresses breast cancer metastasis. Cancer Cell *27*, 370-381.

Liu, D., Chang, C., Lu, N., Wang, X., Lu, Q., Ren, X., Ren, P., Zhao, D., Wang, L., Zhu, Y.*, et al.* (2017). Comprehensive Proteomics Analysis Reveals Metabolic Reprogramming of Tumor-Associated Macrophages Stimulated by the Tumor Microenvironment. J Proteome Res *16*, 288-297.

Lizier, M., Anselmo, A., Mantero, S., Ficara, F., Paulis, M., Vezzoni, P., Lucchini, F., and Pacchiana, G. (2016). Fusion between cancer cells and macrophages occurs in a murine model of spontaneous neu+ breast cancer without increasing its metastatic potential. Oncotarget *7*, 60793-60806.

Lomax, M.E., Folkes, L.K., and O'Neill, P. (2013). Biological consequences of radiation-induced DNA damage: relevance to radiotherapy. Clin Oncol (R Coll Radiol) *25*, 578-585.

Ma, S., Liu, M., Xu, Z., Li, Y., Guo, H., Ge, Y., Liu, Y., Zheng, D., and Shi, J. (2016). A double feedback loop mediated by microRNA-23a/27a/24-2 regulates M1 versus M2 macrophage polarization and thus regulates cancer progression. Oncotarget *7*, 13502-13519.

Maeda, S., Kamata, H., Luo, J.L., Leffert, H., and Karin, M. (2005). IKKbeta couples hepatocyte death to cytokine-driven compensatory proliferation that promotes chemical hepatocarcinogenesis. Cell *121*, 977-990.

Magne, N., Toillon, R.A., Bottero, V., Didelot, C., Houtte, P.V., Gerard, J.P., and Peyron, J.F. (2006). NF-kappaB modulation and ionizing radiation: mechanisms and future directions for cancer treatment. Cancer Lett *231*, 158-168.

Mah, L.J., El-Osta, A., and Karagiannis, T.C. (2010). gammaH2AX: a sensitive molecular marker of DNA damage and repair. Leukemia *24*, 679-686.

Mantovani, A. (2010). Role of inflammatory cells and mediators in tumor invasion and metastasis. Cancer Metastasis Rev *29*, 241.

Mantovani, A., Allavena, P., Sica, A., and Balkwill, F. (2008a). Cancer-related inflammation. Nature *454*, 436-444.

Mantovani, A., Biswas, S.K., Galdiero, M.R., Sica, A., and Locati, M. (2013). Macrophage plasticity and polarization in tissue repair and remodelling. J Pathol *229*, 176-185.

Mantovani, A., and Locati, M. (2013). Tumor-associated macrophages as a paradigm of macrophage plasticity, diversity, and polarization: lessons and open questions. Arterioscler Thromb Vasc Biol *33*, 1478-1483.

Mantovani, A., Romero, P., Palucka, A.K., and Marincola, F.M. (2008b). Tumour immunity: effector response to tumour and role of the microenvironment. Lancet *371*, 771-783.

Mantovani, A., and Sica, A. (2010). Macrophages, innate immunity and cancer: balance, tolerance, and diversity. Curr Opin Immunol *22*, 231-237.

Mazibrada, J., De Andrea, M., Ritta, M., Borgogna, C., Dell'eva, R., Pfeffer, U., Chiusa, L., Gariglio, M., and Landolfo, S. (2010). In vivo growth inhibition of head and neck squamous cell carcinoma by the Interferon-inducible gene IFI16. Cancer Lett *287*, 33-43.

Mazzieri, R., Pucci, F., Moi, D., Zonari, E., Ranghetti, A., Berti, A., Politi, L.S., Gentner, B., Brown, J.L., Naldini, L.*, et al.* (2011). Targeting the ANG2/TIE2 axis inhibits tumor growth and metastasis by impairing angiogenesis and disabling rebounds of proangiogenic myeloid cells. Cancer Cell *19*, 512-526.

Mazzone, M., Menga, A., and Castegna, A. (2017). Metabolism and TAM functions-it takes two to tango. FEBS J.

McCool, K.W., and Miyamoto, S. (2012). DNA damage-dependent NF-kappaB activation: NEMO turns nuclear signaling inside out. Immunol Rev *246*, 311-326.

McGranahan, N., Furness, A.J., Rosenthal, R., Ramskov, S., Lyngaa, R., Saini, S.K., Jamal-Hanjani, M., Wilson, G.A., Birkbak, N.J., Hiley, C.T.*, et al.* (2016). Clonal neoantigens elicit T cell immunoreactivity and sensitivity to immune checkpoint blockade. Science *351*, 1463-1469.

McGranahan, N., and Swanton, C. (2017a). Cancer Evolution Constrained by the Immune Microenvironment. Cell *170*, 825-827.

McGranahan, N., and Swanton, C. (2017b). Clonal Heterogeneity and Tumor Evolution: Past, Present, and the Future. Cell *168*, 613-628.

Melton, D.W., Lei, X., Gelfond, J.A., and Shireman, P.K. (2016). Dynamic macrophage polarization-specific miRNA patterns reveal increased soluble VEGF receptor 1 by miR-125a-5p inhibition. Physiol Genomics *48*, 345-360.

Michiels, C., Tellier, C., and Feron, O. (2016). Cycling hypoxia: A key feature of the tumor microenvironment. Biochim Biophys Acta *1866*, 76-86.

Mieczkowski, J., Kocyk, M., Nauman, P., Gabrusiewicz, K., Sielska, M., Przanowski, P., Maleszewska, M., Rajan, W.D., Pszczolkowska, D., Tykocki, T.*, et al.* (2015). Down-regulation of IKKbeta expression in glioma-infiltrating microglia/macrophages is associated with defective inflammatory/immune gene responses in glioblastoma. Oncotarget *6*, 33077-33090.

Miller, R.C., Lodge, M., Murad, M.H., and Jones, B. (2013). Controversies in clinical trials in proton radiotherapy: the present and the future. Semin Radiat Oncol *23*, 127-133.

Mittal, D., Gubin, M.M., Schreiber, R.D., and Smyth, M.J. (2014). New insights into cancer immunoediting and its three component phases--elimination, equilibrium and escape. Curr Opin Immunol *27*, 16-25.

Miyake, M., Hori, S., Morizawa, Y., Tatsumi, Y., Nakai, Y., Anai, S., Torimoto, K., Aoki, K., Tanaka, N., Shimada, K.*, et al.* (2016). CXCL1-Mediated Interaction of Cancer Cells with Tumor-Associated Macrophages and Cancer-Associated Fibroblasts Promotes Tumor Progression in Human Bladder Cancer. Neoplasia *18*, 636-646.

Mohamad, O., Sishc, B.J., Saha, J., Pompos, A., Rahimi, A., Story, M.D., Davis, A.J., and Kim, D.W.N. (2017). Carbon Ion Radiotherapy: A Review of Clinical Experiences and Preclinical Research, with an Emphasis on DNA Damage/Repair. Cancers (Basel) *9*.

Morgan, M.J., and Liu, Z.G. (2011). Crosstalk of reactive oxygen species and NF-kappaB signaling. Cell Res *21*, 103-115.

Mori, K., Haraguchi, S., Hiori, M., Shimada, J., and Ohmori, Y. (2015). Tumor-associated macrophages in oral premalignant lesions coexpress CD163 and STAT1 in a Th1-dominated microenvironment. BMC Cancer *15*, 573.

Morvan, M.G., and Lanier, L.L. (2016). NK cells and cancer: you can teach innate cells new tricks. Nat Rev Cancer *16*, 7-19.

Movahedi, K., Laoui, D., Gysemans, C., Baeten, M., Stange, G., Van den Bossche, J., Mack, M., Pipeleers, D., In't Veld, P., De Baetselier, P.*, et al.* (2010). Different tumor microenvironments contain functionally distinct subsets of macrophages derived from Ly6C(high) monocytes. Cancer Res *70*, 5728-5739.

Murdoch, C., and Lewis, C.E. (2005). Macrophage migration and gene expression in response to tumor hypoxia. Int J Cancer *117*, 701-708.

Murray, P.J. (2017). Macrophage Polarization. Annu Rev Physiol *79*, 541-566.

Murray, P.J., Allen, J.E., Biswas, S.K., Fisher, E.A., Gilroy, D.W., Goerdt, S., Gordon, S., Hamilton, J.A., Ivashkiv, L.B., Lawrence, T.*, et al.* (2014). Macrophage activation and polarization: nomenclature and experimental guidelines. Immunity *41*, 14-20.

Nagarsheth, N., Wicha, M.S., and Zou, W. (2017). Chemokines in the cancer microenvironment and their relevance in cancer immunotherapy. Nat Rev Immunol *17*, 559-572.

Natale, F., Rapp, A., Yu, W., Maiser, A., Harz, H., Scholl, A., Grulich, S., Anton, T., Horl, D., Chen, W.*, et al.* (2017). Identification of the elementary structural units of the DNA damage response. Nat Commun *8*, 15760.

Natarajan, M., Aravindan, N., Meltz, M.L., and Herman, T.S. (2002). Post-translational modification of I-kappa B alpha activates NF-kappa B in human monocytes exposed to 56Fe ions. Radiat Environ Biophys *41*, 139-144.

Nathan, C., and Cunningham-Bussel, A. (2013). Beyond oxidative stress: an immunologist's guide to reactive oxygen species. Nat Rev Immunol *13*, 349-361.

Newhauser, W.D., and Zhang, R. (2015). The physics of proton therapy. Phys Med Biol *60*, R155-209.

Nishida, N., Yano, H., Nishida, T., Kamura, T., and Kojiro, M. (2006). Angiogenesis in cancer. Vasc Health Risk Manag *2*, 213-219.

Nowell, P.C. (1976). The clonal evolution of tumor cell populations. Science *194*, 23-28.

Nowosielska, E.M., Cheda, A., Wrembel-Wargocka, J., and Janiak, M.K. (2012). Effect of low doses of low-let radiation on the innate anti-tumor reactions in radioresistant and radiosensitive mice. Dose Response *10*, 500-515.

Noy, R., and Pollard, J.W. (2014). Tumor-associated macrophages: from mechanisms to therapy. Immunity *41*, 49-61.

O'Sullivan, T., Saddawi-Konefka, R., Vermi, W., Koebel, C.M., Arthur, C., White, J.M., Uppaluri, R., Andrews, D.M., Ngiow, S.F., Teng, M.W.*, et al.* (2012). Cancer immunoediting by the innate immune system in the absence of adaptive immunity. J Exp Med *209*, 1869-1882.

Ohkuri, T., Kosaka, A., Ishibashi, K., Kumai, T., Hirata, Y., Ohara, K., Nagato, T., Oikawa, K., Aoki, N., Harabuchi, Y.*, et al.* (2017). Intratumoral administration of cGAMP transiently accumulates potent macrophages for anti-tumor immunity at a mouse tumor site. Cancer Immunol Immunother *66*, 705-716.

Ohkuri, T., Kosaka, A., Nagato, T., and Kobayashi, H. (2018). Effects of STING stimulation on macrophages: STING agonists polarize into "classically" or "alternatively" activated macrophages? Hum Vaccin Immunother *14*, 285-287.

Pahl, H.L. (1999). Activators and target genes of Rel/NF-kappaB transcription factors. Oncogene *18*, 6853-6866.

Palucka, A.K., and Coussens, L.M. (2016). The Basis of Oncoimmunology. Cell *164*, 1233-1247.

Parker, K.H., Sinha, P., Horn, L.A., Clements, V.K., Yang, H., Li, J., Tracey, K.J., and Ostrand-Rosenberg, S. (2014). HMGB1 enhances immune suppression by facilitating the differentiation and suppressive activity of myeloid-derived suppressor cells. Cancer Res *74*, 5723-5733.

Pasero, C., Gravis, G., Granjeaud, S., Guerin, M., Thomassin-Piana, J., Rocchi, P., Salem, N., Walz, J., Moretta, A., and Olive, D. (2015). Highly effective NK cells are associated with good prognosis in patients with metastatic prostate cancer. Oncotarget *6*, 14360-14373.

Patidar, A., Selvaraj, S., Sarode, A., Chauhan, P., Chattopadhyay, D., and Saha, B. (2017). DAMP-TLR-cytokine axis dictates the fate of tumor. Cytokine.

Peng, J., Tsang, J.Y., Li, D., Niu, N., Ho, D.H., Lau, K.F., Lui, V.C., Lamb, J.R., Chen, Y., and Tam, P.K. (2013). Inhibition of TGF-beta signaling in combination with TLR7 ligation re-programs a tumoricidal phenotype in tumor-associated macrophages. Cancer Lett *331*, 239-249.

Penny, H.L., Sieow, J.L., Adriani, G., Yeap, W.H., See Chi Ee, P., San Luis, B., Lee, B., Lee, T., Mak, S.Y., Ho, Y.S.*, et al.* (2016). Warburg metabolism in tumor-conditioned macrophages promotes metastasis in human pancreatic ductal adenocarcinoma. Oncoimmunology *5*, e1191731.

Pinto, A.T., Pinto, M.L., Velho, S., Pinto, M.T., Cardoso, A.P., Figueira, R., Monteiro, A., Marques, M., Seruca, R., Barbosa, M.A.*, et al.* (2016). Intricate Macrophage-Colorectal Cancer Cell Communication in Response to Radiation. PLoS One *11*, e0160891.

Plebanek, M.P., Angeloni, N.L., Vinokour, E., Li, J., Henkin, A., Martinez-Marin, D., Filleur, S., Bhowmick, R., Henkin, J., Miller, S.D.*, et al.* (2017). Pre-metastatic cancer exosomes induce immune surveillance by patrolling monocytes at the metastatic niche. Nat Commun *8*, 1319.

Powell, A.E., Anderson, E.C., Davies, P.S., Silk, A.D., Pelz, C., Impey, S., and Wong, M.H. (2011). Fusion between Intestinal epithelial cells and macrophages in a cancer context results in nuclear reprogramming. Cancer Res *71*, 1497-1505.

Qian, B.Z., Li, J., Zhang, H., Kitamura, T., Zhang, J., Campion, L.R., Kaiser, E.A., Snyder, L.A., and Pollard, J.W. (2011). CCL2 recruits inflammatory monocytes to facilitate breast-tumour metastasis. Nature *475*, 222-225.

Qian, B.Z., and Pollard, J.W. (2010). Macrophage diversity enhances tumor progression and metastasis. Cell *141*, 39-51.

Quail, D.F., and Joyce, J.A. (2013). Microenvironmental regulation of tumor progression and metastasis. Nat Med *19*, 1423-1437.

Raggi, F., Pelassa, S., Pierobon, D., Penco, F., Gattorno, M., Novelli, F., Eva, A., Varesio, L., Giovarelli, M., and Bosco, M.C. (2017). Regulation of Human Macrophage M1-M2 Polarization Balance by Hypoxia and the Triggering Receptor Expressed on Myeloid Cells-1. Front Immunol *8*, 1097.

Riabov, V., Gudima, A., Wang, N., Mickley, A., Orekhov, A., and Kzhyshkowska, J. (2014). Role of tumor associated macrophages in tumor angiogenesis and lymphangiogenesis. Front Physiol *5*, 75.

Richter, E., Ventz, K., Harms, M., Mostertz, J., and Hochgrafe, F. (2016). Induction of Macrophage Function in Human THP-1 Cells Is Associated with Rewiring of MAPK Signaling and Activation of MAP3K7 (TAK1) Protein Kinase. Front Cell Dev Biol *4*, 21.

Rodriguez, D., Silvera, R., Carrio, R., Nadji, M., Caso, R., Rodriguez, G., Iragavarapu-Charyulu, V., and Torroella-Kouri, M. (2013). Tumor microenvironment profoundly modifies functional status of macrophages: peritoneal and tumor-associated macrophages are two very different subpopulations. Cell Immunol *283*, 51-60.

Romieu-Mourez, R., Solis, M., Nardin, A., Goubau, D., Baron-Bodo, V., Lin, R., Massie, B., Salcedo, M., and Hiscott, J. (2006). Distinct roles for IFN regulatory factor (IRF)-3 and IRF-7 in the activation of antitumor properties of human macrophages. Cancer Res *66*, 10576-10585.

Roos, W.P., and Kaina, B. (2013). DNA damage-induced cell death: from specific DNA lesions to the DNA damage response and apoptosis. Cancer Lett *332*, 237-248.

Ruffell, B., Chang-Strachan, D., Chan, V., Rosenbusch, A., Ho, C.M., Pryer, N., Daniel, D., Hwang, E.S., Rugo, H.S., and Coussens, L.M. (2014). Macrophage IL-10 blocks CD8+ T cell-dependent responses to chemotherapy by suppressing IL-12 expression in intratumoral dendritic cells. Cancer Cell *26*, 623-637.

Ruoslahti, E. (2002). Specialization of tumour vasculature. Nat Rev Cancer *2*, 83-90.

Saccani, A., Schioppa, T., Porta, C., Biswas, S.K., Nebuloni, M., Vago, L., Bottazzi, B., Colombo, M.P., Mantovani, A., and Sica, A. (2006). p50 nuclear factor-kappaB overexpression in tumor-associated macrophages inhibits M1 inflammatory responses and antitumor resistance. Cancer Res *66*, 11432-11440.

Sahin, E., Haubenwallner, S., Kuttke, M., Kollmann, I., Halfmann, A., Dohnal, A.M., Chen, L., Cheng, P., Hoesel, B., Einwallner, E.*, et al.* (2014). Macrophage PTEN regulates expression and secretion of arginase I modulating innate and adaptive immune responses. J Immunol *193*, 1717-1727.

Schiller, K.C., Habl, G., and Combs, S.E. (2016). Protons, Photons, and the Prostate - Is There Emerging Evidence in the Ongoing Discussion on Particle Therapy for the Treatment of Prostate Cancer? Front Oncol *6*, 8.

Schlaff, C.D., Krauze, A., Belard, A., O'Connell, J.J., and Camphausen, K.A. (2014). Bringing the heavy: carbon ion therapy in the radiobiological and clinical context. Radiat Oncol *9*, 88.

Schreiber, R.D., Old, L.J., and Smyth, M.J. (2011). Cancer immunoediting: integrating immunity's roles in cancer suppression and promotion. Science *331*, 1565-1570.

Schwende, H., Fitzke, E., Ambs, P., and Dieter, P. (1996). Differences in the state of differentiation of THP-1 cells induced by phorbol ester and 1,25-dihydroxyvitamin D3. J Leukoc Biol *59*, 555-561.

Shand, F.H., Ueha, S., Otsuji, M., Koid, S.S., Shichino, S., Tsukui, T., Kosugi-Kanaya, M., Abe, J., Tomura, M., Ziogas, J.*, et al.* (2014). Tracking of intertissue migration reveals the origins of tumor-infiltrating monocytes. Proc Natl Acad Sci U S A *111*, 7771-7776.

Shankaran, V., Ikeda, H., Bruce, A.T., White, J.M., Swanson, P.E., Old, L.J., and Schreiber, R.D. (2001). IFNgamma and lymphocytes prevent primary tumour development and shape tumour immunogenicity. Nature *410*, 1107-1111.

Shao, Y., Zheng, Q., Wang, W., Xin, N., Song, X., and Zhao, C. (2016). Biological functions of macrophage-derived Wnt5a, and its roles in human diseases. Oncotarget *7*, 67674-67684.

Shinohara, H., Kuranaga, Y., Kumazaki, M., Sugito, N., Yoshikawa, Y., Takai, T., Taniguchi, K., Ito, Y., and Akao, Y. (2017). Regulated Polarization of Tumor-Associated Macrophages by miR-145 via Colorectal Cancer-Derived Extracellular Vesicles. J Immunol *199*, 1505-1515.

Shioyama, Y., Tsuji, H., Suefuji, H., Sinoto, M., Matsunobu, A., Toyama, S., Nakamura, K., and Kudo, S. (2015). Particle radiotherapy for prostate cancer. Int J Urol *22*, 33-39.

Short, K.R., Grant, E.J., Vissers, M., Reading, P.C., Diavatopoulos, D.A., and Kedzierska, K. (2013). A Novel Method Linking Antigen Presentation by Human Monocyte-Derived Macrophages to CD8(+) T Cell Polyfunctionality. Front Immunol *4*, 389.

Sica, A., and Mantovani, A. (2012). Macrophage plasticity and polarization: in vivo veritas. J Clin Invest *122*, 787-795.

Sica, A., Saccani, A., Bottazzi, B., Bernasconi, S., Allavena, P., Gaetano, B., Fei, F., LaRosa, G., Scotton, C., Balkwill, F.*, et al.* (2000a). Defective expression of the monocyte chemotactic protein-1 receptor CCR2 in macrophages associated with human ovarian carcinoma. J Immunol *164*, 733-738.

Sica, A., Saccani, A., Bottazzi, B., Polentarutti, N., Vecchi, A., van Damme, J., and Mantovani, A. (2000b). Autocrine production of IL-10 mediates defective IL-12 production and NF-kappa B activation in tumor-associated macrophages. J Immunol *164*, 762-767.

Siegel, R.L., Miller, K.D., and Jemal, A. (2017). Cancer Statistics, 2017. CA Cancer J Clin *67*, 7-30.

Sinha, P., Clements, V.K., Bunt, S.K., Albelda, S.M., and Ostrand-Rosenberg, S. (2007). Cross-talk between myeloid-derived suppressor cells and macrophages subverts tumor immunity toward a type 2 response. J Immunol *179*, 977-983.

Slaney, C.Y., Kershaw, M.H., and Darcy, P.K. (2014). Trafficking of T cells into tumors. Cancer Res *74*, 7168-7174.

Smirnov, A.S., Ruzov, A.S., Budanov, A.V., Prokhortchouk, A.V., Ivanov, A.V., and Prokhortchouk, E.B. (2001). High constitutive level of NF-kappaB is crucial for viability of adenocarcinoma cells. Cell Death Differ *8*, 621-630.

Standiford, T.J., Kuick, R., Bhan, U., Chen, J., Newstead, M., and Keshamouni, V.G. (2011). TGF-beta-induced IRAK-M expression in tumor-associated macrophages regulates lung tumor growth. Oncogene *30*, 2475-2484.

Strauss, L., Sangaletti, S., Consonni, F.M., Szebeni, G., Morlacchi, S., Totaro, M.G., Porta, C., Anselmo, A., Tartari, S., Doni, A.*, et al.* (2015). RORC1 Regulates Tumor-Promoting "Emergency" Granulo-Monocytopoiesis. Cancer Cell *28*, 253-269.

Stutman, M. (1970). Tumor development after 3-methylcholanthrene in immunologically deficient athymic nude mice. Science *183*, 534 - 536.

Su, S., Liu, Q., Chen, J., Chen, J., Chen, F., He, C., Huang, D., Wu, W., Lin, L., Huang, W.*, et al.* (2014). A positive feedback loop between mesenchymal-like cancer cells and macrophages is essential to breast cancer metastasis. Cancer Cell *25*, 605-620.

Takeda, K., and Akira, S. (2004). TLR signaling pathways. Semin Immunol *16*, 3-9.

Tanaka, T., Grusby, M.J., and Kaisho, T. (2007). PDLIM2-mediated termination of transcription factor NF-kappaB activation by intranuclear sequestration and degradation of the p65 subunit. Nat Immunol *8*, 584-591.

Teng, M.W., Swann, J.B., Koebel, C.M., Schreiber, R.D., and Smyth, M.J. (2008). Immune-mediated dormancy: an equilibrium with cancer. J Leukoc Biol *84*, 988-993.

Thomas, ed. (1959). Discussion. in Cellular and Humoral Aspects of hypersensitivity States, Lawrence, H.s. edn.

Tlsty, T.D., and Coussens, L.M. (2006). Tumor stroma and regulation of cancer development. Annu Rev Pathol *1*, 119-150.

Tripathi, C., Tewari, B.N., Kanchan, R.K., Baghel, K.S., Nautiyal, N., Shrivastava, R., Kaur, H., Bhatt, M.L., and Bhadauria, S. (2014). Macrophages are recruited to hypoxic tumor areas and acquire a pro-angiogenic M2-polarized phenotype via hypoxic cancer cell derived cytokines Oncostatin M and Eotaxin. Oncotarget *5*, 5350-5368.

Trivedi, M., Talekar, M., Shah, P., Ouyang, Q., and Amiji, M. (2016). Modification of tumor cell exosome content by transfection with wt-p53 and microRNA-125b expressing plasmid DNA and its effect on macrophage polarization. Oncogenesis *5*, e250.

Tsou, P., Katayama, H., Ostrin, E.J., and Hanash, S.M. (2016). The Emerging Role of B Cells in Tumor Immunity. Cancer Res *76*, 5597-5601.

Turgeon, M.O., Perry, N.J.S., and Poulogiannis, G. (2018). DNA Damage, Repair, and Cancer Metabolism. Front Oncol *8*, 15.

Turrini, R., Pabois, A., Xenarios, I., Coukos, G., Delaloye, J.F., and Doucey, M.A. (2017). TIE-2 expressing monocytes in human cancers. Oncoimmunology *6*, e1303585.

Tyagi, A., Singh, R.P., Ramasamy, K., Raina, K., Redente, E.F., Dwyer-Nield, L.D., Radcliffe, R.A., Malkinson, A.M., and Agarwal, R. (2009). Growth inhibition and regression of lung tumors by silibinin: modulation of angiogenesis by macrophage-associated cytokines and nuclear factor-kappaB and signal transducers and activators of transcription 3. Cancer Prev Res (Phila) *2*, 74-83.

Ugel, S., De Sanctis, F., Mandruzzato, S., and Bronte, V. (2015). Tumor-induced myeloid deviation: when myeloid-derived suppressor cells meet tumor-associated macrophages. J Clin Invest *125*, 3365-3376.

Van den Bossche, J., O'Neill, L.A., and Menon, D. (2017). Macrophage Immunometabolism: Where Are We (Going)? Trends Immunol *38*, 395-406.

Van der Jeught, K., Bialkowski, L., Daszkiewicz, L., Broos, K., Goyvaerts, C., Renmans, D., Van Lint, S., Heirman, C., Thielemans, K., and Breckpot, K. (2015). Targeting the tumor microenvironment to enhance antitumor immune responses. Oncotarget *6*, 1359-1381.

van der Woude, L.L., Gorris, M.A.J., Halilovic, A., Figdor, C.G., and de Vries, I.J.M. (2017). Migrating into the Tumor: a Roadmap for T Cells. Trends Cancer *3*, 797-808.

van Ravenswaay Claasen, H.H., Kluin, P.M., and Fleuren, G.J. (1992). Tumor infiltrating cells in human cancer. On the possible role of CD16+ macrophages in antitumor cytotoxicity. Lab Invest *67*, 166-174.

Vanpouille-Box, C., Alard, A., Aryankalayil, M.J., Sarfraz, Y., Diamond, J.M., Schneider, R.J., Inghirami, G., Coleman, C.N., Formenti, S.C., and Demaria, S. (2017). DNA exonuclease Trex1 regulates radiotherapy-induced tumour immunogenicity. Nat Commun *8*, 15618.

Vanpouille-Box, C., Diamond, J.M., Pilones, K.A., Zavadil, J., Babb, J.S., Formenti, S.C., Barcellos-Hoff, M.H., and Demaria, S. (2015). TGFbeta Is a Master Regulator of Radiation Therapy-Induced Antitumor Immunity. Cancer Res *75*, 2232-2242.

Venneri, M.A., De Palma, M., Ponzoni, M., Pucci, F., Scielzo, C., Zonari, E., Mazzieri, R., Doglioni, C., and Naldini, L. (2007). Identification of proangiogenic TIE2-expressing monocytes (TEMs) in human peripheral blood and cancer. Blood *109*, 5276-5285.

Vergadi, E., Ieronymaki, E., Lyroni, K., Vaporidi, K., and Tsatsanis, C. (2017). Akt Signaling Pathway in Macrophage Activation and M1/M2 Polarization. J Immunol *198*, 1006-1014.

von Boehmer, H., and Daniel, C. (2013). Therapeutic opportunities for manipulating T(Reg) cells in autoimmunity and cancer. Nat Rev Drug Discov *12*, 51-63.

Wan, S., Zhao, E., Kryczek, I., Vatan, L., Sadovskaya, A., Ludema, G., Simeone, D.M., Zou, W., and Welling, T.H. (2014). Tumor-associated macrophages produce interleukin 6 and signal via STAT3 to promote expansion of human hepatocellular carcinoma stem cells. Gastroenterology *147*, 1393-1404.

Wang, M., Zhao, J., Zhang, L., Wei, F., Lian, Y., Wu, Y., Gong, Z., Zhang, S., Zhou, J., Cao, K.*, et al.* (2017a). Role of tumor microenvironment in tumorigenesis. J Cancer *8*, 761-773.

Wang, N., Liang, H., and Zen, K. (2014). Molecular mechanisms that influence the macrophage m1-m2 polarization balance. Front Immunol *5*, 614.

Wang, W., Mani, A.M., and Wu, Z.H. (2017b). DNA damage-induced nuclear factor-kappa B activation and its roles in cancer progression. J Cancer Metastasis Treat *3*, 45-59.

Wang, X., Dai, Z., Wu, X., Wang, K., and Wang, X. (2016a). Distinct RNA transcriptome patterns are potentially associated with angiogenesis in Tie2-expressing monocytes. Gene *580*, 1-7.

Wang, Y., Liu, T., Yang, N., Xu, S., Li, X., and Wang, D. (2016b). Hypoxia and macrophages promote glioblastoma invasion by the CCL4-CCR5 axis. Oncol Rep *36*, 3522-3528.

Wang, Z., Xu, L., Hu, Y., Huang, Y., Zhang, Y., Zheng, X., Wang, S., Wang, Y., Yu, Y., Zhang, M.*, et al.* (2016c). miRNA let-7b modulates macrophage polarization and enhances tumor-associated macrophages to promote angiogenesis and mobility in prostate cancer. Sci Rep *6*, 25602.

Weber, D.C., Ares, C., Lomax, A.J., and Kurtz, J.M. (2006). Radiation therapy planning with photons and protons for early and advanced breast cancer: an overview. Radiat Oncol *1*, 22.

Wenes, M., Shang, M., Di Matteo, M., Goveia, J., Martin-Perez, R., Serneels, J., Prenen, H., Ghesquiere, B., Carmeliet, P., and Mazzone, M. (2016). Macrophage Metabolism Controls Tumor Blood Vessel Morphogenesis and Metastasis. Cell Metab *24*, 701-715.

Wennerberg, E., Lhuillier, C., Vanpouille-Box, C., Pilones, K.A., Garcia-Martinez, E., Rudqvist, N.P., Formenti, S.C., and Demaria, S. (2017). Barriers to Radiation-Induced In Situ Tumor Vaccination. Front Immunol *8*, 229.

Wéra, A.-C., Riquier, H., Heuskin, A.-C., Michiels, C., and Lucas, S. (2011). In vitro irradiation station for broad beam radiobiological experiments. Nuclear Instruments and Methods in Physics Research *269*, 3120 - 3124.

Werno, C., Menrad, H., Weigert, A., Dehne, N., Goerdt, S., Schledzewski, K., Kzhyshkowska, J., and Brune, B. (2010). Knockout of HIF-1alpha in tumor-associated macrophages enhances M2 polarization and attenuates their pro-angiogenic responses. Carcinogenesis *31*, 1863-1872.

Wong, G.H. (1995). Protective roles of cytokines against radiation: induction of mitochondrial MnSOD. Biochim Biophys Acta *1271*, 205-209.

Wong, S.C., Puaux, A.L., Chittezhath, M., Shalova, I., Kajiji, T.S., Wang, X., Abastado, J.P., Lam, K.P., and Biswas, S.K. (2010). Macrophage polarization to a unique phenotype driven by B cells. Eur J Immunol *40*, 2296-2307.

Woo, S.R., Corrales, L., and Gajewski, T.F. (2015). Innate immune recognition of cancer. Annu Rev Immunol *33*, 445-474.

Wu, Q., Allouch, A., Paoletti, A., Leteur, C., Mirjolet, C., Martins, I., Voisin, L., Law, F., Dakhli, H., Mintet, E.*, et al.* (2017). NOX2-dependent ATM kinase activation dictates pro-inflammatory macrophage phenotype and improves effectiveness to radiation therapy. Cell Death Differ *24*, 1632-1644.

Wu, X.Q., Dai, Y., Yang, Y., Huang, C., Meng, X.M., Wu, B.M., and Li, J. (2016). Emerging role of microRNAs in regulating macrophage activation and polarization in immune response and inflammation. Immunology *148*, 237-248.

Wyckoff, J., Wang, W., Lin, E.Y., Wang, Y., Pixley, F., Stanley, E.R., Graf, T., Pollard, J.W., Segall, J., and Condeelis, J. (2004). A paracrine loop between tumor cells and macrophages is required for tumor cell migration in mammary tumors. Cancer Res *64*, 7022-7029.

Wyckoff, J.B., Wang, Y., Lin, E.Y., Li, J.F., Goswami, S., Stanley, E.R., Segall, J.E., Pollard, J.W., and Condeelis, J. (2007). Direct visualization of macrophage-assisted tumor cell intravasation in mammary tumors. Cancer Res *67*, 2649-2656.

Xie, C., Liu, C., Wu, B., Lin, Y., Ma, T., Xiong, H., Wang, Q., Li, Z., Ma, C., and Tu, Z. (2016). Effects of IRF1 and IFN-beta interaction on the M1 polarization of macrophages and its antitumor function. Int J Mol Med *38*, 148-160.

Xing, F., Saidou, J., and Watabe, K. (2010). Cancer associated fibroblasts (CAFs) in tumor microenvironment. Front Biosci (Landmark Ed) *15*, 166-179.

Xu, B., Chen, L., Li, J., Zheng, X., Shi, L., Wu, C., and Jiang, J. (2016). Prognostic value of tumor infiltrating NK cells and macrophages in stage II+III esophageal cancer patients. Oncotarget *7*, 74904-74916.

Yang, J., Hawkins, O.E., Barham, W., Gilchuk, P., Boothby, M., Ayers, G.D., Joyce, S., Karin, M., Yull, F.E., and Richmond, A. (2014a). Myeloid IKKbeta promotes antitumor immunity by modulating CCL11 and the innate immune response. Cancer Res *74*, 7274-7284.

Yang, J., Kantrow, S., Sai, J., Hawkins, O.E., Boothby, M., Ayers, G.D., Young, E.D., Demicco, E.G., Lazar, A.J., Lev, D.*, et al.* (2012). INK4a/ARF [corrected] inactivation with activation of the NF-kappaB/IL-6 pathway is sufficient to drive the development and growth of angiosarcoma. Cancer Res *72*, 4682-4695.

Yang, J., Zhang, Z., Chen, C., Liu, Y., Si, Q., Chuang, T.H., Li, N., Gomez-Cabrero, A., Reisfeld, R.A., Xiang, R.*, et al.* (2014b). MicroRNA-19a-3p inhibits breast cancer progression and metastasis by inducing macrophage polarization through downregulated expression of Fra-1 proto-oncogene. Oncogene *33*, 3014-3023.

Ye, Y., Xu, Y., Lai, Y., He, W., Li, Y., Wang, R., Luo, X., Chen, R., and Chen, T. (2018). Long non-coding RNA cox-2 prevents immune evasion and metastasis of hepatocellular carcinoma by altering M1/M2 macrophage polarization. J Cell Biochem *119*, 2951-2963.

Yeo, E.J., Cassetta, L., Qian, B.Z., Lewkowich, I., Li, J.F., Stefater, J.A., 3rd, Smith, A.N., Wiechmann, L.S., Wang, Y., Pollard, J.W.*, et al.* (2014). Myeloid WNT7b mediates the angiogenic switch and metastasis in breast cancer. Cancer Res *74*, 2962-2973.

Yu, F., Jia, X., Du, F., Wang, J., Wang, Y., Ai, W., and Fan, D. (2013). miR-155-deficient bone marrow promotes tumor metastasis. Mol Cancer Res *11*, 923-936.

Yuan, Y., Jiang, Y.C., Sun, C.K., and Chen, Q.M. (2016). Role of the tumor microenvironment in tumor progression and the clinical applications (Review). Oncol Rep *35*, 2499-2515.

Zafar, F., Seidler, S.B., Kronenberg, A., Schild, D., and Wiese, C. (2010). Homologous recombination contributes to the repair of DNA double-strand breaks induced by high-energy iron ions. Radiat Res *173*, 27-39.

Zeisberger, S.M., Odermatt, B., Marty, C., Zehnder-Fjallman, A.H., Ballmer-Hofer, K., and Schwendener, R.A. (2006). Clodronate-liposome-mediated depletion of tumour-associated macrophages: a new and highly effective antiangiogenic therapy approach. Br J Cancer *95*, 272-281.

Zhang, F., Wang, H., Wang, X., Jiang, G., Liu, H., Zhang, G., Wang, H., Fang, R., Bu, X., Cai, S.*, et al.* (2016). TGF-beta induces M2-like macrophage polarization via SNAIL-mediated suppression of a pro-inflammatory phenotype. Oncotarget *7*, 52294-52306.

Zhang, J., Cao, J., Ma, S., Dong, R., Meng, W., Ying, M., Weng, Q., Chen, Z., Ma, J., Fang, Q.*, et al.* (2014). Tumor hypoxia enhances Non-Small Cell Lung Cancer metastasis by selectively promoting macrophage M2 polarization through the activation of ERK signaling. Oncotarget *5*, 9664-9677.

Zhang, J., Shen, L., and Sun, L.Q. (2015). The regulation of radiosensitivity by p53 and its acetylation. Cancer Lett *363*, 108-118.

Zhang, Y., Zhou, N., Yu, X., Zhang, X., Li, S., Lei, Z., Hu, R., Li, H., Mao, Y., Wang, X.*, et al.* (2017). Tumacrophage: macrophages transformed into tumor stem-like cells by virulent genetic material from tumor cells. Oncotarget *8*, 82326-82343.

Zhao, J., Kong, H.J., Li, H., Huang, B., Yang, M., Zhu, C., Bogunovic, M., Zheng, F., Mayer, L., Ozato, K.*, et al.* (2006). IRF-8/interferon (IFN) consensus sequence-binding protein is involved in Toll-like receptor (TLR) signaling and contributes to the cross-talk between TLR and IFN-gamma signaling pathways. J Biol Chem *281*, 10073-10080.

Zhao, J.L., Huang, F., He, F., Gao, C.C., Liang, S.Q., Ma, P.F., Dong, G.Y., Han, H., and Qin, H.Y. (2016). Forced Activation of Notch in Macrophages Represses Tumor Growth by Upregulating miR-125a and Disabling Tumor-Associated Macrophages. Cancer Res *76*, 1403-1415.

Zhao, S., Zhang, Y., Zhang, Q., Wang, F., and Zhang, D. (2014). Toll-like receptors and prostate cancer. Front Immunol *5*, 352.

Zheng, X., Turkowski, K., Mora, J., Brune, B., Seeger, W., Weigert, A., and Savai, R. (2017). Redirecting tumor-associated macrophages to become tumoricidal effectors as a novel strategy for cancer therapy. Oncotarget *8*, 48436-48452.

Zhong, Y., and Yi, C. (2016). MicroRNA-720 suppresses M2 macrophage polarization by targeting GATA3. Biosci Rep *36*.

Zhou, D., Huang, C., Lin, Z., Zhan, S., Kong, L., Fang, C., and Li, J. (2014). Macrophage polarization and function with emphasis on the evolving roles of coordinated regulation of cellular signaling pathways. Cell Signal *26*, 192-197.

Zhu, L., Zhao, Q., Yang, T., Ding, W., and Zhao, Y. (2015). Cellular metabolism and macrophage functional polarization. Int Rev Immunol *34*, 82-100.

Zhu, Y., Herndon, J.M., Sojka, D.K., Kim, K.W., Knolhoff, B.L., Zuo, C., Cullinan, D.R., Luo, J., Bearden, A.R., Lavine, K.J., *et al.* (2017). Tissue-Resident Macrophages in Pancreatic Ductal Adenocarcinoma Originate from Embryonic Hematopoiesis and Promote Tumor Progression. Immunity *47*, 597.

Abbas, L., Pillai (2015). Cellular and Molecular Immunology, Elsevier edn.

Ahmed, M.M., Hodge, J.W., Guha, C., Bernhard, E.J., Vikram, B., and Coleman, C.N. (2013). Harnessing the potential of radiation-induced immune modulation for cancer therapy. Cancer Immunol Res *1*, 280-284.

Brandsma, I., and Gent, D.C. (2012). Pathway choice in DNA double strand break repair: observations of a balancing act. Genome Integr *3*, 9.

Cai, X., Chiu, Y.H., and Chen, Z.J. (2014). The cGAS-cGAMP-STING pathway of cytosolic DNA sensing and signaling. Mol Cell *54*, 289-296.

Chen, F., Zhang, Y., Bosse, D., Lalani, A.A., Hakimi, A.A., Hsieh, J.J., Choueiri, T.K., Gibbons, D.L., Ittmann, M., and Creighton, C.J. (2017). Pan-urologic cancer genomic subtypes that transcend tissue of origin. Nat Commun *8*, 199.

Chen, Y., and Ahmad, S. (2012). Empirical model estimation of relative biological effectiveness for proton beam therapy. Radiat Prot Dosimetry *149*, 116-123.

DeNardo, D.G., Barreto, J.B., Andreu, P., Vasquez, L., Tawfik, D., Kolhatkar, N., and Coussens, L.M. (2009). CD4(+) T cells regulate pulmonary metastasis of mammary carcinomas by enhancing protumor properties of macrophages. Cancer Cell *16*, 91-102.

Esteller, M. (2011). Non-coding RNAs in human disease. Nat Rev Genet *12*, 861-874.

Franklin, R.A., and Li, M.O. (2014). The ontogeny of tumor-associated macrophages: a new understanding of cancer-elicited inflammation. Oncoimmunology *3*, e955346.

Fridman, W.H., Zitvogel, L., Sautes-Fridman, C., and Kroemer, G. (2017). The immune contexture in cancer prognosis and treatment. Nat Rev Clin Oncol *14*, 717-734.

Gentles, A.J., Newman, A.M., Liu, C.L., Bratman, S.V., Feng, W., Kim, D., Nair, V.S., Xu, Y., Khuong, A., Hoang, C.D.*, et al.* (2015). The prognostic landscape of genes and infiltrating immune cells across human cancers. Nat Med *21*, 938-945.

Grivennikov, S.I., Greten, F.R., and Karin, M. (2010). Immunity, inflammation, and cancer. Cell *140*, 883-899.

Hanahan, D., and Weinberg, R.A. (2000). The hallmarks of cancer. Cell *100*, 57-70.

Hanahan, D., and Weinberg, R.A. (2011). Hallmarks of cancer: the next generation. Cell *144*, 646-674.

Harney, A.S., Arwert, E.N., Entenberg, D., Wang, Y., Guo, P., Qian, B.Z., Oktay, M.H., Pollard, J.W., Jones, J.G., and Condeelis, J.S. (2015). Real-Time Imaging Reveals Local, Transient Vascular Permeability, and Tumor Cell Intravasation Stimulated by TIE2hi Macrophage-Derived VEGFA. Cancer Discov *5*, 932-943.

Hoesel, B., and Schmid, J.A. (2013). The complexity of NF-kappaB signaling in inflammation and cancer. Mol Cancer *12*, 86.

Jakel, O. (2009). Medical physics aspects of particle therapy. Radiat Prot Dosimetry *137*, 156-166.

Ji, H., Cao, R., Yang, Y., Zhang, Y., Iwamoto, H., Lim, S., Nakamura, M., Andersson, P., Wang, J., Sun, Y.*, et al.* (2014). TNFR1 mediates TNF-alpha-induced tumour lymphangiogenesis and metastasis by modulating VEGF-C-VEGFR3 signalling. Nat Commun *5*, 4944.

Jiang, W., Chan, C.K., Weissman, I.L., Kim, B.Y.S., and Hahn, S.M. (2016). Immune Priming of the Tumor Microenvironment by Radiation. Trends Cancer *2*, 638-645.

Joshi, S., Singh, A.R., Zulcic, M., and Durden, D.L. (2014). A macrophage-dominant PI3K isoform controls hypoxia-induced HIF1alpha and HIF2alpha stability and tumor growth, angiogenesis, and metastasis. Mol Cancer Res *12*, 1520-1531.

Kamran, P., Sereti, K.I., Zhao, P., Ali, S.R., Weissman, I.L., and Ardehali, R. (2013). Parabiosis in mice: a detailed protocol. J Vis Exp.

Kerkar, S.P., and Restifo, N.P. (2012). Cellular constituents of immune escape within the tumor microenvironment. Cancer Res *72*, 3125-3130.

Konisti, S., Kiriakidis, S., and Paleolog, E.M. (2012). Hypoxia--a key regulator of angiogenesis and inflammation in rheumatoid arthritis. Nat Rev Rheumatol *8*, 153-162.

Ladra, M.M., and Yock, T.I. (2014). Proton radiotherapy for pediatric sarcoma. Cancers (Basel) *6*, 112-127.

Liu, B., Sun, L., Liu, Q., Gong, C., Yao, Y., Lv, X., Lin, L., Yao, H., Su, F., Li, D.*, et al.* (2015). A cytoplasmic NF-kappaB interacting long noncoding RNA blocks IkappaB phosphorylation and suppresses breast cancer metastasis. Cancer Cell *27*, 370-381.

Mantovani, A., Sozzani, S., Locati, M., Allavena, P., and Sica, A. (2002). Macrophage polarization: tumor-associated macrophages as a paradigm for polarized M2 mononuclear phagocytes. Trends Immunol *23*, 549-555.

McCool, K.W., and Miyamoto, S. (2012). DNA damage-dependent NF-kappaB activation: NEMO turns nuclear signaling inside out. Immunol Rev *246*, 311-326.

McGranahan, N., Furness, A.J., Rosenthal, R., Ramskov, S., Lyngaa, R., Saini, S.K., Jamal-Hanjani, M., Wilson, G.A., Birkbak, N.J., Hiley, C.T.*, et al.* (2016). Clonal neoantigens elicit T cell immunoreactivity and sensitivity to immune checkpoint blockade. Science *351*, 1463-1469.

Mosser, D.M., and Edwards, J.P. (2008). Exploring the full spectrum of macrophage activation. Nat Rev Immunol *8*, 958-969.

Natale, F., Rapp, A., Yu, W., Maiser, A., Harz, H., Scholl, A., Grulich, S., Anton, T., Horl, D., Chen, W.*, et al.* (2017). Identification of the elementary structural units of the DNA damage response. Nat Commun *8*, 15760.

Nathan, C., and Cunningham-Bussel, A. (2013). Beyond oxidative stress: an immunologist's guide to reactive oxygen species. Nat Rev Immunol *13*, 349-361.

Palucka, A.K., and Coussens, L.M. (2016). The Basis of Oncoimmunology. Cell *164*, 1233-1247.

Pouget, J.P., Navarro-Teulon, I., Bardies, M., Chouin, N., Cartron, G., Pelegrin, A., and Azria, D. (2011). Clinical radioimmunotherapy--the role of radiobiology. Nat Rev Clin Oncol *8*, 720-734.

Qi, W., Huang, X., and Wang, J. (2013). Correlation between Th17 cells and tumor microenvironment. Cell Immunol *285*, 18-22.

Qian, B.Z., and Pollard, J.W. (2010). Macrophage diversity enhances tumor progression and metastasis. Cell *141*, 39-51.

Reisz, J.A., Bansal, N., Qian, J., Zhao, W., and Furdui, C.M. (2014). Effects of ionizing radiation on biological molecules--mechanisms of damage and emerging methods of detection. Antioxid Redox Signal *21*, 260-292.

Schlaff, C.D., Krauze, A., Belard, A., O'Connell, J.J., and Camphausen, K.A. (2014). Bringing the heavy: carbon ion therapy in the radiobiological and clinical context. Radiat Oncol *9*, 88.

Schreiber, R.D., Old, L.J., and Smyth, M.J. (2011). Cancer immunoediting: integrating immunity's roles in cancer suppression and promotion. Science *331*, 1565-1570.

Scudellari, M. (2015). Ageing research: Blood to blood. Nature *517*, 426-429.

Siegel, R.L., Miller, K.D., and Jemal, A. (2017). Cancer Statistics, 2017. CA Cancer J Clin *67*, 7-30.

Stout, R.D., and Bottomly, K. (1989). Antigen-specific activation of effector macrophages by IFN-gamma producing (TH1) T cell clones. Failure of IL-4-producing (TH2) T cell clones to activate effector function in macrophages. J Immunol *142*, 760-765.

Ugel, S., De Sanctis, F., Mandruzzato, S., and Bronte, V. (2015). Tumor-induced myeloid deviation: when myeloid-derived suppressor cells meet tumor-associated macrophages. J Clin Invest *125*, 3365-3376.

Van den Bossche, J., O'Neill, L.A., and Menon, D. (2017). Macrophage Immunometabolism: Where Are We (Going)? Trends Immunol *38*, 395-406.

Wang, N., Liang, H., and Zen, K. (2014). Molecular mechanisms that influence the macrophage m1-m2 polarization balance. Front Immunol *5*, 614.

Wéra, A.-C., Riquier, H., Heuskin, A.-C., Michiels, C., and Lucas, S. (2011). In vitro irradiation station for broad beam radiobiological experiments. Nuclear Instruments and Methods in Physics Research *269*, 3120 - 3124.

Zhang, J., Shen, L., and Sun, L.Q. (2015). The regulation of radiosensitivity by p53 and its acetylation. Cancer Lett *363*, 108-118.

Zhao, S., Zhang, Y., Zhang, Q., Wang, F., and Zhang, D. (2014). Toll-like receptors and prostate cancer. Front Immunol *5*, 352.